



# **E**xtension of CFD Codes Application to Two-Phase Flow Safety Problems: Phase 3



**Unclassified**

**English text only**

2 August 2023

**NUCLEAR ENERGY AGENCY  
COMMITTEE ON THE SAFETY OF NUCLEAR INSTALLATIONS**

**Extension of CFD Codes Application to Two-Phase Flow Safety Problems:  
Phase 3**

This document is available in PDF format only.

**JT03523945**

## ORGANISATION FOR ECONOMIC CO-OPERATION AND DEVELOPMENT

The OECD is a unique forum where the governments of 38 democracies work together to address the economic, social and environmental challenges of globalisation. The OECD is also at the forefront of efforts to understand and to help governments respond to new developments and concerns, such as corporate governance, the information economy and the challenges of an ageing population. The Organisation provides a setting where governments can compare policy experiences, seek answers to common problems, identify good practice and work to co-ordinate domestic and international policies.

The OECD member countries are: Australia, Austria, Belgium, Canada, Chile, Colombia, Costa Rica, the Czech Republic, Denmark, Estonia, Finland, France, Germany, Greece, Hungary, Iceland, Ireland, Israel, Italy, Japan, Korea, Latvia, Lithuania, Luxembourg, Mexico, the Netherlands, New Zealand, Norway, Poland, Portugal, the Slovak Republic, Slovenia, Spain, Sweden, Switzerland, Türkiye, the United Kingdom and the United States. The European Commission takes part in the work of the OECD.

OECD Publishing disseminates widely the results of the Organisation's statistics gathering and research on economic, social and environmental issues, as well as the conventions, guidelines and standards agreed by its members.

## NUCLEAR ENERGY AGENCY

The OECD Nuclear Energy Agency (NEA) was established on 1 February 1958. Current NEA membership consists of 34 countries: Argentina, Australia, Austria, Belgium, Bulgaria, Canada, the Czech Republic, Denmark, Finland, France, Germany, Greece, Hungary, Iceland, Ireland, Italy, Japan, Korea, Luxembourg, Mexico, the Netherlands, Norway, Poland, Portugal, Romania, Russia (suspended), the Slovak Republic, Slovenia, Spain, Sweden, Switzerland, Türkiye, the United Kingdom and the United States. The European Commission and the International Atomic Energy Agency also take part in the work of the Agency.

The mission of the NEA is:

- to assist its member countries in maintaining and further developing, through international co-operation, the scientific, technological and legal bases required for a safe, environmentally sound and economical use of nuclear energy for peaceful purposes;
- to provide authoritative assessments and to forge common understandings on key issues as input to government decisions on nuclear energy policy and to broader OECD analyses in areas such as energy and the sustainable development of low-carbon economies.

Specific areas of competence of the NEA include the safety and regulation of nuclear activities, radioactive waste management and decommissioning, radiological protection, nuclear science, economic and technical analyses of the nuclear fuel cycle, nuclear law and liability, and public information. The NEA Data Bank provides nuclear data and computer program services for participating countries.

This document, as well as any data and map included herein, are without prejudice to the status of or sovereignty over any territory, to the delimitation of international frontiers and boundaries and to the name of any territory, city or area.

Corrigenda to OECD publications may be found online at: [www.oecd.org/about/publishing/corrigenda.htm](http://www.oecd.org/about/publishing/corrigenda.htm).

### © OECD 2023

You can copy, download or print OECD content for your own use, and you can include excerpts from OECD publications, databases and multimedia products in your own documents, presentations, blogs, websites and teaching materials, provided that suitable acknowledgement of the OECD as source and copyright owner is given. All requests for public or commercial use and translation rights should be submitted to [neapub@oecd-nea.org](mailto:neapub@oecd-nea.org). Requests for permission to photocopy portions of this material for public or commercial use shall be addressed directly to the Copyright Clearance Center (CCC) at [info@copyright.com](mailto:info@copyright.com) or the Centre français d'exploitation du droit de copie (CFC) [contact@cfcopies.com](mailto:contact@cfcopies.com).

---

## *Committee on the Safety of Nuclear Installations (CSNI)*

The Committee on the Safety of Nuclear Installations (CSNI) addresses Nuclear Energy Agency (NEA) programmes and activities that support maintaining and advancing the scientific and technical knowledge base of the safety of nuclear installations.

The Committee constitutes a forum for the exchange of technical information and for collaboration between organisations, which can contribute, from their respective backgrounds in research, development and engineering, to its activities. It has regard to the exchange of information between member countries and safety R&D programmes of various sizes in order to keep all member countries involved in and abreast of developments in technical safety matters.

The Committee reviews the state of knowledge on important topics of nuclear safety science and techniques and of safety assessments, and ensures that operating experience is appropriately accounted for in its activities. It initiates and conducts programmes identified by these reviews and assessments in order to confirm safety, overcome discrepancies, develop improvements and reach consensus on technical issues of common interest. It promotes the co-ordination of work in different member countries that serve to maintain and enhance competence in nuclear safety matters, including the establishment of joint undertakings (e.g. joint research and data projects), and assists in the feedback of the results to participating organisations. The Committee ensures that valuable end-products of the technical reviews and analyses are provided to members in a timely manner, and made publicly available when appropriate, to support broader nuclear safety.

The Committee focuses primarily on the safety aspects of existing power reactors, other nuclear installations and new power reactors; it also considers the safety implications of scientific and technical developments of future reactor technologies and designs. Further, the scope for the Committee includes human and organisational research activities and technical developments that affect nuclear safety.

## Authors

D. Bestion, H. Anglart, J. Mahaffy, D. Lucas, C.H. Song, M. Scheuerer, G. Zigh,  
M. Andreani, F. Kasahara, M. Heitsch, E. Komen, F. Moretti, T. Morii, P. Mühlbauer,  
B.L. Smith, T. Watanabe

## *Table of contents*

<b>Executive summary .....</b>	<b>8</b>
<b>1. Introduction .....</b>	<b>11</b>
<b>2. Methodology for the application of two-phase CFD and selection of a few nuclear reactor safety issues .....</b>	<b>13</b>
2.1. Multi-step methodology for application of two-phase CFD to nuclear reactor issues.....	13
2.2. Classification of the two-phase CFD modelling options .....	17
2.3. Selection of a limited number of nuclear safety issues .....	29
<b>3. The dry-out investigations .....</b>	<b>34</b>
3.1. Definition of the dry-out issue and identification of all-important flow processes .....	34
3.2. Limits of previous approaches and expected improvements with CFD .....	35
3.3. Selecting the basic model .....	36
3.4. Filtering turbulent scales and two-phase intermittency scales.....	37
3.5. Identification of local interface structure .....	37
3.6. Modelling interfacial transfers.....	38
3.7. Modelling turbulent transfers.....	39
3.8. Modelling wall transfers .....	40
3.9. Status of modelling .....	40
3.10. Matrix of validation test cases .....	40
<b>4. The departure from nucleate boiling .....</b>	<b>48</b>
4.1. Definition of the DNB issue and identification of all-important flow processes.....	48
4.2. Limits of previous approaches and expected improvements with CFD .....	49
4.3. Selecting a basic model.....	50
4.4. Filtering turbulent scales and two-phase intermittency scales.....	51
4.5. ILIS .....	51
4.6. Modelling interfacial transfers.....	51
4.7. Modelling turbulent transfers.....	52
4.8. Modelling wall transfers .....	52
4.9. Status of the modelling .....	53
4.10. Validation matrix for the DNB issue .....	54
<b>5. The pressurised thermal shock.....</b>	<b>76</b>
5.1. Definition of the PTS issue and identification of all-important flow processes .....	76
5.2. Limits of previous approaches and expected improvements with CFD .....	79
5.3. Selecting a basic model.....	79
5.4. Filtering turbulent scales and two-phase intermittency scales.....	81
5.5. ILIS .....	82
5.6. Modelling interfacial transfers .....	84
5.7. Modelling turbulent transfers.....	86
5.8. Modelling wall transfers .....	87
5.9. Validation matrix for the PTS issue.....	87
<b>6. The pool heat exchangers.....</b>	<b>95</b>
6.1. Identification of all-important flow processes of the issue .....	95

6.2. Limits of previous approaches and expected improvements with CFD .....	97
6.3. Selecting a basic model.....	98
6.4. Filtering turbulent scales and two-phase intermittency scales.....	98
6.5. ILIS .....	99
6.6. Modelling interfacial transfers.....	99
6.7. Modelling turbulent transfers.....	100
6.8. Modelling wall transfers .....	100
6.9. Validation matrix for the selected NRS problems .....	100
<b>7. The steam discharge in a pool .....</b>	<b>105</b>
7.1. Identification of all-important flow processes of the issue .....	105
7.2. Limits of previous approaches and expected improvements with CFD .....	110
7.3. Selecting a basic model.....	111
7.4. Filtering turbulent scales and two-phase intermittency scales.....	111
7.5. ILIS .....	112
7.6. Modelling interfacial transfers.....	113
7.7. Modelling turbulent transfers.....	114
7.8. Modelling wall transfers .....	114
7.9. Validation matrix for the steam discharge in a pool .....	115
<b>8. Fire analysis .....</b>	<b>120</b>
8.1. Identification of all-important flow processes of the issues .....	120
8.2. Limits of previous approaches and expected improvements with CFD .....	124
8.3. Selecting a basic model.....	125
8.4. Filtering turbulent scales and two-phase-phase intermittency scales .....	128
8.5. Identification of local interface structure .....	129
8.6. Modelling interfacial transfers.....	129
8.7. Modelling turbulent transfers.....	130
8.8. Modelling wall transfer.....	130
8.9. Validation matrix for fire analysis .....	131
<b>9. Verification test cases of special interest for the selected issues.....</b>	<b>137</b>
9.1. The needs for 3D two-phase CFD codes for open medium.....	137
9.2. The needs for 3D codes for porous medium.....	138
9.3. Selection of a matrix of numerical benchmarks.....	138
9.4. Critical analysis of the list of selected tests. ....	140
9.5. The method of manufactured solutions.....	141
9.6. Conclusion on verification.....	143
<b>10. Proposal of benchmarks relative to the selected issues .....</b>	<b>145</b>
10.1. Proposed benchmark for dry-out .....	145
10.2. Proposed benchmark for DNB.....	146
10.3. Proposed benchmark for PTS .....	146
10.4. Proposed benchmark for pool heat exchangers .....	147
10.5. Proposed benchmark for steam injection in a pool.....	149
10.6. Proposed benchmark for fire analysis.....	150
<b>11. Some guidelines for two-phase CFD application to the selected NRS issues .....</b>	<b>151</b>
11.1. Introduction.....	151
11.2. Guidelines in application of the multi-step methodology .....	152

---

11.3. Definition of errors in CFD simulations .....	156
11.4. Strategies to reduce numerical errors.....	157
11.5. Strategies to reduce model errors.....	159
11.6. Strategies to reduce user errors .....	161
11.7. Strategies to reduce software errors .....	162
11.8. Strategies to reduce application uncertainties.....	162
<b>12. Conclusion.....</b>	<b>164</b>
<b>13. Glossary .....</b>	<b>166</b>
<b>Annex 1. Example of application of the method of manufactured solutions .....</b>	<b>169</b>

## Executive summary

This document is an update of the report NEA/CSNI/R(2014)13 which in turn was an extension of document NEA/SEN/SIN/AMA(2006)2. It was approved by the Committee on the Safety of Nuclear Installations (CSNI) at its 64<sup>th</sup> session on 5-6 December 2018 and prepared for publication by the NEA Secretariat. The original report was produced by the writing group WG3 on the extension of CFD to two-phase flow safety problems, which was formed following the recommendations made at the “Exploratory Meeting of Experts to Define an Action Plan on the Application of Computational Fluid Dynamics (CFD) Codes to Nuclear Reactor Safety Problems”, held in Aix-en-Provence in May 2002.

Extension of CFD codes to two-phase flow may provide insights to smaller scale flow processes, which were not seen by present tools. Using such tools as part of a safety demonstration may bring a better understanding of physical situations, more confidence in the results, and an estimation of safety margins. Subsequent improved computer performance allows for a more extensive use of 3D modelling of two-phase thermal-hydraulics with finer nodalisation. However, models are not as mature as in single-phase flows and much work still remains to be done on the physical modelling and numerical schemes in such two-phase CFD tools. The writing group listed and classified the nuclear reactor safety (NRS) problems where extension of CFD to two-phase flow may bring real benefit and classified different modelling approaches. First ideas were reported about the specification and analysis of needs in terms of validation and verification.

Following the original report mentioned above, it was suggested to focus further activity on a limited number of NRS issues with a high priority and a reasonable chance to be successful in a reasonable period. As a consequence, a second step was taken with WG3, resulting in the report NEA/CSNI/R(2014)13. A few years later it was decided to update that report due to the availability of new experimental data. Thus, in the current version, Section 4.10 has been updated to account for new data in the area of bubbly and boiling flow.

The objectives of the WG3 step-two activity are:

- selection of a limited number of NRS issues where extension of CFD to two-phase flow may bring real benefit;
- identification of the remaining gaps in the existing approaches for each selected NRS issue;
- review of the existing data base for validation of two-phase CFD application to the selected NRS problems; identification of needs for additional experimental validation;
- identification of a matrix of numerical benchmarks of special interest for the selected NRS problems;
- establishment of the foundation of best practice guidelines for two-phase CFD application to the selected NRS problems.

The action was carried out by the writing group WG3. Three meetings were held in the period from March 2006 to May 2007. Tasks were assigned to each group member to supply information on specific NRS issue. Information was gathered from published

literature, from international conferences and from European projects such as NURESIM of the 6th Framework Programme (FP). A close liaison was maintained with the other two CFD Writing Groups and WG3 contributed to the organisation of the CFD4NRS workshop in September 2006 and of the XCFD4NRS workshop in September 2008.

Six NRS problems where two-phase CFD may bring real benefit were selected to be further analysed in more detail:

- dry-out investigations;
- departure from nucleate boiling (DNB) investigations;
- pressurised thermal shock (PTS);
- pool heat exchanger;
- steam discharge in a pool;
- Fire analysis.

These are high priority issues from the point of view of nuclear safety with some investigations currently ongoing and their CFD investigations have a reasonable chance to be successful in a reasonable period. They address both the present generation of PWR and Boiling Water Reactor (BWR) and the generation three water reactors and address all flow regimes so that they may, to some extent, envelop many other issues.

A general multi-step methodology was applied to each issue to identify the gaps in the existing approaches. Many options are possible when using two-phase CFD, for the basic model (one-fluid, two-fluid, multi-field), for the averaging or filtering of turbulent and two-phase scales (using Reynolds Averaged Navier-Stokes (RANS), URANS, Very Large Eddy Simulation [VLES], Large Eddy Simulation [LES]), for the treatment of the interface either by an interface-tracking method (ITM) or statistically by calculating quantities such as a volume fraction or an interfacial area. The choices have to be justified after an in-depth analysis of the issue and an identification of all basic flow processes. Then closure relations have to be selected or developed for interfacial transfers, turbulent transfers and wall transfers and a validation test matrix has to be established to validate all the models in a separate-effect way. Many consistency checks are necessary to build the CFD application on a physically sound basis.

The method was applied to the six selected issues resulting in an updated state of the art, and the gaps were identified in the modelling. Available data for validation were reviewed and the needs of additional data were identified. Verification tests were also identified. A few benchmarks are proposed for future activity.

Although two-phase CFD is still not very mature, a first approach of best practice guidelines (BPG) is given which should be later complemented and updated. As a third step of the WG3 activity, additions and updates were implemented in the present document in the period 2010-2012. In Section 2, a classification of the two-phase modelling options was added. Sections 3, 4 and 5 on dry-out, DNB and PTS were updated. Section 11 was changed and includes four subsections on guidelines in the application of the multi-step methodology.

The main results of this work are summarised here:

For the six selected issues, the theoretical framework was made so clear that the selection of the basic model options was possible, even if some choices remain partly open and require further benchmarking between options. The method for modelling poly-

dispersion in boiling bubbly flow, the use of an ITM or a simpler large interface identification for free surfaces in PTS investigations are examples where further developments and comparisons are still necessary.

For each selected issue, an experimental test matrix already exists which provides very valuable information for model validation. However, in each case, there are still some deficiencies and needs were identified, requiring new “CFD-grade” experiments equipped with advanced local instrumentation. The present status of closure laws used for the selected issues reflects the merits and limits of the validation matrix. Further effort is recommended to propose a strategy of validation with a clear definition of separate-effect tests, global tests, and demonstration tests, and of their respective roles in the whole validation process.

In 2016, it was found that the list of experimental data available for boiling bubbly flow and DNB investigations of the report NEA/CSNI/R(2014)13 had to be updated. It was, then, decided to add information on new experimental data in the Section 4.10.1 on available data for DNB and to update the remaining experimental needs in Section 4.10.2.

The verification issue has to be revisited more systematically and an effort is required to define more specific 3-D benchmarks. Two ways are recommended:

- The use of the method of manufactured solutions should be promoted in two-phase CFD to produce tests with analytical solutions.
- New experiments with simple prototypic flow configurations should be produced with very well defined initial and boundary conditions and well-instrumented local measurements of possibly all principal variables.

Before having a comprehensive verification matrix, it was decided to select a benchmark test (or a few) for each NRS issue to provide at least an evaluation of the present capabilities and limitations, and to promote further progress.

The proposed multi-step methodology gives a first approach to best practice guidelines for two-phase CFD by inviting users to formulate and justify all their choices and by listing some necessary consistency checks. Some methods for the control of numerical errors are also given, as a part of the BPG.

The work performed by the writing group confirms that two-phase CFD is becoming a useful tool, complementary to system codes, for safety investigations. At this point, it cannot be used to perform system safety demonstrations to determine the safety of a plant; however, it provides insights into small-scale flow processes, and provides a better understanding of physical situations. It is already a useful tool for safety analysis and may become a tool for safety demonstration when all the steps of the methodology have been correctly addressed including uncertainty evaluation.

## 1. Introduction

The writing group WG3 on the extension of CFD to two-phase flow safety problems was formed following recommendations made at the “Exploratory meeting of experts to define an action plan on the application of CFD codes to nuclear reactor safety problems” held in Aix-en-Provence, in May 2002. Extension of CFD codes to two-phase flow is significant potentiality for the improvement of safety investigations, by giving some access to smaller scale flow processes, which were not explicitly described by present tools. Using such tools as part of a safety demonstration may bring a better understanding of physical situations, more confidence in the results, and an estimation of safety margins. The increasing computer performance allows a more extensive use of 3D modelling of two-phase thermal hydraulics with finer nodalisation. However, models are not as mature as in single-phase flow and a lot of work has still to be done on the physical modelling and numerical schemes in such two-phase CFD tools.

The writing group listed and classified the nuclear reactor safety (NRS) problems where extension of CFD to two-phase flow may bring real benefit, and classified different modelling approaches in a first report (Bestion et al., 2006). Initial ideas were reported about the specification and analysis of needs in terms of validation and verification.

It was then suggested to focus further activity on a limited number of NRS issues with a high priority and a reasonable chance to be successful in a reasonable period. The WG3-step 2 was decided with the following objectives:

- selection of a limited number of NRS issues having a high priority and for which two-phase CFD has a reasonable chance to be successful in a reasonable period of time;
- identification of the remaining gaps in the existing approaches using two-phase CFD for each selected NRS issue;
- review of the existing database for validation of two-phase CFD application to the selected NRS problems;
- identification of needs for additional experimental validation;
- identification of a matrix of numerical benchmarks of special interest for the selected NRS problems;
- foundation of the best practice guidelines for two-phase CFD application to the selected NRS problems.

This document is an extension of the first report produced by the writing group three. A few NRS problems where two-phase CFD may bring real benefit are first selected to be further analysed in more detail according to some criteria. They must be high priority issues from the point of view of nuclear safety with some investigations going on and CFD investigations must have a reasonable chance to be successful in a reasonable period. They must address both the present generation of PWR and BWR and the generation three water reactors and should possibly address all flow regimes so that they may, to some extent, envelop many other issues.

A general multi-step methodology for application of two-phase CFD to nuclear safety issues is proposed. Many options are possible when using two-phase-CFD, for the basic

model (one-fluid, two-fluid, multi-field, etc.), for the averaging or filtering of turbulent and two-phase scales (using RANS, LES, etc.), for the treatment of the interface either by an ITM or statistically by a volume fraction, an interfacial area equation, ... The choices have to be justified after an in-depth analysis of the issue and an identification of all basic flow processes. Then closure relations have to be selected or developed for interfacial transfers, turbulent transfers and wall transfers, and a test matrix has to be established to validate all the models in a separate-effect way.

The method has been applied to the selected issues resulting in an updated state of the art and gaps were identified in the modelling. Available data for validation were reviewed and needs of additional data were identified.

Verification tests were also identified. A few benchmarks are proposed for future activity.

Although two-phase CFD is still not very mature a first approach of best practice guidelines is given which should be later complemented and updated.

### **Reference**

D. Bestion, H. Anglart, B.L. Smith, J. Royen, M. Andreani, J. Mahaffy, F. Kasahara, E. Komen, P. Mühlbauer and T. Morii (2006), "Extension of CFD Codes to Two-Phase Flow Safety Problems", Technical Note, NEA/SEN/SIN/AMA(2006)2, OECD Publishing, Paris.

## 2. Methodology for the application of two-phase CFD and selection of a few nuclear reactor safety issues

### 2.1. Multi-step methodology for application of two-phase CFD to nuclear reactor issues

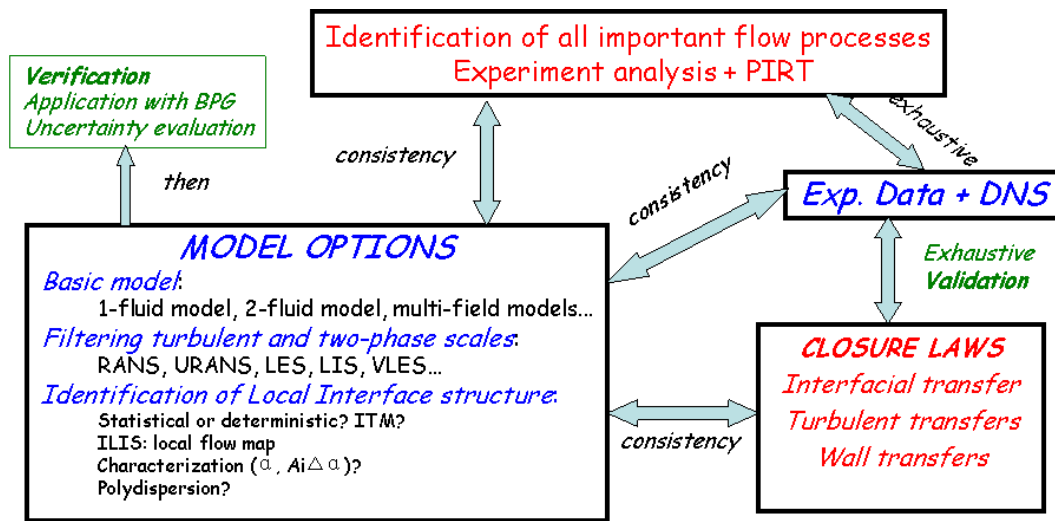
Two-phase CFD is a technology in progress, which may bring very useful new simulation capabilities but the degree of maturity is still rather low. In every new application, attention must be paid to the choice of modelling options, a modelling and validation effort is required, and a clear application methodology has to be followed to obtain reliable results. A general method of work illustrated in Figure 2.1 was proposed (Bestion et al., 2010; Bestion, 2010a) when using two-phase CFD for safety issues with successive steps:

1. Identification of all-important flow processes.
2. Main modelling choices.
  - 2.1 Selecting a basic model.
  - 2.2 Filtering turbulent scales and two-phase intermittency scales.
  - 2.3 Treatment of interfaces.
3. Selecting closure laws.
  - 3.1 Modelling interfacial transfers.
  - 3.2 Modelling turbulent transfers.
  - 3.3 Modelling wall transfers.
4. Verification.
5. Validation.

If the CFD tool is used in the context of a nuclear reactor safety demonstration, one may add a last step:

6. Uncertainty evaluation.

Figure 2.1. General methodology for two-phase CFD application to nuclear reactor safety



### 2.1.1. Identification of all-important flow processes

Any reactor issue involves complex two-phase phenomena in a complex geometry with many basic flow processes, which may play a role. The user must identify all these basic thermal-hydraulic phenomena before selecting the various code options, which are available in most two-phase CFD codes. None of the available codes can be used as a black box, which could take a complex problem and select automatically the adequate options to provide the adequate answer. These basic phenomena have to be ranked with respect to the importance in the reactor issue. This can be achieved by performing a PIRT (Process Identification and Ranking Table) analysis or by a similar approach. The preliminary analysis of some experiments simulating the problem (or part of the problem) may be of great help to identify the phenomena. Considering the inherent complexity of any two-phase flow, this identification of important processes should be revisited several times during the successive steps of the general methodology. Modelling work and validation work may change our mind on the relative importance of each phenomenon. In addition, analysis of some experimental data from the validation matrix may highlight some sensitive phenomenon, which was not identified. The methodology may then be iterative.

### 2.1.2. Modelling choices

Three choices are necessary to select the set of balance equations, which will be used for solving the problem, and they must be consistent with each other. They are related to the separation into fields, to the time and space filtering, and to the treatment of interfaces.

- *The number of fields*

Any two-phase flow may be seen as a juxtaposition of several fields and/or phases. When there is a clear criterion to identify the limits of each field (phase) at each time  $t$ , one may define the field (phase)  $k$  characteristic function  $\chi_k(x,t)$  which is one if the field  $k$  is present at position  $x$  at time  $t$  and zero if it is not present. Then local instantaneous equation for mass, momentum and energy may be multiplied by this  $\chi_k$  function before proceeding to the averaging of the equations.

Then the three balance equations for mass; momentum and energy are averaged for each field  $k$  ( $k=1, N$ -field) resulting in a set of  $3 \cdot N$ -field basic balance equations.

CFD tools offer various approaches, e.g. one-fluid homogeneous model, two-fluid model, multi-field models. A two-phase flow may be seen locally as a possible juxtaposition of a continuous liquid field, a continuous gas field, one or several dispersed gas fields (bubbles) and one or several dispersed liquid fields (droplets). The separation into several fields is particularly necessary when each field has a velocity and/or a temperature significantly different from the others. Then the most complex basic model for two-phase flow would have  $2 + N_b + N_d$  fields and  $3 \cdot (2 + N_b + N_d)$  basic balance equations,  $N_b$  being the number of bubble fields,  $N_d$  being the number of droplet fields. In many cases, it is not necessary to use such a complex model.

- *Filtering turbulent scales and two-phase intermittency scales*

The second important choice is the choice of the type of averaging or filtering of equations. The well-known two-fluid model usually makes a time averaging of equations over a period, which is high enough, compared to turbulence timescales and two-phase intermittency scales. This is fully consistent with the classical RANS equations, which are used in single-phase flow turbulence. This requires that the timescales of the mean flow of interest are significantly larger than the filtered scale by the averaging, which is not always the case.

CFD in single-phase turbulent flow also has alternative models such as URANS (Unsteady RANS), LES, or VLES when some large-scale phenomena have to be deterministically treated.

One may extend these approaches to two-phase CFD by splitting turbulent scales and two-phase intermittency scales into the larger ones, which are simulated whereas a statistical description is applied to the smaller ones.

- *Treatment of interfaces*

Two-phase flows have interfaces with a wide range of geometrical configurations. There are locally “closed interfaces” for dispersed fields, e.g. bubbles and drops, and locally open interfaces free surfaces, interface of a falling film, of a jet, etc.

A deterministic treatment of an interface predicts the position of the interface in the space as function of time and may require an ITM such as the volume of fluid (VOF), the front tracking (FT), the level set (LS), Lattice Boltzmann method (LBM) and others

A statistical approach describes the presence of interfaces through averaged parameters such as a volume fraction, an interfacial area density...

In the case of a pure statistical treatment, one may need an “Identification of the local interface structure” (ILIS) to select appropriate closure laws for the interfacial transfers. Such an ILIS is equivalent to the “flow regime map” used in 1D two-fluid models in system codes.

Three items define a local interfacial structure:

- Presence of dispersed gas field (bubbles).
- Presence of dispersed liquid field (drops).
- Presence and direction of a “large interface”.

In some cases one may combine a deterministic treatment of “large interfaces” with a statistical description of dispersed fields.

In a statistical description of interfaces, they are characterised at least by a volume fraction, but very often, additional information provided by additional equations is required for particle number density, interfacial area density, multi-group volume fractions (e.g. MUSIG method), or any other information on the particle population, probability density function (PDF) of the diameter, etc.

### ***2.1.3. Selecting closure laws***

- *Modelling interfacial transfers*

Any kind of interface may be subject to mass, momentum and energy interfacial transfer. The formulation of these transfers depends on the above modelling choices, filter scale and interface treatment.

If a “large interface” exists (such as a free surface), an adequate model may require the knowledge of the precise position of this interface, either by using an ITM or by any other method.

When an ILIS has defined the interface structure, the choice of adapted closure laws is possible.

All mass momentum and energy interfacial transfers have to be modelled and validated on available separate-effect tests (SETs). Modelling interfacial transfers is a fundamental question in two-phase flow whatever approach is used. CFD approach may make this process easier by using more local information, which allows a more mechanistic approach, but this requires that sufficient local measured data are available for development and validation.

- *Modelling turbulent transfers*

Turbulent transfers have to be modelled and validated on available separate-effect tests (SETs). The formulation of these transfers depends on the above modelling choices on the basic model, filter scale and interface treatment.

- *Modelling wall transfers*

Momentum and energy wall transfers have to be modelled (though adequate wall functions) and validated on available separate-effect tests (SETs).

### ***2.1.4. Verification***

Pure numerical benchmarks may be necessary to check the capabilities of the numerical scheme and to measure the accuracy of the resolution.

The method will be applied to each of the selected issues and gaps will be identified at every step of the method for every issue in the following sections of the report.

When such a methodology will have been applied to a large number of two-phase flow situations, precise guidelines could be given to CFD code users to select the right options appropriate for the specific application. At present, only limited foundations of such best practice guidelines will be given.

### 2.1.5. Validation

A matrix of validation tests (and possibly also of demonstration tests) has to be defined and used. Demonstration tests may be necessary to demonstrate the capability of a modelling approach to capture all the basic flow processes at least qualitatively, and validation tests including separate-effect tests and global tests are necessary to evaluate quantitatively the models for interfacial, turbulent and wall transfer terms of the equations, as far as possible in a separate-effect way. Direct numerical simulation (DNS) results may also be used to some extent as complementary to experimental validation. However, only fully validated DNS simulations may be used as “numerical experiments”.

## 2.2. Classification of the two-phase CFD modelling options

### 2.2.1. Need of a classification

Some attempts to classify the various model approaches were already proposed in the OECD-CSNI WGAMA WG3 reports (2006, 2010). It was presented in detail at CFD4NRS-3 (Bestion, 2010a) and in several papers (Bestion, 2010b, 2010c, 2011a, 2011b). The classification was based on the following aspects:

- Phase averaging or field averaging:
  - homogeneous for a two-phase mixture;
  - two-fluid model;
  - multi-field models.
- Filtering turbulent scales and two-phase intermittency scales:
  - all turbulent scales are filtered (RANS models);
  - only some scales are filtered (two-phase LES);
  - all turbulent scales are simulated (DNS).
- Treatment of interfaces:
  - Use of Interface-Tracking/Capturing Technique;
  - Use of a pure statistical treatment of interfaces;
  - Use of an ILIS;
  - Characterisation of the interfaces through Interfacial area density or other quantities.

However, one would prefer a classification which shows the successive choices with the arborescence of all possible resulting approaches. One may try to give a more detailed classification by considering (see Table 2.1) all treatments of the basic local instantaneous equations for mass (continuity equation), momentum (Navier-Stokes equation), and energy, which are used in the various Eulerian modelling approaches. The selection of the respective approaches can be made by considering five successive choices:

1. Open medium approach or homogenising technique for porous body? Is there a multiplication of basic equations by a fluid characteristic function?

2. How many fields are distinguished? Is there a multiplication of basic equations by a phase characteristic function or field characteristic function?
3. Time averaging or ensemble averaging?
4. Space averaging or filtering.
5. Deterministic interface, filtered interface or statistical interface?

### 2.2.2. Open medium approach and porous body approach

One may distinguish the open medium and porous medium approaches. A simple way to introduce these differences is to consider that local instantaneous equations are first multiplied by fluid/solid characteristic function before any averaging or filtering.

Let  $\chi_f(x,t)$  be the fluid/solid characteristic function

$$\chi_f(x,t) = 1 \text{ when point } x \text{ is in the fluid at time } t$$

$$\chi_f(x,t) = 0 \text{ when point } x \text{ is in the solid at time } t$$

In case of a flow bounded by non-deformable solid structures,  $\chi_f$  is not function of time.

A volume average of  $A$  is defined as:

$$\langle A \rangle(x,t) \cong \frac{1}{V(x)} \int_{V(x)} A(y,t) dV(y)$$

A volume average of  $\chi_f$  is the so-called porosity factor:

$$\phi \cong \langle \chi_f \rangle = \frac{V_f}{V}$$

In the classical porous body approach, after multiplication by  $\chi_f$ , equations are averaged over a fluid volume as follows:

$$\langle A \rangle_f(x,t) \cong \frac{\langle \chi_f A \rangle}{\langle \chi_f \rangle} = \frac{1}{V_f(x)} \int_{V_f(x)} A \chi_f dV$$

Then every local fluid parameter  $A$  may be considered as an average plus a space deviation:

$$A \cong \langle A \rangle_f + \delta A$$

### 2.2.3. The number of fluids or fields

One can separate the two-phase flow in several fields:

- 1-fluid for a model, which considers a mixture of the two phases together;
- 2-fluid for a model, which considers the two phases separately;
- N-field for a model, which splits one or both phases in several fields.

Multi-field models are commonly on the type  $2+nb+nd$  with two continuous fields (continuous gas and continuous liquid) + one or  $nb$  bubble fields and one or  $nd$  droplet fields.

The way to introduce these differences is to consider that local instantaneous equations are multiplied by fluid/field characteristic function before any averaging or filtering.

Let  $\chi_k(x,t)$  be the fluid characteristic function for phase  $k$  or field  $k$  ( $k=1,n$ )

$\chi_k(x,t) = 1$  when point  $x$  is in the phase  $k$  or field  $k$  at time  $t$

$\chi_k(x,t) = 0$  when point  $x$  is not in the phase  $k$  or field  $k$  at time  $t$

One can multiply also by the product  $\chi_k \cdot \chi_f$  for a multi-field model in a porous body approach.

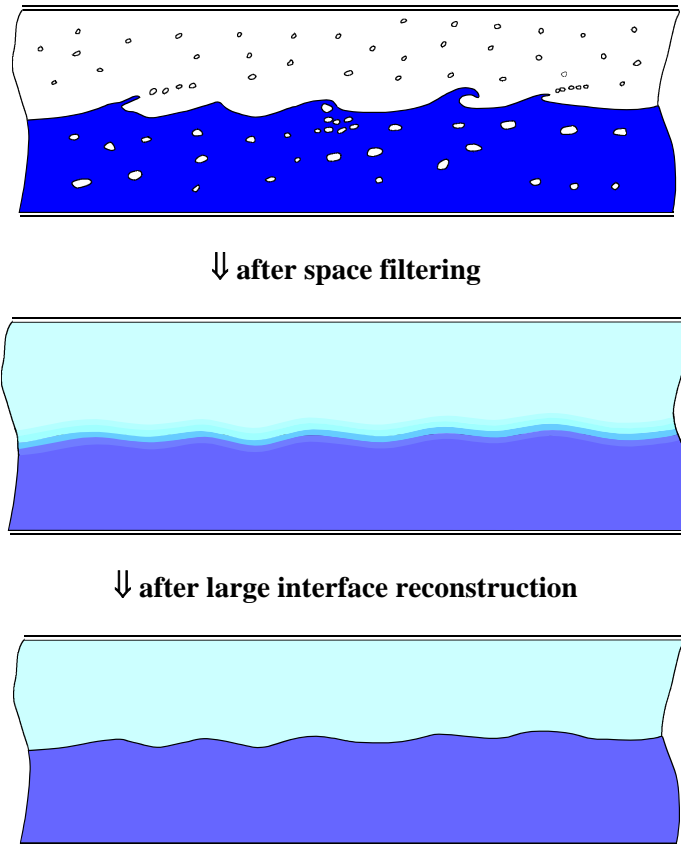
After averaging of the basic equations multiplied by  $\chi_f$ , or  $\chi_k \cdot \chi_f$  for  $k = 1, n$ , the three balance equations (mass, momentum and energy) are written  $n$  times one for each phase or field.

#### ***2.2.4. Time averaging and space averaging***

Time or ensemble averaging is a common way to derive equations for the so-called RANS approach. Although time averaging and ensemble averaging are different, they can be reasonably considered as equivalent (ergodicity) in steady or quasi-steady flows where the RANS approach is applied.

Time averaging filters all turbulent scales and predicts only a mean velocity field. Time averaging does not allow for the prediction of the space and time position of the interfaces of dispersed droplets and dispersed bubbles. It has also a smearing or diffusive effect on the large interfaces between continuous liquid-and continuous gas such as a free surface or the surface of a liquid film along a wall. It is possible to reconstruct a steep large interface by numerical techniques (see Lucas et al., 2009) but waves have disappeared as shown in Figure 2.2.

**Figure 2.2. Loss of information on the structure of a complex stratified flow associated to the application of a space filter. The initial flow structure at the top is simplified as shown in the centre. A reconstruction of a “filtered large interface” is possible as shown at the bottom**

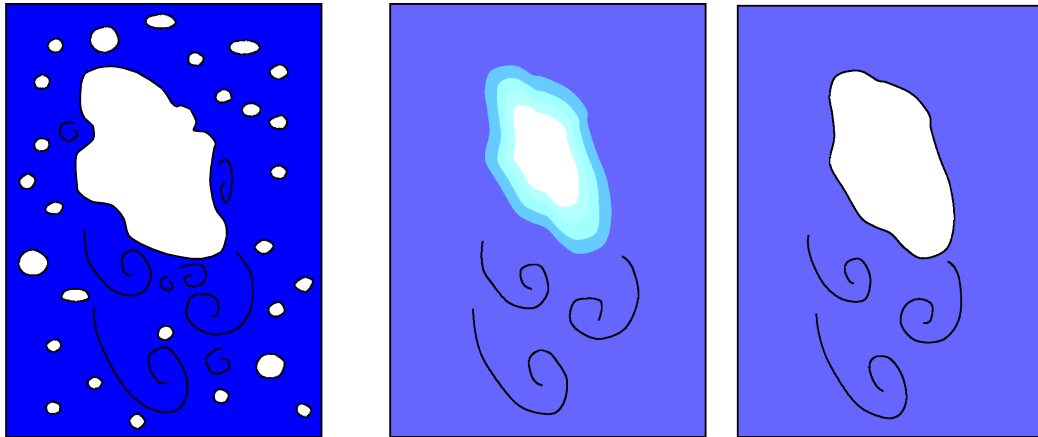


Space averaging is necessary in the porous body approach after having multiplied equations by the fluid/solid characteristic function and possibly also by the fluid (or field) characteristic function.

Space averaging or filtering is also used in the so-called LES of turbulent flow in an open medium context. This technique becomes now increasingly applied in single-phase CFD to be able to simulate some transient flow or to predict large-scale coherent turbulent structures. The filter scale defines the part of the turbulence spectrum, which is simulated and the part, which must be modelled.

Space averaging in two-phase flow filters not only the small eddies but also the interfaces and the density discontinuity is smeared or diffused and replaced by a surface local density gradient. It is possible to reconstruct a steep interface by numerical techniques but small-scale deformations of the interface may have disappeared as shown in Figure 2.3.

**Figure 2.3. Loss of information on the structure of a complex churn flow associated to the application of a space filter. The initial flow structure on the left is simplified as shown in the centre. A reconstruction of a “filtered large interface” is possible as shown on the right**



As advised by European research community on flow, turbulence and combustion (ERCOFTAC) (2008), care should be taken when combining the two-fluid model with the LES for the continuous phase, and the consistence of the governing equation averaging with the LES filtering and sub-grid modelling (particularly the role of grid size) should be checked.

### 2.2.5. *Deterministic interface, filtered interface or statistical interface*

An interface will be said, “**deterministically treated**” when its space and time position is simulated or actually predicted without any simplification. It is clearly the case of a “pseudo-DNS” modelling where neither space nor time averaging is used. The flow on the left on Figure 2.3 is predicted with all eddies and all small deformations of the interface. In single-phase flow, DNS solves exact local instantaneous equations without any physical closure. In two-phase flow, pseudo-DNS methods using an ITM need some closure laws for some very small-scale phenomena such as a film-splitting during a coalescence event. The term “pseudo-DNS” is used to keep in mind that this approach is not as pure as in single-phase DNS.

An interface can also be considered as “deterministically treated” after a space filtering if the reconstructed interface (see Figure 2.3) is not degraded compared to the real interface. A “deterministic interface” requires that all phenomena having an influence on the space and time position of the interface are also simulated. The conditions for this are specified below in the section on LES with deterministic interfaces.

An interface will be said “**statistically treated**” when an averaging or filtering procedure does not allow to predicting its space and time position. Only statistical or averaged information on several interfaces may be predicted through quantities such as a void-fraction, or an interfacial area density. Such a statistical treatment may result either from time averaging or from space averaging.

An interface will be considered as “**filtered interface**” when its space and time position is predicted with some filtering of the smaller scale deformations. Cases illustrated in Figures 2.2 and 2.3 are filtered interfaces. This filtering may result either from space filter or from time averaging.

### 2.2.6. A possible terminology for Eulerian Two-phase CFD approaches

Following the five choices above, one may propose a terminology for Eulerian two-phase CFD approaches.

The nomenclature is a series of four groups of characters: **M . T . I . n**

**M characterises the space averaging or filtering or integration**; it can be:

- O: 3D open medium (no space averaging).
- P: 3D porous medium (space filtering).
- S2: space-averaged 2D (integrated over one space dimension resulting in a 2-D model).
- S1: space-averaged 1D (integrated over two space dimensions resulting in a 1-D model).
- S0: volume-averaged 0D or lumped-parameter model (integrated over three space dimensions resulting in a 0-D model).

S2 does not apply to 2D models, which use some symmetry in a 3D flow to reduce the dimension to two. It applies, e.g. to a 2D modelling of an annular down-comer of a reactor vessel when equations are averaged over the radial direction, keeping a 2D problem in vertical and azimuthal directions ( $Z, \theta$ ).

- **T to characterise the filtering of turbulent scale:**
  - **D** for direct simulation of the whole turbulence spectrum.
  - **R** for Reynolds average approach.
  - **F** for filtered turbulence like LES, DES, etc.
- **I to characterise the treatment of interfaces:**
  - **D** for deterministic interface or simulated interface using an interface-tracking technique.
  - **S** for statistical treatment of interfaces.
  - **F** for filtered interfaces: an interface-tracking or reconstruction technique is used but it does not predict smaller scale deformations of this interface.
  - **FS** for hybrid methods where the larger scale interfaces are known by an interface-tracking or reconstruction technique and the smaller scale interfaces are only statistically treated.
- **n is the number of fluids or fields:**
  - **One** for the classical one-fluid approach, e.g. homogeneous model.
  - **Two** for the classical two-fluid approach.
  - **N for a n-field model.**

**Table 2.1. Time and space resolution in the various modelling approaches of two-phase CFD**

		Open medium					Porous medium
Time & space filtering		No filter No averaging	Space filtering			Time averaging	Time averaging
<b>Turbulence</b>	DNS LES VLES RANS, URANS	DNS	LES	LES VLES	LES VLES	RANS, URANS	RANS, URANS
<b>Interfaces</b>	Simulated Filtered Statistical	Simulated	Simulated	Filtered & Statistical	Statistical	(Filtered) Statistical	Statistical
<b>Nb of fields</b>	1-F 2-F n-F	1-F	1-F	1-F 2-F n-F	1-F 2-F n-F	1-F 2-F n-F	
<b>Type of models</b>		O.D.D.1  Pseudo  DNS	O.F.D.1  LES  with simulated interfaces	O.F.FS.2 O.F.FS.n  Hybrid LES  with filtered & statistical interfaces	O.F.S.2 O.F.S.n  LES  with statistical interfaces	O.R.FS.2 O.R.FS.n  RANS URANS  statistical interfaces	P.R.S.2 P.R.S.n  Porous medium approach  statistical interfaces

### ***2.2.7. The pseudo-DNS approach***

The pseudo-DNS does not apply any space or time averaging of the equations. However, some additional equation or numerical treatment is required to track the interface and to add the physics of the liquid-solid interface or of a triple line (liquid-solid-gas). There is no need to solve equations for several fields and a one-fluid approach is generally used with some additional equation or technique to track the interface position. Additional models are often required for example for implementing a film-splitting criterion when two bubbles coalesce or for the contact angles at a triple line solid-liquid-gas. Such additional models are the reason why in two-phase flow the word DNS must be replaced by pseudo-DNS since some very small-scale physics is not solved but only modelled.

Since no averaging or filtering is used, pseudo-DNS should be able to predict the smaller scale eddies (up to the Kolmogorov dissipative scale), the smaller scale interface deformations and smaller scale distance between interfaces. This would be extremely difficult for liquid films between two bubbles when they collide before coalescence since it would require mesh sizes in the order of the micrometre. Therefore, such very thin films are often not predicted to allow larger mesh sizes. It may affect the prediction of some phenomena such as coalescence or breakup phenomena but one may still consider that such extension still belongs to the pseudo-DNS approach.

Pure DNS resolving only exact equations without any modelling does not exist in two-phase flow and pseudo-DNS techniques also have to be validated against experimental data to see how the models and the simplifications affect the predictions.

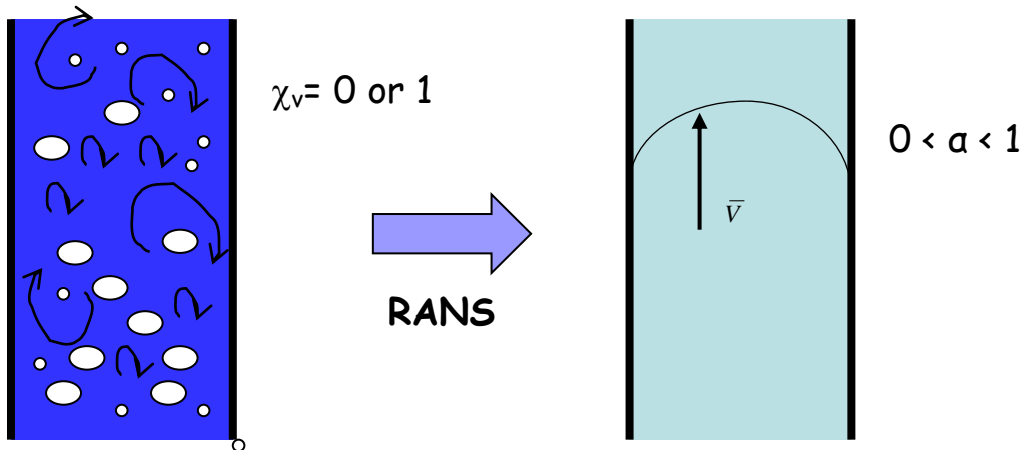
Since even pseudo-DNS require extremely expensive CPU cost, its use is restricted to the investigation of very small-scale flow processes as a complement to experimental investigations and as a support for the modelling and validation of more macroscopic approaches.

### ***2.2.8. The RANS approach***

This is the simplest, the cheapest (in terms of CPU), the most advanced, and the most used available two-phase CFD method. The RANS approach for two-phase flow consists in applying an ensemble averaging or a time averaging which filters all turbulent scales and all two-phase intermittency scales. The method is applied to steady flows or quasi-steady flows when the timescales of variation of mean variables are larger than the largest timescales of turbulence and two-phase intermittency.

The Figure 2.4 below illustrates how a two-phase flow is simplified by a RANS like approach.

Figure 2.4. Illustration how a RANS like approach simplifies a two-phase flow



No velocity fluctuation is predicted and only time-averaged velocities are solved. The presence of interfaces is treated statistically by averaged parameters such as the void-fraction or the interfacial area density.

#### Compatibility of RANS with flow regimes

RANS is in principle compatible with all two-phase flow regimes provided that they are steady or quasi-steady. The condition is that the time scale of mean flow variations is significantly larger than the timescales of turbulence and two-phase intermittency (time between passage of two interfaces at a given point). Depending on the flow regime, the RANS procedure may induce some loss of information on the flow structure:

- For dispersed-bubbly flow (see Bestion et al., 2009) or dispersed-droplet flow, the condition is easy to satisfy.
- For separate-phase flows (stratified flow, annular flow), the averaging procedure filters interfacial waves in a way which is not fully clear: although the modelling of turbulent diffusion prevents simulation of large eddies, it does not prevent irrotational waves to be predicted resulting from Kelvin-Helmholtz instability.
- for slug and churn flow regimes with large bubbles (either Taylor bubbles in slug flows or distorted large bubbles in churn flow) the intermittency due to the passage of these bubbles corresponds to rather large timescales; since the RANS filters even these large-scales it is unable to predict this intermittency.

#### Compatibility of RANS with the number of fields

RANS is compatible with all the possible choices for the number of fields, including single-fluid, two-fluid and all kinds of multi-field models.

#### Compatibility of RANS with interface treatments

Due to the time (or ensemble) averaging, RANS is not compatible with a deterministic treatment of interfaces since interface movements and deformations are influenced by eddies which are not simulated by the RANS approach.

RANS is fully compatible with the statistical treatment of interfaces.

RANS is also compatible with some “filtered interface” for some large interfaces as shown in Figure 2.2 with a free surface, which is parallel to the mean flow velocity (Coste et al. 2008).

### 2.2.9. The LES with deterministic interfaces

The LES with deterministic interface (O.F.D.1) combines a filtering of turbulent fluctuations with an ITM used for all interfaces. This method was developed and used by Bois et al (2010), Toutant et al. (2009a, 2009b), Magdeleine (2010), Lakehal (2008a, 2008b), in both dispersed flow and free surface flow.

A “deterministic interface” requires that all phenomena having an influence on space and time position of the interface are also simulated. The smaller scale deformations of the interfaces are influenced by the turbulent fluctuations and the surface tension.

A limiting value of a Weber number should define the limits of applicability of LES together with a deterministic interface.

$$We = \frac{\rho v(l)^2 l}{\sigma} \leq We_{\text{lim}}$$

$v(l)$  is the velocity scale of turbulent fluctuations for eddies of size equal to  $l$ .

For a given turbulence spectrum it may give a maximum value of the filter scale  $l_{\text{filter}}$ :

$$l_{\text{filter}} \leq We_{\text{lim}} \frac{\sigma v(l_{\text{filter}})^2}{\rho}$$

For a given filter scale  $l_{\text{filter}}$  the maximum value of the turbulent fluctuating velocity  $v(l)$  at scale  $l_{\text{filter}}$  is:

$$v(l_{\text{filter}}) \leq \sqrt{We_{\text{lim}} \frac{\sigma}{\rho l_{\text{filter}}}}$$

Another limit, which is often less restrictive, is related to the Laplace scale:

$$l_{\text{filter}} \leq \frac{1}{n} \sqrt{\frac{\sigma}{g \Delta \rho}}$$

The Laplace scale is related to the smallest wavelength of free surface waves (capillary waves) or film waves when there is no high turbulence intensity. The required value of  $n$  (probably in the range five to ten) should be determined.

Finally, if there are very small bubbles much smaller than the Laplace scale, e.g. in boiling flow, the filter scale should allow a good description of the interfaces of these smallest bubbles of diameter  $d_{\text{min}}$ , which results in a severe limitation:

$$l_{\text{filter}} \leq \frac{1}{m} d_{\text{min}}$$

According to Magdeleine (2010),  $m$  can be taken as six at best without degrading the results.

All these limitations make this “LES with deterministic interface” method less CPU consuming than pseudo-DNS (up to one or two orders of magnitude) but still rather expensive. It is still used as a research tool as a support for the modelling and validation of more macroscopic approaches and cannot address a real industrial-scale problem.

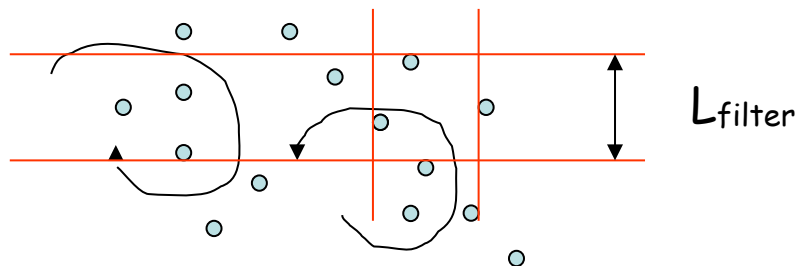
### 2.2.10. The LES with statistical interfaces

When the largest two-phase intermittency scale is rather small and significantly smaller than the largest turbulent eddies (see Figure 2.5), a LES method is applicable with a smaller filter scale than the large eddies but larger than the two-phase scale to allow a statistical treatment of interfaces (O.F.S.2 or O.F.S.n). This was already applied with some success to some turbulent dispersed flow by Dhotre et al. (2007) and Ničeno et al. (2009).

These authors have applied the so-called Milleli criterion about the smallest  $l_{filter}$  scale,  $d_{min}$  being the smallest bubble or droplet size.

$$l_{filter} > 1.5 d_{min}$$

**Figure 2.5. A dispersed flow treated by a LES with statistical interfaces**



Such a method is clearly much less CPU consuming than the pseudo-DNS and the LES with deterministic interface but it is restricted to some flow situations, typically the dispersed bubble or dispersed drops where the large eddies are much larger than the largest bubbles or eddies. In slug or churn flow where the largest bubbles and the largest eddies are of the size of the geometrical dimensions of the flow (such as a hydraulic diameter) this method is clearly not applicable.

This method is compatible with the two-fluid model and multi-field models where size groups may treat the dispersed bubbles or droplets.

### 2.2.11. The hybrid LES method with both filtered and statistical interfaces

Looking for a method, which may address all flow regimes with a more reasonable CPU cost than the pseudo-DNS and the LES methods above, one may imagine a hybrid method, which filters the smaller eddies and treats statistically the small droplets or bubbles while the other interfaces are simply filtered (O.F.FS.2). This is illustrated in Figure 2.3. The space filter eliminates the smaller bubbles, which are treated statistically, and it thickens and filters the interface of the large bubble, which may be reconstructed with a simplification of the shape as shown on the right side view.

Although this method has not been clearly defined and applied, some analyses with a two-fluid model without any turbulence model may be somewhat similar to it (Bartosiewicz et al., 2007, 2008).

It may be a promising way of modelling the most complex two-phase flow (such as churn or slug flow) at a reasonable CPU cost without filtering the two-phase structures like RANS does. However, the closure issue is rather complex and the present state of the art is not very well advanced.

This method is compatible with the two-fluid approach and with multi-field models. A four-field model with a continuous gas field, a continuous liquid field, a dispersed bubble field and dispersed-droplet field may help to reconstruct the large filtered interfaces.

### ***2.2.12. The CFD in porous medium approach***

The CFD in porous medium approach (P.R.S.2 or P.R.S.n) uses a space averaging or filtering of time-averaged basic equations multiplied by  $\chi_f$  or by the product  $\chi_k \cdot \chi_f$  as defined in Section 2.2.2 above. It is adapted to the macroscopic 3D description of two-phase flow in reactor components such as the core or the steam generator. The minimum filter scale in such components is the sub-channel scale. This approach is used with some simplifying assumptions in the component codes for core and SGs.

Due to the time, averaging, additional terms such as Reynolds stresses  $\overline{u'_i u'_j}$  or turbulent diffusion of heat  $\overline{u'_i \theta'}$  appear in balance equations. Due to space filtering, dispersion terms of momentum and energy (related to  $\langle \delta u_i \delta u_j \rangle$  and  $\langle \delta u_i \delta \theta \rangle$ ) appear in the equations which would require some modelling.

In the present state of the art, no modelling of dispersion terms exists and only very simple turbulent diffusion models are used.

This method is compatible with the single-fluid model, the two-fluid model, and any kind of multi-field model. In the nuclear community, the most complex models are using the three-field model with a gas field, a continuous liquid field, and a droplet field, which is adequate for annular-mist flow.

### ***2.2.13. Classification of dispersed flow modelling approaches made by ERCOFTAC***

The CFD modelling and simulation of dispersed flows (although limited to adiabatic conditions) is addressed in the ERCOFTAC best practice document (ERCOFTAC, 2008). There the disperse flows are first classified depending on the various possible combinations of carrier (continuous) and dispersed phase, such as gas/solid, liquid/solid, liquid/droplet (case of immiscible fluids), gas/droplet, liquid/gas. All of those configurations can be encountered in other nuclear plant related situations, the last two being particularly relevant to the issues selected for the present report.

Another useful criterion for the classification of dispersed flows is whether they are “dense” or “diluted”, with reference to the spacing between particles. If the spacing is relatively small (i.e. less than ten times the particle diameter) then the dispersed phase, flow is dominated by the interactions (e.g. collisions) between particles, which combined with the interaction between phases lead to a so-called “four-way coupling” regime. When on the other hand the spacing if the dispersed phase is relatively large, the inter-particle interactions play a negligible role and a “two-way coupling” regime occurs. If the dispersed phase is sufficiently diluted (average distance over particle diameter ratio  $\approx 80$ ) then its influence on the carrier flow becomes negligible as well, and the resulting regime can be regarded as a “one-way coupling”. The degree of coupling strongly affects the requirements

in terms of modelling; this aspect is further discussed in the following sections when bubbly flows are addressed.

The ERCOFTAC document indicates the following modelling approaches for the simulation of dispersed flows:

- DNS.
- Discrete particle modelling (DPM).
- Eulerian-Lagrangian.
- Eulerian-Eulerian.

The present report mainly focuses on the last two approaches, also referred to as particle tracking and two-fluid methods. They are more popular and less computationally expensive, although still challenging as concerns the accurate and reliable modelling of turbulence, inter-phase transfers and particle interactions.

The two-fluid model, in its classical formulations, exhibits mathematical ill-posedness due to the non-hyperbolic nature of the equation system (Dinh et al., 2003), which can lead to instability problems. Several numerical artifices or alternate methods have been proposed and adopted to cope with the ill-posedness; however, it is necessary to be aware of the problem and place even stronger emphasis on the need of comprehensive validation for specific applications.

DNS (called pseudo-DNS here above) aims at resolving the particles and the flow around them (i.e. the micro-scales referred to in the following) and tracking the interfaces. Its computational costs are usually prohibitive, but its capabilities are promising, also because it could provide more insight into basic phenomena (e.g. boiling crisis) and closure relations for higher-scale modelling approaches.

DPM is another promising method that aims at resolving the discrete particle flow by a “granular dynamics simulation” approach. It is also computationally expensive and relatively less developed than the methods based on averaging, and, like the DNS, may be a tool for calibrating closure relations.

### 2.3. Selection of a limited number of nuclear safety issues

#### 2.3.1. Selection criteria

A limited number of issues for which two-phase CFD has a reasonable chance to be successful in a reasonable period were selected according to the following criteria:

- *High priority issues*: the selected issues should be considered as high priority from the point of view of nuclear safety. The existence of some ongoing investigations in the industry or research projects related to these issues was also considered.
- *Chance to be successful*: only issues having a reasonable chance to be successful in a reasonable period have been selected, this reasonable period being about five years. It depends in particular on the maturity of present numerical tools to handle the issue. The ranking of issues performed in the previous report (Bestion et al., 2006) was used in this selection. “high” maturity was applied to the case in which sufficient information was available, all related phenomena were well identified, and models were developed for each phenomenon, improvements being welcome for some of them. “medium” maturity was applied when a publicised background exists, most basic phenomena are supposed to be well identified, and some models

exist which require improvements and validation. “Low” maturity was applied to the case in which no trusted information was available on the validity of existing models. Only “high” maturity and “medium” maturity issues were considered.

- *Availability of data:* only issues for which some data sources are available to allow a validation of the physical models were considered. CFD-grade data with a high density of local measurements are often necessary for a validation of the physical models in a “separate-effect” way. More global experimental data, with mixed effects, are also required to check the consistency of the whole model.
- *Covering all water reactors:* the selected list of issues should address both present generation of PWR and BWR and the advanced (generation three) water reactors including passive reactors.
- *Covering all flow regimes:* the selected list of issues should cover all flow configurations (dispersed-bubbly, dispersed-droplet flow, free surface flow, etc.) so that they may, to some extent, envelop many other issues.

Remark: After review of the state of the art for each selected issue, it appears that a period of five years may be largely optimistic, first for getting a credible and numerically operational physical CFD type modelling, secondly for getting the necessary missing detailed experimental data and finally for incorporating the experimental findings in the models.

### ***2.3.2 The selected issues***

The issues about Critical Heat-Flux (CHF) (both DNB and dry-out) and PTS were investigated in the NURESIM integrated project of the 6<sup>th</sup> Framework Programme where 14 partners (CEA, EDF, FZD, GRS, Paul Scherrer Institute (PSI), ASCOMP, KTH, University of Pisa, JSI, LUT, VTT, UCL, KFKI, NRI) are using and developing two-phase CFD.

PWRs are clearly concerned with DNB and PTS issues; BWRs are clearly concerned with dry-out and “steam discharge in a pool”, whereas “pool heat exchanger” and “steam discharge in a pool” are important issues for all advanced passive reactors.

The opportunity of selecting the issue about “containment thermal-hydraulics” was discussed. This topic will not be treated here in order to avoid overlapping with other GAMA activities.

The opportunity of selecting the issue about re-flooding was also discussed. Although this is a very old issue, the present simulation tools (the system codes) will appear very old fashioned in one, two or three decades in comparison to what will exist in the CFD world. First attempts to use CFD should be made at least to attract some young scientists and to keep some expertise on this important accidental sequence. However due to the lack of an experiment having enough local measured data, the issue was not selected.

Fire analysis is the only considered issue which is not dealing with steam-water flows and it belongs to a rather different domain from the others. However, it was found that CFD investigations of fires and of the steam-water issues encountered very similar difficulties and have many common features.

Six issues have been finally selected for detailed study:

- dry-out investigations;
- DNB investigations;

- PTS;
- pool heat exchanger;
- steam discharge in a pool;
- fire analysis.

Looking at all possible local interface configurations of two-phase flows, there are a limited number of possibilities:

- dispersed bubbles in a continuous liquid;
- dispersed droplets or particles in a continuous gas-phase;
- separate-phase flow at the vicinity of the interface such as a free surface in a stratified flow or a surface of a liquid film; in both cases there are only two continuous fields;
- presence of two continuous fields and two dispersed fields; this is the case of a stratified flow when droplets are above the liquid surface and bubbles below, a situation which may be found when there are waves with droplets entrained at the wave crests and when breaking waves are trapping bubbles below the free surface.

Looking at all possible heat transfers, there may be heating walls, cooling walls, vaporisation or condensation, and heat sources due to chemical reactions.

Bubbly flows are encountered in DNB investigations and in pool heat exchangers, droplet flows and particle flows in dry-out investigations and fire analyses, free surfaces are encountered in PTS and pool heat exchangers, liquid films are encountered in dry-out investigations. Heating walls and vaporisation are present in both DNB and dry-out investigations, condensation in PTS and steam discharge in a pool. A free surface with bubbles below the surface is found in pool heat exchangers and at emergency core-cooling (ECC) injection when investigating PTS. The most complex situation with two continuous fields and two dispersed fields is not present in the selected issues. Considering the relative low maturity of two-phase CFD tools, it is expected that the selected five issues give the opportunity to cover many flow configurations, leaving aside only the most complex situations.

## References

Bartosiewicz, Y., J. Laviéville and J.M. Seynhaeve (2007), "A Validation Case for the NEPTUNE\_CFD Platform: Instabilities in a Stratified Flow. Experimental, Theoretical and Code to Code Comparisons", *NURETH-12*, Pittsburgh, Pennsylvania, United States, 30 September-4 October 2007.

Bartosiewicz, Y., J.-M Laviéville and J.-M Seynhaev (2008), "A first Assessment of the NEPTUNE\_CFD code: Instabilities in a Stratified Flow, Comparison between the VOF Method and a Two-Field Approach", *International Journal of Heat and Fluid Flow*, vol. 29, pp. 460-478.

Bestion, D., H. Anglart, B.L. Smith, J. Royen, M. Andreani, J. Mahaffy, F. Kasahara, E. Komen, P. Mühlbauer and T. Morii (2006), *Extension of CFD Codes to Two-Phase Flow Safety Problems*, Technical Note, NEA/SEN/SIN/AMA(2006)2, OECD Publishing, Paris.

Bestion, D., H. Anglart, D. Caraghiaur, P. Péturaud, B. Smith, M. Andreani, B. Ničeno, E. Krepper, D. Lucas, F. Moretti, M. C. Galassi, J. Macek, L. Vyskocil, B. Končar, and G. Hazi (2009), Review of Available Data for Validation of NURESIM Two-Phase CFD Software Applied to CHF Investigations, *Science and Technology of Nuclear Installations*, Volume 2009 (2009), Article ID 214512.

Bestion, D., H. Anglart, J. Mahaffy, D. Lucas, C.H. Song, M. Scheuerer, G. Zigh, M. Andreani, F. Kasahara, M. Heitsch, E. Komen, F. Moretti, T. Morii, P. Mühlbauer, B.L. Smith, T. Watanabe (2010), “Extension of CFD Codes to Two-Phase Flow Safety Problems”, NEA/CSNI/R(2010)2, OECD Publishing, Paris, [https://oecd-nea.org/jcms/pl\\_18898](https://oecd-nea.org/jcms/pl_18898).

Bestion, D. (2010a), Applicability of two-phase CFD to nuclear reactor thermal-hydraulics and elaboration of best practice guidelines, presented at CFD4NRS-3, Washington, sept 2010, accepted for publication in *Nuclear Engineering and Design*, 2011.

Bestion, D. (2010b), Extension of CFD Code application to Two-Phase Flow Safety Problems, *Nuclear Engineering and Technology*, VOL.42 NO.4 August 2010.

Bestion, D. (2010c), From the DNS to system codes – Perspective for the Multi-scale analysis of light water reactor (LWR) Thermal-hydraulics, *Nuclear Engineering and Technology*, VOL.42, NO.6, December 2010.

Bestion, D., P. Coste, B. Ničeno and S. Mimouni (2011a), Two-phase CFD: the various approaches and their applicability to each flow regime, *Multi-phase Science and Technology*, Volume 23, Issue 2-4.

Bestion, D. (2011b), Status and perspective for a multiscale approach to LWR thermal-hydraulic simulation, NURETH-14, Toronto, Ontario, Canada, 25-30 September 2011, to be published in a topical issue of *Nuclear Engineering and Design*, 2012.

Bois, G., D. Jamet and O. Lebaigue (2010), “Towards LES of two-phase flow with phase-change: DNS of a pseudo-turbulent two-phase condensing flow”, 7th International Conference on Multi-phase Flow, ICMF 2010, Tampa, FL, United States, 30 May-4 June 2010.

Coste, P., J. Pouvreau, J. Laviéville and M. Boucker (2008), Status of a two-phase CFD approach to the PTS issue, XCFD4NRS, 10-12 September 2008, Grenoble, France.

Dhotre, M.T., B. Smith and B. Ničeno (2007), “CFD Simulation of Bubbly Flows: Random Dispersion Model”, *Chem. Eng. Sci.*, 62, 7140-7150.

Dinh, T.N., R. R. Nougaliév and T. G. Theofanous (2003), Understanding the ill-posed two-fluid model, The 10th International Topical Meeting on Nuclear Reactor Thermal-Hydraulics (NURETH-10), Seoul, Korea, 5-9 October 2003.

ERCOFTAC (2008), Best practice guidelines for computational fluid dynamics of dispersed multi-phase flows, edited by M. Sommerfeld, B. van Wachem, R. Oliemans, Version 1, October 2008.

Lakehal, D. (2008a), “Large eddy and interface simulation (LEIS) for the Prediction of Turbulent Multi-fluid Flows Applied to Thermal-Hydraulics Applications”, XFD4NRS, Grenoble, 10-12 September 2008.

Lakehal, D., M. Fulgosi, S. Banerjee and G. Yadigaroglu (2008b), “Turbulence and heat-transfer in condensing vapour-liquid flow”, *Phys. Fluids*, 20, 065101.

Liovic, P. and D. Lakehal (2007a), "Interface-turbulence interactions in large-scale bubbling processes", *International Journal of Heat and Fluid Flow*, vol. 28, pp. 127-144.

Liovic, P. and D. Lakehal (2007b), "Multi-physics treatment in the vicinity of arbitrarily deformable gas-liquid interfaces", *Journal of Computational Physics*, vol. 222, no. 2, pp. 504-535.

Magdeleine, S., B. Mathieu, O. Lebaigue and C. Morel (2010), "DNS up-scaling applied to volumetric interfacial area transport equation, 12 p., 7th International Conference on Multi-phase Flow", ICMF 2010, Tampa, FL, United States, 30 May-4 June 2010.

Ničeno, B., M. Boucker, and B. L. Smith (2009), "Euler-Euler LES of a Square Cross-Sectional Bubble Column Using the Neptune\_CFD Code", *STNI*, Volume 2009, Article ID 410272.

Toutant, A., M. Chandesris, D. Jamet and O. Lebaigue (2009), "Jump conditions for filtered quantities at an under resolved interface. Part 1: theoretical development", *Int. J. Multi-phase Flow*, Vol. 35, No. 12, pp. 1100-1118, December 2009.

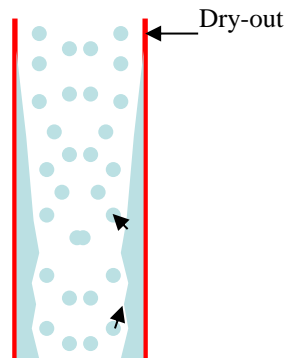
Toutant, A., M. Chandesris, D. Jamet and O. Lebaigue (2009), "Jump conditions for filtered quantities at an under resolved interface. Part 2: a priori tests", *Int. J. Multi-phase Flow*, Vol. 35, No. 12, pp. 1119-1129, December 2009b.

### 3. The dry-out investigations

#### 3.1. Definition of the dry-out issue and identification of all-important flow processes

One of the major limiting factors in the safe operation of BWRs is the occurrence of dry-out, which manifests itself with breakup or disappearance of the liquid film in adiabatic annular two-phase flows. Due to dry-out, the heat-transfer between cladding and coolant is significantly deteriorated and, as a result, the cladding temperature rapidly increases. This, in turn, can cause damage to the cladding and can lead to a release of fission products to the coolant. Figure 3.1 shows a typical configuration of annular flow in a heated channel. The liquid phase exists as a liquid film, which is attached to walls, and as droplets, which are carried in the central part of the channel by the vapour phase. The mass flow rate in the liquid film is changing due to several mass transfer mechanisms. Due to hydrodynamic forces acting on the liquid film surface, a certain amount of liquid from the liquid film is entrained into the vapour core as droplets. The entrainment rate of droplets from the liquid film is usually expressed in units of  $\text{kg}/\text{m}^2/\text{s}$ , which corresponds to the mass of liquid entrained from a unit film surface in a unit time interval. Clearly, the liquid film is depleted due to the drop entrainment. Another mechanism that is causing liquid film depletion is associated with evaporation due to heating applied to walls. These two mechanisms must be counter-balanced by the drop deposition from the vapour core to the liquid film surface to avoid the film dry-out.

Figure 3.1. Schematic of annular flow and liquid film dry-out



There are several possible mechanisms that have been postulated for dry-out (Hewitt, 1982). The first one is as suggested above: the liquid film dries by progressive entrainment and evaporation, which prevail in comparison to deposition and dry-out occurs when the film has gone. Another possible mechanism is associated with a formation of a dry patch within the liquid film, causing such wall temperature increase that it cannot be rewetted. In some situations a sudden disruption of liquid film may occur beyond which the wall surface is dry. The disruption mechanism is not fully understood yet, however, hydrodynamic mechanisms for the disruption are postulated. For very thin liquid films dry-out occurs when the rate of evaporation of droplets at the surface exceeds the rate at which they arrive at the surface due to deposition. For thicker liquid films it is postulated that dry-out may

occur due to a vapour film formation under the liquid film. The mechanism of forming this vapour film might be of the same type as described for the DNB mechanisms.

Annular flow pattern usually is the predominant flow regime in upper core regions in BWRs. The factor that limits the total power obtained from each assembly is the risk of occurrence of dry-out. Increasing the heat-flux above some critical value can lead to dry-out that is associated with a sudden increase in the wall temperature, which, in turn, can destroy the cladding material and allow the radiation releases into the primary system. Due to inaccuracy in dry-out prediction as well as uncertainties in determining operating conditions, the operational heat-flux must not approach the CHF by some safety margin. In order to optimise the operating conditions, the CHF must be accurately predicted with smaller margins than the ones existing today.

As already mentioned, the annular regime in boiling two-phase flow is characterised by a thin liquid film flowing on the channel walls and a gas core flowing in the central part of the channel. Droplets in the gas core represent a larger interfacial area than the liquid film and thus can dominate heat and mass transport between the phases. System pressure drop is increased by droplet acceleration in the gas core and depositing droplets contribute to corrosion by increasing local wall friction.

The basic phenomenological model of dry-out takes into account deposition, entrainment and film evaporation to determine the location of dry-out. Solving the mass, momentum and energy-conservation equations, a location of the point of complete liquid film depletion can be found. This approach was initiated in 1970s by Hewitt and his co-workers (Whalley et al., 1974; Whalley and Hewitt 1978; Whalley et al., 1982) and has been further developed by many research groups since then. In a boiling channel the approach requires boundary conditions for the initial film thickness at the point of the onset of annular flow. Both these parameters are quite uncertain and contribute the uncertainty in determining the location of the dry-out point.

The important phenomena that influence the occurrence of dry-out have several different scales:

- macro-scales, with order of magnitude of the channel hydraulic diameter, and governed by channel-wide parameters, such as system pressure, mass flow rate, disturbance waves, overall flow quality, cross-flows, flow obstacles;
- meso-scales, with order of magnitude of droplet sizes and initial film thickness, governing the droplet concentration distribution, entrainment rates and deposition rates;
- micro-scales, with order of magnitude of 10  $\mu\text{m}$  or less, that govern liquid film breakup into rivulets, creation and stability of dry patches, dynamic contact angle at the edge of liquid film, turbulence in liquid film and gas core.

### 3.2. Limits of previous approaches and expected improvements with CFD

The currently existing approaches to predict the occurrence of dry-out in nuclear fuel assemblies are as follows:

- application of a co-relation which is predicting the critical power based on bundle-mean values of major flow and heat-transfer parameters, such as the mass flux, the thermodynamic mean quality and the power distribution;

- application of a sub-channel code in connection with a phenomenological model to predict the liquid film distribution on heated rods.

In both these cases, a significant amount of experimental data is needed to develop the correlations and to calibrate the phenomenological liquid film models. As a result, the predictive tools are limited just to the assemblies in which the data were obtained and are not applicable to general dry-out predictions.

The expected major improvements while employing CFD approach are as follows:

- capability to capture the influence of geometry details on dry-out;
- mechanistic formulation of models based on local values of the governing parameters, leading to a predictive tool applicable to a wide range of the operating conditions;
- including the effects of turbulence on two-phase flow features such as spatial distribution of drops, distribution of drop sizes and deposition of drops on liquid film, leading to more accurate predictions;
- capability to capture from first principles the influence of spacer grids on drop size and deposition rates;
- better understanding of the dry-out phenomenon by analysing detailed information provided by CFD simulations.

### 3.3. Selecting the basic model

The computation of annular flows can be performed either using the Eulerian-Eulerian (two-fluid) or Eulerian-Lagrangian framework for the steam-droplet core flow. Due to presence of a liquid film on walls, special wall functions must be applied to account for the liquid film movement and the interface roughness seen by the core flow. The most common approach to model the effect of drop dispersion and drop/vapour heat-transfer is by means of the Lagrangian approach. This method is based on tracking of individual droplets in the continuous vapour phase by integrating their equations of motion. To simulate the effect of drop dispersion, the gas velocity is randomly sampled along trajectories, where characteristic properties of turbulence are determined from mean vapour flow properties (see Anglart and Caraghiaur, 2011).

Heat and mass transfer of droplets is accounted for by solving the droplet mass and energy equations. For dry-out predictions it is essential to consider interactions between droplets and a wall covered with a liquid film. However, for near-dry-out and post-dry-out heat-transfer conditions, interactions between droplets and the dry wall should be considered as well. The liquid film itself can be treated as a third field with mass, momentum and energy balance equations.

The liquid film can be included into the basic model in two ways: as an additional field with pertinent conservation equations of mass, momentum and energy, or as a dedicated model that either resolves the liquid layer on the wall surface and calculates the liquid film thickness based on the mass, momentum and energy balances. In the former case, a consistent three-field model is obtained with conservation equations formulated separately for vapour, droplet and liquid film. The model must be supplemented with closure laws for interfacial mass, momentum, energy and turbulence transfer between the fields, as well as with model for adhesion effects, which are responsible for the film susceptibility to move along walls. In the latter case, the model of the steam-droplet core flow (which can be

formulated in either Eulerian-Eulerian or Eulerian-Lagrangian framework) is coupled with the film model through transfers of mass, momentum and energy at the film-core interface.

Both above-mentioned modelling approaches can be formulated in two- and three-dimensional frameworks. Two-dimensional framework is especially valuable for model testing, which is typically performed for axi-symmetric (pipe) flow conditions, and whenever computational time is of concern. Three-dimensional approach is recommended for most practical applications. In this approach, all continuous fields are represented in 3D, with one notable exception for the liquid film, which can be modelled using either 1D, 2D or 3D approach. The mesh size should be such as to allow resolving the geometry details.

### 3.4. Filtering turbulent scales and two-phase intermittency scales

The present prediction tools are not including the modelling of turbulence and have limited capabilities to resolve the internal two-phase scales. Thus, major improvement is expected while employing the CFD approach, in which these issues can be addressed.

The most promising approach which can be applied for practical cases is based on the two-fluid, multi-field RANS modelling of the gas core and the liquid film, where ensemble averaging is applied to the vapour, liquid film and the dispersed-droplet field. The equations are closed with droplet-vapour interaction terms that describe the exchange of mass, momentum and energy. The liquid film thickness and the interface between the liquid film and the gas core is resolved in the ensemble-averaged sense, that is the mean liquid film thickness is calculated, whereas the wavy structure of the interface is not resolved and is accounted for with closure relationships for the interfacial mass, momentum and energy transfer. Another approach could employ LES, in which only the smallest eddies, smaller than droplets and wave structure on the liquid film, will be filtered. This approach would enable inclusion of the wave motion on the film surface, and in particular would take into account the influence of disturbance waves on the dry-out occurrence.

### 3.5. Identification of local interface structure

ILIS requires employment of mechanistic closure laws, which are based on local values of the governing flow parameters. This type of approach is practically impossible for current prediction tools, since they are using typically area-averaged and bulk parameters. In contrast, CFD approach lends itself for the resolution of the local interface structure.

The interface in annular two-phase flows has two distinct scales: a large-scale interface exists between the liquid film and the continuous vapour and a small-scale interface exists between the continuous vapour and droplets. The large-scale interface is determined by the liquid film surface, which has a wavy structure on top of the base film thickness. The most important from the dry-out point of view are so-called disturbance waves, the wave height being several times larger than the base film thickness, and, which propagate with velocities, which exceed the mean velocity of the liquid film. However, the thickness of the base film is also important since the triggering of dry-out is due to the evaporation of the base film between two disturbance waves. The interfacial area can be considered proportional to the wall surface area and the additional area due to interfacial waves can be only considered as a roughness effect on interfacial transfers.

The small-scale interface is determined by the drop size, which is an important parameter that affects the deposition rates and thus the dry-out phenomenon. The drop size

can be calculated from an algebraic expression as a function of local parameters. In a more sophisticated approach, the drop size can be determined from predictions of drop breakup and collisions. Various models for drop breakup have been developed, e.g. the TAB (Taylor Analogy Breakup) model (O'Rourke and Amdsen, 1987) and the Reitz Diwakar model (Reitz and Diwakar, 1987).

### 3.6. Modelling interfacial transfers

Modelling of the interfacial transfer rates requires detailed information about local values of major flow parameters such as flow velocity, fluid temperature and turbulence intensity. This type of information is not available in present predictive tools, thus, the interface transfer rates are evaluated from co-relations, which are using bulk parameters. Such formulation may lead to inconsistent results and is not applicable outside of specified ranges. CFD approach is free from these limitations and can be applied for modelling of interfacial transfer rates in a wide spectrum of conditions. This is particularly true in complex geometries, such as spacer grids, where the influence of geometry features on interfacial transfer rates can be captured.

The liquid phase in typical dry-out situation exists in two different structures: as a continuous liquid film moving on walls and as a disperse phase (droplets) carried by the continuous vapour phase. Thus, there are three types of interactions that have to be considered: liquid film – vapour interactions, liquid film–droplet interactions and droplet – vapour interactions.

The liquid film – vapour interactions include mass transfer due to evaporation of the liquid film and the momentum transfer due to interfacial shear and evaporation. Since usually the liquid film and the vapour phase are assumed to be at the saturation temperature, the energy transfer is determined by the evaporation rate, which results from the local value of the heat-flux, thus its modelling is quite straightforward.

The mass, momentum and energy transfer between droplets and the liquid film is usually modelled by accounting for the entrainment of droplets from the liquid film into the gas core and the deposition of droplets from the gas core to the liquid film. Both these effects are strongly influencing the liquid film thickness and thus need to be accurately predicted. Their modelling is discussed in a more detail below.

Liquid droplets carried by a turbulent gas stream deposit on bounding walls. Deposition rate depend on drop dispersion in turbulent flow where particle motion is primarily governed by interactions with eddies of various scales. Depending on the ratio of the particle response time to the eddy characteristic time the dispersion can have different characters. If this ratio is very small, particles are following the continuous flow structure. When the ratio is close to one (the time constants of eddies and particles are of the same range of magnitude) the dispersion of drops can be even bigger than that observed in the carrier fluid. Finally, for high values of the ratio particles remain largely unaffected by eddies. Due to the complexity of involved processes, the deposition rate is modelled in various ways. Typically, drop deposition is associated with two mechanisms: the diffusion process and the free flight to the wall. For proper prediction of the deposition rate of droplets, both these mechanisms have to be taken into account. In addition, impinging conditions of a drop on a liquid surface have to be considered. When a single droplet impinges a liquid film, various phenomena can occur. The droplet can bounce from the surface or merge with the liquid film. Splash can occur when the drop kinetic energy is

high enough. For conditions typical for BWRs, the liquid film is thin and the velocity of droplets is high, thus splashing and merge are the key phenomena involved.

Several mechanisms of drop entrainment from the liquid film have been identified. The dynamic impact of gas core causes generation of waves on the film surface, with droplets being separated and entrained from the crests of these waves. Important role in the drop entrainment process plays the creation and breakup of the disturbance waves. Another entrainment mechanism is associated with splashing associated with drop deposition. Finally, in a heated channel with nucleate boiling in the film, entrainment can occur due to the action of vapour bubbles, which induce splashing. Entrainment of droplets from liquid film due to core dynamic action will not occur if certain critical conditions of the onset of film atomisation are not satisfied. A number of empirical and semi-empirical correlations have been suggested in the literature for prediction of the critical conditions and the rate of the entrainment. Obviously, such correlations should include both the liquid film and the film interface properties.

The droplets – gas core interactions include mainly the transfer of momentum due to drag, lift and turbulent dispersion forces. The mass and energy transfer terms are usually neglected since in non-dry-out annular flows, the two fields are in the thermodynamic equilibrium and no phase-change takes place. An important parameter that governs the transfer rates is the local value of the interfacial area concentration, which, in turn, depends on the local drop diameter. Thus, the drop diameter is a part of the solution and has to be predicted from a model, which takes into account the breakup, and collision effects as well as drop interactions with turbulence of the continuous field.

### 3.7. Modelling turbulent transfers

Turbulence plays an important role in two-phase annular flows since it influences the transfer rates of mass and momentum between the gas core and the liquid film. When drop concentrations are very small, the influence of drops on turbulence in the continuous field (so-called turbulence modulation) is small and can be neglected. This type of approach is referred to as the one-way coupling approach, since only the influence of the turbulence in the continuous field on drop distribution is modelled. With moderate drop concentration a two-way coupling approach is used. In this approach, the turbulence modification in the continuous phase due to droplets is taken into account. For high drop concentration (which is the case for most practical situations of interest) even particle-particle interactions have to be considered.

The simplest approach to vapour turbulence will employ a two-equation turbulence model (either  $k-\epsilon$  or  $k-\omega$ ), in which additional source terms are introduced to account for the turbulence sources and turbulence dissipation caused by droplets and liquid film interface. Turbulence transfer at the film interface is usually modelled using the standard law-of-the wall approach, possibly with a modification to account for the wavy structure of the interface.

In a more advanced approach based on LES, turbulence transfer between the liquid film and gas core can be computed directly, provided that only eddies smaller than film surface waves and drops are filtered. Modelling would be required for the turbulence transfer resulting from interface structures, which are smaller than the smallest resolved turbulent eddies.

### 3.8. Modelling wall transfers

Prior to dry-out occurrence the walls are covered with liquid films, where velocity, temperature and turbulence distributions can be obtained in principle in the same way as it is done for single-phase flows. However, the film may be modelled more simply with balance equations being integrated over the film thickness and classical wall friction coefficients are used. It should be noted that even though the liquid is superheated in the film, the evaporation takes place at the film interface rather than on the wall or in the bulk. When a dry patch is created at the onset of dry-out, evaporation takes place at the wall surface and at its vicinity. In the dry patch, the convective heat-transfer to vapour and heat-transfer to the impinging droplets must be taken into account. To this end, the total wall heat-flux must be partitioned into two corresponding parts, which will cause the vapour superheat and drop evaporation. Prediction of the wall surface temperature will require a simultaneous solution of heat conduction in the solid wall.

### 3.9. Status of modelling

CFD modelling of dry-out is still severely limited due to the lack of proper closure relationships for the two-fluid approach. The major difficulty is to model the liquid film, which is a thin continuous layer sticking to walls. The flow of gas core and liquid film as such has a character of two-phase separate flow, where the two-phases are separated with a large-scale interface. The best approach to model this type of flow would be either interface-tracking or interface-capturing method. This approach should be combined with two-fluid treatment of the dispersed flow in the gas core. Since such hybrid two-phase solvers are not available yet, the common approaches are:

- two-fluid approach to resolve the gas core combined with a separate, one- or two-dimensional model for liquid film propagation along walls;
- two-fluid three-field approach where the liquid film is treated as a separate continuous field, in addition to a continuous vapour film and a dispersed-droplet film.

### 3.10. Matrix of validation test cases

Early experiments were focused on the measurements of the total power, which was necessary for the dry-out occurrence in a heated channel. A vast number of these experiments were performed for different conduit geometries in different flow conditions, with constant and variable axial and radial heat-flux distributions. The measurements for steam-water were done in round ducts, annuli and rod clusters. The round duct experiments covered diameters between 3.93 and 24.95 mm (about 14 diameters), heated lengths in a range 400-7100 mm, and, pressures from atmospheric to 200 bar (Becker et al., 1963; Becker, 1962; Becker, 1965; Becker and Hernborg, 1961; Becker et al., 1970; Becker and Ling; 1970; Becker et al., 1971; Söderqvist et al., 1994; Becker et al 1969; Becker, Persson, Nilsson and Eriksson, 1963). As a result of these measurements, the effects of diameter, heated length, pressure, mass flux, inlet sub-cooling and non-uniform power profile on CHF were studied and correlations derived. The measurements in annuli covered the inner tube diameters of 9.92 – 13.8 mm and outer tube diameters of 17.42 – 26.0 mm; heated lengths of 600 – 3650 mm and pressures of 30, 50 and 70 bar (Becker and Letzer, 1981; Persson, 2001). Additionally to the effects mentioned for the round ducts, the influence of pin and grid spacers on the CHF was studied for the annuli. Rod clusters of 3, 6, 7 and 36

rods in round and square arrangements were subject to experiments in the pressure range of three – 46 bar (Becker et al., 1964; Becker and Hernborg, 1964; Nilsson et al., 1983; Becker, 1967). Radial as well as axial non-uniform heat profiles were applied.

For a validation of models based on the analysis of wall film flows, experimental data of pressure drops, including wall shear stress and interfacial shear stress, which characterise liquid film thickness and the onset of entrainment, respectively, are required. In addition, actual measurements of film flows, film thickness, wave amplitude, frequencies and wave velocities are needed for the validation. Moreover, because complete physical models for droplet entrainment and droplet deposition are still not available, experimental data of these are needed to develop reliable correlations and/or computational models.

#### Pressure Drop in Annular flow

More than several thousand pressure drop measurements for steam-water and air-water mixtures in annular flow are reported in the literature. Würtz (1978) has reported more than 2 700 measurements for steam-water. The measurements in tubes were carried out within the following intervals: tube diameter 3.2–55.9 mm, pressure one – 212 bar, mass flux 99–8210 kg/m<sup>2</sup>s. The summary of the selected measurements of pressure drop is given in Table 3.1.

**Table 3.1. Data sets of pressure drops (shear stress) for validation of dry-out models**

No	Measured value	Geometry	Fluid Heating	Flow conditions	Reference
1	$\Delta P$	Tubular test section: $D_i = 10$ mm, $L_h = 9.0$ m Annular test section: $d_1 = 17$ mm, $d_2 = 26$ mm, $L_h = 8.0$ m	Steam-water Adiabatic and diabatic	P: 30, 50, 70 and 90 bar G: 500–3000 kg/m <sup>2</sup> s	Würtz, 1978
2	$\Delta P$	Plexiglass tube $D_i = 24$ mm $L = 5$ m	Air-water Adiabatic conditions	P: atmospheric $G_l: 9.73 \times 10^{-3} - 200.3 \times 10^{-3}$ kg/s $G_g: 17.5 \times 10^{-3} - 50.3 \times 10^{-3}$ kg/s	Andreussi, 1983
3	$\Delta P$ $\tau_w$ $\tau_l$	LOTUS test rig Tubular section $D_i = 31.8$ mm $L = 23$ m	Air-water Adiabatic conditions	P: 2.4 bar $G_l: 100, 200, 300$ and 500 kg/m <sup>2</sup> s $G_g: 70$ –240 kg/m <sup>2</sup> s Temperature ambient	Govan et al., 1989

$D_i$ : internal diameter

$L_h$ : heated length

$\tau_w$  wall shear stress

$\tau_l$  interfacial shear stress

### Film flow rates

A review of film flow measurements in steam-water mixtures in annular flow was performed by Würtz (1978). The film flows were measured both in tubes and in annuli. The diameters of the tubes were in range from 9.3 to 20 mm and the diameters for annuli were (all dimensions in mm) 19.7/23.8, 17.0/27.2 and 17.0/26.0. Pressures were in range from 2.4 to 100 bars and mass flux from 275 to 4000 kg/m<sup>2</sup>s. Most of the film flow measurements were done in 60s – 70s. A summary of selected measurements is presented in Table 3.2.

**Table 3.2. Summary of selected measurements of film flow rates**

No	Measured value	Geometry	Fluid heating	Flow conditions	Reference
1	Film flow Wave velocity	acrylic resin tube D <sub>i</sub> : 9.525 mm	Air-water Adiabatic	P: 2 bar G <sub>g</sub> : 18.14 & 31.75 kg/h Temperature ambient	Cousins and Hewitt, 1968
2	Film flow Film thickness Wave frequency Wave velocity	Tubular test section: D <sub>i</sub> : 10 mm, L <sub>h</sub> : 9.0 m Annular test section: d <sub>1</sub> =17 mm, d <sub>2</sub> =26 mm, L <sub>h</sub> : =8.0 m L <sub>h</sub> : =3.5 m	Steam-water Adiabatic & diabatic	P: 30, 50, 70 and 90 bar G: 500-3000 kg/m <sup>2</sup> s	Würtz, 1978
3	Film flow	Tubular test section D <sub>i</sub> : 13.9 mm L <sub>h</sub> : 3.65 m various power profiles	Steam-water Diabatic conditions	P:70 bar G: 500 – 1750 kg/m <sup>2</sup> s	Adamsson and Anglart, 2006

### Deposition rates

An extensive review of existing measurements of deposition rate has been presented by Okawa et al. (2005). The deposition rates were predominantly measured in air-water systems with low pressures. The techniques employed are the double film extraction, thermal method and tracer method. The internal diameters of the tubes for deposition rate measurements range from 9.5 mm to 57.2 mm. The proposed data sets of measured deposition rates for the present study are presented in Table 3.3.

It was experimentally proven that the mode of the deposition is dependent on the droplet size. Observations of droplet motion (Andreussi, 1983) show that larger droplets travel across the gas core at about their initial velocity in a constant direction until they are deposited. This mechanism of deposition has been called direct impaction. At higher gas velocities, where the droplets are comparatively smaller, the effect of the initial momentum on droplet motion becomes negligible. In this case, the eddy diffusion mechanism of deposition prevails. Bates and Sheriff (1992) have presented a summary of the previous work done on droplet size/velocity in vertical annular air-water two-phase flow. All above-mentioned researchers have been performing measurements at atmospheric or close to the atmospheric pressure. The internal diameters of the tubes were 9.5, 32 and 51 mm. Various

techniques have been employed for the measurements, among which such as photography, diffraction, visibility (SPC –single particle counter), LPM (SPC) and Phase Doppler (SPC). The sizing ranges span between 5.5 and 2 500  $\mu\text{m}$ . A summary of selected measurements are presented in Table 3.3.

**Table 3.3. Summary of selected measurements of deposition rates**

No	Measured value	Geometry	Fluid heating	Flow conditions	Reference
1	Deposition mass transfer coefficients Droplet concentration	Stainless steel tube $D_i$ : 5 mm L: 3670 mm	Air – water	P: 1.4 – 7.6 bar Temperature ambient $G_i$ : 201-1264 $\text{kg/m}^2\text{s}$ $G_g$ : 173 – 627 $\text{kg/m}^2\text{s}$	Okawa et al., 2005
2	Deposition rates	LOTUS test rig Tubular section $D_i$ : 31.8 mm L: 23 m	Air-water Adiabatic conditions	P: 2.4 bar $G_i$ : 100, 200, 300 and 500 $\text{kg/m}^2\text{s}$ $G_g$ : 70-240 $\text{kg/m}^2\text{s}$ Temperature ambient	Govan et al., 1989
3	Deposition rates / Drop size	Vertical tube $D_i$ :10.26 mm	Air-water Helium/water	P: ambient & 1.5 bar $T^\circ$ : ambient $G_i$ : 40-147 $\text{kg/m}^2\text{s}$ $G_g$ : 7.33-80.3 $\text{kg/m}^2\text{s}$	Jepson et al., 1989
4	Drop size distribution	Stainless steel duct $D_i$ : 9.67 mm L: 3.4 m	Nitrogen-water	Pressure 3.4 and 17 bar Temperature 38 $^\circ\text{C}$ $Q_i$ : 0.0157 and 0.126 $\text{kg/s}$ $J_g$ : 5, 7, 17 and 23 $\text{m/s}$	Fore et al., 2002
5	Drop size distribution	Vertical tube $D_i$ : 50.8 mm L: 7.6 m	Air-water (1cP liquid) Air-water+glycerine (50% mix) (6 cP liquid)		Fore and Dukler, 1995

### Entrainment rates

When a gas-phase is flowing over a liquid film, several different flow regimes are possible depending on the magnitude of the gas velocity. For a very small gas velocity, the interface is relatively stable, however, as the gas velocity increases the interfacial waves appear. The amplitude and irregularity of waves became pronounced as the gas velocity is further increased. At sufficiently high gas flow, the capillary waves transform into large amplitude roll waves (disturbance waves). Near the transition to the roll wave or at a still higher gas velocity, the onset of entrainment occurs.

It is not easy to make measurements of a complex process such as entrainment from film into the gas core. In the case of deposition, unidirectional experiments can be carried out such that entrainment is not occurring. No such simple scheme is available for measuring entrainment rates. It is not possible to remove the drops from the gas core

without causing significant disturbance to the flow. Equally, it is not possible to get close to the source of entrainment, namely the disturbance waves from which the drops are created, primarily because they are moving along the walls. One way to measure entrainment is to reach a quasi-equilibrium state in the system where it is considered that deposition rate is equal to the entrainment rate. Okawa et al. (2005) presented a summary of existing experiments for the equilibrium entrainment rate. The measurements were performed in air-water as well as steam-water. The system pressure varied between one and 90 bars. Internal diameter of the tube was from 9.3 to 57.1 mm. A summary of selected measurements is shown in Table 3.4.

**Table 3.4. Summary of selected measurements of entrainment rates**

No	Measured value	Geometry	Fluid heating	Flow conditions	Reference
1	Equilibrium entrainment rate	Stainless steel tube D <sub>i</sub> : 5 mm L: 3670 mm	Air – water	P: 1.4 – 7.6 bar Temperature ambient G <sub>i</sub> : 201-1264 kg/m <sup>2</sup> s G <sub>g</sub> : 173 – 627 kg/m <sup>2</sup> s	Okawa et al., 2005
2	Fraction of liquid entrained by gas, Rate of liquid interchange	Plexiglass tube D <sub>i</sub> : 24 mm L: 5 m	Air-water Adiabatic	Pressure: atmospheric Q <sub>i</sub> : 9.73x10 <sup>-3</sup> – 200.3x10 <sup>-3</sup> kg/s Q <sub>g</sub> : 17.5x10 <sup>-3</sup> – 50.3x10 <sup>-3</sup> kg/s	Andreussi, 1983
3	Entrainment rate	acrylic resin tube D <sub>i</sub> : 9.525 mm	Air-water Adiabatic	P: 2 bar Q <sub>g</sub> : 18.14 and 31.75 kg/h Temperature ambient	Cousins and Hewitt, 1968

Even though the validation database for dry-out is quite extensive, it does not cover the needs as far as the validation of CFD models is concerned. A specific feature of CFD closure laws is that they are formulated in terms of local values of major flow parameters, such as velocity, temperature, and phasic volume fraction and turbulence intensity. In principle, a thorough validation of CFD models requires that all these parameters are measured simultaneously and used in the validation. Thus, the present experimental database should be extended with simultaneous measurements of several parameters such as velocity (both vapour and drops), drop size, drop volume fraction, turbulence intensity and liquid film thickness. A properly validated CFD model for dry-out should be able to predict all these parameters at the same time. In particular, the following data concerned with micro-scale phenomena are needed:

- droplet dynamics, coalescence, breakup and interactions in turbulent gas core flow;
- liquid film dynamics and its coupling to a local entrainment rate;
- stability condition of a dry patch in a liquid film;
- liquid film minimum wetting rate under annular two-phase flow conditions;
- velocity and turbulence distribution in a liquid film;
- interfacial shear stress on the liquid film surface;
- speed and propagation of disturbance waves and their interactions with liquid film.

## References

Adamsson, C. and H. Anglart (2006), “Film flow measurements in high pressure diabatic annular flow in tubes with various axial power distributions”, *Nuclear engineering and Design*, Vol. 236, pp. 2485-2493.

Andreussi, P. (1983), “Droplet transfer in two-phase annular flow”, *Int. J. Multiphase Flow*, Vol. 9, No. 6, pp. 697-713.

Anglart, H. and D. Caraghiaur (2011), “CFD modelling of boiling annular-mist flow for dryout investigations”, *Multiphase Science and Technology*, 23(2-4): 223-251.

Azzopardi, B.J. (1997), “Drops in annular two-phase flow”, *Int. J. Multiphase Flow*, Vol. 23, pp.1-53.

Bates, C.J. and J.M. Sheriff (1992), “High data rate measurements of droplet dynamics in a vertical gas-liquid annular flow”, *Flow Meas. Instrum.*, Vol. 3, pp. 247-256.

Becker, K.M., R.P. Mathisen, O. Eklind and B. Norman (1963), “Measurements of hydrodynamic instabilities, flow oscillations and burnout in a natural circulation loop”, Arbetsrapport R4-176, RPL-681, Aktiebolaget Atomenergi.

Becker, K.M. (1962), “Measurements of burnout conditions for flow of boiling water in vertical round ducts”, AE 87, Aktiebolaget Atomenergi.

Becker, K.M. (1965), “An analytical and experimental study of burnout conditions in vertical round ducts”, AE 178, Aktiebolaget Atomenergi, Stockholm, Sweden.

Becker, K.M. and G. Hernborg (1961), “An experimental study of burnout conditions for flow of boiling water in a vertical round duct”, Arbetsrapport, R4-133, IPL-90, Aktiebolaget Atomenergi, Stockholm, Sweden.

Becker, K.M., G. Strand, M. Bode and C. Österdahl (1970), “Burnout and post-burnout measurements for flow of water in a round tube at high pressures”, RINL-11, Royal Institute of Technology, Stockholm, Sweden.

Becker, K.M. and C.-H. Ling (1970), “Burnout measurements in a round tube of 7100 mm heated length” Paper presented at the Two-Phase Flow meeting, Milano, Italy, 8-12 June 1970, KTH report NEL-13.

Becker, K.M., G. Strand, D. Djursing, O. Eklind, K. Lindberg and C. Österdahl (1971), “Round tube burnout data for flow of boiling water at pressures between 30 and 200 bar”, KTH report, NEL-14.

Becker, K.M., G. Hernborg, K. Bergman and S. Lange (1969), “Measurements of burnout conditions in vertical round tubes with non-uniform axial heat flux”, Aktiebolaget, Atomenergi, Arbetsrapport, AE/RL-1153.

Becker, K.M., P. Persson, L. Nilsson and O. Eriksson (1963), “Measurements of burnout conditions for flow of boiling water in vertical round ducts (Part 2)”, Aktiebolaget, Atomenergi, AE-114.

Becker, K.M. and A. Letzer (1981), “An experimental study of the effect of the axial heat flux distribution on the dryout conditions in a 3650-mm long annulus”, *Int. J. Multiphase Flow*, Vol. 7, pp 47-61.

Becker, K.M., G. Hernborg and J.E. Flinta (1964), “Measurements of burnout conditions for flow of boiling water in vertical 3-rod and 7-rod clusters”, Aktiebolaget, Atomenergi, AE-153.

Becker, K.M. and G. Hernborg (1964), “Measurements of the effects of spacers on the burnout conditions for flow of boiling water in a vertical annulus and a vertical 7-rod clusters”, Aktiebolaget, Atomenergi, AE-165.

Becker, K.M. (1967), “A burnout correlation for flow of boiling water in vertical rod bundles”, Aktiebolaget, Atomenergi, AE-276.

Cousins, L.B. and G.F. Hewitt (1968), “Liquid phase mass transfer in annular two-phase flow: droplet deposition and liquid entrainment”, AEA Report, AERE-R 5657.

Fore, L.B. and A.E. Dukler (1995), “The distribution of drop size and velocity in gas-liquid annular flow”, *Int. J. Multiphase Flow*, Vol. 21, No. 2, pp. 137-149.

Fore, L.B., B.B. Ibrahim and S.G. Beus (2002), “Visual measurements of droplet size in gas-liquid annular flow”, *Int. J. Multiphase Flow*, Vol. 28, pp. 1895-1910.

Gosman, A.D. and E. Ioannides (1983), “Aspects of computer simulations of liquid-fueled combustor”, *Journal of Energy*, 7(6), pp. 482-490.

Govan, A.H., G.F. Hewitt, D.G. Owen and T.R. Bott (1988), “An Improved CHF Modelling Code”, 2nd UK National Heat Transfer Conference, Glasgow, United Kingdom.

Govan, A.H., G.F. Hewitt, D.G. Owen and G. Burnett (1989), “Wall shear stress measurements in vertical air water annular two-phase flow”, *Int. J. Multiphase Flow*, Vol. 15, No. 3, pp. 307-325.

Hewitt, G.F. (1982), “Burnout”, in Handbook of multiphase systems, G. Hetsroni Ed. ISBN 0-07-028460-1, Hemisphere Publishing Corporation, United States.

Jepson, D.M., B.J. Azzopardi and P.B. Whalley (1989), “The effect of gas properties on drops in annular flow”, *Int. J. Multiphase Flow*, Vol. 15, pp 327-339.

Kataoka, I., M. Ishii and K. Mishima (1983), “Generation and size distribution of droplets in annular two-phase flow”, *Trans ASME, J. Fluids Eng.* 105, 230-238.

Mori, S. and T. Fukano (2004), “Influence of a flow obstacle on the occurrence of burnout in boiling two-phase upward flow with a vertical annular channel”, *Nucl. Eng. Des.* Vol. 225, 49.

Nilsson, L., et al. (1983), “FIX-II – LOCA blowdown and pump trip heat transfer experiments”, Studsvik Report/NR-83/274.

Okawa, T., A. Kotani, I. Kataoka and M. Naito (2003), “Prediction of Critical Heat Flux in Annular Flow Using a Film Flow Model”, *J. Nucl. Sci. Technol.*, Vol. 40 No. 6.

Okawa, T., A. Kotani and I. Kataoka (2005), “Experiments for liquid phase mass transfer rate in annular regime for a small tube”, *Int. J. Heat and Mass Transfer*, Vol. 48, pp. 585-598.

Persson, P. (2001), “Measurements and analysis of dry out in annular geometry with two sided heating with uniform and nonuniform axial power and the influence of spacers and spacer positions”, SKI/KSU/KTH Project.

Reitz, R.D. and R. Diwakar (1987), “Structure of high-pressure fuel sprays”, SAE Technical Paper 870598.

O’Rourke, P.J. (1981), “Collective drop effects on vapourizing liquid sprays”, PhD thesis, Princeton University, Department of Mechanical and Aerospace Engineering.

O'Rourke, P.J. and A.A. Amsden (1987), "The TAB method for numerical calculation of spray droplet breakup," SAE Technical Paper 872089.

Söderqvist, B., S. Hedberg and G. Strand (1994), "Critical heat flux measurements in vertical 8 mm round tubes", KTH report, ISSN 1104-4020, ISRN KTH/NEL/R-56-SE.

Tatterson, D.F., J.C. Dallman and T.J. Hanratty, "Drop size in annular gas-liquid flows", AIChE J. 23, 68-76 (1977).

Whalley, P.B., P. Hutchinson and G.F. Hewitt (1974), "The calculation of critical heat flux in forced convective boiling", Proc. 5th Int. Heat Transfer Conf., Versailles, Vol. 4, pp. 290-294.

Whalley, P.B. and G.F. Hewitt (1978), "The correlation of liquid entrainment fraction and entrainment rate in annular two-phase flow", Report AERE-R9187, UKAEA Harwell.

Whalley, P.B., B.J. Azzopardi, G.F. Hewitt and R.G. Owen (1982), "A physical model for two-phase flows with thermodynamic and hydrodynamic non-equilibrium", Paper CS29, 7th Heat Transfer Conf., Munich.

Würtz, J. (1978), "An experimental and theoretical investigation of annular steam-water flow in tubes and annuli at 30 to 90 bar", Risø Report No. 372, Risø National Laboratory.

## 4. The departure from nucleate boiling

### 4.1. Definition of the DNB issue and identification of all-important flow processes

DNB is the CHF process, which is likely to occur when a PWR core deviates from its nominal conditions. Empirical co-relations that have been developed from specific measurements currently estimate DNB in LWRs. Applicability of such co-relations is limited to the experimental conditions and to geometry of test sections, in which the measurements have been performed. Extrapolation of co-relations beyond these limits will not assure the required accuracy and, in general, is not possible. This particular feature makes co-relations useless in development of new fuel assembly designs, and full-scale measurements are required instead. Due to that, the design process is quite costly and time-consuming.

In addition to co-relations, there are several phenomenological models, that have been developed to predict DNB. For example, when investigating DNB conditions, it has been observed, that small bubbles near the heated surface are merging into large bubbles (Jiji and Clark 1964, Hino and Ueda 1985). Large bubbles, in turn, form a vapour blanket, which is separated from the heated wall by a thin liquid macro layer. DNB condition occurs when the macro layer evaporates and the wall temperature rises above the rewetting temperature (Haramura and Katto, 1983; Celata, 1994; He et al., 2001).

There are several phenomenological models of the DNB condition based on the macro layer dry-out concept. Following Zuber (1958), Haramura & Katto (1983) invoke the Helmholtz instability mechanism, include a three-layer liquid velocity distribution, a Magnus effect, and buoyancy and drag forces on the vapour blanket (Lee & Mudawwar 1988) and finally, add energy balance in the liquid macro layer (Ho et al. 1993). It should be mentioned, that, besides the concept of dry-out of the liquid macro layer, there exist other phenomenological models, based on other principles. Zhao et al. (2002) propose a micro-layer vaporisation process, Theofanous et al. (2002a, 2002b) a micro-layer rupture, Beysens et al. (2003) a recoil force instability. Several authors mention a possible dry spot spreading (Unal et al., 1992; Bricard, 1995; Ha & No, 2000; Le Corre, 2007) or the heating of the wall in the dry spot up to Leidenfrost temperature (Unal et al., 1992; Bricard, 1995; Le Corre, 2007). Other phenomenological models can be shortly described as: liquid layer superheat limit model, boundary layer separation model, liquid flow blockage model and vapour removal limit and near-wall bubble crowding model.

Three scales have important flow processes influencing the DNB:

#### **Macro-Scale (order of about 1 cm)**

- Phenomena at this scale are the mixing between sub-channels, cross-flows, turbulence and grid spacer effects on averaged flow parameters  $P$ ,  $G$ ,  $X_{th}$ .
- Averaged flow parameters (pressure  $P$ , mass flux  $G$ , and thermodynamic quality  $X_{th}$ ) can be predicted with a sub-channel code.
- DNB can be empirically correlated at this scale as a function of  $P$ ,  $G$ ,  $X_{th}$ .

**Meso-scale (order of about 1 mm)**

- Phenomena at this scale are the bubble transport and dispersion, bubble-growth and collapse, coalescence, breakup, turbulent transfers of heat and momentum, local effects of grid spacers.
- Local flow parameters (pressure  $P$ , phase velocities  $V_l$ ,  $V_v$ , liquid temperature  $T_l$ , void-fraction  $\alpha$ , and bubble diameter  $d_b$ ) within sub-channels can be predicted with a CFD code.
- DNB could be empirically correlated at this scale as a function of  $P$ ,  $V_l$ ,  $V_v$ ,  $T_l$ ,  $\alpha$ ,  $d_b$ .

**Micro-scale (order of 10  $\mu\text{m}$ , 1  $\mu\text{m}$  or less)**

- Phenomena at this scale are the activation of nucleation sites, the growing of attached bubbles, a possible sliding of attached bubbles along the wall, coalescence of attached bubbles, bubble detachment, wall rewetting after detachment.
- Prediction of pressure, velocity and temperature, and of positions of all interfaces is necessary to simulate these small-scale flow processes with DNS Techniques and ITM.
- DNB is no longer co-related but can theoretically be predicted by DNS and ITM.

**4.2. Limits of previous approaches and expected improvements with CFD**

As mentioned above, DNB in LWRs is currently estimated by empirical correlations that have been developed from specific measurements, applicable only to the experimental conditions and to geometry of test sections, in which the measurements have been performed. Such co-relations cannot be used for the development of new fuel assembly designs,

To overcome the above-mentioned shortcomings of CHF correlations and phenomenological models, it is desirable to develop a mechanistic model to predict CHF conditions in a boiling channel based on local parameters. The model has to take into account:

- a) the heater characteristics (physical properties, geometry, and surface roughness);
- b) the fluid characteristics (physical properties, near-surface macro layer hydrodynamics, and far-surface flow features); and
- c) the heater-fluid interface characteristics (contact angle, active site density).

All these parameters span over several different scales, starting from micro-scales (e.g. surface roughness), through meso-scales (e.g. bubble or drop size), till macro-scales (e.g. sub-channel size). Such mechanistic model should be applicable to any flow and heat-transfer conditions and should accommodate arbitrary geometry features of the boiling channel.

System codes and component codes cannot be used to model phenomena where interactions between such different scales exist. On the contrary, CFD technique is the proper tool to be used in such situations, since it combines the far-surface effects (e.g. flow distribution in a rod bundle) with near-surface effects (e.g. bubble nucleation at the heated surface). Still, further development of models is necessary for proper treatment of the phenomena. The major improvements include, but are not limited to: (a) model of the

interfacial area transport, (b) model of two-phase boundary layer, (c) model of the controlling mechanism for CHF and quenching.

A better understanding of the DNB phenomenon and an improved accuracy of CHF predictions requires that flow processes to be simulated at each relevant scale including CFD codes and pseudo-DNS models with ITM. Models at scale  $n$  can be based either on analysis of experimental data or on numerical experiments using scale  $n-1$  simulations. Improvements of the methodologies related to DNB might be achieved by performing the following R&D actions:

**Micro-scale**

- Further develop and improve pseudo-DNS methods.
- Perform local visualisation experiments.
- Perform simulations with several nucleation sites up to DNB.

**Meso-scale**

- Further develop and improve two-phase CFD models on the basis of experiments and on the basis of pseudo-DNS simulations.
- Experiments with local measurements in a heated channel.
- Validate CFD model with data.

**Macro-scale**

- Use CFD predictions to improve models in sub-channels codes.
- Experiments in an assembly.
- Couple sub-channel codes with CFD codes to predict DNB.

*Coupling between scales may be useful.*

### 4.3. Selecting a basic model

In boiling bubbly flows, the gas is a dispersed phase with many small bubbles in a continuous liquid phase. The two-fluid model is naturally used in this flow conditions to benefit from the possibility to model all interfacial forces acting on the bubbles such as drag, lift, turbulent dispersion, wall lubrication and virtual mass forces which control the void repartition in a boiling channel. The balance equations of the two-fluid model include two mass balance equations, two momentum balance equations and two energy balance equations (see Morel et al , 2003, 2005, Krepper et al., 2011, Končar et al., 2011).

The only choice, which remains partly open is the way to model poly-dispersion effects. Bubbles may have a rather wide diameter distribution and it may be necessary to model the behaviour of bubbles depending on their size, in particular for the interfacial heat and mass transfers associated with vaporisation and condensation or for momentum transfer since the lift force may change sign depending on the bubble-size (Tomiyama, 1998). Multi-group models exist with mass (and momentum) equations written for several bubble sizes. The two-fluid model is then extended to some kind of multi-fluid model with the MUSIG method (see Lucas et al. 2007, Krepper et al. 2009). The method of the statistical moments (Morel et al., 2009) can also be used to characterise the poly-dispersion. The two methods should be further evaluated and compared.

#### 4.4. Filtering turbulent scales and two-phase intermittency scales

Considering flow in a PWR core in conditions close to nominal, when boiling occurs, a high-velocity steady flow regime takes place with timescales associated with the passage of bubbles being very small ( $10^{-4}$ ,  $10^{-3}$  s) and with bubble diameter being rather small ( $10^{-5}$  to  $10^{-3}$  m) compared to the hydraulic diameter (about  $10^{-2}$  m). These are perfect conditions to use a time average or ensemble average of equations as usually done in the RANS approach. All turbulent fluctuations and two-phase intermittency scales can be filtered since they are significantly smaller than scales of the mean flow. Interfaces are not simulated, they are just statistically treated.

The use of a LES approach is also possible in dispersed-bubbly flow. This requires that there is a filter scale smaller than the large eddies of the liquid flow and larger than the bubble-size. Compared to the RANS approach, using the LES will allow the simulation of large coherent structures of liquid turbulence and the associated bubble dispersion, instead of modelling it. LES was applied to a bubbly plume with some success (Reddy Vanga et al., 2005, Ničeno et al. 2007, 2009, Dhotre and Smith 2007, Dhotre et al. 2007). This LES approach was also evaluated and compared to the RANS approach for boiling flows and it was found that it does not bring a real added value since there is not a sufficient difference between the large eddy size and the size of the largest bubbles. The associated CPU cost may be prohibitive since smaller meshes are necessary, but LES application to simplified situations may bring valuable information on interactions between bubbles and eddies which are shaded phenomena in the RANS approach.

#### 4.5. ILIS

ILIS is necessary to select the adequate interfacial transfer laws. This ILIS is similar to the use of flow regime maps in system codes. Here there is a unique interfacial structure corresponding to a dispersed gas-phase in a continuous liquid. As long as bubbly flow is encountered, there is no need to develop an automatic ILIS and there is no need to use an ITM. However, going to DNB occurrence, a continuous gas layer appears changing the interface structure and a criterion must be implemented for identifying this occurrence.

The description of the interface structure in bubbly flow may require addition of transport equations such as IAT (interfacial area transport) or bubble number density transport. More generally the method of the statistical moments can be used to characterise the poly-dispersion of the bubbles or a multi-group model (MUSIG method) with mass (and momentum) equations written for several bubble sizes. These two methods were evaluated to some extent, and compared to data. The MUSIG method with several mass equations for different bubble sizes and at least two momentum equations have shown good capabilities for capturing all qualitative effects in TOPFLOW (Krepper et al., 2007) vertical pipe tests in adiabatic conditions. The main difficulty is the modelling for source and sink terms associated with bubble coalescence and fragmentation which becomes very complex in both approaches.

#### 4.6. Modelling interfacial transfers

Momentum interfacial transfers control the void distribution and it is necessary to model all the forces acting on the bubbles. The virtual mass force is not expected to play a very important role, and rather reliable models exist for the drag force. More effort should be paid to the modelling and validation of lift force, turbulent dispersion force and wall force

since available models are still often tuned. In particular, since the lift force may depend on the bubble-size (Tomiyaama, 1998); it may be necessary to model poly-dispersion to take this into account. However, in most cases of boiling flows at high-velocity there will be only bubbles below the critical diameter where the lift force changes its sign.

Interfacial heat and mass transfers also depend on the bubble-size distribution. It was found that a given heat-transfer coefficient applied to a population of poly-dispersed bubbles or to an “averaged bubble diameter” could result in very different condensation rates, which demonstrates the importance of a poly-dispersion modelling of boiling flows. Moreover, condensing bubbles in sub-cooled liquid are often modelled with heat-transfer coefficients derived for solid spheres and the effect of decreasing radius is not taken into account. Neither the MUSIG method nor the method of statistical moments is provided with a complete set of validated closure relations applicable to the whole domain of simulation.

#### 4.7. Modelling turbulent transfers

Liquid turbulence plays a very important role in boiling flows. It influences liquid temperature diffusion, bubble dispersion, bubble detachment, bubble coalescence and breakup which affect the interfacial area. Then the liquid turbulent scales have to be predicted correctly to model all these processes and this will require additional transport equations. The k-epsilon or shear stress transport (SST) methods were used with some success in DEBORA (Morel et al. 2003) and TOPFLOW (Lucas et al, 2005). If the swirling flow past a spacer grid vane must be modelled, it is shown (Mimouni et al., 2008, 2009) that the SST models can perform better than the k-epsilon model. The LES approach has been evaluated in the simulations of deep bubble column experiment (Ničeno et al., 2007). LES can only be used in situations for which the bubble-size is small enough compared to large turbulent eddies and it must be further evaluated and compared to the RANS approach for boiling flows in confined conditions.

#### 4.8. Modelling wall transfers

The wall function for momentum should be adapted to the boiling flow situation, should not be too sensitive to the mesh size, and should allow converged solutions with reasonably coarse-mesh size close to a heating wall. Such wall functions are used (see Končar et al., 2011). A wall function which models the effects of the roughness due to attached bubbles was validated on Arizona State University (ASU) tests (Končar, 2007, 2009). A “wall force” exerted on bubbles close to a wall is often used in the models without a consensus on its expression (Antal, 1991, and Tomiyama, 1998).

The boiling model of Kurul and Podowski (1991) and the Ünal (1976) correlation for bubble detachment diameter are often used in boiling flows. They do not perform uniformly well in all test conditions and they may be sensitive to mesh size when the near-wall properties are calculated from the state in the first wall-adjacent cell. Further progress is still necessary for energy wall functions.

The DNB criterion in local variables also remains to be found. First demonstration calculations used a limiting value of the void-fraction in the first cell close to the heating wall as DNB criterion and simulated boiling flow conditions in real WWER type core assemblies within the NURESIM project. CHF in heated tube with steam-water is predicted with a 10% accuracy in a large domain of parameters (Vyskocil and Macek, 2010). Although the simulation results are not so far from the experiments, it is clear that the issue

is still fully open. The basic phenomenon responsible for the DNB occurrence being still unclear, one may expect that new experiments or possibly DNS simulations will be necessary to clarify the DNB process before proposing physically based local DNB criterion. This criterion may be also empirically correlated as a function of local variables, on the basis of experimental data.

#### 4.9. Status of the modelling

The average accuracy of CFD predictions of boiling bubbly flow is still not fully satisfactory and one would expect improvements in order to meet the final objectives. However, in two-phase flow modelling, the past experience of system codes shows that at least two decades of R&D may be necessary to bring a new modelling approach to the maturity.

The last advances in the understanding of flow processes and in the modelling were obtained in the following fields:

- Wall function laws for momentum specific for boiling bubbly flow were validated on the TAMU boundary layer data.
- Mechanical laws including interfacial forces and turbulence were extensively validated.
- Poly-dispersion effects were investigated in adiabatic flow and in presence of boiling and condensation.
- CFD was validated on the local data obtained in real rod bundle geometry (BWR Full-size Fine-mesh Bundle Test (BFBT) and PWR sub-channel and bundle tests (PSBT)).
- Many attempts to develop a physically based local DNB criterion were made. They were not successful and a very simple criterion on the local void-fraction or the Podowski and Podowski criterion is still the best available predictor.

Further progresses are expected on each of these topics but at least, the relative importance of each process is now well identified.

In order to progress in the understanding of micro-scale phenomena and of the DNB mechanism itself, micro-scale simulation tools were further developed, and applied to some investigations. Many parametric studies are available on nucleation, growing and detachment of bubbles with effects of cavities, interactions between nucleation sites. These simulations are still limited to pool boiling and one may expect that they may bring in the future also useful information in convective boiling.

Although the accuracy of CFD predictions is not yet fully satisfactory, CFD can already be used for some parametric studies and as a tool for helping the fuel design. If CFD cannot yet replace the experimental validation of a new fuel design in full-size experiments like LWL for VVER, it can already be used in the design optimisation phase.

In addition, the maturity of the models seems sufficient to try to analyse the so-called “non-uniform heat-flux effect” on DNB: CHF depends on the history of the power received by the fluid and not only on total heat received at location where it occurs. It is supposed that this effect is related to the development of the two-phase boundary layer close to the heating wall. CFD can allow a more physically based modelling of this effect for CHF prediction by sub-channel analysis.

The analysis of BFBT and PSBT rod bundle data with CFD, system codes and sub-channel codes illustrated the benefit of a multi-scale analysis. Today even the average void-fraction is not better predicted by CFD than by 1D simulation tools, but CFD brings a lot of information for improving system codes and sub-channel codes. In particular, the transverse mixing in a rod bundle may be more physically modelled in sub-channel codes by using models derived from CFD. CFD can quantify the various effects of turbulence diffusion of heat and momentum, of turbulent dispersion of bubbles, of spacer grids and of dispersion effects due to averaging over the sub-channel section and will allow future progress of sub-channel codes.

#### 4.10. Validation matrix for the DNB issue

##### 4.10.1. Available data for DNB

A review of existing experimental data, which may be used to validate CFD application to DNB was made within the NURESIM project (Bestion et al., 2006, 2007). Table 4.1 summarises the main characteristics of this database and shows what basic model of CFD tools may be validated by each experiment. The following experimental programmes were considered.

##### **Texas A&M boiling flow experiment in rectangular vertical channel**

The experimental test section was designed to investigate the sub-cooled boiling of refrigerant HFE-301 at low system pressure. The refrigerant was pumped through a vertical, rectangular 530 mm long channel made of transparent polycarbonate of nearly square cross-sectional area (Estrada-Perez and Hassan, 2010). A thin heater was attached 320 mm from the channel inlet to one of the lateral walls of the channel. The channel cross-section has width to height ratio close to unity and a hydraulic diameter of 8.2 mm, which resembles the coolant sub-channels of boiling and pressurised nuclear water reactors (BWR, PWR). Time-averaged velocities, turbulence intensities and Reynolds stresses in axial and normal direction were measured by the means of PTV. The data were recorded at three different Reynolds numbers 3309, 9926, 16549 and 13 different heat fluxes ranging from 0 to 64 kWm<sup>-2</sup>.

An important advantage of considered experiments is that they provide useful information on the flow behaviour close to the wall including the shear velocity. However, one of the main weaknesses is unavailability of the gas-phase measurements, such as void-fraction, bubble-size and bubble-velocity. These data can be acquired using the shadowgraph technique, which is envisaged for the upcoming experiments.

##### **DEDALE air-water bubbly flow tests**

DEDALE is an adiabatic air-water experiment performed at EDF/DER (Grossetête, 1995) analysing the axial development of a bubbly flow in a vertical pipe up to the transition to slug flow with local information for the validation of dynamics-related models in CFD tools.

##### **CHAPTAL adiabatic water-Freon tests in a pipe**

The CHAPTAL test section is a 5 m long vertical pipe with an inside diameter of 38 mm. The working liquid fluid is water. Gas bubbles are made of R116 refrigerant fluid. The resulting flow is an adiabatic two-phase flow.

The local measurements characterise each phase along diameters at different elevations ( $Z= 7.5D$ ,  $54.5D$  and  $115.5D$ ) with bi-hot-film and bi-optical probes. Liquid mean and

fluctuating velocity is measured. As concern the gaseous phase, void-fraction, interface velocity, interfacial area concentration and mean Sauter diameter are measured by bi-optical probes.

The combined effects of bubble dynamics and bubble-size distribution are investigated in adiabatic vertical upward two-phase flow in a pipe.

#### **DEBORA boiling flow tests in a heated pipe**

The DEBORA experiment (Garnier et al. 2001) was carried out at the Commissariat à l'Énergie Atomique et aux Énergies Alternatives (French Alternative Energies and Atomic Energy Commission) to provide a reliable local data base on boiling phenomena (up to DNB) in PWR T/H condition ranges. The test section is an electrically heated vertical tube with upward R12 boiling flow simulating PWR in-core T/H conditions, with local measurements along a diameter within the outlet tube cross-section of both steam phase characteristics (void-fraction, interfacial area concentration, bubble-size and mean axial velocity) and liquid phase parameter (temperature). Temperature of the tube wall outer surface was also measured at a few locations close to the tube outlet.

#### **DEBORA tests in a heated pipe with a turbulence promoter/enhancer (swirl flows)**

The “DEBORA-promoter” (see Boucker et al., 2006) tests with a vane type turbulence promoter/enhancer were carried in addition to the previous ones, to characterise the two-phase boiling flow behaviour in a complex geometry representing a spacer grid.

#### **AGATE single-phase tests**

The AGATE experiment has been developed in CEA Grenoble (see Bestion et al., 2006). Two test sections were used:

- “AGATE-grid” consists of a 5X5 rod bundle inside a squared-section housing with a mixing vane grid.
- “AGATE-promoter” with a similar geometry as “DEBORA-promoter” one (i.e. pipe with a three vane turbulence enhancer).

Non-heated water flows upward in the vertical test section and velocity measurements are made using laser doppler anemometry (LDA). Both the mean velocity and velocity fluctuations are measured in order to investigate the effects of the grid or promoter.

The data allow validation of the turbulence modelling with spacer grid (or turbulence promoter/enhancer) effects in single-phase conditions. They were used for validation of a 1D model with a  $k-\varepsilon$  turbulence model (Serre et al., 2005).

#### **ASU tests of boiling flow in a heated annular channel**

Experiments of turbulent sub-cooled flow in a vertical annular channel were carried out at the ASU (Roy et al., 1994, 1997, 2002; Kang et al., 2002) to provide detailed information on average flow structure, temperature, and gas and liquid flow fields in fully developed nucleate boiling, as well as on turbulent variables controlling transport mechanisms. In the experiment, R-113 was the working fluid.

Measurements used simultaneously a two-component LDV for liquid velocity and a fast response cold-wire for the temperature field, as well as a dual-sensor fibre optic probe for the vapour fraction and vapour axial velocity.

### **Purdue University (PU/NE) tests of boiling flow in a heated annular channel**

Experiments have been carried out at the Purdue University School of Nuclear Engineering in an internally heated annulus to provide local measurements of void-fraction, interfacial area concentration and interfacial velocity in sub-cooled boiling (Bertel et al., 1999, 2001, Situ et al., 2004). Water at atmospheric pressure was the working fluid. Influence of inlet liquid temperature, heat-flux and inlet liquid velocity on local flow parameters was specially investigated. The chosen geometry and set of conditions were aimed at scaling the conditions of a BWR. Although properties at 70 bars could not be represented, geometrical, hydrodynamic and thermal similarities for the flow boiling processes were preserved.

Additionally, the experimental results have been complemented by visual observations of the boiling processes, which provided essential information on the displacement between the location of net vapour generation (NVG) and the location of bubble detachment. More recent photographic studies of bubble lift-off diameters have been presented by Situ et al. (2004, 2005).

### **Korea Atomic Energy Research Institute (KAERI) tests of boiling flow in a heated annular channel**

Experiments have been carried out at KAERI in two separate internally heated annulus test channels using water and R134a to provide local measurements of void-fraction and phase velocities in sub-cooled boiling (Yun et al., 2010(a), 2010(b), Chu et al., 2017). Water at low-pressure (one to two bars) and R134a (13 to 27 bars) are the working fluids. The aim was to provide a database for sub-cooled boiling modelling, including aspects such as force balances for departing vapour bubbles and bubble population balance.

The test channel for water boiling is a vertical concentric annulus, 4.165 m long with a heated inner tube. The inner tube includes a 3.087 m heated section. The inner diameter of the outer wall is 35.5 mm, and the outer diameter of the inner wall (heated rod) is 9.98 mm. Measurements of steam phase characteristics (radial profiles of void-fraction, interfacial area concentration, bubble-size, and axial velocity) were taken using a double-sensor optical fibre probe. Radial profiles of water velocity were measured by Pitot tubes, correcting for the effect of bubbles (Reimann et al., 1983) and radial profiles of water temperature were measured by thermo-couples with 0.25 mm diameter. Wall temperatures were measured by thermo-couples embedded on the heated rod.

The test channel for R134a boiling is a vertical concentric annulus 2.88 m long with a heated inner tube. The inner tube includes a 1.75 m heated section. The inner diameter of the outer wall is 27.2 mm, and the outer diameter of the inner wall (heating tube) is 9.5 mm. Measurements of vapour phase characteristics (radial profiles of void-fraction, interfacial area concentration, bubble-size, and axial velocity) were taken using a double-sensor optical fibre probe. Local wall temperature distributions were measured by two moving thermo-couples, which were installed inside the heating tube.

### **Experimental data on TOPFLOW loop on two-phase flow in a vertical tube**

The structure of an adiabatic air-water and of steam-water flow with reduced condensation and with slight sub-cooling in a vertical pipe of 195.3 mm inner diameter (DN200) was studied using wire-mesh sensors. The experiments were performed at the Two-Phase Flow Test Facility (TOPFLOW) of Safety Research of Forschungszentrum Dresden-Rossendorf e.V. (see Prasser et al., 2006). Beside experimental data for air-water flow at ambient conditions, also data obtained for steam-water flows under nearly adiabatic conditions as well as with slightly sub-

cooled water are available for pressures of one and two MPa. Wire-mesh sensors can characterise the shape of large bubbles, since they acquire the phase distribution in the entire cross-section.

The DN200 pipe is equipped with a variable gas injecting system that allows injection of air or steam at 18 different vertical positions upstream of the measuring position to study the evolution of the flow structure along the flow (Prasser et al., 2007).

Radial gas fraction profiles as well as bubble-size distributions can be calculated (Prasser et al., 2002). Radial gas velocity profiles were obtained by means of a point-to-point cross-correlation between the signals of both sensors placed in a distance of 63 mm behind each other (Prasser et al., 2002a). Bubble-size distributions were extracted from the measuring data.

### **TOPFLOW tests with condensation**

For the condensation experiments, some extensions were implemented in the facility. The test section consists of a vertical steel pipe with an inner diameter of 195.3 mm and a length of about eight metres.

The measurement plane, which consists of a pair of wire-mesh sensors and a lance with thermo-couples is located at the upper end of the test section.

The supply of the liquid phase allows for sub-cooling of the water of several Kelvin depending on the flow rates.

In addition to the measurement of the two-phase flow characteristics by wire-mesh sensors, also information on local temperatures was determined. For this reason, a lance of thermo-couples is mounted directly above the wire-mesh sensor. It spans over the whole pipe diameter. The single positions of the thermo-couples can be assigned to single measuring points of the wire-mesh sensor. This allows to combine the information on local void-fraction and local temperature, and to determine the liquid temperature from measured mixture temperature by co-relating the temporal signals of both measurements.

### **BFBT data on void-fraction distribution in BWR fuel assembly**

Experimental tests for measuring the void-fraction distribution inside BWR fuel assemblies have been conducted by the Nuclear Power Engineering Corporation (NUPEC) by the use of an experimental facility referred to as BFBT. Data provided by such facility are currently being used for CFD code assessment in the framework of an OECD-NEA/US NRC Benchmark. An X-ray CT scanner and X-ray densitometers are employed to measure the void-fraction distribution in a BWR full-scale fuel assembly under steady-state and transient conditions (Inoue et al., 1995). The void-fraction data have a  $0.3 \times 0.3 \text{ mm}^2$  resolution. Such a high-resolution makes those data useful for CFD code validation.

The test section consists of a full-scale BWR fuel assembly simulator, which is made of electrically heated rods able to reproduce the actual power profiles generated by nuclear fission. The instrumentation allows measurements of temperature, flow rate, pressure and, mainly, void-fraction.

### **PSBT data on void-fraction distribution in PWR fuel assembly**

The NUPEC PSBT constitute an experimental database on the fluid flow and heat-transfer in nuclear reactor coolant channels, useful to support model and code development and validation, both at sub-channel and microscopic scale. An exhaustive description of the PSBT database can be found in the benchmark specifications (Rubin et al., 2010).

The test facility can reproduce typical PWR operating conditions (working fluid, pressure, temperature). Different tests section can be used on the same loop, to simulate either a single coolant sub-channel or an entire 5x5 rod bundle, electrically heated rods being always used in place of fuel pins. Two test sections, respectively, are used for void distribution measurement tests; a third one, of 6x6 rod bundle-type, is used for DNB measurements.

A  $\gamma$ -ray computer tomography scanner is used to provide steady-state measurement of the void-fraction distribution over a cross-section with a spatial resolution of 0.5 mm.  $\gamma$ -ray densitometer measurements of chordal-averaged void-fraction are provided as well.

Both steady-state and unsteady tests are performed; the latter feature transient variations of the operating and inlet conditions.

### **CHF tests in tubes**

Russian Academy of Sciences produced a series of standard tables of CHF as a function of the local bulk mean water condition and for various pressures and mass velocities for fixed tube diameter of eight mm (Collier, 1981, USSR Academy of Sciences, 1976). These tables are valid for length/diameter ratio equal or greater than 20. For the tube diameters other than eight mm the CHF values are given by the approximate relationship valid for tube diameter in range between four mm and 16 mm.

### **Large water loop experimental test facility**

The large water loop has been built at the nuclear machinery plant, ŠKODA, Plzen Ltd. The loop is non-active pressurised-water equipment with technological and thermal parameters corresponding to those of PWR. The CHF experimental facility (a part of large water loop) has been designed for the research of CHF in water flow through a bundle of electrically heated rods. Some information was reported in the NURESIM project (see Bestion, Macek et al., 2007).

Seven formed the test sections or 19 parallel electrically heated rods with external diameters of nine mm; axially and radially uniform or non-uniform heat-flux distribution and water up flow were used in the tests. The rods (3 500 mm long) were placed in regular hexagonal geometry with a pitch of 12.5-13 mm. Critical conditions were obtained under constant thermal-hydraulic conditions by gradually increasing heat input.

### **Gaertner et al (1965) test facility**

A photographic study was made of saturated nucleate pool boiling at a pressure of one atmosphere. Over 1 000 still photographs and 12 high-speed motion pictures were taken of water boiling from a two-in-dia flat horizontal surface facing upward. Two surfaces were studied: a 2/0 polished platinum surface and a 4/0 polished copper surface. The platinum surface was studied in the heat-flux range of 14 700 to 176 000 Btu/hr, sq ft, and the copper surface from the incipient boiling heat-flux of 10 500 Btu/hr, sq ft to the maximum flux of 493 000 Btu/hr, sq ft. Data were obtained for the break-off diameters of discrete bubbles, and for the populations of active sites at heat fluxes up to 58 600 Btu/hr, sq ft. At least three, and possibly four heat-transfer regions were found to exist in nucleate boiling, depending upon the mode of vapour generation. The vapour structures on the surface progressed through a sequence of first discrete bubbles, then vapour columns and vapour mushrooms, and finally vapour patches, as the surface temperature was increased. These individual vapour structures, or combinations of them, determine the mechanism of heat-transfer in the four nucleate boiling regions. It was concluded that any heat-transfer model

or design equation, which is based on the dynamics of individual bubbles, or on any other single mechanism, must be in serious error.

#### **Liu and Bankoff's test facility**

In his PhD thesis (Liu and Bankoff, 1993a and 1993b), Liu investigated the structure of air-water turbulent bubbly flows in a vertical pipe. Liu and Bankoff carried out a series of 42 experiments at atmospheric pressure and a temperature of 10°C. This database is ideal for model testing and validation in the low Eötvös number regime ( $0.5 < Eo < 2$ ), typically characterised by small roughly-spherical bubbles (average bubble-size in the range of 2-4 mm) and wall-peaked void-fraction distributions. Marfaing et al (2018) present a benchmark simulation of these experimental runs with different two-phase flow models, performed by American and European teams. An uncertainty quantification study is carried out.

The experimental test section was a 2 800 mm long, vertical smooth acrylic tubing, with inside diameter 38 mm. A mixture of water and air bubbles was injected at the bottom of the pipe with prescribed superficial velocities  $J_l$  and  $J_g$ . According to the authors, the injection method ensured a uniform bubble-size distribution at the pipe inlet. The average flow was observed to be steady and axi-symmetric. The Reynolds number ranged from 15 000 to 55 000. A measuring station was located at a height of 36 hydraulic diameters, or 1.4m, and recorded the radial profiles of liquid/gas velocity, velocity fluctuations, bubble diameters, void-fraction.

#### **Nakoryakov et al.'s test facility**

Nakoryakov et al. (1996) investigated the structure of low Reynolds number bubbly flows in a vertical pipe. Their test section was a vertical cylindrical pipe with internal diameter 14 mm and height 6.5 m, at the bottom of which a mixture of gas and liquid was injected. The gas was air. The liquid used was an aqueous solution of sodium hydroxide, potassium ferri- and ferrocyanide, to which glycerine was added to increase the viscosity. In the reported experiments, the Reynolds number was comprised between 875 and 1860. For such low Reynolds numbers, the corresponding single-phase flow would be "laminar". The observed liquid velocity fluctuations ("pseudo-turbulence") are due to the presence of bubbles. The flow was observed to be statistically steady and axi-symmetric – statistically meaning that the average flow, not its fluctuations, is steady and axi-symmetric. A measuring station, located at the top of the pipe, recorded the radial profiles of void-fraction, liquid velocity and velocity fluctuations. Measurements were made with an electro-diffusional method, based on the rate of mass transfer from a microelectrode to the liquid. The probe was able to get to a distance  $y$  from the wall of one tenth of a bubble diameter. Marfaing et al (2016, 2017a, 2017b) analyse the void-fraction distribution in the near-wall region, both analytically and numerically. Nakoryakov's measurements, which go very close to the wall in comparison to other experimental data from the literature, can be used to estimate the bubble dispersion near the wall.

#### **Milenkovic's test facility (2005)**

This PhD thesis was conducted at ETH Zurich. The main motivation is to better understand bubble trapping in eddies in free turbulent shear flows and the interaction between bubble motion and liquid velocity.

The experiments have been carried out with liquid-and bubbly jet flows generated by a gas/liquid injector. Bubbly jet flows are formed by a vertical water jet containing bubbles of various well-controlled sizes and volume fraction. The jet is injected into a water volume

contained in a large plexiglas tank to minimise wall effects. If the jet is periodically excited with controllable frequency and amplitude, it is called triggered jet. The excitation is achieved by periodically modulating the jet shear layer by means of a coaxial water layer injected close to the jet exit through an annular nozzle.

Two-camera PIV, double optical sensor (DOS), and laser-induced fluorescence (LIF) were the main experimental techniques used. In order to study trapping phenomena, simultaneous PIV and shadow graphic were applied for tracking the large vortices and bubble structures.

The DOS results indicate clustering of the bubbles in coherent vortex structures, with a periodic variation of void-fraction during the excitation period.

### **PETHER test facility**

The objective of PETHER test facility (Bucci, 2017; Richenderfer et al., 2017) is to improve the understanding of sub-cooled pressurised flow boiling and DNB mechanisms by elucidating the relationship between surface properties, fundamental boiling quantities, heat-flux partitioning and boiling crisis (DNB). The facility leverages advanced high-speed IR and video cameras and elaborated post-processing tools. Engineered surfaces with modified wettability and surface morphology (in order to control the nucleation site density and the bubble departure frequency) as well as prototypical fresh and oxidised zircaloy surfaces (to mimic actual reactor conditions) are used.

High-speed IR thermometry enables measurements of time-dependent temperature and heat-flux distributions exactly on the boiling surface (space resolution down to 20-30  $\mu\text{m}/\text{pixel}$ , time resolution up to 10 000 fps, total imaged area 1 x 1  $\text{cm}^2$ ). In turn, temperature and heat-flux distributions enable measurements of fundamental boiling quantities such as nucleation site density, wait time, growth time, bubble departure frequency, dry area fraction, contact line density, bubble thermal footprint surface distribution, etc., as well as direct measurement of the wall heat-flux partitioning (e.g. to quantify the importance of micro-layer evaporation and other heat-transfer mechanisms), from sub-cooled forced convection up to CHF. The formation and the growth of dry spots (leading to CHF) can also be imaged. The flow field is also visualised with high-speed video systems.

With conventional heaters, average wall temperature and heat-flux are measured. The flow field is also visualised with high-speed video systems. These experiments are run with zircaloy plates (same morphology and thickness as reactor cladding), fresh or oxidised.

### **Central Research Institute of Electric Power Industry (CRIEPI) test facility**

The test facility is situated at CRIEPI in Tokyo, Japan (Furuya et al., 2017). The height of the facility is approximately six metres. Experiments are performed in air-water flow. The test facility consists of a water circulation pump, air compressor, air receiver tank, air-water separation tank, heat exchanger and a test pipe. The water temperature is maintained at 30°C by the heat exchanger. The test pipe is a bubble column of the round PVC (polyvinyl chloride) pipe, whose internal diameter,  $D$ , is 224 mm. The upstream section is more than 4.5 m (20.3  $D$ ) long from the height where the WMS is inserted. The superficial liquid velocity,  $j_L$ , is 0.63 m/s. The superficial gas velocity,  $j_G$ , is 0.63 m/s, as well. The non-dimensional distances of WMS from the air nozzle,  $z/D$  are 1.78, 3.57, 7.14, and 10.7. In order to acquire three-dimensional two-phase flow structures at high temporal and spatial resolutions necessary for the development and validation of the computational multi-fluid dynamics (CMFD) code models, an algorithm was developed to measure three-dimensional

velocity of individual bubble with a bubble-pairing scheme. The bubble-pairing scheme finds a pair of bubble in two sets of wire-mesh sensor data to determine the direction and magnitude of velocity vector for each bubble. The sampling rate of the WMS is 1 000 frames/s and the acquisition time is five seconds. The direction and magnitude of velocity vector is determined by the differences in position and time of centre mass of the paired bubbles. The algorithm is applied to the bubble column in the vertical pipe (i.e. 224 mm) at 0.64 m/s for both the same air and water superficial velocities.

### **SUBFLOW test facility**

The SUBFLOW facility (Ylönen, 2013; Ničeno et al., 2013; Ylönen et al., 2011) is an adiabatic test loop with a fuel rod bundle model. The European pressurised reactor (EPR) is used as reference reactor for the rod bundle. An important aspect of the facility is the use of wire-mesh sensors to achieve high temporal and spatial resolution of experiment results. It must also be noted that this was the first facility in the world to employ WMS in a rod bundle.

The experimental set-up is scaled up linearly with a factor of about 2.6 from real fuel elements because the coolant is modelled as adiabatic air-water flow instead of water-steam flow. Acrylic glass pipes of 25 mm outer diameter and 19 mm inner diameter, filled with demineralised water, act as fuel rods in the set-up. This leads to hydraulic diameter  $DH$  of 33.9 mm for the sub-channel. The channel walls and half pipes on the walls were all made of same transparent material for visualisation purposes. The overall test section is square with dimensions 136×136 mm.

The wire-mesh sensor provides instantaneous (local) two-dimensional gas fraction distributions over the whole cross-section. With data processing, time-averaged void fractions can be calculated. Using two sensors, also bubble-velocity profiles, bubble-size distributions and bubble-size resolved radial gas fraction profiles can be calculated. In addition, the axial evolution of these profiles can be attained.

### **LINX facility**

The LINX facility is described in detail by Simiano (2005) and Zboray and Cachard (2005). It consists of a cylindrical vessel (stainless steel) two metres in diameter and 3.4 m in height, with a total volume of 9.42 m<sup>3</sup>. A specially designed injector at the bottom of the vessel, consisting of 716 capillary tubes of two mm inner diameter distributed uniformly over a circular area of 15 cm diameter, enables air injection to take place with a constant and equal flow rate per needle. With this arrangement, a broad, axi-symmetric bubble plume with a narrow bubble-size distribution diameter of around two to three mm is obtained. Isothermal tests are performed at atmospheric pressure. The test parameters are the inlet gas mass flux and the immersion depth (i.e. the pool height above the injector). The uniqueness of the measurements lies the fact that they were acquired simultaneously for the bubble and liquid velocities, together with the volume fraction of the gas-phase. Therefore, the relative velocity (after local averaging) is the true mean of the difference between the instantaneous bubble and liquid velocities, and not the difference of the means obtained from two separate sets of measurements. This distinction is important because it reveals true relative velocity and enables accurate closure laws based on relative velocity to be tested.

The data gathered in the tests, and available for assessment of the physical modelling, include: radial void-fraction profiles (obtained using optical probes), liquid-and bubble-velocity distributions inside the plume (obtained using particle image velocimetry, PIV), 3D velocity information on the recirculation flow around the plume (obtained using an

electromagnetic, current metre); bubble-size and shape information (obtained using photographic techniques). The relative uncertainty of the measured void-fraction is usually between 2% and 4%, for bubble-velocity somewhat higher (8-9%) and for liquid velocity 10-12% (for details, see Simiano, 2005). The uncertainty in the recirculation liquid velocity is about 10-15%.

#### **Kubasch's test facility (2001)**

Kubasch's PhD thesis (ETH Zurich, 2001) aims at better understanding of two-phase flow under pool scrubbing conditions, i.e. injection of high airflow rates through a single nozzle into a large water pool. The experiments were carried out in the context of severe accident research for advanced power plants.

The pool was 1 metre in diameter and pool depths up to 3 metres were investigated. Air was injected through a single nozzle (diameters of 5, 10 and 20 mm) at the bottom. The flow rate was varied between 0.42 and 3.33 dm<sub>n</sub>/s. The local measurements were performed with a DOS and a hot-film anemometer. Void-fraction, bubble and water velocity, and bubble chord length distributions were measured. Void-fraction, bubble and water velocity radial profiles collected at different elevations provided information about the expansion of the bubble plume in the horizontal direction. Bubble chord length data indicate that bubble breakup is dominant over coalescence in a plume.

#### **PUMA test facility**

The experimental work was performed using a thermo-hydraulic loop placed at the Energy Engineering Institute in Polytechnic University of Valencia (Spain). The PUMA loop (Muñoz-Cubo et al., 2012, 2017) consists of a test section, a round transparent tube made by plexiglas with constant section, an upper plenum and a lower plenum where air and water are mixed. The test section has a 52 mm inner diameter and a length of 3340 mm. Two centrifugal pumps controlled by a frequency controller circulated the water.

An LDA equipment provides the liquid phase velocity moments while a four-sensor probe is used to identify the phase and to measure the gas-phase velocity.

Several sets of experiments were performed in PUMA facility with different  $j_g$  and  $j_l$  values:

- Set A (55 runs) was devoted to studying the transition from the bubbly flow regime to the slug flow and the evolution of the void-fraction peak at the wall.
- Sets B, C, D, E (80 runs) enabled to measure the effect of changes in the surface tension on the local parameters of the two-phase flow. concentrations of 1-Butanol for the sets B,C,D, E are: 0, 9, 39, 75 ppm.
- Set F (70 runs) aimed at measuring the main local parameters of the two-phase flow at three axial locations and 15 radial positions for each particular run, measuring the turbulence intensity and the liquid velocity at two axial positions.

**Table 4.1. Available data relative to DNB investigations – Data in adiabatic flow and heated flow in simple geometry - Correspondence between the data sources and the basic phenomena at the meso-scale**

PHENOMENA	DEDALE	TOPFLOW	CHAPTAL	NAKORYAKOV	AGATE (&AGATE-PRO MOTER)	TEXAS A&M	TEXAS A&M 2016	MILENKONVIC (2005)
<b>Geometry</b>	Tube L=6 m D=0.0381 m	Tube D=195.3mm	Tube L=5 m D=0.0381 m	Tube D= 14 mm and L= 6.5 m	Rod Bundle (Tube+Promoter)	Rectangular Duct L=0.53m Dh=8.2mm	Square Duct L = 0,24m Dh = 10 Mm	Liquid-and bubbly jet flows in a large tank
<b>Fluid/flow conditions</b>	Air-Water Adiabatic	Air-Water And Steam-Water Adiabatic	Water-Freon Adiabatic	Air Aqueous solution + glycerine Room pressure and temperature	Water Adiabatic	Refrigerant Hfe-3 01 Heated	Refrigerant Hfe-3 01 Heated, Atmospheric Pressure, Inlet Temperature 20-30 °C, 3000 < Re < 15000, 0,01 < Eo < 1	Air-water room te mperature and pre ssure
<b>Local measureme nts</b>	$\alpha, A_i, \delta_B, F_{\delta}, V_{lz}, V'_{lz}, V_{bz},$ at Z/D = 8, 55 & 155	$\alpha, \delta_B, V_{bz}, F_{\delta}$	$\alpha, A_i, \delta_B, F_{\delta}, V_{bz}, V_{lz}, V'_{lz},$ at Z/D = 7.5, 54.5 & 115.5	$\alpha, \delta_B, V_{lz}, V'_{lz}, V_{bz}$	$V_{lz}, V'_{lz}, V_{lx}, V'_{lx}$	$V_{lz}, K_z$	$\delta_B, T_w, V_{bz},$ Bubble departure Frequency, Heat-Transfer Coefficient	$\alpha, V_{bx}, V_{by}, V_{bz}, V_1, V_x, V_y, V_{lz}, \delta_b,$ vorticity
<b>Wall to fluid heat -transfer</b>							x	
<b>Wall friction</b>				x		x		
<b>Bubbles transport &amp; dispersion</b>	x	x	x	x				x
<b>Vaporisation -Condensation</b>		x					x	
<b>Coalescence &amp; breakup of bubbles</b>	x	x	x				x	x
<b>Turbulent transfers of heat &amp; momentum</b>	x	x	x	x	x	x		x
<b>Effects of poly-dispersion</b>		x	x					x
<b>Effects of grids</b>					x			

**Table 4.2. Available data relative to DNB investigations - Data in heated flow in simple and complex geometry Correspondence between the data sources and the basic phenomena at the meso-scale**

PHENOMEN A	DEBORA	DEBORA PROMOTER	ASU	PURDUE BOILING	LIU AND BARKOFF	KAERI WATER BOILING	KAERI R134 BOILING	BFBT	PSBT	LWL
<b>Geometry</b>	Tube D=0.0192m	Tube + Promoter	Annulus Di=15.78mm De=38.02mm	Annulus Di=19.1mm De=38.1mm	Tube D=38mm L=2.8m	Annulus Di=9.98mm De=35.5mm	Annulus Di=9.5mm De=27.2mm	Rod Bundle	Rod Bundle	Rod Bundle
<b>Fluid/Flow Conditions</b>	R12	R12	R113	Steam-Water	Air-water, room temperature and pressure	Steam-water, Sub-cooled Boiling 1-2 Bar	R134a Sub-cooled Boiling 13-27 Bar	Steam/water	Steam/water	Steam/water
<b>Local Measurements</b>	$\alpha$ , Ai, Ti, Tw, $\delta B$ , Vbz	$\alpha$ , Ai, Ti, Tw, $\delta B$ , Vbz	$\alpha$ , Vlz, V'lz, V'lx, Vbz, Tw, T'w, Turbulent Heat Fluxes	$\alpha$ , Ai, $\delta b$ , Vbz At Z/D=52.6 + Visual observations	$\alpha$ , Ai, $\delta b$ , Vlz, Vbz	$\alpha$ , Ai, $\delta b$ , Vlz, vzb, Ti, Tw Visual observations	$\alpha$ , Ai, $\delta B$ , Vlz, vzb, Ti, Tw Visual observations	$\alpha$ $\phi_{Crit}$	$\alpha$ $\phi_{Crit}$	$\phi_{Crit}$
<b>Wall to Fluid Heat</b>	X		X	X		X	X			
<b>Bubbles Transport &amp; Dispersion</b>	X		X	X	X	X	X			
<b>Vaporisation - Condensation</b>	X		X	X		X	X			
<b>Coalescence &amp; Breakup of Bubbles</b>	X		X	X	X	X	X			
<b>Turbulent Transfers of Heat &amp; Momentum</b>	X	X	X	X	X	X	X			
<b>Effects of Polydispersion</b>	X									
<b>Effects of Grids</b>		X								
<b>Combined Effects in Real Geometry</b>								BWR		PWR WWER

**Table 4.3. Available data relative to DNB investigations - Data in heated flow in simple and complex geometry Correspondence between the data sources and the basic phenomena at the meso-scale**

PHENOMENA	Gaertner (1965)	PETher	SUBFLOW	LINX	CRIEPI	KUBASCH (2001)	PUMA
<b>Geometry</b>	Heated horizontal plate 5cm diameter	1x3 cm2 rectangular channel	4x4 rod bundle	Cylindrical vessel 2m in diameter 3.4m in height	Bubble column Height 6m Diameter 224mm	Pool diameter 1m Depth 3m Bubble plume	Cylindrical with i.d 52mm and a length of 3.34m
<b>Fluid / Flow Conditions</b>	Water/pool boiling Atmospheric pressure Wall temperature btw 110°C and 140°C	Water, sub-cooled boiling Up to ten bar Up to Re ~100000	Water (+tracer) or air-water 20°C one bar Reynolds: 9800 to 51000 Eötvös :0.5 to ~16	Air-water Atmospheric pressure axi-symmetric bubble plume	air-water 30 °C	Air-water, atmospheric pressure, room temperature	air-water + 1-butanol atmospheric pressure, room temperature
<b>Local Measurements</b>	heat-transfer coefficient, heat-flux q'', nucleation site density as a function of wall superheat, $\delta_b$	$T_w$ , nucleation site density, heat-flux, bubble departure frequency, dry area fraction	At the outlet : dimensionless mixing scalar, $\alpha$ , $V_b$ , $\delta_b$	$\alpha$ , $V_{bx}$ , $V_{by}$ , $V_{bz}$ , $V_{lx}$ , $V_{ly}$ , $V_{lz}$ , $\delta_b$ , bubble shape	$\alpha$ , $V_{bx}$ , $V_{by}$ , $V_{bz}$ , $\delta_b$	$\alpha$ , $V_{bx}$ , $V_{by}$ , $V_{bz}$ , $V_{lx}$ , $V_{ly}$ , $V_{lz}$ , $\delta_b$	$\alpha$ , $V_{bx}$ , $V_{by}$ , $V_{bz}$ , $V_{lx}$ , $V_{ly}$ , $V_{lz}$ , $\delta_b$ , $v'_{lx}$ , $v'_{ly}$ , $v'_{lz}$
<b>Wall to Fluid Heat</b>	X	X					
<b>Bubbles Transport &amp; Dispersion</b>			X	X	X	X	XX
<b>Vaporisation – Condensation</b>	X						
<b>Coalescence &amp; Breakup of Bubbles</b>	X		X	X	X	X	X
<b>Turbulent Transfers of Heat &amp; Momentum</b>			X	X	X	X	X
<b>Effects of Poly-dispersion</b>				X	X	X	X

**Table 4.3. Available data relative to DNB investigations - Data in heated flow in simple and complex geometry Correspondence between the data sources and the basic phenomena at the meso-scale (Continued)**

PHENOMENA	Gaertner (1965)	PETher	SUBFLOW	LINX	CRIEPI	KUBASCH (2001)	PUMA
Effects of Grids			X				
Combined Effects in Real Geometry							

$\alpha$ : local void-fraction,  $A_i$ : local interfacial area density,  $\delta_b$ : local average bubble diameter,  $F_\delta$ : bubble-size distribution,  $V_{lz}$ : axial mean liquid velocity,  $v'_{lz}$ : rms axial liquid velocity,  $V_{bz}$ : axial mean bubble-velocity,  $T_l$ : liquid temperature,  $T_w$ : wall temperature,  $T'_w$ : rms value of wall temperature,  $V_{lx}$ : radial component of mean liquid velocity,  $V'_{lx}$ : rms radial component of liquid velocity,  $\phi_{crit}$ : CHF.

#### 4.10.2. Remaining experimental needs

A rather extensive database was collected for boiling bubbly flow and DNB investigations. However, the measurement difficulties are still penalising the progress of the modelling for the following reasons:

- No experiments provide all principal variables of the model and very few provide together void-fraction, velocities and bubble-size. Turbulence measurements are either absent or very limited.
- No experiment provides sufficient information for a full validation of the poly-dispersion modelling with either a MUSIG approach or a method of statistical moments since effects of breakup, coalescence, nucleation, collapse and mass transfers may co-exist without any possibility to separate them.
- No experiment provides sufficient information to validate the various parts of the wall boiling heat-transfer modelling (density of sites, frequency of bubble detachment, bubble departure diameter, etc.)
- No experiment provides information on the DNB mechanism itself, neither in pool boiling nor in convective boiling.
- In rod bundles the number of measured parameters is even more limited.

In this situation the main recommendations for new experimental programmes and DNS applications are:

1. Experiment providing information on the wall boiling heat-transfer and on the DNB mechanism by using innovative measurement or visualisation techniques are expected.

Experiment providing several parameters together such as velocities, void-fraction, bubble-size, liquid turbulence and wall and fluid temperatures would be very useful. Existing test facilities in simple geometries should make efforts to add new measurement devices.

Of course, efforts to provide data with evaluation of measurement uncertainty and with the minimum possible uncertainty may also be recommended.

Micro-scale simulation techniques should be further developed and applied to wall boiling investigations first in pool boiling and then in convective boiling.

Data are needed for a broad range of micro-scale phenomena. The most crucial to be addressed are:

- *CHF mechanism under convective boiling conditions.* A specific need exists for experiments under flow boiling conditions, as other mechanisms have been proposed to prevail than in pool boiling. In particular, direct observation of the liquid micro-layer vaporising on the heater surface will be required to clarify the role of its rupture in the onset of DNB. Complementary experiments on nano-scale phenomena such as the evaporating extended meniscus (ultra-thin liquid layer below the bubble) are also necessary, as the evaporation of liquid layers and advancement or receding of interfaces are controlled by this nano-scale physics.
  - *Bubble dynamics and boiling characteristic points in a flow channel* Recent experiments provide a better understanding of the size of the bubble at detachment (and lift-off), the points of inception or onset of nucleate boiling (ONB), NVG, and

Onset of Significant Voiding (OSV). This data can now be used to verify the models affecting the micro-scale. Further developments could be to perform experiments over a broad range of pressure: the dependence of the bubble diameter at detachment and of the bubble release frequency on heat-flux should be better investigated in new experiments at high pressure.

- *Nucleation* Recent experiments under forced convection conditions are now available to address the co-relation between CHF and nucleation site density, as well as the co-relation (available for pool boiling conditions only) between active nucleation sites and wall superheat. Several types of heaters (both “fresh” and “aged”) heaters were used, which will be useful to understand how the state of the surface influences the activation of nucleation sites for increasing wall superheats. Further studies are needed to investigate over a wide range of pressures the interaction between coalescence and site activation mechanisms, which at low-pressure has been reported to produce a smaller lift-off diameter for merging bubbles than for single bubbles.
- *Basic tests on bubble transversal migration and sliding bubbles* The detachment and reattachment of bubbles (this last phenomenon being observed at high sub-cooling under low-pressure conditions) have significant influence on the cross-sectional area-averaged void-fraction and consequently on heat-transfer. On the other hand, for small sub-cooling and low-pressure, bubbles slide along the wall. To understand this variety of bubble behaviours and their relevance over a wide range of conditions, basic tests to determine the forces acting on the individual bubbles after detachment are needed, where a parametric variation of number density, pressure, flow rate and sub-cooling is carried out.
- *Basic tests on heat-flux partitioning* recently obtained experimental data has to be used to improve our understanding of heat-flux partitioning in nucleation processes. A remaining issue is the relative weight of micro-layer evaporation and transient conduction under pool boiling conditions. Attempts to obtain quantitated information have been reported. These studies could not resolve the controversy with respect to the dominant heat-transfer mechanism, thus more work is still needed for pool boiling. Progress in that area will provide the basis for experiments under convective flow conditions, which eventually will also be needed.

## References

Antal, S.P., R.T. Lahey Jr. and J.E. Flaherty (1991), Analysis of phase distribution in fully developed laminar bubbly two-phase flow, *Int. J. Multi-phase Flow*, Vol. 17, No. 5, pp. 635-652.

Bestion, D., D. Caraghiaur, H. Anglart, P. Péturaud, M. Andreani, B. Smith, E. Krepper, H.M. Prasser, D. Lucas, D. Mazzini, F. Moretti and J. Macek (2006), Review of existing data basis for validation of models for CHF, [www.nuresim.com](http://www.nuresim.com).

Bestion, D., H. Anglart, P. Péturaud, B. Smith, E. Krepper, F. Moretti and J. Macek (2007), Review of available data for validation of NURESIM two-phase CFD software applied to CHF investigations, 2007, 12<sup>th</sup> Int. Topical Meeting on Nuclear Reactor Thermal-Hydraulics (NURETH-12), Pittsburgh, Pennsylvania, United States, 30 September-4 October, also published in Science and Technology of Nuclear Installations, Volume 2009 (2009), Article ID 214512.

Bertel, M. (1999), Experimental investigation of sub-cooled boiling, M.S.N.E. Thesis, Purdue University, West Lafayette, IN, United States.

Bertel, M., M. Ishii, Y. Mi, T. Masukawa, R. Situ and M. Mori (1999), Experimental Investigation of Sub-cooled Boiling under BWR Flow Conditions, NURETH-9, San Francisco, CA, United States, 3-8 October.

Bertel, M., M. Ishii, T. Masukawa, Y. Mi and R. Situ (2001), Interfacial area Measurements in Sub-cooled Flow Boiling, *Nucl. Eng. Design*, 210, 135-155.

Beysens, D., V. Nikolayev and Y. Garrabos (2003), Vapour spreading and the boiling crisis, *J. Phys.: Condens. Matter* 15, pp. S435-S442.

Boucker, M., A. Guelfi, S. Mimouni, P. Péturaud, D. Bestion and E. Hervieu (2006), Towards the prediction of local thermal-hydraulics in real PWR core conditions using NEPTUNE\_CFD software, Workshop on Modelling and Measurements of Two-Phase Flows and Heat-Transfer in Nuclear Fuel Assemblies, KTH, Stockholm, Sweden, 10-11 October 2006.

Bricard, P. (1995), “Modélisation de l'ébullition sous-saturée et de la crise d'ébullition par caléfaction en convection forcée”, Thèse de Doctorat, Ecole Centrale Paris.

Bucci, M. (2017), “Advanced Diagnostics to Resolve Long-Lasting Controversies in Boiling Heat-Transfer”, 13<sup>th</sup> International Conference on Heat-Transfer, Fluid Mechanics and Thermodynamics (HEFAT 2017), Portoroz, Slovenia, 17-19 July 2017.

Celata, G.P., M. Cumo, A. Mariani, M. Simoncini and G. Zummo (1994), Rationalisation of existing mechanistic models for the prediction of water sub-cooled flow boiling CHF, *Int. J. Heat & Mass Transfer*, Vol. 37, Suppl. 1, pp. 347-360.

Chu, I.-C., S.-J. Lee, Y. J. Youn, J. K. Park, H. S. Choi, D.-J. Euh and C.-H. Song (2017), Experimental evaluation of local bubble parameters of sub-cooled boiling flow in a pressurised vertical annulus channel, *Nucl. Eng. Des.*, Vol. 312, pp.172-183.

Collier, J.G. (1981), “Convective Boiling and Condensation”, McGraw-Hill.

Dhotre, M.T. and B. Smith (2007), CFD simulation of large-scale bubble plumes: Comparisons against experiments, *Che. Eng. Sci.*, 62, 6615-6630.

Dhotre, M.T., B. Smith and B. Ničeno (2007), CFD Simulation of Bubbly Flows: Random Dispersion Model, *Chem. Eng. Sci.*, 62, 7140-7150.

Estrada-Perez, C.E. and Y.A. Hassan (2010), PTV experiments of sub-cooled boiling flow through a vertical rectangular channel, *Int. J. Multi-phase Flow* 36, 691-706.

Furuya, M., T. Kanai, T. Arai, H. Takiguchi, H-M. Prasser, U. Hampel and E. Schleicher (2017), Three-dimensional velocity vector determination algorithm for individual bubble identified with Wire-Mesh Sensors, *Nuclear Engineering and Design*, <https://doi.org/10.1016/j.nucengdes.2017.06.022>

Garnier, J., E. Manon and G. Cubizolles (2001), Local measurements on flow boiling of refrigerant 12 in a vertical tube, *Multi-phase Science and Technology*, Vol. 13, pp. 1-111.

Gaertner, R.F. (1965), “Photographic study of nucleate pool boiling on a horizontal surface”, *J. Heat-Transfer* 87 (1965) 17–27.

Grossetête, C. (1995), “Caractérisation expérimentale et simulations de l’évolution d’un écoulement diphasique à bulles ascendant dans une conduite verticale”, Thèse de L’Ecole Centrale Paris.

Haramura, Y. and Y. Katto (1983), “A New Hydrodynamic Model of CHF, Applicable Widely to Both Pool Boiling and Forced Convection Boiling Submerged Bodies in Saturated Liquids”, *Int. J. Heat Mass Transf.*, 26, p. 389.

Hewitt, G.F. and A.H. Govan (1990), “Phenomenological Modelling of Non-equilibrium Flow With Phase-Change”, *Int. J. Heat Mass Transfer*, 33, No. 2, p. 229.

Ha, S.J. and H.C. No (2000), A dry spot model of CHF applicable to both pool boiling and sub-cooled forced convection boiling, *Int. J. Heat & Mass Transfer*, 43, pp. 241-250.

Haramura, Y. and Y. Katto (1983), A new hydrodynamic model of CHF applicable widely to both pool and forced convection boiling on submerged bodies in saturated liquids, *Int. J. Heat & Mass Transfer*, Vol. 26, No. 3, pp. 389-399.

He, Y., M. Shoji and S. Maruyama (2001), Numerical study of high heat-flux pool boiling heat-transfer, *Int. J. Heat & Mass Transfer*, 44, pp. 2357-2373.

Hino, R. and T. Ueda (1985) “Studies on Heat-Transfer and Flow Characteristics in Sub-cooled Flow Boiling – Part 2, Flow Characteristics”, *Int. J. Multi-phase Flow*, 11, p. 283.

Ho, W.H., K.C. Tu, B.S. Pei and C.J. Chang (1993), “A Theoretical CHF Model for Low-Pressure, Low Mass Flux, and Low-Steam-Quality Conditions”, *Nucl. Technol.*, 103, p. 332.

Inoue, A. et al. (1995), Void-Fraction Distribution in BWR Fuel Assembly and Evaluation of Sub-channel Code, *Journal of Nuclear Science and Technology*, 32, 629~640, July 1995.

Jiji, L.M. and J.A. Clark (1964), “Bubbly boundary Layers and Temperature Profiles for Forced Convection Boiling in Channel Flow”, *Trans. ASME, Ser. C., J. Heat-Transfer*, 86, p. 50.

Kang, S. and R.P. Roy (2002), “Vapour Phase Measurements in Sub-cooled Boiling Flow”, *Journal Heat-Transfer*, 124, pp. 1207-1209.

Kataoka, I., S. Kodama, A. Tomiyama and A. Serizawa (1997), “Study on Analytical Prediction of Forced Convective CHF Based on Multi-Fluid Model”, *Nucl. Engrg Des.*, 175, p. 107.

Končar, B., I. Kljenak and B. Mavko (2004), “Modelling of local two-phase flow parameters in upward sub-cooled flow boiling at low-pressure”, *Int. J. Heat Mass Transfer*, 47, 1499-1513.

Končar, B., I. Kljenak and B. Mavko (2004), Nucleate Boiling Flow simulation with Coupling of Eulerian and Lagrangian Methods, Proc. of HT2005, 2005 ASME Summer Heat-Transfer Conference, 17-22 July, San Francisco, CA, United States.

Končar, B. (2007), Use of two-phase wall function for simulation of boiling flow, companion paper proposed at NURETH 12, Pittsburgh, Pennsylvania, United States, 30 September-4 October 2007.

Končar, B., and E. Krepper (2008), CFD simulation of convective flow boiling of refrigerant in a vertical annulus, *Nucl. Eng. Des.*, Volume 238, Issue 3, 2008, pp. 693-706.

Končar, B., C. Morel, S. Mimouni, L. Vyskocil, G. Hazi and M.C. Galassi (2011), CFD modelling of boiling bubbly flow for DNB investigations, *Multi-phase Science and Technology*, Volume 23, Issue 2-4.

Krepper, E., C. Morel, B. Ničeno and P. Ruyer (2011), CFD modelling of adiabatic bubbly flow, *Multi-phase Science and Technology*, Volume 23, Issue 2-4.

Krepper, E., T. Frank, D. Lucas, H.-M. Prasser and P.J. Zwart (2007), Inhomogeneous MUSIG model – a population balance approach for poly-dispersed-bubbly flows, The 12<sup>th</sup> International Topical Meeting on Nuclear Reactor Thermal-Hydraulics (NURETH-12), 30 September-4 October 2007, Pittsburgh, United States.

Krepper, E., P. Ruyer, M. Beyer, D. Lucas, H.-M. Prasser and N. Seiler (2009), CFD Simulation of Poly-dispersed Bubbly Two-Phase Flow around an Obstacle, *Science and Technology of Nuclear Installations*, Volume 2009 (2009), Article ID 320738.

Kurul, N. and M.Z. Podowski (1991), Multi-dimensional effects in forced convection sub-cooled boiling, International Heat-Transfer Conference, Jerusalem, Vol. 1, Paper BO-04, pp. 31-45.

Le Corre, J.M. and S.C. Yao (2007), A mechanistic model of CHF under sub-cooled flow boiling conditions for application to one and three-dimensional computer codes, NURETH-12, Pittsburgh, Pennsylvania, United States, 30 September-4 October.

Lee, C.H. and I. Mudawwar, “A Mechanistic CHF Model for Sub-cooled Flow Boiling Based on Local Bulk Flow Conditions”, *Int. J. Multi-phase Flow*, 14, 711 (1988).

Lee, T.H., G.C. Park and D.J. Lee (2002), “Local Flow Characteristics of Sub-cooled Boiling of Water in a Vertical Concentric Annulus”, *Int. J. Multi-phase Flow*, 28, 1351-1368.

Liu, T.J. and S.G. Bankoff (1993a), “Structure of air-water bubbly flow in a vertical pipe—I. liquid mean velocity and turbulence measurements”, *International Journal of Heat and Mass Transfer*, Volume 36, Issue 4, March 1993, pp. 1049-1060.

Liu, T.J. and S.G. Bankoff (1993b), “Structure of air-water bubbly flow in a vertical pipe—II. Void fraction, bubble velocity and bubble size distribution”, *International Journal of Heat and Mass Transfer*, Volume 36, Issue 4, March 1993, pp. 1061-1072.

Lucas, D., E. Krepper and H.M. Prasser (2007), “Modelling of the evolution of large bubbly flow along a vertical pipe”, 2007, *Nuclear Technology*, 158, 291-303.

Marfaing, O., M. Guingo, J. Laviéville, G. Bois, N. Méchitoua, N. Méricoux and S. Mimouni, (2016), “An Analytical Relation for the Void-Fraction Distribution in a Fully Developed Bubbly Flow in a Vertical Pipe”, *Chemical Engineering Science*, 152: 579–585.

Marfaing, O., M. Guingo, J. Laviéville and S. Mimouni (2017a), Analytical Void-Fraction Profile near the Walls in Low Reynolds Number Bubbly Flows in Pipes: Experimental Comparison and Estimate of the Dispersion Coefficient, *Oil and Gas Science and Technology – Reviews IFP*.

Marfaing, O. and J. Laviéville (2017b), “Bubble Force Balance Formula for Low Reynolds Number Bubbly Flows in Pipes and Channels: Comparison of Wall Force Model”, *International Journal of Chemical Reactor Engineering*, 2017; 20170053.

Marfaing, O., M. Guingo, J. Laviéville, S. Mimouni, E. Baglietto, N. Lubchenko, B. Magolan, R. Sugrue and B. T. Nadiga (2018), Comparison and Uncertainty Quantification

of Two-Fluid Models for Bubbly Flows with NEPTUNE\_CFD and STAR-CCM+, accepted for publication in *Nuclear Engineering and Design*.

Mimouni, S., F. Archambeau, M. Boucker and J. Laviéville (2008), CFD Modelling of sub-cooled boiling in the NEPTUNE\_CFD code and application to fuel assembly analysis, XCFD4NRS, GRENOBLE, FRANCE, 10-12 September 2008.

Mimouni, S., F. Archambeau, M. Boucker, J. Laviéville and C. Morel (2009), “A Second-Order Turbulence Model Based on a Reynolds Stress Approach for Two-Phase Flow—Part I: Adiabatic Cases”, *Science and Technology of Nuclear Installations*, Volume 2009, Article ID 792395.

Morel, C., W. Yao and D. Bestion (2003), Three-Dimensional modelling of boiling flow, The 10<sup>th</sup> International Topical Meeting on Nuclear Reactor Thermal-Hydraulics (NURETH-10), Seoul, Korea, 5-9 October 2003.

Morel, C., S. Mimouni, M. Laviéville and M. Boucker (2005), R113 Boling Bubbly Flow in an annular Geometry simulated with the NEPTUNE code, 11<sup>th</sup> Int. Topical Meeting on Nuclear Reactor Thermal-Hydraulics (NURETH-11), Avignon, France, 2-6 October.

Morel, C. and J.M. Laviéville (2009), Modelling of Multisize Bubbly Flow and Application to the Simulation of Boiling Flows with the NEPTUNE CFD Code, *Science and Technology of Nuclear Installations*, Volume 2009, Article ID 953527.

Muñoz-Cobo, J.L., S. Chiva, M. Ali Essa and S. Méndez-Díaz (2012), “Tracking of Bubble Trajectories in Vertical Pipes in Bubbly Flow Regime by Coupling Lagrangian, Eulerian and 3D Random Walks Models: Validation with Experimental Data”, *The Journal of Computational Multi-phase Flows*, 4. 309-326. 10.1260/1757-482X.4.3.309.

Muñoz-Cobo, J.L., S. Chiva, S. Méndez, G. Monrós, A. Escrivá and J.L. Cuadros (2017), Development of Conductivity Sensors for Multi-Phase Flow Local Measurements at the Polytechnic University of Valencia (UPV) and University Jaume I of Castellon (UJI), *Sensors* 2017, 17, 1077, doi:10.3390/s17051077.

Nakoryakov, V.E., O.N. Kashinsky, V.V. Randin and L.S. Timkin (1996) Gas-liquid bubbly flows in vertical pipes, *J. Fluids Eng.* 118, 377-382, Experimental data are available online at: <https://scholar.lib.vt.edu/ejournals/JFE/data/JFE/DB96-377/>.

Neykov, B. (2005), NUPEC BFBT Benchmark, Volume I: Specifications, NEA/NSC/DOC(2005)5, May 2005.

Ničeno, B., B. Smith and M.T. Dhotre (2007), Euler-Euler LES of a square cross-section bubble column using the NURESIM CFD platform, companion paper proposed at NURETH 12, Pittsburgh, Pennsylvania, United States, 30 September-4 October 2007.

Ničeno, B., M. Boucker and B.L. Smith (2009), Euler-Euler LES of a Square Cross-Sectional Bubble Column Using the Neptune\_CFD Code, *Science and Technology of Nuclear Installations*, Volume 2009, Article ID 410272.

Ničeno, B., F. Reiterer, A. Ylönen and H-M. Prasser (2011), Simulation of single-phase mixing in fuel rod bundles, using an immersed boundary method, *Physica Scripta*, 2013, Topical articles: 3<sup>rd</sup> International Conference on Turbulent Mixing and Beyond (TMBW'11), August 2011, Trieste, Italy.

Prasser, H.-M., A. Böttger and J. Zschau (1998), A new electrode-mesh tomograph for gas-liquid flows, *Flow Measurement and Instrumentation*, 9 (1998), 111-119.

Prasser, H.-M., E. Krepper and D. Lucas (2002), Evolution of the two-phase flow in a vertical tube - de-composition of gas fraction profiles according to bubble-size classes using wire-mesh sensors, *International Journal of Thermal Sciences*, 41 (2002) 17-28.

Prasser, H.-M., J. Zschau, D. Peters, G. Pietzsch, W. Taubert and M. Trepte (2002a), Fast wire-mesh sensors for gas-liquid flows - visualisation with up to 10 000 frames per second, ICAPP 2002, Hollywood, Florida, paper #1055.

Prasser, H.-M., M. Beyer, H. Carl, A. Manera, H. Pietruske, P. Schütz and F.-P. Weiß (2006), The multipurpose thermal-hydraulic test facility TOPFLOW: an overview on experimental capabilities, instrumentation and results, *Kerntechnik* 71, 163-173.

Prasser, H.-M., M. Beyer, H. Carl, S. Gregor, D. Lucas, H. Pietruske, P. Schütz, F.-P. Weiss (2007), Evolution of the structure of a gas-liquid two-phase flow in a large vertical pipe, *Nuclear Engineering and Design* 237, 1848-1861.

Reddy Vanga, B.M., M.A. Lopez de Bertodano, E. Krepper, A. Zaruba and H.M. Prasser (2005), Two-fluid model LES of a bubble column, 11<sup>th</sup> Int. Topical Meeting on Nuclear Reactor Thermal-Hydraulics (NURETH-11), Avignon, France, 2-6 October.

Reimann, J., H. Kusterer and H. John (1983), Two-phase mass flow rate measurements with Pitot tube and density measurements. In: *Measuring Techniques in Gas-Liquid Two-Phase Flows*, Symposium, Nancy, France.

Richenderfer, A., A. Kossolapov, J.H. Seong, G. Saccone, E. Demarly, R. Kommajosyula, E. Baglietto, J. Buongiorno and M. Bucci (2018), "Investigation of sub-cooled flow boiling and CHF using high-resolution diagnostics," *Experimental Thermal and Fluid Science*, Volume 99, pp.35-58.

Richenderfer, A., A. Kossolapov, T. McKrell, M. Bucci and J. Buongiorno (2017), "The application of Modern Experimental Techniques to the Study of Sub-cooled Flow Boiling CHF", 17<sup>th</sup> International Topical Meeting on Nuclear Reactor Thermal-Hydraulics (NURETH-17), Xi'an, China, 3-8 September 2017.

Richenderfer, A., A. Kossolapov, J.H. Seong, G. Saccone, T. McKrell, M. Bucci and J. Buongiorno (2017), "Direct Measurement of Heat-Flux Partitioning in Boiling Heat-Transfer", ASME 2017 Fluids Engineering Division Summer Meeting (FEDSM), Waikoloa, Hawaii, 2017.

Richenderfer, A., A. Kossolapov, J.H. Seong, T. McKrell, M. Bucci and J. Buongiorno (2017), "Investigation of Sub-cooled Flow Boiling and CHF Using High-Resolution Diagnostics", 9<sup>th</sup> World Conference on Experimental Heat-Transfer, Fluid Mechanics and Thermodynamics, Iguazu Falls, Brazil, 12-15 June 2017.

Roy, R.P., V. Velidandla, S.P. Kalra and P. Péturaud (1994), Local Measurements in the Two-Phase Region of Turbulent Sub-cooled Boiling Flow, *Journal Heat-Transfer*, 116, 660-669.

Roy, R.P., V. Velidandla and S.P. Kalra (1997), Velocity Field in Turbulent Sub-cooled Boiling Flow, *Journal Heat-Transfer*, 119, 754-766.

Roy, R.P., S. Kang, J.A. Zarate and A. Laporta (2002), Turbulent Sub-cooled Boiling Flow – Experiments and Simulations, *Journal Heat-Transfer*, 124, 73-93.

Rubin, A. et al. (2010), OECD/NRC Benchmark Based on NUPEC PSBT, Volume I: Experimental Database and Final Problem Specifications, NEA/NSC/DOC(2010)1, January 2010.

Serre, G. and Bestion D. (2005), Progress in improving two-fluid model in system code using turbulence and interfacial area equations, 11<sup>th</sup> International Topical Meeting on Nuclear Reactor Thermal-Hydraulics, NURETH-11, Avignon, France, 2-6 October.

Simiano, M. (2005), Experimental Investigation of Large-Scale Three-dimensional Bubble Plume dynamics, Diss. EH. No. 16220, Swiss Federal Institute of Technology, Zurich.

Situ, R., T. Hibiki, X. Sun, Y. Mi and M. Ishii (2004a), Flow structure of sub-cooled boiling in an internally heated annulus, *Int. J. Heat Mass Transfer*, 47, 5351-5364.

Situ, R., T. Hibiki, M. Ishii and M. Mori (2004b), Photographic study of bubble behaviours in Forced Convection Sub-cooled Boiling, *Int. J. Heat Mass Transfer*, 47, 3659-3667.

Situ, R., T. Hibiki, M. Ishii and M. Mori (2005), Bubble Lift-Off Size in Forced Convection Sub-cooled Boiling Flow, *Int. J. Heat Mass Transfer*, in press.

Theofanous, T.G., J.P. Tu, A.T. Dinh and T.N. Dinh (2002a), The boiling crisis phenomenon. Part I: nucleation and nucleate boiling heat-transfer, *Experimental thermal and fluid science* 26, pp. 775-792.

Theofanous, T.G., T.N. Dinh, J.P. Tu and A.T. Dinh (2002b), The boiling crisis phenomenon. Part II: dry-out dynamics and burnout, *Experimental thermal and fluid science* 26, pp. 793-810.

Tomiyama, A. (1998), Struggle with computational bubble dynamics, in: Proceedings of Third International Conference on Multi-phase Flow, ICMF 98, Lyon, France, 8-12 June 1998.

Tomiyama, A. and N. Shimada (1998), Numerical simulations of bubble columns using a 3D multi-fluid model, 3<sup>rd</sup> Int. Conf. Multi-phase Flow ICMF'98, Lyon, France, 8-12 June.

Tu, J.Y., G.H. Yeoh, G.C. Park and M.O. Kim (2005), On Population Balance Approach for Sub-cooled Boiling Flow Prediction, *J. Heat-Transfer*, 127, 253-264.

Ünal, H.C. (1976), "Maximum bubble diameter, maximum bubble-growth time and bubble-growth rate during the sub-cooled nucleate flow boiling", *International Journal of Heat and Mass Transfer*, Volume 19, pp. 643-649.

Ünal, C., V. Daw and R.A. Nelson (1992), Unifying the controlling mechanisms for the CHF and quenching: the ability of liquid to contact the hot surface, *J. Heat-Transfer*, Vol. 114, pp. 972-982.

Vyskocil, L. and J. Macek (2010), CFD Simulation of CHF in a Tube, CFD4NRS-3: CFD for Nuclear Reactor Safety Applications, OECD/NEA and IAEA, Bethesda, MD, United States, 14-16 Sept. 2010.

Vyskocil, L. and J. Macek (2010), CFD Simulation of CHF in a Rod Bundle, CFD4NRS-3: CFD for Nuclear Reactor Safety Applications, OECD/NEA and IAEA, Bethesda, MD, United States, 14-16 Sept. 2010.

Working Party of the Heat and Mass Transfer Section of the Scientific Council of the USSR Academy of Sciences (1976), "Tabular data for calculating burnout when boiling water in uniformly heated round tubes", *Teploenergetika* 23 (9), pp. 90-92.

Yeoh, G.H. and J.Y. Tu (2004), A Bubble Mechanistic Model for Sub-cooled Boiling Flow Predictions, Numerical Heat-Transfer, Part B, 45, 475-49;

Yeoh, G.H. and J.Y. Tu (2005), Thermal-Hydrodynamic modelling of Bubbly Flows with Heat and Mass Transfer, *AIChE J.*, 51, 8-27.

Ylönen, A.T. (2013), High-Resolution Flow Structure Measurements in a Rod Bundle, PhD thesis, ETH Zurich, 2013.

Ylönen, A.T., W-M. Bissels and H-M. Prasser (2011), “Single-phase cross-mixing measurements in a  $4 \times 4$  rod bundle”, *Nuclear Engineering and Design*, 241:2484–2493, 2011, ISSN 0029-5493, DOI: 10.1016/j.nucengdes.2011.04.014.

Ylönen, A.T. and H-M. Prasser (2011), Two-phase flow and cross-mixing measurements in a rod bundle, in Proceedings of the 14<sup>th</sup> International Topical Meeting on Nuclear Reactor Thermal-hydraulics (NURETH-14), number 068, September 2011.

Yoo, J., C.E. Estrada-Perez and Y.A. Hassan (2016), Experimental study on bubble dynamics and wall heat-transfer arising from a single nucleation site at sub-cooled flow boiling conditions - Parts 1 and 2, *IJMF* 84.

Yun, B.J., B.U. Bae, D.J. Euh, G.C. Park and C.-H. Song (2010), Characteristics of the local bubble parameters of a sub-cooled boiling flow in an annulus, *Nucl. Eng. Des.*, Vol. 240, pp. 2295-2303.

Yun, B.-J., B.-U. Bae, D.-J. Euh and C.-H. Song (2010), Experimental investigation of local two-phase flow parameters of a sub-cooled boiling flow in an annulus, *Nucl. Eng. Des.*, Vol. 240, pp. 3956-3966.

Zboray, R. and F. de Cachard (2005), “Simulating large-scale bubble plumes using various closure and two-phase turbulence models”, *Nuclear Engineering and Design*, 235, 867-884.

Zhao, Y.H., T. Masuoka and T. Tsuruta (2002), Unified theoretical prediction of fully developed nucleate boiling and CHF based on a dynamic micro-layer model, *Int. J. Heat & Mass Transfer*, 45, pp. 3189-3197.

Zuber, N. (1958), On the stability of boiling heat-transfer, *Transactions of the ASME*, pp. 711-720.

## 5. The pressurised thermal shock

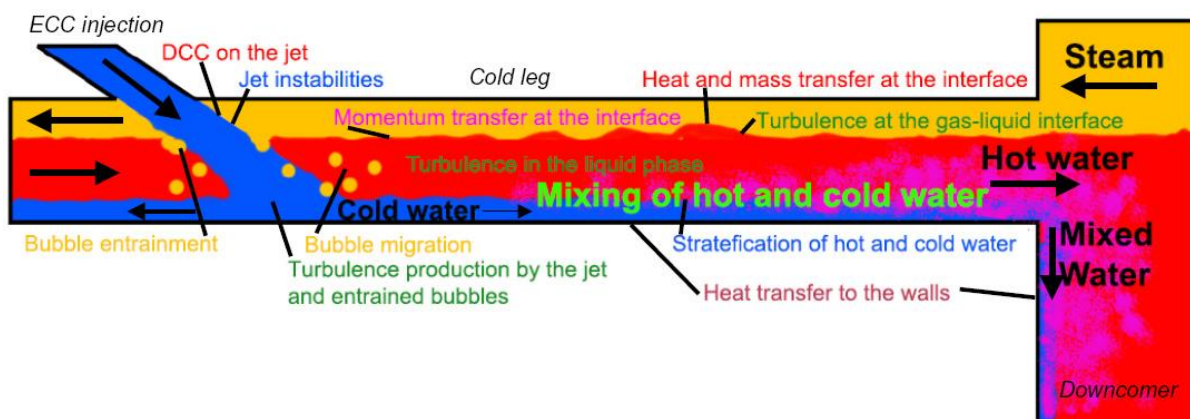
### 5.1. Definition of the PTS issue and identification of all-important flow processes

PTS in general denotes the occurrence of thermal loads on the reactor pressure vessel (RPV) under pressurised conditions.

A thermal-hydraulic evaluation of PTS was made for United States Nuclear Regulatory Commission (USNRC) (Bessette). PTS was first investigated using system codes (see Arcieri et al., Fletcher et al.) and the thermal-hydraulic uncertainties issue was addressed (Chang et al.). PTS was also considered in the scaling analysis the OSU APEX-CE integral test facility (Reyes). We are now considering here the possibility to use two-phase CFD as a support to the safety analysis of some scenarios with two-phase situations.

PTS was also identified by the EUROpean project for Future Advances in Sciences and Technology for Nuclear Engineering Thermal-Hydraulics (EUROFASTNET) (Bestion et al., 2003) project as one of the most important industrial needs related to safety. The most severe PTS scenario limiting the RPV lifetime is cold-water ECC injection into the cold leg during a hypothetical small break loss of coolant accident the mixture flows towards the down-comer where further mixing with the ambient fluid there takes place (Figure 5.1). Such a scenario may lead to extreme thermal gradients in the structural components and consequently to very high stresses. Therefore, the loads upon the RPV must reliably be assessed. Either the fluid present in the cold leg at the location of the injection can be in single-phase or in two-phase condition, depending on the leak size, on its location, and on the operating conditions of the considered nuclear power plant. In this report only the two-phase case, i.e. a cold leg partially filled with hot water or a downcomer water level below the cold leg nozzle is considered.

**Figure 5.1. Most important flow phenomena during a PTS situation with partially filled cold leg**



As shown in Figure 5.1 locally different flow phenomena occur. There are different flows with separated surfaces (jet interface, horizontal interface) but also dispersed flows

occur due to bubble entrainment (at jet impingement and possibly in the horizontal flow region by entrainment caused by waves). Since there is a strong thermal non-equilibrium at these interfaces, momentum transfers as well as heat and mass transfers, have to be considered. The various two-phase phenomena-taking place are strongly coupled with each other and with the heat transfers at the system walls. The single phenomena depend on very different characteristic length scales from the size of the smallest eddy up to the system scale. Some of the involved phenomena are not yet well understood regarding their physics. The simulations of the whole system during the ECC process, and then the accurate reproduction of the thermal loads on the RPV are thus a big challenge.

In detail the following flow regions connected with the listed single phenomena can be distinguished for the two-phase PTS situation (compare e.g. Bestion et al., 2006):

- (A) Free liquid jet
  - (a) Momentum transfer at the jet interface, including instabilities
  - (b) Splitting of the jet
  - (c) Condensation on the jet surface
- (B) Zone of the impinging jet
  - (a) Surface deformation by the jet including generation of waves
  - (b) Bubble entrainment
  - (c) Bubble migration and de-entrainment
  - (d) Turbulence production below the jet
- (C) Zone of horizontal flow
  - (a) Momentum exchange at the gas-liquid interface including generation of waves and growth or damping of these waves
  - (b) Heat and mass transfer (condensation) at the gas-liquid interface including its influence on the phenomena (C,a)
  - (c) Heat-transfer with the walls
  - (d) Turbulence production at the interface
  - (e) Turbulence production at the walls
  - (f) Influence of the phase transfer (condensation) on turbulence
  - (g) Mixing/stratification of hot and cold-water
- (D) Flow in the down-comer in case of partially filled cold leg
  - (a) Turbulence production at the walls
  - (b) Mixing/stratification of hot and cold-water
  - (c) Heat-transfer to the walls
- (E) Flow in the down-comer in case of a water level below the cold leg nozzle
  - (a) Separation of the incoming water jet from the down-comer wall or not

- (b) Momentum transfer at the jet interface, including instabilities
- (c) Splitting of the jet
- (d) Phase transfer on the jet surface
- (e) Heat-transfer to the walls

As mentioned above there is a strong coupling between all these phenomena. Also in case of condensation, the effect of non-condensable gases has to be considered. Although the above list was not ranked with respect to their relative importance for the PTS simulation, it is generally agreed that the most sensitive processes are the condensation at the free surface and the turbulent transfers within the liquid, the major source of turbulence being due to the jet impact.

Two-phase PTS is one of the most challenging exercises for a CFD simulation since it involves almost all two-phase flow phenomena, which may occur in gas-liquid flows. Presently available CFD tools are not able to accurately reproduce the entire single phenomena-taking place in the cold leg and the down-comer during the ECC injection, let alone an accurate simulation of the whole process. This becomes also clear from benchmark simulations done for an experimental set-up in frame of the European project NURISP (Apanasevich et al., 2012). Strong deviation were observed in the results of pre-test simulations done for a steam-water configuration using the NEPTUNE\_CFD, FLUENT and CFX codes with different model options. On the other hand, simulations done with NEPTUNE\_CFD and TransAT of COSI- and LIM-experiments show promising agreements with experimental data. In any case, strong improvements of the two-phase modelling capabilities have to be done to qualify the codes for the simulation of such flows. An accurate simulation of the two-phase PTS situation will be possible only in the far future when this qualification will be completed.

The simulation of each single phenomenon requires the choice of the most adapted model but no available model can simulate all the details of the whole ECC process, starting from the injection location to the inner down-comer. However, simulations of isolated parts have already been performed with more or less success. The most critical problems identified during these computations are the treatment of the liquid/gas interfaces including all interfacial transfers, the turbulence modelling (for both the liquid-and the gas phases, and the coupling of these two turbulence fields) and finally the needs of accurate experimental data for the models validation. If several two-phase flow regimes with different interface structures (i.e. dispersed-bubbly flow, free surface flow, jet flow,...) co-exist in the same isolated region (thus, in the same computation), it is critical to identify these various regimes for applying the adequate model. In general models for the “recognition of the local interface structure” to skip automatically from one model to another model (i.e. activating bubbly flow models or free surface flow models, or other,...) exist, i.e. the Algebraic Interfacial Area Density model (AIAD, Höhne et al., 2011), but they are not mature. For this reason in most of the presently available CFD codes, the use of different models at different locations of the simulation domain is not possible or very limited. Finally, isolated phenomena may be well modelled but the coupling between all these phenomena is not yet well understood. The instabilities at the jet surface are indeed more or less well reproduced, but their effects on the air entrainment at the plunging point are not well modelled.

## 5.2. Limits of previous approaches and expected improvements with CFD

Until now simulations by system codes combined with experimental correlations are used for the estimation of the thermal loads on the RPV wall in case of two-phase PTS analyses. This is a strong limitation since system codes are only able to predict an average liquid temperature in the 1D mesh of the cold leg or a coarse 1D or 3D mesh in the down-comer. Since this does not give the minimum local temperature, which may lead to brittle fracture, additional conservative assumptions are applied. It is obvious that only a 3D simulations tool with a finer space resolution have the general capability to predict the mixing process of hot and cold-water, the condensation rates and finally the resulting thermal loads on the RPV wall properly. Thus, the expected improvement with CFD consists in a reliable prediction of the transient space resolved thermal loads on the RPV wall.

For this reason, CFD codes have to be applied to the two-phase PTS problem in future. On the other hand, two-phase CFD is not mature. In case of two-phase PTS several different local flow regions and their coupling have to be modelled as discussed in the previous section. For each flow, region different phenomena have to be considered. For many of these phenomena universal closure models are not yet available. Special attention has to be paid to improvements regarding:

- turbulence modelling;
- models for the heat-transfer coefficient for direct contact condensation (DCC);
- modelling of the momentum transfer at the free surface;
- consideration of the influence of bubble entrainment on the mixing;
- consideration of the influence of non-condensable gases.

A more detailed discussion on the required model improvements is given below. Once a successful qualification of CFD for two-phase PTS will be obtained, a general approach of the thermal-hydraulic part of a PTS analysis may consist of two steps:

- a) a system code simulation of the scenario leading to ECC injection to determine the boundary conditions for a CFD simulation;
- b) CFD simulation determining the transient and spatial resolved thermal loads on the RPV wall.

This can be done first as two successive steps; in future also, a coupling between both scales would be useful. Up to now, such a coupled approach was only conducted for a single-phase ROSA-experiment on PTS (Scheuerer et al. 2010).

## 5.3. Selecting a basic model

Since the PTS situation is strongly connected with phase transfers, it is clear that a two-fluid model with the complete set of transient balance equations for mass, momentum and energy separately for each phase is the basic choice. Specific efforts have to be paid to some closure relations depending on the phenomenon.

### 5.3.1. Free liquid jet

The cold liquid jet injected into the horizontal cold leg pipe interacts first with the hot surrounding steam environment. These interactions are strongly dependent on the contact surface between the cold-water and the hot gaseous environment. ITMs are needed for this

reason. Depending on various characteristics of both the liquid-and the gas, such as the relative velocity between the two-phases or the turbulence properties, instabilities at the surface of the jet can be generated. The changes in these instabilities are responsible for the variations in the heat and mass transfers. Models for DCC at the jet surface have to be applied. The condensation process (Weiss, 1989) can directly generate instabilities. The behaviour of the instabilities also influences the gas entrainment at the impingement point by capturing gas before the entrainment. An adequate modelling of the interface in connection with a suitable coupling of the turbulence fields of the single phases and local mass and heat-transfer is needed. The basic topological model for the interface is a free surface model, but in case of jet instabilities also drops may be created. This would require a combination with a model for a dispersed liquid phase.

### ***5.3.2. Zone of the impinging jet***

An appropriate modelling of the turbulence production below the jet is most important, since turbulence is responsible for the mixing of the fluid. The jet kinetic energy is the main source of turbulence below the free surface and must be correctly taken into account by the turbulence modelling. Gas entrainment below the free surface by the jet impingement slightly influences the characteristics of the turbulence below the free surface. The properties of the entrained gas (e.g. the size of the bubbles, the penetration depth, the horizontal migration and the total amount of entrained gas) are dependent on various properties of both the liquid-and the gas environment. The jet velocity is one of the most critical parameters for the entrainment of gas below the free liquid surface (Bin, 1993; Davoust et al., 2002). The modelling of the impinging jet zone requires a simultaneous consideration of separated (surface) und dispersed (bubbles) flow within one flow domain. Due to the entrained bubbles, the topology of this zone has to be reflected by a model for the dispersed gas-phase. For the bubble entrainment, itself a transition from a continuous gas-phase to a dispersed gas-phase has to be considered.

### ***5.3.3. Zone of horizontal flow***

Further, in the horizontal cold leg pipe, a stratified flow is observed, i.e. the topology of the interface is characterised by a free surface separating the continuous gas or liquid phases. Depending on the velocities of both the gas and the liquid phases, the liquid/gas interface is more or less perturbed. For low velocities, the interface is a quasi-plane interface. For higher velocities, the interface is perturbed and small waves are generated and amplified depending on the operating conditions. Since the steam flow is generated by the condensation, it depends mainly on the ECCS injection flow rate. For most situations of interest for PTS investigations, the ECCS flow rate is such that a rather calm stratified flow is expected to occur in the cold leg with a smooth or moderately wavy interface (the free falling jet previously presented may generate some waves). In this flow, density stratifications effects play a significant role on turbulence transfers from the free surface to the bottom of the fluid. Heat transfers between the fluids and the wall of the cold leg pipe have also to be considered.

In cases with higher ECCS flow rate generating higher relative velocities, the waves may be strongly amplified, and a slug flow with a complex system of interactions between the two-phases can occur which include separated phases, bubbles and drops. Thus the modelling again requires a simultaneous consideration of separated (surface) und dispersed (bubbles and drops) flow within one flow domain. In such situation, the Kelvin-Helmholtz instability is strongly influenced by the strong condensation and an ITM, able to model surface tension effects (Bartosiewicz and Seynhaeve, 2006) may be required. Lucas et al.

(2011) discusses three different approaches on the modelling of free surface flows with and without phase transfer.

#### ***5.3.4. Flow in the down-comer***

The two-phase flow in the cold leg finally enters in the down-comer. In the case with a water level in the down-comer below the cold leg nozzle, a complex two-phase flow regime occurs and another jet impingement region has to be considered. Depending on the water velocity when entering in the down-comer and on the nozzle geometry, a detachment of the flow from the walls can be observed. If this detachment occurs, the heat transfers between the water and the walls are decreased. Because of the variations in the flow regime and the presence of waves in the cold leg pipe, the velocity is not constant when the liquid enters in the down-comer. Some strong temperature gradients occur at various places on the down-comer wall, and are responsible for the mechanical stresses taking place in the down-comer. The phenomena-taking place in this particular situation are similar to those encountered at the impingement region below the free falling jet. In addition, the effects of the down-comer walls have to be considered during the computations. The presence of the walls modifies the liquid flow behaviour, by changing the turbulence properties, the liquid temperature and the velocity field. Some calculations of the flow in the down-comer have been performed (Willemsen, 2005), and have reproduced with more or less success the water oscillations in the down-comer.

### **5.4. Filtering turbulent scales and two-phase intermittency scales**

#### ***Free liquid jet***

Numerous theories related to mechanisms on generation and growing of jet instabilities exist. Several numerical approaches have already been used, such as DNS or LES for the prediction of their behaviour using various conditions (Pan and Suga, 2004). Even if the individual effect of some parameters such as gravity, nozzle internal flow and so on has been separately studied, no computation taking into account all these effects simultaneously is reported. Actually, some models for the treatment of these instabilities are based on restrictive assumptions, which limit strongly their applicability. Probably the LES approach is most suitable for the modelling of this flow situation, but the best choice in context of the simulation of whole PTS domain is still open. However, the ECCS jet has a very short length before entering the free surface and turbulent transfers within the liquid jet do not play an important role in the whole PTS process.

#### ***5.4.1. Zone of the impinging jet***

The most important effect of the impinging jet is the turbulence generation below the jet. Two parts have to be considered, the main effect being the turbulence generated by the impingement of the jet itself and then, the influence of entrained bubbles on turbulence. In most simulations the effect of the liquid turbulence on the bubbles is modelled, but the opposed effect corresponding to the influence of the bubble on the liquid turbulence field is only considered for the turbulent viscosity, e.g. using the Sato model (Sato et al., 1981), despite this effect is important in the dense bubble region (near the impingement point). Some studies (both experimental and theoretical) have thus to be conducted for the understanding and the modelling of the coupling between these various processes. LES or RANS models, which apply for two-phase turbulence, should be used for the simulation of the zone of the impinging jet.

### ***5.4.2. Zone of horizontal flow***

Turbulence also plays a dominant role for the stratified flow configuration. The turbulence characteristics influence the interfacial transfer rates, especially turbulence close to the interface. On the other hand, the mixing of hot and cold-water is determined by turbulence, with a strong influence of the density gradient. Unsteady RANS models, i.e.  $k-\varepsilon$  or  $k-\omega$  models or combinations of both are frequently applied. In Vallée et al. (2006) fluid-dependent SST turbulence models were selected for each phase. The  $k-\omega$  based SST model (Menter, 2002) accounts for the transport of the turbulent shear stress and gives good predictions of the onset and the amount of flow separation under adverse pressure gradients. The qualitative slug formation in the simulations (ANSYS-CFX) was in good agreement with the experiment. LES or VLES were also successfully applied in combination with interface-tracking (Lakehal, 2010).

### ***5.4.3. Flow in the down-comer in case of partially filled cold leg***

In this case, the flow in the down-comer is assumed to be single-phase. RANS models should apply for filtering turbulent scales in this case.

### ***5.4.4. Flow in the down-comer in case of a water level below the cold leg nozzle***

Since such a flow situation is characterised by a liquid jet coming from the cold leg and impinging into the water in the down-comer afterwards, similar flow situations as discussed for the free liquid jet and for the zone of jet impingement occur. In this case, the same modelling as discussed there should be applied.

## **5.5. ILIS**

### ***Free liquid jet***

The interface has to be identified and modelled carefully, since the condensation process as well as the generation and development of instabilities strongly depends on the interface structure. Instabilities of the jet surface have to be reflected in the simulations. For this reason ITM have to be applied. They have also to account for the interactions with the condensation process on the jet surface. However, due to the short jet length, the jet instabilities are not well developed and cannot affect significantly the condensation on the jet, and then should not play an important role in the whole PTS process.

### ***5.5.1. Zone of the impinging jet***

In the impinging jet zone, four different interface structures have to be considered: 1) the surface of the jet; 2) the free surface of the pool (i.e. liquid level in the cold leg); 3) the entrained bubbles; and 4) the complicated surface structure in the region where the jet hits the surface. Separated flows (jet surface and pool surface) as well as dispersed flow (bubbles) exist simultaneously in one flow domain. Most difficult is to model the transitions between both types of interfaces (i.e. bubble entrainment and de-entrainment). For the different interfacial structures different closure models are needed, e.g. for drag of bubbles and drag on separated interfaces. The identification of the interfaces for separated flows is thus of crucial importance. Some computations of the whole plunging jet process have been performed with more or less successes (Egorov, 2004). Even if the entrainment process has been qualitatively well reproduced numerically, the total volume flow rate of entrained gas

has been largely overestimated. One of the most critical problems pointed out during these computations is the treatment of the liquid/gas interfaces. To overcome the discrepancies, the two kinds of interface mentioned above have to be automatically identified and modelled using two different models, which is not possible in most presently available CFD codes. This point is for the moment one of the most important limitations for the two-phase flow computations (and not only for the plunging jet calculations) in which several similar flow regimes co-exist simultaneously. As a first approximation, priority should be given to the adequate modelling of the turbulence generated by the jet and to the free surface condensation.

### ***5.5.2. Zone of horizontal flow***

The modelling of the two-phase stratified flow in the horizontal cold leg pipe is based on various models and numerical approaches (see e.g. Lucas et al., 2011). Most of them are dedicated to the treatment of the free surface where the most important phenomena take place. This interface is characterised by intense exchanges between the liquid and the gas phases (heat, mass, momentum, turbulence), which are strongly coupled with each other and have to be reproduced as accurately as possible. Numerical models for free surface flow may be divided according to Zwart (2005) into three categories: surface-adaptive methods, interface-capturing methods and ITMs. One may also simply use the two-fluid model with an identification of the free surface based on the void-fraction. In any case, the knowledge of the free surface location is necessary for a good modelling of the interfacial transfers, since many models in boundary layers on both gas and liquid sides depend on the distance to the interface.

Surface-adaptive methods are typically single-phase approaches in which the kinematic condition is used to update the location of the free surface interface and the mesh boundary conforms to this interface at all times. These methods inherently involve mesh motion.

These limitations may be overcome by having a fixed mesh, which spans the interface location. The interface is captured or tracked within the mesh by some algorithm. Most commonly, the algorithm makes use of the continuity equation for one of the phases, in which the dependent variable is the volume fraction of that phase; these methods are called VOF methods (Hirt and Nichols, 1981). VOF methods differ widely in their detailed implementation. Many of them are interface-capturing and solve the VOF equation using a continuum advection scheme. If standard techniques are used for the advection operator, numerical diffusion will lead to significant smearing of the interface. A variety of compressive advection schemes has been devised to minimise this diffusion. Other VOF methods are interface-tracking and explicitly track the free surface interface. For a particular volume fraction field, the interface is reconstructed using a piecewise representation (constant, linear, or parabolic) in each cell. The volume fluxes may be calculated either geometrically or using an advection operator as described above. Further details of these algorithms can be found in Rudman (1997) and Kothe et al. (1996). Another fixed grid strategy for free surface flow problems involves the use of level sets (Sussman et al., 1998).

The LEIS, (Lakehal, 2010) combines ITMs with LESs. The model was successfully applied for the simulation of COSI test.

Modelling surface tension effects is challenging because it is a potentially large force, which is concentrated on the free surface interface. The continuum surface force method (Brackbill et al., 1992) formulates the surface tension force as a volumetric force. A key ingredient of this method is evaluating the interface curvature; it is challenging because it

in effect requires second derivatives of the discontinuous volume fraction field. Care must be used in order to avoid errors in this calculation. Kothe et al. (1996) discuss further details.

Due to the geometrical scale, it is in most cases not possible to resolve the spatial structure of the free surface into the micro-scale with the CFD model. A free surface simulation can therefore not cover onset of Kelvin-Helmholtz instabilities at the interface with wave formation. The interface drag law applied to the free surface must consider the influence of these waves on the macro-scale flow properties. Additionally, the movement of the free surface at the inlet boundary condition can introduce instabilities.

Although an ITM seems to be more adequate for a free surface flow, other simpler approaches have to be further evaluated before selecting a general method for reactor PTS simulations. A simple identification of the free surface by the “large interface model” proposed by Coste et al (2008) was applied to adiabatic and condensing stratified flow with some success. A similar approach is the AIAD model (Höhne et al., 2011)

### ***5.5.3. Flow in the down-comer***

Only in the case of a water level below the cold leg nozzle, gas-liquid interface has to be considered. Since such a flow situation is characterised by a liquid jet coming from the cold leg and impinging into the water in the down-comer afterwards, similar flow situations as discussed for the free liquid jet and for the zone of jet impingement occur. In this case, the same modelling as discussed there should be applied.

## **5.6. Modelling interfacial transfers**

### ***Free liquid jet***

The DCC at the jet surface resulting from the temperature difference between the two-phases is responsible for a non-negligible part of the total condensation in the considered flow domain of the cold leg (Janicot and Bestion, 1993). The heat and mass transfers at an interface have been largely studied and several models have been proposed. The resulting co-relations are often only valid for the corresponding geometry, scales or operating conditions, e.g. some fluid properties are neglected such as the liquid internal recirculation and the temperature profile in the liquid or in the gas-phase. Such models have to be validated by including these effects for the free falling jet configuration. The influence of non-condensable gases has to be considered.

### ***5.6.1. Zone of the impinging jet***

The free surface close to the jet impingement is highly agitated due to jet-induced turbulence and is subject to high heat and mass transfers. Both the liquid to interface heat-flux and the turbulence, which diffuses the heat from the surface to the bottom of the liquid, must be well modelled in this zone since they are the dominant processes affecting the PTS. Available experimental data do not allow a precise validation of these models and information that is more detailed is expected from the future TOPFLOW-PTS experimental programme.

The interfacial momentum transfer at the place where the jet enters the free surface governs the bubble entrainment. In previous simulations, the rate of entrained bubbles was overestimated, since a drag coefficient for bubbles was used. According to the different types of interfaces mentioned in Section 5.4, different models for momentum transfer,

e.g. different drag laws have to be applied. This is not possible in presently available CFD codes.

Several forces acting on individual bubbles determine the behaviour of the entrained gas below the free liquid surface. The most important of these forces are drag force, virtual mass force, lift force and turbulent dispersion force. All these forces are strongly dependent on the bubble-size (see e.g. Tomiyama, 1998). For bubbly flow in vertical pipes a set of Tomiyama lift- and wall force together with the Favre averaged drag force (Burns 2004) was found to reflect the experimental findings in poly-dispersed flows (Lucas et al., 2004). In the case of developing flows, some differences have been pointed out between calculations and experimental data (Lucas et al., 2005). In most of the cases, during the computations the bubble diameters are supposed to be constant. In principle CFD models, which allow the consideration of a number of bubbles classes exist (Krepper et al. 2005), but they are very time-consuming. The bubbles size distribution is strongly influenced by bubble coalescence and breakup, for which various models exist in the literature. The models for bubble forces as well as the models for bubble coalescence and breakup have consequently to be validated for the plunging jet configuration.

In addition, models for interfacial heat and mass transfer have to be applied to the bubbles, which are expected to condense quickly. For these models, it is also necessary to distinguish between the bubble interfaces and the free surface, since different heat-transfer coefficients have to be applied for separated flows and for bubbly flows.

### ***5.6.2. Zone of horizontal flow***

Heat, mass and momentum interfacial transfers have also to be considered along the stratified flow in the cold leg. These transfers are closely connected with turbulent transfers. In the case of the turbulence predicted by the  $k-\epsilon$  model, the interfacial friction can be modelled by using several closure laws. The interfacial sub-layer model (ISM, Yao et al., 2003) in the gas-phase supposes, due to the significant difference between the gas and liquid density, that the interface can be treated as a “moving solid wall” with a velocity equal to the liquid velocity. The gas region close to the interface is modelled with the two sub-layer model, which is similar to the wall function concept. It is also possible to use the average viscosity assumption (AVM, Yao et al., 2003). This model is based on the simplified momentum equation in the case of a thin layer near a smooth interface without phase-change, which permits evaluation of the interfacial friction and velocity.

Some simulations exist on the safety analysis of nuclear reactor where rapid contact condensation of vapour occurs during the emergency injection of cold-water (Bankoff, 1980; Hughes and Duffey, 1991; Murata et al., 1992; Zhang et al., 1993; Chu et al., 2000). The recent models for the interfacial transfers can be mainly separated in two classes, one based on the surface renewal concept (e.g. Hughes and Duffey, 1991) another based on the eddy diffusivity concept (e.g. Yamamoto, 2001). The use of the first class of models with the steam-water flow is theoretically questionable. The modelling of the interfacial heat-transfer is based on approaches similar to the interfacial friction transfer. Schiestel (1993) and Jayatilke (1969) have proposed relations for the temperature profile and the Prandtl number, using a formulation similar to the interfacial sub-layer model (SIM, Yao et al., 2003). Shen et al. (2000) have investigated the asymptotic behaviour of the eddy viscosity and found that in the boundary layer the turbulent viscosity follows a Gaussian function. Using a surface renewal concept with small eddies (HDM), Barnejee (1978), has proposed a relation for the heat-transfer, and Hughes and Duffey (1991) have modified the relation by introducing the Kolmogorov time scale for the small eddies. Simulations using the

surface renewal theory show that the condensation rate is under-estimated by such a modelling (Tiselj et al. 2006). New experimental data (TOPFLOW-PTS) are required to validate interfacial heat-transfer in presence of condensation with accurate measurement of temperature, velocity and turbulence fields.

### ***5.6.3. Flow in the down-comer***

Only in the case of a water level below the cold leg nozzle must interfacial transfers be considered. Since such a flow situation is characterised by a liquid jet coming from the cold leg and impinging into the water in the down-comer afterwards, similar flow situations as discussed for the free liquid jet and for the zone of jet impingement occur. In this case, the same modelling as discussed there should be applied.

## **5.7. Modelling turbulent transfers**

### ***Free liquid jet***

Turbulent transfers at the jet interface are strongly coupled with heat and mass transfers. The question of a suitable modelling of these transfers is fully open.

#### ***5.7.1. Zone of the impinging jet***

RANS or LES models can be used for the simulation of turbulence in the impinging jet zone. A simple k- $\epsilon$  model was applied (Galassi et al., 2007) to a plunging jet experiment with reasonable predictions. Entrained bubbles modify the turbulence in the zone below the jet. This turbulence modulation has to be considered in addition to the turbulence generated by the jet itself. In addition, turbulent transfers have to be considered at the pool interface. Here the same models have to be applied as in the zone of horizontal flow.

#### ***5.7.2. Zone of horizontal flow***

The turbulence fields for both the liquid-and the gas phases and the coupling between these two turbulence fields play an important role on the regime of the two-phase stratified flow in the cold leg, and for the transition between the different regimes (smooth surface, wavy flow and slug flow). Close to the interface, three turbulence sources have been identified: turbulence diffused from wall boundaries, turbulence production by the interfacial friction and turbulence induced by interfacial waves. Another important problem close to the interface is the anisotropy of the turbulence, which is not reproduced by any classic model. In most of the cases, the turbulence is modelled using the k- $\omega$  or the k- $\epsilon$  (classic or modified) models with specific hypothesis at the interface (Akai et al., 1981; Issa, 1988), especially for the turbulent kinetic energy. Without any special treatment of the free surface, the high-velocity gradients at the free surface generate too high turbulence when using eddy viscosity models like the k- $\epsilon$  or the k- $\omega$  model. Therefore, (Egorov, 2004) proposed a symmetric damping procedure for the solid wall-like damping of turbulence in both gas and liquid phases.

#### ***5.7.3. Flow in the down-comer***

Only in the case of a water level below the cold leg nozzle turbulent transfers have to be considered. Since such a flow situation is characterised by a liquid jet coming from the cold leg and impinging into the water in the down-comer afterwards, similar flow situations as

discussed for the free liquid jet and for the zone of jet impingement occur. In this case, the same modelling as discussed there should be applied.

### 5.8. Modelling wall transfers

The prediction of the transient and local heat-transfer to the RPV wall is the final aim of the thermal fluid-dynamic simulation of the PTS situation. In addition, the heat-transfer to the cold leg wall has to be considered, since there is also a feedback from the wall temperatures to the flow. The various flow regimes taking place in the different regions influence the heat transfers at the walls. The numerical reproduction of the transfers with the walls is strongly dependent on the accuracy of the prediction of all the others phenomena. The variations of the temperature fields for both the liquid-and the gas phases are strongly dependent on the mixing between the phases, which results in the local phenomena. Inversely, these heat transfers at the walls influence the behaviour of the others phenomena by changing the temperature fields of the fluids.

For the simulation of the wall heat-transfer, models valid for single-phase should be sufficient. Various models exist and have been largely studied. In most of the CFD codes some heat-transfer models with a solid wall are available. These models require the definition of the wall properties, depending on their composition. These models have already been used successfully with various configurations.

### 5.9. Validation matrix for the PTS issue

An overview on suitable experimental data for the validations of the relevant flow processes in a PTS situation is given in a report, which was elaborated in the frame of the NURESIM project (Lucas, 2005a). The Table 5.1 below was taken from this report. It gives an assignment of experiments to the local physical phenomena they are related to. For the cells marked with a **v** the measured data can be used for validation of such local CFD models. There is a measurement, which is directly related to the phenomenon. **p** means, that the physical phenomenon is **p**resent in the experiment, but cannot be used for the validation of the single effect modelling. There is a lack of precise measurement to quantify it. This allows only a global validation of the code. The effect is mixed with other effects. A more detailed description and characteristics of the experiments can be found in Lucas (2005a).

Table 5.1. Available experimental data for validation of two-phase CFD applied to PTS simulation

	JET	JET	SLUG FLOW	Fabre data	DCC	DCC	PMK-2 WH	HYBISCUS	UPTF-TRAM C1	COSI	ROSA IV OECD Tests
Air-water / Steam-water	A-W	A-W	A-W	A-W	S_W	S_W	S_W	A-W	S_W	S_W	S_W
Test section geometry		Cyl.	Rect.	Rect	Rect		pipe	Cold leg, SI, downcomer	Reactor	Cold leg, SI	reactor
Author Ref	Bonetto & Lahey 1993	Iguchi & al,1998	Vallee & al., 2005	Fabre & al. 1987	Lim & al, 1984	Goldbrunner & al., 2000	Prasser & al., 2004	Bichet & al. 2005	UPTF report, 1996	Janicot, Bestion 1993	
Instabilities of the ECC jet								p	p	p	p
Condensation on the jet before mixing									p	p	p
Entrainment of steam bubbles below the water level	v	p						p	p	p	p
Migration of entrained bubbles	v	p						p	p	p	p
Turbulence production below the jet	p	v							p	p	p
Interfacial transfer of momentum at free surface			v	v	p	p	v	p	p	p	p
Interfacial transfer of heat & mass at free surface					v	v	v		p	p	p
Effects of turbulent diffusion upon condensation					p	p			p	p	p
Turbulence production in wall shear layers & in interfacial shear layer			p	v		p			p	p	p
Interactions between interfacial waves and interfacial turbulence production				p	p	p		p	p	p	p
Effect of condensation upon interfacial structure and wave structure					p	p			p	p	p
Effects of temperature stratification upon turbulent diffusion					p	p			p	p	p
Interface configuration in top of downcomer									v		p
Flow separation or not in downcomer at cold leg nozzle									v		p
Influence of non-condensable gases on condensation						v	p		p	p	p
Heat transfers with cold leg and RPV walls									v		p

For the following physical phenomena one or more experiments exists with data measured, which can be used for the validation:

- Entrainment of steam bubbles below the water level.
- Migration of entrained bubbles.
- Turbulence production below the jet.
- Interfacial transfer of momentum at free surface.
- Interfacial transfer of heat and mass at free surface.
- Turbulence production in wall shear layers and in interfacial shear layer.
- Interface configuration in top of down-comer.
- Flow separation or not in down-comer at cold leg nozzle.
- Influence of non-condensable gases on condensation.
- Heat transfers with cold leg and RPV walls.

In general, most of the experiments show a lack of well-defined instrumentation. For this reason, some data cannot be used for the separate-effect modelling and validation, although the phenomenon occurs in the experiment. Of course, they have a more or less pronounced influence on other measured data, but this allows only vague conclusions on the considered phenomenon. In the reviewed data basis, there is no direct information on the following single effect local physical models:

- Instabilities of the jet from ECC injection.
- Condensation on the jet itself before mixing.
- Effects of turbulent diffusion upon condensation.
- Interactions between interfacial waves and interfacial turbulence production.
- Effect of condensation upon interfacial structure and wave structure.
- Effects of temperature stratification upon turbulent diffusion.

These phenomena are important for a reliable simulation of the PTS situation and a prediction of the thermal loads. Thus, e.g. the condensation on the liquid jet from the ECC injection represents a relatively large part of the total condensation, since there are huge temperature differences between the jet and the steam.

If there are data available for a single phenomenon, they often do not cover the parameter ranges of two-phase PTS situations. E.g. the nozzle diameter in the Bonetto and Lahey data is much smaller than in case of ECC injection into the cold leg. In addition, the jet is perpendicular to the pool surface but may have different angles in the PTS-relevant case. Even more important is the fact that the experiment is done only for air-water and not for water-steam. Since CFD codes should have some capabilities to extrapolate to other parameter ranges, these data can be also used, but for comprehensive validation the validity of the models has to be shown also for the required parameter range.

The HYBISCUS, UPTF-TRAM C1, COSI and ROSA experiments aim on an integral simulation of two-phase PTS scenarios. For this reason, most of the single effect phenomena are present, but all these experiments were weakly instrumented. The data available from these experiments can be used for validation of the integral process in

principle, but only few data can be compared. For a well-founded validation, measurements of different parameter with a high-resolution in space and time are needed.

A new experiment on the PTS issue was recently conducted at the TOPFLOW facility of the Helmholtz-Zentrum Dresden-Rossendorf e.V. (HZDR) in Germany. Beside HZDR the consortium comprises EDF, CEA, AREVA-NP and IRSN in France along with PSI and ETH Zurich, Switzerland. The reference reactor for the tests is the CPY, 900 MWe plant operated in France. The test mock-up comprises the cold leg and a part of the down-comer in a geometrical scale of 1:2.5. It was installed inside the pressure tank of TOPFLOW in order to allow operation at a pressure of up to five MPa in pressure equilibrium with the inner atmosphere of this tank. This allows building the flow channel from components with thin walls, which ensures optimal access with instrumentation. Besides the operational standard instrumentation (pressure, differential pressure, temperature, flow rates), the instrumentation comprises thermo-couples, heat-flux probes, wire-mesh sensors, local void probes equipped with a micro-thermocouple, high-speed camera observation and infrared camera observations. These measuring techniques provided data with high-resolution in space and time. Steady-state as well as transient tests were performed. Since the data are, property of the consortium the availability is limited.

## References

Akai, M., A. Inoue, S. Aoki and K. Endo (1980), “A concurrent stratified air-mercury flow with wavy interface”, *International Journal of Multi-phase Flow*, vol. 6, pp. 173–190.

Apanasevich, P., D. Bestion, P. Coste, C. Raynaud, C. Heib, M. Scheuerer, B. Ničeno, D. Lakehal, I. Tiselj and D. Lucas (2012), “Synthesis and conclusions on PTS modelling”, EU-Project NURISP, Deliverable D2.5.1.

Arcieri, W.C., R.M.S. Beaton, C.D. Fletcher and D.E. Bessette (2004), “RELAP5 Thermal-Hydraulic Analysis to Support PTS Evaluations for the Oconee-1, Beaver Valley-1, and Palisades Nuclear Power Plants”, ISL, Inc., NUREG/CR-6858, ML051780284.

Bestion, D., H. Paillère, A. Latrobe, A. Laporta, V. Teschendorff, H. Städtke, N. Aksan, F. d’Auria, J. Vihavainen, P. Meloni, G. Hewitt, J. Lillington, A. Prošek, B. Mavko, J. Macek, M. Malacka, F. Camous, F. Fichot and D. Monhardt (2003), EUROFASTNET, FISA-2003, EU Research in Reactor Safety, 10-13 November 2003, EC Luxembourg.

Bankoff, S.G. (1980), “Some condensation studies pertinent to LWR safety”, *International Journal of Multi-phase Flow*, vol. 6, pp. 51–67.

Barnejee, S. (1978), “A surface renewal model for interfacial heat and mass transfer in transient two-phase flow”, *International Journal of Multi-phase Flow*, vol. 4, pp. 571–573.

Bartosiewicz, Y. and J.-M. Seynhaeve (2006), “Numerical investigation on the Kelvin-Helmholtz instability in the case of immiscible fluids”, 13<sup>th</sup> International Conference on Fluid Flow Technologies, Budapest, Hungary, (2006).

Bessette, D. (2005), Thermal-Hydraulic Evaluation of PTS, USNRC, NUREG-1809, ML051780303.

Bestion, D. et al. (2006), “Extension of CFD Codes to Two-phase Flow Safety Problems”, Technical Note, NEA/SEN/SIN/AMA(2006)2, OECD Publishing, Paris.

Bichet, T., A. Martin and F. Beaud (2005), “Stratified flow and free surface of an uncovered RPV cold leg. Water-air experimental results”, ASME Fluids Engineering Summer Conference, Houston, Texas, 19-23 June 2005.

Bin, A.K. (1993), “Gas entrainment by plunging liquid jets”, *Chemical Engineering Science*, vol. 48, pp. 3585-3630.

Bonetto, F. and R.T. Lahey Jr. (1993), “An experimental study on air carryunder due to a plunging liquid jet”, *International Journal of Multi-phase Flow*, vol. 19, pp. 281–294.

Brackbill, J.U., D.B. Kothe and C. Zemach (1992), “A continuum method for modelling surface tension. *Journal of Computational Physics*”, vol. 110, pp. 335–353.

Burns, A.D., T. Frank, I. Hamill and J.-M. Shi (2004), “The Favre averaged drag model for turbulence dispersion in Eulerian multi-phase flows”, 5<sup>th</sup> Int. Conf. on Multi-phase Flow, ICMF'2004, Yokohama, Japan.

Chang, Y.H., K. Almenas, A. Mosleh and M. Pour-Gol (2004), “Thermal-Hydraulic Uncertainty Analysis in PTS Risk Assessment”, University of Maryland, NUREG/CR-6899, ML043570541.

Chu, I.C., M.K. Chung, S.O. Yu and M.H. Chun (2000), “Interfacial condensation heat-transfer for counter-current steam-water stratified flow in a circular pipe”, *Journal of the Korean Nuclear Society*, no. 32, pp. 142–156.

Coste, P., J. Pouvreau, J. Laviéville and M. Boucker (2008), Status of a two-phase CFD approach to the PTS issue, XCFD4NRS, Grenoble, France, 10-12 Sept. 2008.

Davoust, L., J.L. Achard and M. El Hammoumi (2002), “Air entrainment by a plunging jet: the dynamical roughness concept and its estimation by a light absorption technique”, *International Journal of Multi-phase Flow*, vol. 28, pp. 1541–1564.

Demuren, A.O. and R. W. Wilson (1999), “Streamwise vorticity generation in laminar and turbulent jets”, NASA/CR-1999-209517. ICASE report No. 99–33.

Dhotre, M.T., B. Ničeno and B.L. Smith (2006), “LES of a bubble column”, 6<sup>th</sup> EURATOM Framework Programm NURESIM, Deliverable D2.1.6.1.

Egorov, Y., M. Boucker, A. Martin, S. Pigny, M. Scheuerer and S. Willemsen (2004), “Validation of CFD codes with PTS-relevant test cases”, 5<sup>th</sup> EURATOM Framework Programme ECORA project.

Fabre, J., L. Masbernat and C. Suzanne (1987), “Stratified flow, Part I : local structure”, *Multi-phase Science and Technology*, 3, Ed. by G. F. Hewitt, J. M. Delhaye, and N. Zuber, 285-301.

Fletcher, C.D., D.A. Prelewicz and W.C. Arcieri (2004), “RELAP5/MOD3.2.2 $\gamma$  Assessment for PTS Applications”, ISL, Inc., NUREG/CR-6857, ML061170401.

Galassi, M.C., C. Morel, D. Bestion, J. Pouvreau and F. D’Auria (2007), Validation of NEPTUNE CFD module with data of a plunging water entering a free surface, 12<sup>th</sup> International Topical Meeting on Nuclear Reactor Thermal-Hydraulics (NURETH-12), Pittsburgh, Pennsylvania, United States, 30 September-4 October 2007.

Goldbrunner, M., J. Karl and D. Hein (2000), “Experimental Investigation of Heat-Transfer Phenomena during DCC in the Presence of Non-Condensable Gas by Means of Linear Raman Spectroscopy”, 10<sup>th</sup> International Symposium on Laser Techniques Applied to Fluid Mechanics, Lisbon.

- Higbie, H. (1935) “The rate of absorption of a pure gas into a still liquid during short periods of exposure”, *Transaction of the AIChE*, vol. 31, pp. 365–388.
- Hirt, B. and B. Nichols (1981), “VOF method for the dynamics of free boundaries”, *Journal of Computational Physics*, vol. 39, pp. 201-225.
- Höhne, T., Deendarlianto and D. Lucas (2011), “Numerical simulations of counter-current two-phase flow experiments using an interfacial area density model”, *International Journal of Heat and Fluid Flow* 32, 1047-1056.
- Hughes, E.D. and R.B. Duffey (1991), “DCC and momentum transfer in turbulent separated flows”, *International Journal of Multi-phase Flow*, vol. 17, pp. 599–619.
- Iguchi, M., K. Okita and F. Yamamoto (1998), “Mean velocity and turbulence characteristics of water flow in the bubble dispersion region induced by plunging water jet”, *Int. J. Multi-phase Flow*, 24, 523-537.
- Issa, R.I. (1988), “Prediction of turbulent, stratified, two-phase flow in inclined pipes and channels”, *International Journal of Multi-phase Flow*, vol. 14, pp. 141–154.
- Janicot, A. and D. Bestion (1993), “Condensation modelling for ECC injection”, *Nuclear Engineering & Design*, vol. 145, pp. 37–45.
- Jayatileke, C.L.V. (1969), “The influence of Prandtl number and surface roughness on the resistance of the laminar sub-layer to momentum and heat-transfer”, *Progress in Heat and Mass Transfer*, vol. 1, p. 193.
- Krepper, E., D. Lucas and H.-M. Prasser (2005), “On the modelling of bubbly flow in vertical pipes”, *Nuclear Engineering & Design*, 235, 597.
- Kothe, D.B., W.J. Rider, S.J. Mosso and J.S. Brock (1996), “Volume-tracking of interfaces having surface tension in two and three dimensions”, *AIAA Paper 96-0859*.
- Lakehal, D. (2006), “Turbulence structure at interfacial two-phase flow”, 6<sup>th</sup> EURATOM Framework Program NURESIM, Deliverable D2.1.7.1.
- Lakehal, D. (2010), “LEIS for the prediction of turbulent multi-fluid flows for thermal-hydraulic applications”, *Nuclear engineering and Design* 240, pp. 2096-2106.
- Lim, I.S., R.S. Tankin and M.C. Yuen (1984), “Condensation measurement of horizontal co-current steam-water flow”, *Journal of Heat-Transfer*, vol. 106, pp. 425-432.
- Lucas, D., J.-M. Shi, E. Krepper and H.-M. Prasser (2004), “Models for the forces acting on bubbles in comparison with experimental data for vertical pipe flow”, 3<sup>rd</sup> International Symposium on Two-Phase Flow Modelling and Experimentation, Pisa, Italy, Paper ha04.
- Lucas, D., E. Krepper and H.-M. Prasser (2005), “Modelling of the evolution of bubbly flow along a large vertical pipe”, The 11<sup>th</sup> International Topical Meeting on Nuclear Reactor Thermal-Hydraulics (NURETH-11), Popes’ Palace Conference Centre, Avignon, France.
- Lucas, D. (Editor) (2005a), Review of the existing data basis for the validation of models for PTS, EU-project NURESM, Deliverable D2.1.2, [www.nuresim.com](http://www.nuresim.com).
- Lucas, D., P. Coste, T. Höhne, D. Lakehal, Y. Bartosiewicz, D. Bestion, M. Scheuerer and M.C. Galassi (2011), CFD modelling of free surface flow with and without condensation”, *Multi-phase Science and Technology* 23, 253-342.

Menter, F., B. Hemstrom, M. Henriksson, R. Karlsson, A. Latrobe, A. Martin, P. Mühlbauer, M. Scheuerer, B. Smith, T. Takacs and S. Willemsen (2002), “CFD best practice guidelines for CFD code validation for reactor-safety applications”, EC-report EVOL-ECORA-D01.

Murata, A., E. Hihara and T. Saito (1992), “Prediction of heat-transfer by DCC at a steam-sub-cooled water interface”, *International Journal of Heat and Mass Transfer*, vol. 35, pp. 101–109.

Pan, Y. and K. Suga (2004), “Direct simulation of water jet into air”, 5<sup>th</sup> International Conference on Multi-phase Flow, ICMF’04, Yokohama, Japan, Paper vol. 377.

Prasser, H.M., G. Ezsol and G. Baranyai (2004), “PMK-2 water-hammer tests, condensation caused by cold-water injection into main steam-line of VVER-440-type PWR - Data Evaluation Report (DER)”, WAHALoads project deliverable D51.

Reyes, J.N. (2003), “Scaling Analysis for the OSU APEX-CE Integral Test Facility,” Oregon State University, NUREG/CR-6731, ML 051790419.

Reyes, J.N., et. al. (2006), “Final Report for the OSU APEX-CE Integral Test Facility,” Oregon State University, NUREG/CR-6856, ML051790416.

Rudman M. (1997), “Volume-tracking methods for interfacial flow calculations”, *International Journal for Numerical Methods in Fluids*, vol. 24, pp. 671–691.

Sato, Y., M. Sadatomi and K. Sekoguchi (1981), “Momentum and heat-transfer in two-phase bubble flow-I”, *Int. J. of Multi-phase Flow*, vol. 7, pp. 167-177.

Scheuerer, M. and J. Weiß (2010), “Transient Computational Fluid Dynamics of ECC Injection at natural circulation conditions”, CFD4NRS-3, Washington DC, United States, September.

Schiestel, R. (1993), “Modélisation et simulation des écoulements turbulents”, Hermès, Paris.

Shen, L., G.S. Triantafyllou and D.K.P. Yue (2000), “Turbulent diffusion near a free surface”, *Journal of Fluid Mechanics*, vol. 407, 145–166.

Siemens, AG (1996), Report “UPTF-TRAM Versuch C1/C2 - Strähnen- und Streifenkühlung der RDB-Wand“, Quick Look Report, NT31/96/17, Siemens A.G., Erlangen, Bereich Energieerzeugung, März.

Sussman, M., E. Fatemi, P. Smereka and S. Osher (1998), “An improved LS method for incompressible two-phase flows”, *Computers and Fluids*, vol. 27, pp. 663–680.

Taitel Y. and A. E. Dukler (1976), “A theoretical approach to the Lockhart-Martinelli correlation for stratified flow”, *International Journal of Multi-phase Flow*, vol. 2, pp. 591–595.

Tiselj, I., L. Štrubelj and A. Prošek (2006), “DCC in horizontally stratified flow of AEKI PMK-2 device”, 6<sup>th</sup> EURATOM Framework Program NURESIM, Deliverable D2.1.13.1.

Tomiyaama, A. (1998), “Struggle with computational bubble dynamics”, Third International Conference on Multi-phase Flow, ICMF’98, Lyon, France, 8-12 June.

Vallée, C., T. Höhne, H.-M. Prasser and T. Sühnel (2006), “Experimental investigation and CFD simulation of horizontal air/water slug flow”, *Kerntechnik*, vol. 71, pp. 95-103.

Weiss, P. (1989), “UPTF experiment: principal full-scale test results for enhanced knowledge of large-break loss of coolant accident (LOCA) scenario in PWR’s”, Fourth International Topical Meeting on Nuclear Reactor Thermal-Hydraulics, Karlsruhe.

Willemsen, S.M. and E.M.J. Komen (2005), “Assessment of RANS CFD modelling for PTS analysis”, The 11<sup>th</sup> International Topical Meeting on Nuclear Reactor Thermal-Hydraulics (NURETH-11), Avignon, France.

Yamamoto, Y., T. Kunugi and A. Serizawa (2001), “Turbulence statistics and scalar transport in an open-channel flow”, *Journal of Turbulence*, no. 2, pp. 1–16.

Yao, W., P. Coste, D. Bestion and M. Boucker (2003), “Two-phase PTS investigations using a 3D two-fluid modelling of stratified flow with condensation”, *Proceedings of the NURETH-10*, Seoul, Korea.

Zhang, Q., G. F. Hewitt and D. C. Leslie (1993), “Nuclear safety code modelling of condensation in stratified flow”, *Nuclear Engineering & Design*, vol. 139, pp. 1–15, 1993.

Zwart, P.J. (2004), “Industrial CFD applications of free surface and cavitating flows”, In VKI Lecture Series: Industrial Two-Phase Flow CFD, (2005), “Validation of CFD codes with PTS-relevant test cases”, 5<sup>th</sup> EURATOM Framework Programme ECORA project.

## 6. The pool heat exchangers

### 6.1. Identification of all-important flow processes of the issue

Pool heat exchangers are important elements of advanced passive safety systems for the Westinghouse AP1 000 (W.E. Cummins, et al., 2003), the GE ESBWR, and other proposed passive designs. In pressurised-water reactors, the pool heat exchanger associated with the passive residual heat removal (PRHR) system is primarily intended to take the thermal load from decay heat when the steam generators are not available in situations such as loss of feed-water (including feed-water-line breaks) or a steam-line break. However, the PRHR can also play a significant role in loss of coolant accidents, contributing substantial cooling before the system pressure drops enough to permit gravity draining from the in reactor water storage tank (IRWST) into the vessel. In BWRs, the analogous pool heat exchangers are part of isolation condenser system (ICS), used as a heat sink when normal steam flow is disrupted. A similar set of pool heat exchangers are used in the ESBWR's passive containment cooling system (PCCS). This system performs the same function as condensation on the steel shell of the AP1 000 containment during a LOCA.

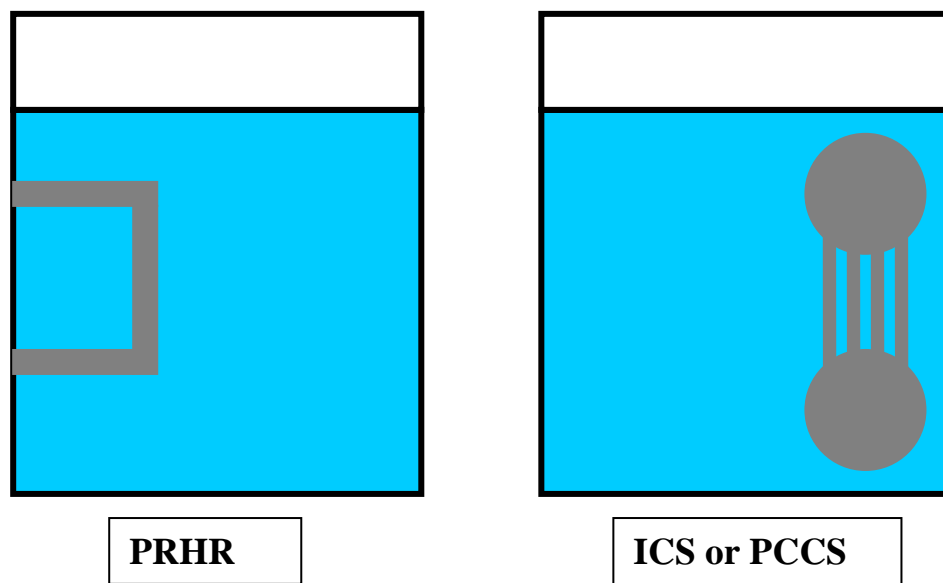
This section focuses on flow processes on the poolside of the heat exchangers, so many details of the PRHR, ICS and PCCS will not be discussed. The PRHR uses C shaped tubes, while the ICS and PCCS use tubes that are basically vertical. The general shapes of these heat exchangers are illustrated in Figure 6.1, but no representation of scale is intended in these drawings, and no attempt was made to represent the bundle configuration of the C tubes for the PRHR. Two important features to note in these drawings are that:

1. The PRHR has substantial horizontal runs in the heat exchanger tubes.
2. The ICS and PCCS heat exchangers have manifolds at top and bottom that will affect the flow pattern.

The primary safety issue associated with these heat exchangers is whether they can remove energy from the reactor at the rate it is being added by decay heat from the core. If so, it is also useful to know how long they will function at this level, before outside intervention is required to supply additional cooling water to the pool. Within the intended uses of the pool heat exchangers, any safety issue related to flow in the pools has been considered to be resolved through experiments and relatively simple heat-transfer calculations. Behaviour of the PRHR has been studied in conjunction with the SPES (C. Medich et al., 1995), ROSA (Y. Kukita et al., 1996), and APEX (Lafi and Reyes, 2000; Hochreiter and Reyes, 1995; Welter et al., 2005) test facilities. The ICS and PCCS have been studied through experiments at the PANDA (Dreier et al., 1996) and PUMA (Bandurski et al., 2001; Ishii et al., 1998) facilities. As the performance of these units under certain accident conditions depends on the heat-transfer on primary and poolsides, a brief discussion of certain important processes in the primary side has to be included here. Indeed, for certain transient scenarios with presence of large concentrations of non-condensable gases in the tubes the heat removal also depends on the distribution of these gases (air or hydrogen or other gases, depending on accident scenario and on whether the containment is inerted). In particular, in presence of a light gas, the flow distribution among the tubes could become very complex and flow reversal and gas accumulation in some tubes could occur. This would lead to a substantial reduction of the active primary heat-transfer area (partial blanketing) with reduction in the overall condensation rate, consequent

transport of a substantial amount of steam into the suppression pool, and, finally, increase of the long-term pressure. This issue has been experimentally tackled in a number of tests in the scaled facility PANDA, which provided some evidence that substantial degradation is not to be expected. However, as the PCC units installed in PANDA represent just a slice of the ESBWR full-scale unit, scale-up to plant size could be an issue that would need further clarification, and this can only be achieved by means of validated, three-dimensional models. The following tasks require a refined TH analysis: 1) Predict the condensation rates in the tubes and its effect on flow and gas concentration distribution; and 2) Predict the heat-transfer rate (boiling) on the poolside.

**Figure 6.1. Heat Exchangers in AP1000 and ESBWR**



Flow in the pool is buoyancy-driven natural circulation, starting with a simple single-phase flow, and evolving to a two-phase flow as the pool is slowly heated. Upward flow is concentrated in close proximity to the heat exchanger. In any horizontal plane, the area occupied by the bulk of the upward mass flow is very small in comparison to the total pool surface area. As a result, the heated flow will spread relatively slowly across the surface, and downward flow velocities in the circulation pattern will be very small. Behaviour of this natural circulation pattern will be significantly different from the widely studied Bénard convection (Daly 1974, Zboray and de Cachard 2005), but will share two key properties observed early in the study classic Bénard problems. Turbulence can be expected to be anisotropic, and once the flow is established, turbulence will be primarily produced through shear effects already represented in standard turbulence models. Turbulence production by special buoyancy effects will be far less important, and may not need special models. However, over most of the water tank, a thermally stratified pattern will exist in which buoyancy effects will act to suppress any turbulence, and depending on the level of fidelity required for the numerical simulation, terms may be needed in the turbulence model to account for this effect. Other considerations for turbulence modelling include the effect of bubbles on turbulence in the continuous liquid field, and the influence of the free surface at the top of the pool.

Early in any transient, heat-transfer from the tubes will be dominated by sub-cooled nucleate boiling at the higher elevations (inlet for interior flow) and by convective heat-transfer lower on the tubes where the interior flow has been cooled enough to permit tube outer surface temperatures below the saturation temperature. Later in a transient, a saturated layer develops in the upper level of the pool and the upper portions of the tube will be in standard nucleate boiling. For a PRHR heat exchanger, experiments at the APEX facility indicate that the top horizontal run of the C will carry most of the heat load, so that experience with nucleate boiling in horizontal tube heat exchangers will be more valuable than standard reactor experience with rod bundles.

## 6.2. Limits of previous approaches and expected improvements with CFD

Heat removal systems implementing heat exchangers, like the isolation condenser (SBWR) and PRHR (AP600), have been modelled in the past with the most well-known system codes (RELAP, CATHARE, ATHLET), in order to calculate their performance and the plant response at different accident conditions. The overall behaviour of heat exchangers with vertical tube bundles, as proposed in these systems, are generally well reproduced in the latest code versions both for pure steam and in presence of non-condensable gases. Nevertheless, the description of the condensation along the interior of the tubes requires further qualification of the related models, while the simulation of the three-dimensional convection in the pool needs a more accurate model than the one-dimensional nodalisation usually adopted.

As concerns the primary side, a specially challenging problem arises in the analysis of severe accident conditions, as the presence of a light gas (hydrogen) leads to very complex conditions in the multi-tube geometry, with possibility of flow reversal in several of the tubes, and strongly inhomogeneous deposition of aerosols. As these conditions could eventually lead to a substantial deterioration of the performance of the condenser, and no credit can be given to simulation performed with 1-D codes, costly experiments are needed for addressing these issues.

As regards the simulation of the poolside heat-transfer, one-dimensional tools cannot provide any reliable prediction for the long-term cooling phase, if the water level drops below the top of the tube bundle. In fact, for an increasingly dry tube bundle, the changing boiling conditions determined by natural-convection below the decreasing water level cannot be represented.

In order to evaluate the reliability and the efficiency of such innovative safety systems in a wide spectrum of accident conditions and to develop a design economically competitive, there is a need of more accurate and better qualified TH numerical tools, able to provide a realistic prediction of all the physical phenomena concerned. A more accurate representation for the pool needs a specific 3D 2-phase module with turbulence effects. The better solution is the modelling of two-phase flows with methods similar to the ones used for multi-dimensional single-phase flows (CFD), including turbulence and free surface effects. This approach may prove to be sufficient transients, but it is expected to be challenged by the most severe scenarios, when bundle dry-out occurs. For these conditions, with a large area of the tubes in contact with a high-quality mixture, the representation of a droplet field may be required, for both improving physical modelling and circumventing numerical problems related to the propagation of the boil-down front under very low (atmospheric) pressure conditions.

For mixing in the suppression pool under long-term decay heat removal conditions, CFD codes are required (using RANS or LES approaches) for calculating the mixing-

induced by the bubble plumes (condensing steam or a mixture of gas and steam) generated by the low flow rate venting.

### 6.3. Selecting a basic model

Modelling of the full pool will require treatment of bubbles as a sub-grid phenomenon. The relatively large void-fraction in the plume later in a transient means that a fully Eulerian rather than Eulerian-Lagrangian approach is preferable for modelling the two-phases. As a minimum, a two-fluid model will be needed with separate mass, energy and momentum equations for each phase. These equations should be supplemented by an equation to follow either bubble number density or interfacial area. The bubble momentum equation will need special terms and corresponding models for standard interfacial drag lift forces, turbulent dispersion forces and momentum exchange associated with phase-change. Virtual mass is very unlikely to produce significant contributions to a model of the full tank, but may be appropriate in special localised calculations in which details are resolved of bubble motion within turbulent eddies. Zboray and de Cachard (2005) can find a more detailed discussion of these source terms for the momentum equation in a paper. Phase-change away from the wall can be handled by a heat conduction limited model, and use of accepted models for interfacial heat-transfer coefficients. Phase-change at the wall will need special contributions to the phase-change source terms and associated interfacial area source term to account for nucleate boiling.

Knowledge of nucleate boiling at the tube surfaces could be enhanced by use of more detailed models employing DNS, or near DNS, including use of a VOF (Hirt and Nichols, 1981) or LS (Osher and Fedkiw, 2001; Shepel et al., 2005) approach to locating the interfaces bounding bubbles. Yadigaroglu (2005) can find a discussion of the potential for this approach in a recent paper.

Because bubbles originating at different locations on the tube's surfaces will be mixed in the flow above the heat exchanger, additional sets of mass, momentum and area transport equations for representative bubble fields may be justified. Work supervised by M. Ishii (Hibiki et al., 1998; Suna et al., 2004) at Purdue University is a good starting point for source terms representing bubble coalescence and breakup in the field equations.

### 6.4. Filtering turbulent scales and two-phase intermittency scales

RANS analysis with a second order Reynolds stress model for turbulence has worked well in the past for single-phase natural-convection. This has the advantage that conflicts will not arise between the filtering scales used for turbulence and for the two-phase model. Given the range of scales between tube spacing and tank dimensions, full LES is probably not a viable choice for full tank simulation, but a hybrid approach may prove to be valuable. If LES is used within the bubbly plume, no conflict of scales is likely as long as the liquid has no superheat. However, once the bulk fluid crosses the saturation line at and above the upper extent of the heat exchanger, bubbles will grow rapidly in size as they rise to the pool's surface. Interactions between turbulent eddies and bubbles in this region will not be simulated well without a great deal of new work on model equations.

## 6.5. ILIS

Thought must be given to both the interface at the surface of the pool, and the interfaces between submerged bubbles and the pool. The simplest model for a pool surface is a flat mesh boundary with free slip boundary conditions. This may be adequate for some purposes, but longer-term simulations need to account for a decreasing water level as pool inventory is boiled away. In addition, a more accurate representation of the fluid dynamics may need to account for surface deviations from horizontal due to the strong upward flow in the bubble plume. An additional consideration is interaction with flow above the pool surface. Basic analysis of the PRHR, ICS or PCCS systems can end with the surface. However, as more integrated system analysis is attempted and pool contributions beyond the heat exchangers are explored, feedback with the containment through the surface becomes more important.

The pool surface may be tracked with an adaptive mesh, or via some surface tracking method within a fixed mesh. The VOF and LS approaches discussed above for bubble surface tracking are both good candidates for following the surface. These numerical technologies have been used and refined over many years, and something is available in just about any commercial, or full featured laboratory CFD package.

Modelling of the bubble interfaces comes at two levels of complexity. The first is for a sub-grid (two-fluid) approach to bubble modelling. Here the interface for each bubble is normally assumed to be spherical, and the IAT equation is used to determine the total bubble interfacial area in any computational volume. This model can be refined by using information on velocities and bubble sizes to introduce other bubble surface shapes (e.g. cap bubble) into underlying calculations for constitutive relationships. The second level of complexity occurs when the mesh is fine enough to resolve some range of bubbles. This becomes a more complicated version of tracking the pool surface, and LS or VOF approaches are applied to locate the surface of each resolved bubble. Software and hardware technology are far from ready to handle this level of detail for a full pool heat exchanger simulation. However, it will be needed to provide the combination of grid resolved and sub-grid modelling of bubbles consistent with LES.

## 6.6. Modelling interfacial transfers

Models are already available for interfacial heat-transfer coefficients associated with bubbly flow from two-phase thermal-hydraulic codes, and should be used when bubbles are treated as a sub-grid phenomenon. These provide direct information on interfacial energy transfer, and indirect information on interfacial mass transfer via a heat conduction limited phase-change model. The interfacial area across which heat and mass are transferred should come from an IAT equation. In this problem with rising bubbles, details of the bubble geometry depend on its history, and cannot be obtained solely from local conditions. Models are also available for terms in the momentum equations representing for standard interfacial drag, lift forces, turbulent dispersion forces, virtual mass, and momentum exchange associated with phase-change. Work is needed to improve existing interfacial heat and momentum transfer coefficients by including the information from the turbulence model.

### 6.7. Modelling turbulent transfers

As previously mentioned the first choice should be a Reynolds stress model for turbulence. This requires addition of transport equations for each component of the Reynolds stress tensor, instead of a single transport equation for turbulent kinetic energy. The presence of bubbles can have a significant effect on turbulence, but this can be modelled as source terms within the chosen set of single-phase turbulence transport equations for the continuous liquid field. For internal flows, bubbles have been observed to have a net damping effect on turbulence intensity near walls. In regions with little shear, turbulence in the liquid is enhanced by wake turbulence from the bubbles. The turbulence transport equations also need to include specific terms to account for buoyancy and for effects from the pool's free surface.

### 6.8. Modelling wall transfers

Momentum transfer at tank walls can be handled by standard wall functions, since the flow there will be single-phase. However, different treatment will be required along tube walls that are producing nucleate boiling. Results analysed by Troshko and Hassan (2001) show significant discrepancies between a standard single-phase model for near-wall velocities and some experimental results in bubbly flow by Sato et al (1981). Troshko and Hassan developed a two-phase wall function model, but further improvements are needed.

Cheung and Liu (1999) have shown that the nucleate boiling heat-transfer and the CHF point depend strongly on the spatial orientation of the heated surface. Detailed experiments and perhaps detailed (near DNS) flow simulations will be needed to obtain high-quality heat-transfer wall functions for the exterior of C-tube or U-tube pool heat exchangers. For some lower accuracy applications, it is possible to adapt heat-transfer correlations from the large volume of literature on horizontal tube heat exchangers to the top and bottom runs of the C tubes (e.g. Cornwell and Houston, 2000). However, most such correlations are based on bulk fluid properties, and need to be adapted with care. Models for nucleate boiling heat-transfer are available that are based upon local fluid conditions at the wall (e.g. Steiner et al., 2005), but anyone adapting them must understand applicability to different surface orientations relative to vertical.

### 6.9. Validation matrix for the selected NRS problems

Separate effects validation for the pool heat exchanger problem should begin with the experiments listed in the previous section on DNB. Unfortunately, these experiments are focused on flows along vertically oriented rods or tubes. To validate simulations of C-tube heat exchangers, CFD-grade data will also be needed for cross flow over horizontally oriented heated rods. Because the pool is sub-cooled over a significant time, simple experiments will be needed to validate condensation models.

CFD-grade validation data is not available from experiments modelling passive reactor pool heat exchangers. However, bubble plume data from the LINX facility (Zboray and de Cachard, 2005; Simiano, 2005; Simiano et al., 2004, 2005, and 2006) is directly applicable to testing most modelling capabilities for the heat exchangers, providing data on velocities, turbulence and void distributions. In addition, temperatures are available at 11 axial locations in the scaled IRWST of the APEX facility, and on its heat exchanger tubes (Welter et al., 2005). These can be used to check a code's ability to produce the correct overall energy balances, and to predict the time evolution of the tank's thermal

stratification. Useful data could also be obtained from ROSA (Kukita et al., 1996). In addition general capabilities of a CFD code to model two-phase natural-convection can be tested against experiments at Forschungszentrum Rossendorf (FZR) (Aszoke et al., 2000) using a cylindrical tank with heated walls. This series of experiments produced excellent data on liquid temperature and void distributions, but nothing on flow velocities or turbulence intensities. For a full spectrum of validation, CFD-grade data will be needed from experiments with scaled prototypic pool heat exchangers.

For the specific issue of the performance of the PCC units of the ESWBR, no CFD-grade validation data is available. However, the capability of the codes to predict the overall performance of the PCCs in presence of a light gas (helium as simulant of hydrogen) in the primary side can be tested using the data of experiments performed in PANDA within the fifth EU-FWP project TEMPEST (2004). These data include mainly temperature distributions in selected tubes, and total condensation rates, but no in-tube gas concentration or velocity measurements. Analyses of one of these experiments (Lyclama and Nijeholt, 2003), where only two PCCs were in operation, have been performed with two CFD codes (Tuomainen, 2003), which produced encouraging results with respect to the qualitative behaviour of one PCC, although using simplified CFD models. The complexity of the phenomena (including different behaviour of the PCC units) and a number of uncertainties in the boundary conditions (especially poolside heat-transfer) prevented, however, a quantitative analysis capturing the details of the gas distribution within the tubes. Future use of these data for code assessment is thus limited to the comparison of the calculated total condensation rate with the experimental results. Furthermore, it should be considered that the CFD model must include representation of all PCC units in operation and appropriate assumptions should be made with respect to the pool heat-transfer.

Validation tests are also available at a much smaller scale from an entirely different field of research. Two-phase natural circulation is also an important phenomenon in electrochemical cells. Gas produced at the anode and cathode of such a cell drives circulation patterns that can be important to the performance of the cell. Data (LDV, PIV, and image processed bubble-size distributions) taken by Boissonneau and Byrne (2000) in a small electrochemical cell could be useful in validation of a two-phase CFD model in the realm of natural circulation. However, additional equations would be needed to model transport of ions, electric current in the fluid, and bubble production at the anode and cathode. One example is a recent analysis by Mat and Aldas (2005) using the CFD code PHOENICS to explore convection patterns in a simple hypothetical electrochemical cell. They found that the flow pattern depended strongly on assumed bubble-size.

## References

Aszoke, A., E. Krepper and H.M. Prasser (2000), "Experimental and numerical investigation of one and two-phase natural-convection in storage tanks," *Heat and Mass Transfer*, Vol. 36, pp. 497-504.

Boissonneau, P. and P. Byrne (2000), "An experimental investigation of bubble-induced free convection in a small electrochemical cell", *Journal of Applied Electrochemistry*, Vol. 30, pp. 767-775.

Bandurski, T., M. Huggenberger, J. Dreier, C. Aubert, F. Putz, R.E. Gamble and G. Yadigaroglu (2001), "Influence of the distribution of non-condensable on passive containment condenser performance in PANDA, Nuclear Engineering and Design Vol. 204, pp. 285–298.

Cheung, F.B. and Y.C. Liu (1999), "Natural-Convection Boiling on the Downward-Facing Side of a Hemispherical Annular Channel," *Experimental Heat-Transfer*, Vol. 12, pp. 17-32.

Cornwell, K. and S.D. Houston (2000), "Assessment of convective pool boiling on horizontal tubes," *Multi-phase Science and Technology*, Vol. 12, n 3-4, pp. 103-128.

Cummins, W.E., M.M. Corletti and T.L. Schulz (2003), "Westinghouse AP1000 Advanced Passive Plant," *Proceedings of ICAPP 03*, Paper 3235.

Daly, B.J. (1974), "A numerical study of turbulence transitions in convective flow", *J. Fluid Mech*, Vol. 64, pp. 129-165.

Dreier, J., M. Huggenberger, C. Aubert, Th. Bandurski, O. Fischer, J. Healzer, S. Lomperski, H.-J. Strassberger, G. Varadi and G. Yadigaroglu (1996), "First PANDA tests," *Proceedings of the 1996 4th ASME/JSME International Conference on Nuclear Engineering, ICONE-4. Part 1B*, pp. 843-852, New Orleans, March 10-14.

Hibiki, T., S. Hogsett and M. Ishii (1998), "Local measurement of interfacial area, interfacial velocity and liquid turbulence in two-phase flow," *Nuclear Engineering and Design* Vol. 184, pp. 287–304.

Hirt, C.W. and B.D. Nichols (1981), "VOF method for the dynamics of free boundaries," *J.Comput. Phys.* Vol. 39, p. 201.

Hochreiter, L.E. and J.N. Reyes (1995), "Comparison of SPES-2 and APEX tests to examine AP600 integral system performance," *Proceedings of the 1995 International Joint Power Generation Conference. Part 2*, pp. 41-56, ASME Nuclear Engineering Division, Minneapolis, 8-12 October.

Ishii, M., S.T. Revankar, T. Leonardi, R. Dowlati, M.L. Bertodano, I. Babelli, W. Wang, H. Pokharna, V.H. Ransom, R. Viskanta and J.T. Han (1998), "The three-level scaling approach with application to the Purdue University Multi-Dimensional Integral Test Assembly (PUMA)," *Nuclear Engineering and Design*, Vol. 186 pp. 177–211.

Krishnamurti, R. (1973), "Some further studies on the transition to turbulent convection," *J. Fluid Mech.*, Vol. 60, pp 285-303.

Kukita, Y., T. Yonomoto, H. Asaka, H. Nakamura, H. Kumamaru, Y. Anoda, T.J. Boucher, M.G. Ortiz, R.A. Shaw and R.R. Schultz (1996), "ROSA/AP600 testing: facility modifications and initial test results," *Journal of Nuclear Science and Technology*, Vol. 33, pp. 259-265.

Lafi, A.Y. and J.N. Reyes (2000), "Comparative study of station blackout counterpart tests in APEX and ROSA/AP600", *Nuclear Technology*, Vol. 130, pp. 177-183.

Lyclama a' Nijeholt, J.A. (2003), "Modelling of the ESBWR Passive Containment Cooling System – CFD analysis of the Effect of Helium on the Performance of the PCCS in PANDA Test T1.2", NRG internal Report 20407/03.56479/C (CONFIDENTIAL).

Mat, M.D. and K. Aldas (2005), "Application of a two-phase flow model for natural-convection in an electrochemical cell", *Int. J. of Hydrogen Energy*, March 2005, Vol. 30, pp. 411-420.

Medich, C., M. Rigamonti, M. Tarantini, R. Martinelli and L. Conway (1995), “SPES-2, the full-height, full-pressure, test facility simulating the AP600 plant: Main results from the experimental campaign” Proceedings of the 1995 International Joint Power Generation Conference. Part 2, pp. 33-40, ASME Nuclear Engineering Division, Minneapolis, 8-12 October.

Osher, S. and R.P. Fedkiw (2001), “LS methods: an overview and some recent results,” *J. Comput. Phys.* Vol. 169, pp. 463–502.

Paladino, D., O. Auban, M. Huggenberger, P. Candreia and H.J. Strassberger (2003), “Hydrogen Impacts on PCCS and Accident Mitigating Design Features”, Deliverable D06, Part C, PSI internal Report, TM-42-03-03, ALPHA-03-03-0.

Troshko, A.A. and Y.A. Hassan (2001), “Law-of-the wall for two-phase turbulent boundary layers”, *International Journal of Heat and Mass Transfer*, Vol. 44, pp. 871-875.

Sato, Y., M. Sadatomi and K. Sekoguchi (1981), Momentum and heat-transfer in two-phase bubble flow, Parts I and II, *International Journal of Multi-phase Flow* Vol. 7 pp. 167-190.

Shepel, S.V., B.L. Smith and S. Paolucci (2005), “Implementation of a LS ITM in the FIDAP and CFX-4 Codes,” *Transactions of the ASME*, Vol. 127, pp. 674-685.

Simiano, M., R. Zboray, F. de Cachard, D. Lakehal and G. Yadigaroglu (2004), Extensive measurements of the hydrodynamic characteristics of large-scale bubble Plumes. Proc. 5<sup>th</sup> International Conference on Multi-phase Flow, ICMF’04, Yokohama, Japan, 30 May-4 June 2004.

Simiano M., F. de Cachard and G. Yadigaroglu (2006), “Comprehensive experimental investigation of the hydrodynamics of large-scale, 3D, oscillating bubble plumes”, *International Journal of Multi-phase Flow* (ISSN 0301-9322), 32, 1160-1181.

Simiano, M., R. Zboray, F. de Cachard, D. Lakehal and G. Yadigaroglu (2005), “Advanced Processing of Liquid-Bubble PIV Measurements in Large Bubble Plumes”, 11<sup>th</sup> Int. Topical Meeting on Nuclear Reactor Thermal-Hydraulics (NURETH-11), 2-6 October 2005, Avignon, France, CD-ROM (ISBN 2-9516195).

Simiano, M. (2005), “Experimental investigation of large-scale three-dimensional bubble plume dynamics”, Thesis Nr. 16220, ETHZ Zurich.

Suna, X., S. Kima, M. Ishii and S.G. Beus (2004), “Modelling of bubble coalescence and disintegration in confined upward two-phase flow,” *Nuclear Engineering and Design* Vol. 230, pp. 3–26.

Steiner, H., A. Kobor and L. Gebhard (2005), “A wall heat-transfer model for sub-cooled boiling flow”, *International Journal of Heat and Mass Transfer*, Vol. 48, pp. 4161–4173.

TEMPEST (Testing and Enhanced Modelling of Passive Evolutionary Systems Technology for Containment Cooling) (2004), Final Synthesis Report, 5<sup>th</sup> EURATOM Framework Programme Contract FIKS-CT-2000-00095.

Tuomainen, M. (2003), “Fluent simulation of PCC Behaviour in PANDA Test T1.2”, Deliverable D09b, VTT internal Report PRO1/P7016/03.

Welter, K.B., S.M. Bajorek, J.N. Reyes and G.S. Rhee (2005), “APEX-AP1000 Confirmatory Testing To Support AP1000 Design Certification,” Nuclear Regulatory Commission Report, NUREG-1826.

Xu, Y., M. Ishii and M.A. Feltus (2004), “Safety analysis of multiple-failure of passive safety systems in SBWR-1200 SBLOCA,” Nuclear Engineering and Design Vol. 230 pp. 107–119.

Yadigaroglu, G. (2005) “Computational Fluid Dynamics for nuclear applications: from CFD to multi-scale CMFD,” Nuclear Engineering and Design Vol. 235 pp. 153–164..

Zboray, R. and F. de Cachard (2005), “Simulating large-scale bubble plumes using various closure and two-phase turbulence models,” Nuclear Engineering and Design Vol. 235, pp. 867–884.

## 7. The steam discharge in a pool

### 7.1. Identification of all-important flow processes of the issue

#### Reactors adopting the relevant system

Several types of LWR adopt a concept of steam discharge into a sub-cooled water pool as a safety-related system. Here the steam is discharged either from a reactor coolant system (RCS) or from a compartment of a containment system (CS), as a pure steam or a mixture of steam and non-condensable, for depressurisation or gas venting of relevant systems. An example can be found in BWR suppression pool [USNRC, 1981]. Some of advanced LWRs (ALWR) also adopts a similar design concept. They include a pressure suppression pool in SBWR [Gamble et al., 2001], an IRWST pool with the automatic depressurisation system (ADS) in AP1000 [Cummins et al., 2003], and an IRWST pool with the safety depressurisation and vent system (SDVS) in APR1400 [Lee et al., 2003; Song et al., 2006].

The pressure suppression pool (SP) of SBWR is equipped with two different discharging devices: main vents with several side holes and a down-comer with one downward discharge hole of large diameter [Gamble et al., 2001]. Discharge from the main vents consists of three phases: water clearing for very short period, a discharge of steam with a high concentration of non-condensable, and successively a continuous discharge of steam with low concentration of non-condensable over a wide range of mass fluxes. The discharge from the down-comer shows a rather low steam mass flux, often leading to the chugging, which is one of the unstable condensation modes. In the case of the IRWST for advanced PWR designs such as APR1400 or AP1000, many discharging devices called the sparger or quencher are installed, of which the shape is typically either the I-type without side arms or more complicated shape (X-type or T-type) with side arms. Each sparger or arm has many discharging holes with small diameter of typically about ten mm. As an example, in APR1400, each sparger has 144 side holes with ten mm in diameter and 1 bottom hole with 25 mm in diameter [Song et al., 2006]. This case, in general, shows three different discharging phases typically for an abnormal operation like a total loss of feed-water (TLOFW) [Song et al., 2002; Song et al., 2003]: a water clearing at the beginning of discharge, followed by an air clearing for very short period, and finally a continuous discharge of pure saturated steam usually under very high steam mass flux for a long time.

There are practically at least two kinds of technical concern during the actuation of discharging devices. The one is a concern on thermo-hydraulically induced mechanical loads on the structures of relevant systems, which are induced either by the direct influence of discharging process or by resultant thermo-fluid-dynamic processes such as periodic expansion/contraction of large air bubbles or pressure oscillation due to unstable condensation of discharged steam in a water pool. The other concern is on the thermal mixing in a water pool. At an early stage of steam discharge, the steam is condensed effectively by mixing with sub-cooled pool water. As time goes on, however, the pool water temperature increases locally or globally above a certain limit due to a continuous influx of high-energy steam [USNRC, 1981; Kang and Song, 2006(a); Kang et al., 2005]. Accordingly, the condensation efficiency becomes decreasing and an unstable condensation, such as condensation oscillation or chugging, may occur due to a high pool water temperature. In fact, some structural failures due to the condensation oscillation have been previously reported in BWR SP [USNRC, 1981]. From a viewpoint of unstable

condensation, we can consider a local hot spot, which may exist due to an unfavourable thermal mixing in a large pool and resultantly affect the stability of condensation during a long-term bleed-feed operation in TLOFW [Song et al., 2006]. From a global viewpoint, we can also consider a thermal stratification, which usually form in the upper part of water pool.

During the venting process in ALWR, the steam discharge into a water pool is commonly considered along with a possible inclusion of non-condensable from the viewpoints of both mechanical loads and the thermal mixing. With the CFD application to nuclear reactor safety problems in mind (at least within the context of this report), it may be preferable to confine our attention only to the case of DCC of a pure steam discharged into a sub-cooled water pool through immersed spargers. So excluded hereafter for discussion is our interests in condensation-induced pressure oscillation, the steam-gas mixture effect on DCC and the resultant thermal mixing, and DCC occurring in rather flat condensing interfaces (e.g. condensation in a stratified or separated two-phase flow situation).

### **Basic flow processes**

The DCC of steam discharged in a pool is very much dependent on the design of steam sparger, which can affect significantly the efficiency and stability of condensation as well as the thermal mixing in pool. DCC of our interest is revealed when saturated or superheated steam flow contacts with a highly sub-cooled liquid. Typically, in this situation, the liquid has a low-velocity or is quasi-stagnant whereas steam flows into a pool as a jet with very high-speed. This leads to a rapid condensation of steam and the resultant turbulent mixing. Usually pressure also oscillates locally when a certain volume of steam is condensed radically leading to an unstable flow behaviour or thermally non-uniform state in a pool.

The process of steam jetting into a pool are normally associated with several elementary flow phenomena, such as the steam jet, turbulent jet, impinging jet, wall jet, and the resultant local and global flow circulation. Figure 1(a) shows a flow pattern induced by a horizontally discharging steam jet, which is typically observed in a sub-cooled water pool. Steam, discharged usually at the choking condition through spargers in PWR cases, forms a steam jet just downstream of the sparging hole or nozzle. In general, the steam jet consists of the vapour core and two-phase mixing region. The steam jet acts as either a forced jet under a high discharging mass flux, which penetrates the pool horizontally with very little upward motion, or a *buoyant plume* under a low flux condition with distinctly upward motion near the exit of a sparger due to buoyancy effect, as experimentally observed in Figure 1(b) in the B&C facility at KAERI [Cho et al., 2002]. As the steam jet penetrates horizontally into a water pool and entrains liquid from the pool water, it induces a turbulent jet, of which the velocity decays slowly along its axial distance. Once the turbulent jet becomes a perpendicularly impinging jet hitting on the pool wall, it will expand into a wall jet, which is a radial jet moving out along the wall in all directions. This situation is true for a high discharging mass flux especially under a large pool sub-cooling condition. When a pool temperature increases, however, the circulation flow pattern induced by the horizontal turbulent jets diminishes and instead, a type of buoyant plume appears distinctively near the sparger due to the decrease of condensation efficiency and the increased effect of buoyancy.

Figure 7.1. Circulation flow pattern induced by a horizontal steam discharge in a pool

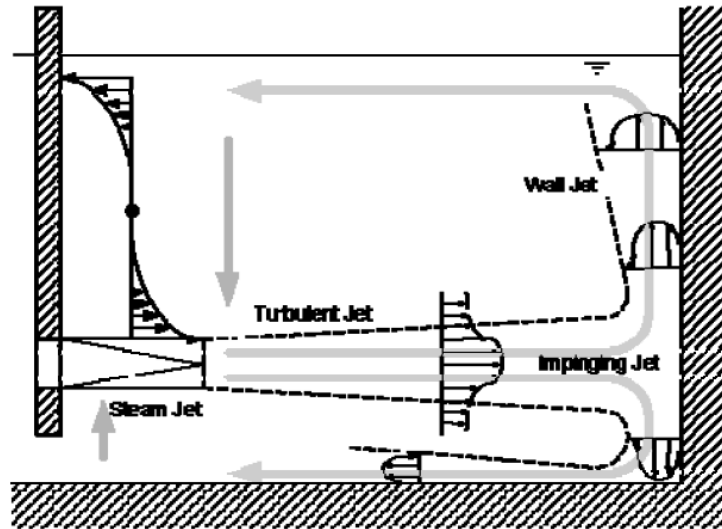
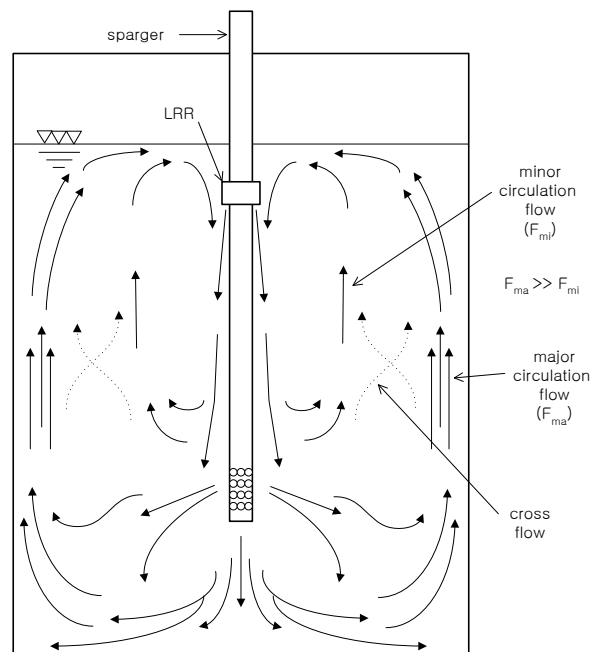


Figure 7.2. Flow pattern reconstructed from the temperature measurements in a scaled facility to simulate APR1400: Two types of steam jets shown [Cho et al., 2002]

(Typical of APR1400)



### Major thermal-hydraulic phenomena

A steam sparger, in general, consists of a number of discharging holes: hole or nozzle type, and horizontal or vertical orientation in upward or downward direction. Therefore, it is very important to understand the discharging behaviour of a single jet in a pool.

Many investigators have previously studied the condensing behaviour of a single jet analytically or experimentally. They proposed some empirical or semi-analytical models for the heat-transfer coefficient over a wide range of steam mass flux conditions [e.g. Aya and Nariai, 1991; Young et al., 1974; Fukuda, 1982; Cumo et al., 1978; Kerney et al., 1972; Chun et al., 1996]. Also empirical co-relations of the steam jet length was proposed by many investigators [e.g. Del Tin et al., 1983; Kerney et al., 1972; Weimer et al., 1973; Chun et al., 1996]. Song et al. (1998) also investigated experimentally the shapes of steam jet, steam jet length, heat-transfer coefficients, and axial and radial temperature distributions in a steam jet over a wide range of test conditions with different nozzle diameters. Three different shapes of steam jet have been identified, which include the conical, ellipsoidal and divergent types, as typically shown in Figure 7.2. Stable steam jets, such as conical and ellipsoidal shapes, have been observed under a high steam mass flux with a large pool sub-cooling in small hole sizes.

Figure 7.3. Different types of steam jet in a sub-cooled water pool [Song et al., 1998]

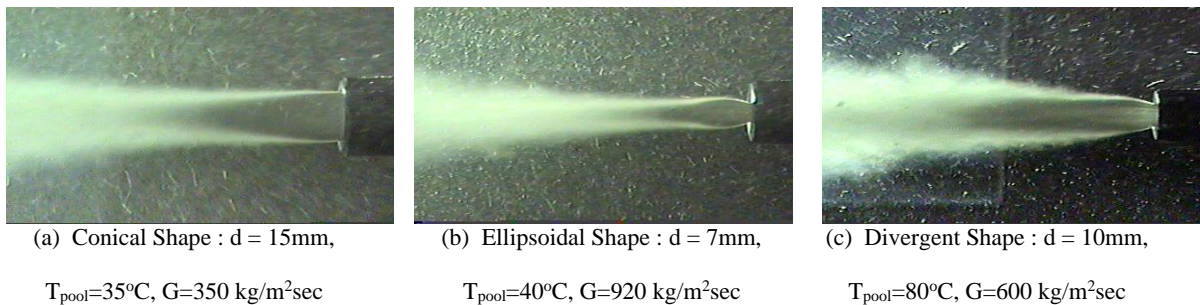


Figure 7.4. Condensation regime map for a single-hole sparger [Cho et al., 1998]

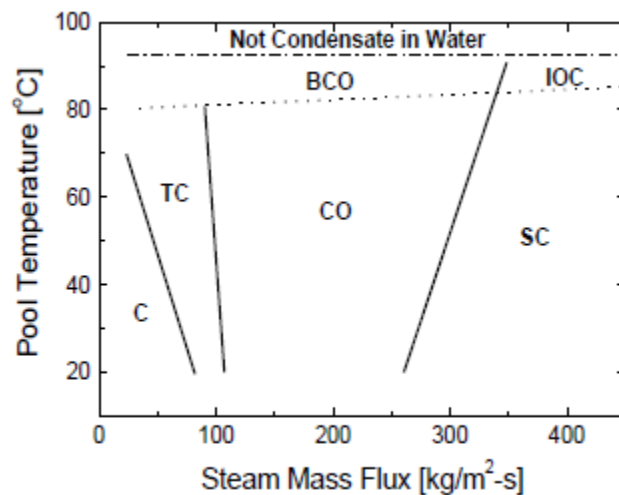
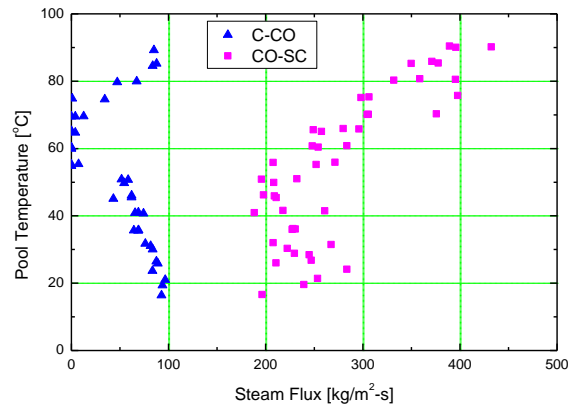


Figure 7.5. Condensation regime map for a multi-hole sparger [Kim and Song, 2003]



Recently Cho et al. (2004) observed different behaviours of thermal mixing in a pool, which are dependent on the arrangement of discharging holes for multi-holed sparger and this attributes to different behaviour of the interaction between adjacent steam jets. Gamble et al. (2001) investigated the interaction of adjacent steam jets for typical conditions in a SBWR blowdown flow. There is an overlap between adjacent jets, and the cumulative jet looks more like a rectangular jet where there is no growth in the vertical direction and the jet expands in the horizontal direction.

It is well-known that the interfacial transfer of momentum, heat and mass during the DCC of steam in a pool is highly dependent on the condensation regime. It is not likely that a correct prediction can be found for an associated heat-transfer rate unless the mechanism of condensation is well understood and the condensation regime is identified properly. Condensation regime maps, which is mostly dependent on the steam mass flux and pool temperature (more exactly sub-cooling), have been proposed by many investigators, including Nariai and Aya (1986) and Fukuda (1982) in vertical nozzle, and Young et al. (1974) in a horizontal nozzle for rather limited range of steam mass flux, among others. Chun et al. [6] extended the steam mass flux range to 1 500 kg/m<sup>2</sup>·s for small horizontal nozzles. Recently Cho et al. (1998) proposed a condensation regime map of single nozzle where the condensation mode could be classified into six regions: chugging (C), transitional (TC), condensation oscillation (CO), stable condensation (SC), bubbling condensation oscillation (BCO) and interfacial oscillation condensation (IOC) as shown in Figure 7.4. Recently Kim and Song (2003) developed a new condensation regime map, which consider the effect of multiple discharging, as shown in Figure 7.5. The regime map for the case of multiple holes shows the trends of C-CO (for higher temperature region) and CO-SC (for lower temperature region), which are slightly different from those of the single nozzle case.

### Multi-scale approach

The physical processes to affect a thermal mixing due to the DCC of steam in a pool have three different scales, typically shown in Figure 7.1 and Figure 7.6 can be summarised as follows:

- **Macro-scale (Pool):** Typical phenomena having this scale are the turbulent jet, impinging jet and wall jet, and the mixing between these jets and quasi-stagnant surrounding water in a pool. These have a length of order of about several tenth cm

or one m. Single-phase mixing pattern affected by these jets can be reasonably described by using standard CFD analysis tools or even by adopting multi-dimensional models with very fine-mesh in system analysis codes.

- **Meso-scale** (Jets region): Phenomena at this scale include the formation of steam jets and the interaction between adjacent ones, all of which have a length of order of about one cm. Since the turbulent jet forms due to the momentum interaction between discharged steam jet and its surrounding liquid, the details of steam jet behaviour should be well predicted, especially in terms of momentum transfer to its neighbouring liquid, for understanding the behaviour of turbulent jets and their resultant effects on impinging jets. Once the information on meso-scale parameters is known, the macro-scale information, such as a temperature distribution in pool, can be easily predicted using state-of-the-art CFD tools.

For accurate calculation of the behaviour of a condensing steam jet, much smaller scale (micro-scale) information shall be required a priori to simulate the detailed phenomena at the condensing interfaces, especially on the boundary layer of surrounding liquid side.

- **Micro-scale** (Interfacial region between steam jet and pool water): Phenomena at this scale include the local characteristics of heat and mass transfer at the interfaces between steam jets and surrounding liquid. Also included is the interaction of some of the isolated micro-bubbles in the two-phase mixing region near the surface and the downstream of a vapour core, and the collapse of bubbles in turbulent mixing region by condensation. All of these parameters have a length of order of about one mm or smaller.

Since the interaction between vapour core and surrounding liquid at the condensing interfaces is microscopic, the details of a condensing jet and the resultant mixing phenomena in a pool should be dealt with based on the *multi-scale* approach as pointed out by Yadigaroglu (2005). The most important phenomena to be treated in CFD analysis of the macroscopic behaviour of thermal mixing-induced by the steam discharge in a pool, however, are associated with the meso-scale phenomena such as the momentum interaction between a group of discharged steam jets and its surrounding liquid, as pointed out by Kang and Song (2008).

## 7.2. Limits of previous approaches and expected improvements with CFD

To predict the behaviour of steam discharge in a pool requires three-dimensional capabilities since the liquid temperature in a pool, which affects the condensation efficiency, depends on turbulent mixing and/or possibly gravity-driven circulation with density stratification.

Even though, there are some applications of system analysis codes with multi-dimensional capabilities based on the two-fluid model, such as Gamble et al. (2001), Bang et al. (2005), B.D. Chung et al. (2005), they might be applicable only to the cases of rough estimation of relevant phenomena due to the limitations of at least both the attainable mesh size and the treatable minimal size of physical length scales in the codes. In fact, it is very difficult to properly simulate two different kinds of steam jet behaviour, such as a forced jet or a buoyant plume, which directly affect the momentum transfer from a steam jet to a subsequent turbulent liquid jet. Without proper simulation of this momentum transfer among others, it will be hard to accurately predict the overall behaviour of mixing pattern in a large pool.

A better results can be obtained based on the CFD approach for multi-dimensional analysis of condensing two-phase flows and the resultant thermal mixing phenomena: (i) Conventional CFD methods for single-phase flow analysis with some simplified or sophisticated models specific to simulating the steam jet and its interaction with pool water; (ii) CFD methods based on the classical two-fluid model; (iii) CFD methods based on the two-fluid model along with the ITM; and (iv) also the use of advanced numerical methods based on the single-fluid approach.

The most promising analysis tools for the future will be the adoption of CMFD along with an ITM based on the detailed understanding of microscopic phenomena in and around the condensing interfaces. Now, there is no single numerical tool well adapted to predict the DCC phenomena in a pool with a sufficient accuracy. There are certain limitations of lumped-parameter and coarse-mesh approaches to certain classes of thermal-hydraulic phenomena relevant to nuclear reactor safety. As pointed out by Yadigaroglu (2005), the physics of the flow may be amenable to appropriate prediction by scale-specific strategies at each level of multiple scales, and the linking of the solutions for each scale will be required to consider the inter-scale interaction and to close the problem of interest with a multiplicity of scales.

### 7.3. Selecting a basic model

The behaviour of impinging jet and wall jet, which affect both locally the thermal mixing near the elevation of steam discharging and macroscopically the global circulation flow pattern in a pool, can be rather easily predicted using the state-of-the-art CFD tools with appropriately chosen turbulence models and these prediction can also be easily validated using experimental data.

One of the key issues for solving the problems related to the steam discharge in a pool is how to practically deal with and determine the phasic interfaces. The phasic interfaces related to the steam discharge in a pool can be classified into two cases: one case is the *condensing interface* between the vapour core region of the steam jet and the surrounding water pool, and between small vapour bubbles finely dispersed in the two-phase mixing region of steam jet and the surrounding water. This interface is intrinsically unstable in a microscopic sense and may be violent in some conditions. The other case is the *free surface* of the pool water, which is rather stagnant or somewhat wavy due to sloshing in a rather confined pool. This is a moving interface between two immiscible phases that can be encountered diversely in practical applications.

Both the condensing interface and the free surface can be simulated using the sophisticated ITMs, which are still in an early stage of development. Tracking the interface of jetting, expanding or rising vapour bubbles is required for determining the interfacial area and its concentration, which are mostly important for the transfer of momentum, heat and mass in the DCC process.

### 7.4. Filtering turbulent scales and two-phase intermittency scales

Considering the condensing flow in a pool, there will be macroscopically several different cases of flow structure: a high-velocity vapour core region surrounded by a continuous liquid phase, medium-velocity two-phase mixture region surrounded by a continuous liquid phase, impinging jet and wall jet regions, and the low-velocity global circulation zone, as illustrated in Figure 7.1.

Depending on the existing phases and flow velocity range in each region, the characteristics of flow turbulence will be different. At the interface between a vapour core and its surrounding liquid, an interfacial model applicable to the case of separated flow might be used, whereas in the two-phase mixture region, another model, which is applicable to the case of a finely dispersed bubble flow, could be valid. Around the flow stagnation point on the wall, the impinging jet hits the pool wall to form a wall jet, where the Reynolds Analogy will not be used in the turbulent energy equation any more due to a large pressure drop near the wall caused by the impinging jet [Bae and Sung, 2001].

In general, the RANS approach may be a suitable choice for the CFD analysis of the steam discharge in a pool considering the computational economics and the characteristics of a jet flow under the choking condition. A time average or ensemble average of equations as in the RANS approach can be applied. All turbulent fluctuations and two-phase intermittency scales can be filtered in this approach if they are significantly smaller than scales of the mean flow. When a detailed estimation is trying to resolve the eddy motion of two-phase mixtures using the RANS model with simple turbulence models such as the eddy viscosity model or using the isotropic turbulence model, however, it must be applied very carefully since this may lead to a wrong velocity profile.

In the continuous liquid phase, the LES approach can be applied [Smith et al., 2003]. This requires that there is a filter scale smaller than the large eddies of the liquid flow and larger than the bubble-size. Compared to the RANS approach, using the LES will allow simulation of bubble dispersion by the liquid turbulence instead of modelling it.

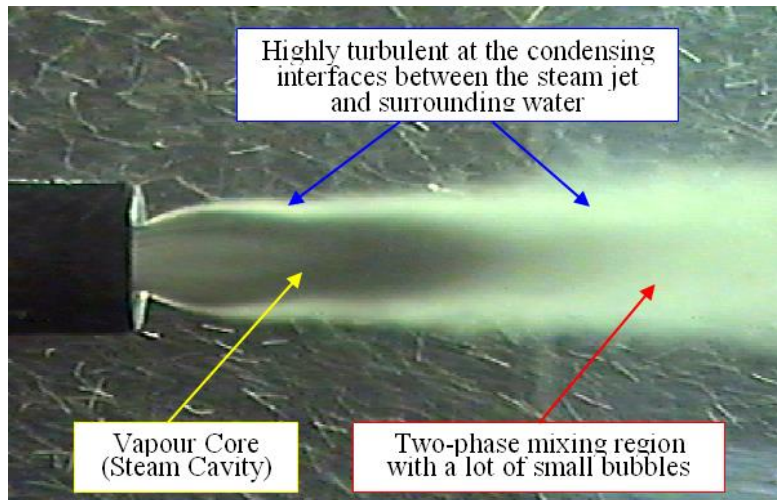
## 7.5. ILIS

In the case of the steam discharge in a pool, where a high condensation rate due to a large temperature difference between the two-phases is achievable, the condensation process can directly generate instabilities. The behaviour of these condensation instabilities also influences the liquid entrainment into a steam jet region. The changes in these instabilities are responsible for the variations in the transfer of heat and mass on the surface of steam jet.

The DCC-related heat-transfer rate and the resultant mixing in a pool can be predictable only when the condensation mechanism is well understood and both the hydrodynamic and condensation regimes can be identified properly. Determination of the interfacial area and its concentration at the interface of jetting, and the expanding or rising of vapour or gas bubbles is mostly important for predicting the transfer of momentum, heat and mass in this mixing phenomena accompanied by the DCC process.

The important local interfacial structure to be modelled for the steam discharge in a pool is the shape and dimensions of the vapour core as typically shown in Figure 7.6 [Song et al., 1998]. Transport phenomena at the interface between the steam jet and the surrounding pool water as well as between the steam jet and the turbulent jet regions is important. The characteristics of momentum and heat transfers at the phasic interfaces are dependent on each phase or field.

Figure 7.6. Steam jet of high mass flux in a sub-cooled pool [Song et al., 1998] (Nozzle dia.: 10.15 mm, Mass Flux: 600 kg/m<sup>2</sup>s, Pool Temp.: 40°C)



### 7.6. Modelling interfacial transfers

In the case of steam discharge in a pool, there are two kinds of liquid-gas interface coexisting simultaneously in different regions of the computational domain: the *condensing interface* between the vapour core or bubbles and pool liquid, and the *free surface* of pool liquid. Either these interfaces have to be modelled using two different models or at least the same model with different values for the parameters. In order to apply the adequate model, the phasic interface has to be identified during CFD analysis. Concerning the phasic interfaces to affect the heat and mass transfer in the case of the steam discharge in a pool, two continuous regions of gas and liquid, and one dispersed bubbles region located near the vapour core boundary around the steam jet are typically observed.

The heat-transfer rate and the resultant mixing in a pool can be predictable when the thermo-fluid-dynamic information at the *condensing interfaces* is available. The *interfacial area* and *its concentration* at the interface of jetting, and broken-up or rising bubbles are mostly important for the transfer of momentum, heat and mass in the DCC process, and it is very much dependent on the condensation regimes. For proper simulation of condensation process of the steam jet and its interaction with surrounding sub-cooled liquid, the shape and dimension (length and expansion ratio, etc.) of the vapour core should be properly predictable.

Since, the flow regions of interest are the vapour core surface and the two-phase mixture region in the steam jet, and, the interface between these jet regions and the surrounding pool water, as far as the interfacial transfer is concerned; a correct estimation of the momentum, heat and mass transfer at those regions should be performed to model the interfacial transfer phenomena. When the pool water is entrained into the vapour core and two-phase mixture jet regions, the interfacial friction should be importantly considered.

## 7.7. Modelling turbulent transfers

There are many challenging issues remaining in the development of reliable turbulence models for two-phase flow. Most of CFD analysis for bubbly flow, which corresponds to the interface region between the vapour core and its neighbouring liquid, is based on the RANS *approach*. In case of two-phase flow application of this approach, the turbulent dispersion force should be considered in addition to other interfacial forces such as drag and non-drag forces. Adequate models of these forces are needed based on mechanistic approaches for universal application.

To model the turbulent transfer for a two-phase flow, it is one way that the *two-equation model* (i.e.  $k$ - $\varepsilon$  or  $k$ - $\omega$  model) of the single-phase turbulence needs to be expanded into two-phase flow by adding an interfacial transfer term for *k-equation* and  *$\varepsilon$ -equation*. The contribution of these terms into each equation, however, is not clear. The effort is needed to quantify these transfer phenomena. The bubbles and the liquid in the two-phase mixture region in a steam jet may enhance the turbulence of the continuous phase. This additional turbulence effect should also be modelled. In fact, the turbulent intensity in the inlet region of the turbulent jet has been experimentally observed to be non-isotropic and be an order of 20~25 % in its magnitude, which is much larger than the default value of max. Ten per cent in commercial CFDD codes (van Wissen et al., 2005; Kang and Song, 2008; Choo and Song, 2008).

The LES-based techniques can be used for simulating the turbulence in liquid phase of bubbly flow [e.g. Smith et al., 2003; Meier, 1999; Lakehal et al., 2002]; based on the rationale such that large-scale turbulent motions, which are captured explicitly within the LES methodology, will interact strongly with bubbles themselves, and thereby be mostly responsible for macroscopic bubble motion [Smith et al., 2003]. In this approach, however, the sub-grid-scale (SGS) would be less important, affecting only small-scale interactions.

The characteristics of liquid turbulence for both the impinging jet and wall jet regions, which might be much different from the case of conventional single-phase flow field such as a confined channel or open space, affect the exchange of momentum between these jet regions and the surrounding liquid. Since the turbulence model for these jet regions, however, is already developed from other application fields, and they might be applied to the case of pool mixing of current interest.

## 7.8. Modelling wall transfers

In general, the primary effect of the wall on the steam discharge in a pool may be the wall lubrication force implemented in the source term of momentum equation with the two-fluid model. This force, however, is meaningful only for the case that the steam is discharged closely to the wall and there exists a bubbly flow near the wall. Since in most cases of steam discharging into a pool for nuclear reactor applications, the steam jet discharged from the sparger or subsequently forming turbulent jet is usually far from the pool wall, and thereby it is not necessary to consider practically the wall lubrication force applicable to two-phase flow field. Instead, the conventional no-slip condition should be applied for the thermal mixing phenomena in a pool.

As to, laterally discharged steam jet near the wall, we have to consider two different cases, depending on the steam mass flux discharged, to affect the relative importance of impinging jet: the case of high mass flux shows significantly an impinging jet due to the momentum-controlled jetting, whereas the other case of low mass flux shows practically

no impinging jet due to the buoyancy-controlled plume. Two different kinds of momentum transfer from the steam cavity to surrounding water as well as the interaction of induced impinging jet with wall should be well described in the analysis to properly model the wall transfer.

Another wall effect may be associated with the existence of a stagnation point on the wall when the impinging jet hits the pool wall to form a wall jet. Around the flow *stagnation point* on the wall, the Reynolds Analogy usually used in the turbulent energy equation may no longer valid [Bae and Sung, 2001].

### 7.9. Validation matrix for the steam discharge in a pool

The condensing behaviour of steam discharged in a sub-cooled water pool and the resultant thermal mixing requires: a tool with three-dimensional prediction capabilities since the liquid temperature, which affects the condensation efficiency, depends usually on turbulent mixing and possibly on the gravity-driven circulation due to a buoyancy effect especially under a density stratification situation or a low discharge flow condition. So it is generally needed to validate the CFD tools against both *local* information on the interfacial area and the transfer of momentum, heat and mass in and around the steam jet, and the *global* information on the temperature and velocity distributions and flow circulation pattern in a pool.

Experiments on the steam discharge in a pool can be classified into two types of testing: basic test and integral test. The *basic* test is required for understanding the mechanism of the DCC of steam jet and its momentum transfer to subsequent turbulent jet. It is likely to our understanding that a proper prediction of the DCC-associated heat-transfer rate and resultant mixing cannot be realised unless the condensation mechanism is understood and both the hydrodynamic and condensation regimes are identified correctly. Basic tests should reveal the local characteristics of flow and heat-transfer in and around the steam jet region, such as the temperature, phasic boundary and interfacial area of vapour core, as well as the velocity and temperature distribution in the turbulent jet region under well-defined initial and boundary conditions.

*Integral* tests should provide detailed information on the macroscopic flow pattern in a pool, such as global circulation pattern, overall mixing and thermal stratification behaviours, as well as the interaction of steam jet-induced impinging jet with the wall and the phenomena in and near the free surface of the pool. These tests should also cover the condensing and mixing behaviours induced differently by either the buoyant plumes forming under low steam mass flux condition or the forced jet forming under high steam mass flux condition.

Currently available experimental data sets for developing physical models for local phenomena of various jetting and jets-induced local mixing as well as the macroscopic mixing patterns in a large pool include the followings:

(1) Basic tests:

- GIRLS: Vertical upward or horizontal venting nozzle with single or multiple holes immersed in a circular tank for steam ejection to a water pool. [Kim and Song, 2003].
- JICO: Vertical upward venting nozzle with a single-hole immersed in a circular tank for steam ejection to a water pool, highly instrumented to measure

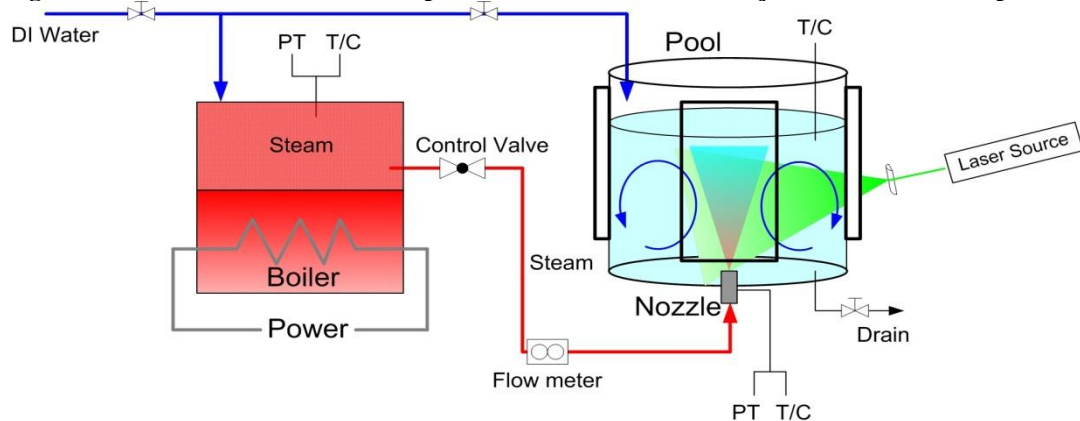
two-dimensional distribution of velocity in and around the steam jet, as schematically shown in Figure 7.7. [Choo and Song, 2008].

- LINX: Vertical venting tube with downward injection of steam [Smith et al., 2003].
- The LINX facility consists of a cylindrical vessel (stainless steel) of two m diameter and 3.4 m height, with a total volume of 9.42 m<sup>3</sup>. A specially designed injector at the bottom of the vessel, consisting of 716 capillary tubes of two mm inner diameter, distributed uniformly over a circular area of 15 cm diameter, enables air injection to take place with a constant and equal flow rate per needle. With this arrangement, a broad, axi-symmetric bubble plume with a narrow bubble-size distribution diameter of around two to three mm is obtained.
- PSU: Horizontal venting nozzle (Eden and Mahaffy, 2002).
- Experiments were conducted for steam into water, air into water, and air into air. Tables are provided of pressure along the centreline of the jet for a wide range of inlet conditions. Pressure expansion ratios for the jet were set at two, three and four. Reynolds numbers at the nozzle were between  $1.4 \times 10^5$  and  $3.2 \times 10^5$ . Density ratios (ambient to nozzle exit) ranged from 450-860 for steam-in-water, from 170-340 for air-in-water, and from 0.2 to 0.4 for air in air experiments. High-speed photographs are available for the steam-in-water and air-in-water jets, as a means of checking CFD predictions of the extent of the vapour region.

(2) Integral tests:

- B&C: Prototypic scale of vertical downward pipe sparger with multiple holes for quasi-steady or transient steam ejection in a large pool with about hundreds thermo-couples installed in the water pool. (Kang et al., 2005; Kang and Song, 2006a).
- COMA: Thermal mixing in an annulus shape of condensing pool is experimentally simulated for prototypic situation in APR1400 IRWST. Several multi-holed spargers are installed for long-term steam ejection in a large pool with about hundreds of thermo-couples installed in the water pool. (C.K. Park et al., 2009).

Currently available experimental information on the macroscopic flow pattern in a pool, such as global circulation pattern, overall mixing and thermal stratification behaviours, seems to be sufficient for validating appropriate analysis tools including CFD codes due to some experimental programmes, among others, such as B&C, COMA and LINX. However, the information on the local interaction of steam jet with surrounding pool water in terms of hydrodynamic and thermal viewpoints is still needed in order to understand better the relevant phenomena and validate appropriate CFD tools against those local phenomena, which eventually affect the global mixing behaviour.

**Figure 7.7. Schematic of the JICO experiment to simulate a steam jet into a sub-cooled pool**

### References

- Antal, S.P., S. Nagrath and M.Z. Podowski (2001), "Multi-dimensional Simulations of Two-Phase Flows in Large Volumes with Injection Spargers", Proc. Fourth Int'l Conf. on Multi-phase Flow (ICMF'01), New Orleans, Louisiana, United States, 27 May-1 June 2001.
- Aya, I. and H. Nariai (1991), "Evaluation of Heat-Transfer Coefficient at Direct Condensation of Cold-Water and Steam", *Nucl. Eng. & Design*, Vol. 131, pp. 17-24,
- Bae, S.W. and H.J. Sung (2001), "Breakdown of the Reynolds Analogy in a Stagnation Region Under Inflow Disturbances," *Theoretical and CFD*, 14, 377.
- Bang, Y.S. et al. (2005), "Prediction of Thermal Mixing by Steam Discharging into Water Tank", Proc. ANS Conf..
- Bejan, A. (1995), *Convection Heat-Transfer*, 2<sup>nd</sup> Ed., John Wiley & Sons, Inc. p. 317.
- Chung, B.D. et al. (2005), *MARS Code Manual Vol. IV: Developmental Assessment Report*, KAERI/TR-3042/ 2005, KAERI.
- Cho, S. et al. (1998), "Experimental Study on Dynamic Pressure Pulse in DCC of Steam Jets Discharging into Sub-cooled Water", Proc. 1<sup>st</sup> Korea-Japan Symposium on Nuclear Thermal-Hydraulics and Safety (NTHAS1), Pusan, Korea.
- Cho, S. et al., (2002), "Characteristics of Thermal Mixing and Pressure Load during Continuous Steam Discharging phase", Proc. KNS Spring Conf., KNS [in Korean].
- Cho, et al. S. (2004), "Effect of Multiple Holes on the Performance of Sparger during DCC of Steam", *Exp. Thermal & Fluid Science*, Vol. 28, pp. 629-638.
- Choo, Y.J. and C.H. Song (2008), "PIV Measurements of Turbulent Jet and Pool Mixing Produced by a Steam Jet in a Sub-cooled Water Pool", Proc. XCFD4NRS workshop, Grenoble, Sept. 10 (also accepted for Publication in *Nuclear Engineering & Design*).
- Chun, M.H., Y.S. Kim and J.W. Park (1996), "An Investigation of Direct Condensation of Steam Jet in Sub-cooled Water", *Int. Comm. Heat & Mass Transfer*, Vol. 23, No. 7, pp. 947-958.

- Cumo, M., G.E. Farello and G.E. Ferrari (1978), "Heat-Transfer in Condensing Jets of Steam-in-Water", Proc. 6<sup>th</sup> Int. Heat-Transfer Conf., Toronto, Vol. 5, pp. 101-106.
- Cummins, W.E., M.M. Corletti and T.L. Schultz (2003), "Westinghouse AP1000 Advanced Passive Plant", Proc. ICAPP'03, Cordoba, Spain, 4-7 May 2003.
- Davis, J. and G. Yadigaroglu (2004), "DCC in Himenz Flow Boundary Layers", *Int. J. of Heat and Mass Transfer*, Vol. 47, p. 1863.
- Del Tin, G., E. Lavagno and M. Malandrone (1983), "Thermal and Fluid-Dynamic Features of Vapour Condensing Jets", *Heat & Technology*, Vol. 1, No. 1, pp. 13-35.
- Eden, T. and J.H. Mahaffy (2002), "Experimental Results for Condensing Jets," Joint IAEA/NEA Technical Meeting on the use of CFD Codes for Safety Analysis of Reactor Systems, Pisa, Italy, Nov. 11-13.
- Fukuda, S. (1982), "Pressure Variation due to Vapour Condensation in Liquid (II): Phenomena at Large Vapour Mass Flow Rate", *J. Atomic Energy Soc. Japan*, Vol. 24, No. 6, pp. 466-474.
- Gamble, R.E. et al. (2001), "Pressure SP Mixing in Passive Advanced BWR Plants", *Nuclear Eng. & Design*, Vol. 204, pp. 321-335.
- Gerber, A.G. and M.J. Kermani (2004), "A Pressure-Based Eulerian-Eulerian Multi-phase Model for Non-equilibrium Condensation in Transonic Steam Flow", *Int'l J. Heat & Mass Transfer*, Vol. 47, pp. 2217-2231.
- Kang, H.S. et al. (2005), "CFD Analysis for Thermal Mixing Phenomena at the Discharge of a Low Steam Mass Flux in a Sub-cooled Water," Proc. ICAPP'05, Seoul, Korea, 15-19 May, 2005.
- Kang, H.S. and C.H. Song (2006a), "CFD Analysis of a Thermal Mixing in a Sub-cooled Water Pool Under a High Steam Mass Flux", Proc. CFD4NRS workshop, Garching, Germany, 5-7 Sept. 2006.
- Kang, H.S. and C.H. Song (2006b), "Sensitivity Analysis for the CFD Calculation of Thermal Mixing Test", Proc. KNS Spring Conference, Gangchon, Korea, 25-26 May 2006.
- Kang, H.S. and C.H. Song (2008), "CFD Analysis of a Turbulent Jet Behaviour Induced by a Steam Jet Discharged through a Single-Hole in a Sub-cooled Water Pool", Proc. XCFD4NRS workshop, Grenoble, Sept. 10 (2008) (also accepted for Publication in *Nuclear Engineering & Design*).
- Kerney, P.J., G.M. Faeth and D.R. Olson (1972), "Penetration Characteristics of Submerged Jet," *AIChE J.*, Vol. 18, No. 3, pp. 548-553.
- Kim, Y.S. et al. (1997), "An Experimental Investigation of Direct Condensation of Steam Jet in Sub-cooled Water," *J. of Korean Nuclear Society*, 29[1], 45.
- Kim, Y.S. and C.-H. Song (2003), "Condensation Regime Map for a 4-Hole Sparger", Proc. ANS 2003 Annual Mtg., San Diego, United States, June 2003.
- Kim, Y.S., J.W. Park and C.-H. Song (2004), "Investigation of the Steam-Water DCC Heat-Transfer Coefficients Using Interfacial Transport Models", *Int. Comm. Heat and Mass Transfer*, Vol.31, No.3, pp.397-408.
- Laine, J. and M. Puustinen (2006), "Condensation pool experiments with steam using insulated DN200 blowdown pipe", 6<sup>th</sup> EURATOM Framework Program NURESIM, Deliverable D2.1.15.1.

- Lakehal, D., B. Smith and M. Milelli (2002), "LES of Bubble Turbulent Shear Flows", *IOP Journal of Turbulence*, Vol. 3, No. 25, pp. 1-21.
- Lee, S.W., Y.S. Jang and H.J. Ko (2003), "APR1400 CS Design and Analysis", Proc. ICAPP'03, Cordoba, Spain, 4-7 May 2003.
- Meier, M., G. Yadigaroglu and M. Andreani (2000), "Numerical and Experimental Study of Large Steam-Air Bubbles Injected in a Water Pool", *Nuclear Science and Engineering*, Vol. 136, pp. 363-375, Nov..
- Milelli, M. (2002), "A Numerical Analysis of Confined Turbulent Bubble Plumes", Ph.D. Thesis (#14799), Swiss Federal Institute of Technology (ETHZ), Zurich.
- Nariai, H. and I. Aya (1986), "Fluid and Pressure Oscillations Occurring at DCC of Steam Flow with Cold-Water", *Nucl. Eng. & Des.*, Vol. 95, pp. 35-45.
- Park, C.K. et al. (2009), "Preliminary Analysis of Mixing Tests in an Annular Vessel", Proc. KNS 2009 Spring mtg., Jeju, 22 May 2009.
- Smith, B.L., M. Milelli, S. Shepel and D. Lakehal (2003), "A Generic Study of Phenomena Affecting Two-Phase Mixing in BWR Suppression Pools during Passive Removal", Proc. NURETH-10, Seoul, Korea, 5-9 Oct. 2003.
- Song, C.-H. et al. (1998), "Characterisation of DCC of Steam Jets Discharging into a Sub-cooled Water", Proc. IAEA Technical Committee Mtg., PSI, Villigen, 14 Sept. 1998.
- Song, C.-H. et al. (2002), "Overview of Thermal-Hydraulic Test Program for Evaluating or Verifying the Performance of New Design Features in APR1400 Reactor", Proc. of ICAPP'-02, Hollywood, Florida, 9-13 June 2002.
- Song, C.-H. et al. (2003), "Multi-dimensional Thermal-Hydraulic Phenomena in Advanced Nuclear Reactor Systems: Current Status and Perspectives of the R&D Program at KAERI," Proc. NURETH-10, Seoul, Korea, 5-9 October 2003.
- Song, C.-H. et al. (2006), "Development of the PIRT for Thermal Mixing Phenomena in the APR1400 IRWST", Proc. 5<sup>th</sup> Korea-Japan Symposium on Nuclear Thermal-Hydraulics and Safety (NTHAS5), Jeju, Korea, 26-29 Nov. 2006.
- Young, R.J., S.K. Yang and J.L. Novonty (1974), "Vapour Liquid Interaction in a High-Velocity Vapour Jet Condensing in a Coaxial Water Flow", Proc. 5<sup>th</sup> Int. Heat-Transfer Conf., Tokyo, Vol. 3, pp. 226-230.
- US NRC (1981), SP Temperature Limits for BWR Containments, NUREG-0783.
- van Wissen, R.J.E. et al. (2005), "Particle Image Velocimetry Measurement of a Steam-Driven Confined Turbulent Water Jet", *J. Fluid Mech.*, Vol. 530, pp. 358-368 (2005).
- Weimer, J.C., G.M. Faeth & D.R. Olson (1973), "Penetration of Vapour Jets Submerged in Sub-cooled Liquids", *AIChE J.*, Vol. 19, No. 3, pp. 552-558.
- Yadigaroglu, G. (2005), "Computational Fluid Dynamics for Nuclear Applications: from CFD to Multi-scale CMFD", *Nuclear Eng. & Design*, Vol. 235, pp. 153-164.

## 8. Fire analysis

### 8.1. Identification of all-important flow processes of the issues

The fire scenarios in commercial nuclear power plants are large and diverse. These scenarios may have characteristics or attributes that cannot be modelled using computational fire models, and/or no experimental data is available to support a verification and validation study of that particular characteristic or attribute. Improvements in these two specific limitations of limited fire modelling capabilities and/or insufficient experimental data are needed. The generic list of scenarios includes fires in the switchgear room (SWGR), cable spreading room (CSR), main control room (MCR), pump room, turbine building, multiple compartment (corridor) scenarios, multi-level building, containment (PWR), battery room, diesel generator room, computer room and outdoors.

#### 8.1.1. Fire analysis

A variety of fires modelling tools employing different features is currently available. The most appropriate model for a specific application often depends on the objective for modelling and fire scenario conditions. Fire models have been applied in nuclear power plants in the past to predict environmental conditions inside a compartment room of interest. The models typically try to estimate parameters such as temperature, hot smoke gas layer height, mass flow rate, toxic species concentration, heat-flux to a target, and the potential for fire propagation in the pre-flashover stage compartment fire.

Fire models are generally limited by their intrinsic algorithms and by other factors impacting the range of applicability of a given model feature. These features are inherent in the model's development and should be taken into consideration in order to produce reliable results that will be useful in decision-making.

The engineer must bear in mind that most fire models were developed for general application and not specifically for the conditions and scenarios presented in nuclear power plants. A fire models features and ability to address these conditions should be considered when selecting an appropriate fire model. These considerations can affect the accuracy or appropriateness of the fire dynamics algorithms used for a unique analysis of a given space. The conditions can include but are not limited to the following:

- The types of combustibles and heat release rates.
- Types and location of ignition sources.
- The quantity of cables in cable trays and other in situ fire loads in compartments.
- Location of fire sources with respect to targets in the compartments.
- High-energy electrical equipment.
- Ventilation methods.
- Concrete building construction, large metal equipment and cable trays that will influence the amount of heat lost to the surroundings during fire.

- Compartments that vary in size but typically have a large volume with high ceilings.
- Transient combustibles associated with normal maintenance and operations activities.

The CFD models can provide detailed information on the fluid dynamics of an enclosure fire in terms of three-dimension field, pressure, temperature, enthalpy, radiation and kinetic energy of turbulence. These models have been used to model a variety of complex physical phenomena such as the impact of a suppression system (e.g. a sprinkler system or water mist system) on a specific type of fire. Alternatively, smoke movement in a large compartment with complex details such that detection can be optimised. CFD models can provide a fundamental understanding of the flow field models for known compartment geometry, along with the physical phenomena that interact with the flow field.

Fire differs significantly in its behaviour from other fluids and gases flow due to its complex chemical, thermal and turbulent behaviour phenomena interaction, and the multi-phase nature. Because of this complexity, any simulation tool must be capable of handling the chemical reactions; the turbulent flows and radiative and convective heat-transfer within the analysis. Additionally, fire suppression using mist-spray is an additional factor to take into account when choosing a CFD tool to analyse fire.

### ***8.1.2. Smoke particulate***

Fire is a complex, dynamic, physico-chemical event and is a result of a rapid chemical reaction that generates smoke. Each fire is different. Smoke composition and heat generated in a fire depends on type of burning materials and environment conditions. Smoke is the airborne solid and liquid particulates and gases evolved when a material undergoes pyrolysis or combustion. Smoke particles are actually an aerosol (or a mist) of solid particles and liquid droplets. The composition of smoke depends on the nature of the burning fuel and the condition of combustion. The smoke particulates participate in radiation and play an important role in the absorption and scattering of radiative heat-transfer.

In CFD, as the volume fraction of the smoke particulate is low (less than 10 %); discrete phase model can be used to model the flow of smoke particulates. A soot formation model is needed to predict the amount of smoke particulate in the combustion product. Magnussen combustion model is an example of models that can be used in CFD to predict the rate of smoke particles creation and destruction.

### ***8.1.3. Sprinkler***

When activated, sprinklers spray water droplets on the hot smoky environment. Discrete phase model can be used to track the water droplet trajectories from the sprinklers to the floor or the burning commodity, as well as heat and mass transfer to/from them. The coupling between the phases and its impact on both the discrete phase trajectories and the continuous gas-phase flow should be included.

DPM can be used to model sprinkler sprays. For sprays, however, there are models available to predict the droplet size and velocity distributions. Models are also available for droplet breakup and collision, as well as a dynamically varying drag coefficient, which accounts for variation in droplet shape. These models for realistic spray simulations are described in this section.

#### ***8.1.4. Time and length scales***

The numerical simulation of fires is a challenging task. The principle scientific challenge is the coupling of multiple disciplines across a range of timescales from fempto-seconds for some of the reactions occurring during the explosion to days for burnout of spilled fuel in the accidental fire. Each of these timescales has an associated spatial scale. These spatial dimensions range across nanometres for molecular events to kilometre for large-scale mixing in the fire simulation itself. The fire simulation work is motivated by exploring the possibility of uniquely designing quenching devices to rapidly extinguishing accidental fires.

Pool fires are characterised by large-scale vertical structures driven by buoyancy with a puffing frequency that scales with the diameter of the pool. The size of the largest eddies is about the diameter of the pool fire as its base. Yet these large-scale structures are generated by buoyancy generated by heat release from chemical rate processes occurring at the molecular scale. Information from the microscopic to the macroscopic scales is important to fire simulations.

##### *Fire suppression*

Fire suppression involves a multitude of phenomena from convection of suppression of turbulent flow to strain modified-diffusion of suppressant into flame zones, to thermal and chemical interactions at the molecular level between the suppressant and fuel/air reactions species. It is important to recognise the length and timescales for suppression phenomena have a very large range. The smallest length scales of interest are the molecular collisional scales defined by the mean free path of the molecules, which are about  $10^{-7}$  to  $10^{-6}$  m, depending on the temperatures at ambient pressure. The largest length scales are defined by the application under consideration, typically a compartment length-scale about metres. The smallest timescales of interest are the molecular collisional times defined by the collision frequency of molecules, which is about  $10^{-10}$  sec depending on the temperature at ambient pressure. The largest timescales are defined by the need to prevent thermally induced damage of structural boundaries, composite or steel by conduction heat-transfer timescales, typically about seconds to ten s of seconds. Therefore, representation of some seven order of magnitude in length-scale and some ten to 11 orders of magnitude in time scale are required to capture all the process in fire suppression from molecular chemistry to the systems level.

##### *Pool fire*

Within the fire itself, global characteristics alone are not sufficient to define the extensive physical/chemical processes and their coupling. For example, [Delichatios, 1987] distinguishes between the scaled overall heat release rate,  $Q$ , which is used to define global fire scales, and a reduced gravity,  $(\Delta\rho/\rho)g$ , associated with turbulent eddies at smaller scales where combustion interactions occur. Time and length-scale estimates for non-premixed combustion are found in the combustion literature. Non-premixed combustion is typically defined by a time scale alone [Vervisch, 1998], as thickness is not an intrinsic property [Sung, 1995]. However, length scales can be estimated by using the Damkohler number (i.e. the ratio of physical process time scale and a chemical time scale). If the chemical time scale and the corresponding Damkohler number are known, by definition the time scale for the corresponding transport process is known. For all transport processes, there is a length-scale associated with every time scale for a given process. Therefore, a length-scale can be determined for the physical process that occurs over the chemical process time scale. Typically, for diffusion flames not near extinction, i.e. large  $Da$ , the length-scale associated

with diffusion flames is not dependent on chemistry directly, but is a balance between diffusive and advective transport processes resulting in a thickness, that is dependent on the square root of the local strain rate [Sung, 1995]. For fires, [Cox, 1995] gives estimates of combustion properties in terms of velocity and length scales.

It should be obvious that a necessary condition for modelling a process is an understanding of it. For fires, it is necessary to understand the physical/chemical processes that contribute to the fire sustenance/spread, which include time and length scales ranges between soot production and global radiative deposition.

The smallest scales in sooty, turbulent fires that are of direct interest are those that contribute to thermal radiation, since radiative transport couples this energy back into larger length scales including fuel pyrolysis/vaporisation. Soot grows from molecular length scales  $O$  (nm) to  $O$  (100 nm) in large fires [Mulholland, 1996; Williams, 1998]. Since continuum approximations start at length scales about  $O$  (100 s nm) depending on the temperature at ambient pressure [Vincente, 1975], fundamentally, soot formation is a heterogeneous, non-continuum, chemical process. Continuum representations, such as Arrhenius-rate-equation based kinetic sets, must be considered as models for the real molecular-transport-processes.

The large end of the length-scale range depends on application. For laboratory experiment, fire sizes from  $O$  (cm to m), for building fires from  $O$  (m to 10 s m), and for forest fires  $O$  (0.1km to km s). Another factor in determining the scale is if the primary interest is within the fire itself, or in the fire-induced flow, which can exceed fire length scales by several orders of magnitude. For numerical simulation purposes, even if the interest is in the fire itself, often boundary conditions are set at a considerable distance  $O$ (3-10 diameters from the fire) to avoid errors [Nicolette, 1996]. When comparing small- scales and large-scales, it can immediately be concluded that a first principles description of fire requires the coupling of some six to ten or more orders of magnitude depending on the problem of interest.

The timescales involved depend on the length scales and process rates. Non-continuum transport is very rapid, due to high molecular velocities, typically about 500 m/s at ambient temperature and pressure [Williams, 1985]. Continuum velocities on the other hand are quite low, ranging from  $O$ (0.1 mm/sec to cm/sec) at the fuel source [Babrauskas, 1986] up to  $O$ (10 s m/sec) at the top a large  $O$ (10 s m base) fire [Schneider, 1989].

Continuum transport processes are expressed in terms of conservation of mass, momentum, energy and equations of states [Williams, 1985]. Dimensionless numbers are obtained from non-dimensionalising the equations [Williams, 1985] and [Drysdale, 1985]. The highest rate, i.e. shortest time scale terms are dominant. Details of the partial non-dimensionalisation may be found in [Tieszen, 2000].

For momentum transport, the terms are:

$$\text{Buoyancy: } \tau_{ref} \approx \sqrt{\frac{L_{ref}}{(\rho_{\infty} - \rho_{ref})g}} / \rho_{ref}$$

$$\text{Advection: } \tau_{ref} \approx \frac{L_{ref}}{u_{ref}}$$

$$\text{Diffusion: } \tau_{ref} \approx \frac{L_{ref}^2}{v_{ref}}$$

When comparing these terms, it can be seen that they have different length-scale dependencies. Thus, each term dominates at a different length-scale. At small scales, diffusion dominates because of the high molecular-velocities relative to the bulk velocities. Molecular walk processes, which define diffusion, are inefficient at larger length scales and bulk advection becomes dominant. At still larger scales, buoyancy dominates. Since there is a turbulent-mixing-limited combustion-phenomena, which has a spectrum of length scales that is driven by radiation with its own length-scale spectrum from non-continuum soot emission to absorption at global application scales, all length scales play a role in this coupled multi-physics/multi-length-scale problem. Therefore, while one process may dominate at a given length-scale, it cannot be said that any one of these terms dominates the entire coupled process overall length scales.

The advection to diffusion ratio is the Reynolds number. In flames with fast chemistry, ( $Da \gg 1$ ) the balance of these forces defines the width of the diffusion flame as a function of the imposed velocity gradient across it. A two order of magnitude increase in imposed velocity will decrease the flame thickness one order of magnitude until finite-rate chemistry results in extinction. Flames are typically O (mm) depending on the imposed strain. Above this length-scale, advection and buoyancy dominate transport processes.

The role of advection cannot be said to be well understood because its non-linear behaviour is the source of turbulent processes with their concomitant scale changing behaviour, creating the broad spectrum known as the “turbulent cascade”. However, the role of buoyancy has received much less attention. Its role is perhaps best understood from the vorticity transport equations (curl of Navier-Stokes equations). These equations may be loosely thought of as transport equations for rotational motion, since vorticity is twice a solid body rotation rate. The gravitational (hydrostatic pressure) and local acceleration (hydrodynamic pressure) terms survive the curl operation to become explicit source terms for vorticity. The local acceleration can be important relative to the gravitational term when accelerations are high, as at the base of the fire [Mell, 1996].

An important point is that buoyancy expresses itself through vorticity generation. Since baroclinic vorticity generation is the result of misalignment of the density with the local acceleration field, it scales on this product. Therefore, vorticity will be generated at all density gradients unless they are aligned with the local acceleration field. Experimental support for this view comes from measurements that show vorticity is found at the fire edge where density gradients are located [Zhou, 1995 and 1996]. Vorticity will be generated at a length-scale related to the density gradient length-scale. Due to turbulent mixing processes in a fire, density gradients will exist across a broad spectrum of length scales from diffusive to integral scale of the turbulent eddies. Therefore, buoyancy will express itself as vorticity over the same broad length-scale spectrum. Experimental evidence for this view can be found in non-reacting buoyant plume data [Kotsovinos, 1991].

## 8.2. Limits of previous approaches and expected improvements with CFD

Techniques used to model the transfer of energy, mass, and momentum associated with fires fall into three major categories:

- Single equations: used to predict specific parameters of interest in nuclear power plant applications such as adiabatic flame temperature, heat of combustion of fuel

mixtures, flame height, mass loss rate, and so forth. These equations can be steady-state or time-dependent. The results of the single equation can be used either directly or as input data to more sophisticated fire modelling techniques.

- Zone models zone models assume a limited number of zones, typically two or three zones, in an enclosure. Each zone is assumed to have uniform properties such as temperature, gas concentration, and so forth. Zone models solve conservation equations for mass, momentum, energy, and in some examples, species. However, zone models usually adopt simplifying assumptions to the basic conservation equations to reduce the computational demand for solving these equations.
- Field models: field or CFD models divide an enclosure into large number of cells and solve the Navier-Stokes equations in three dimensions of the flow field. CFD models also require the incorporation of sub-models for a wide variety of physical phenomena, including convection, conduction, turbulence, radiation and combustion. The resulting flow or exchange of mass, energy, and momentum between computational cells are determined so that the three quantities are conserved. Accordingly, CFD models need intensive computational power, but these models can be run on high-end PC computers. The CFD models can provide detailed information on the fluid dynamics of fires in terms of three-dimension field, pressure, temperature, enthalpy, radiation and kinetic energy of turbulence. These models have been used to model a variety of complex physical phenomena such as the impact of a suppression system (e.g. a sprinkler system or water mist system) on a specific type of fire. On the other hand, smoke movement in a large compartment with complex details such that detection can be optimised. CFD models can provide a fundamental understanding of the flow field models for known compartment geometry, along with the physical phenomena that interact with the flow field.

Fire differs significantly in its behaviour from other fluids and gases flow due to its complex chemical, thermal and turbulent behaviour phenomena interaction, and the multi-phase nature. Because of this complexity, any simulation tool must be capable of handling the chemical reactions; the turbulent flows and radiative and convective heat-transfer within the analysis. A right and robust radiation model is required to assess heat-flux to the walls and targets from fire. This can be accomplished only by CFD models. The other two options are lumped-parameter methods, and can predict only bulk value, which can be far away from the local temperature considering how high fire temperature can reach. As such, CFD is needed in fire analysis and will bring tremendous improvement in the prediction of target variables such as temperature, heat-flux, visibility attenuation due presence of smoke and others.

### 8.3. Selecting a basic model

#### 8.3.1. Species transport equations

In fire analysis, conservation equations for each chemical species are solved. The local mass fraction of each species,  $Y_i$ , is predicted through the solution of a convection-diffusion equation for the  $i$ th species. This conservation equation takes the following general form:

$$\frac{\partial}{\partial t}(\rho Y_i) + \nabla \cdot (\rho \vec{v} Y_i) = -\nabla \cdot \vec{J}_i + R_i + S_i$$

Where  $R_i$  is the net rate of production of species  $i$  by chemical reaction and  $S_i$  is the rate of creation by addition from the dispersed phase. An equation of this form will be solved for  $N-1$  species where  $N$  is the total number of fluid phase chemical species present in the system. Since the mass fraction of the species must sum to unity, the  $N$ th mass fraction is determined as one minus the sum of the  $N-1$  solved mass fractions.

### 8.3.2. *The generalised finite-rate formulation for reaction modelling*

The reaction rates that appear as source terms in the species conservation equation described in Section 8.2.1 can be computed by one of three models:

- Laminar finite-rate model: the effects of turbulent fluctuations are ignored, and reaction rates are determined by Arrhenius expressions;
- Eddy-dissipation model: reaction rates are assumed to be controlled by the turbulence, so expensive Arrhenius chemical kinetic calculations can be avoided;
- Eddy-dissipation-concept (EDC) model: detailed Arrhenius chemical kinetics can be incorporated in turbulent flames.

The generalised finite-rate formulation is suitable for a wide range of applications including laminar or turbulent reaction systems, and combustion systems with premixed, non-premixed, or partially premixed flames.

### 8.3.3. *Modelling non-premixed combustion*

When modelling turbulent non-premixed combustion, it is common to employ a chemical conserved scalar, usually referred to as mixture fraction, as a co-ordinate for the computational of reactive scalar behaviour. For pure gas-phase combustion, mixture fraction can be defined as an appropriate linear combination of reactive and inert species mass fractions such that it has no chemical source term. Since mixture fraction is defined as being conserved under chemical reaction, it is solely a measure of the mass fraction of mass present that originated from one of the two mixing streams. As such, its value is only subject to change due to mixing. This makes it an effective co-ordinate in which to solve conditionally averaged reactive scalar equations free from large mixing-induced fluctuations.

In non-premixed combustion, fuel and oxidiser enter the reaction zone in distinct streams. This is in contrast to premixed systems, in which reactants are mixed at the molecular level before burning. Examples of non-premixed combustion include pulverised coal furnaces, diesel internal-combustion engines and pool fires. Non-premixed combustion can be greatly simplified to a mixing problem (see the mixture fraction approach).

#### *Mixture fraction $f$*

Under certain assumptions, the thermochemistry can be reduced to a single parameter: the mixture fraction. The mixture fraction, denoted by  $f$ , is the mass fraction that originated from the fuel stream. In other words, it is the local mass fraction of burnt and unburnt fuel stream elements (C, H, etc.) in all the species ( $\text{CO}_2$ ,  $\text{H}_2\text{O}$ ,  $\text{O}_2$ , etc.). The approach is elegant because atomic elements are conserved in chemical reactions. In turn, the mixture fraction is a conserved scalar quantity, and therefore its governing transport equation does not have a source term. Combustion is simplified to a mixing problem, and the difficulties associated with closing non-linear mean reaction rates are avoided. Once mixed, the chemistry can be modelled as being in chemical equilibrium with the equilibrium model,

being near chemical equilibrium with the steady Laminar Flamelet model, or significantly departing from chemical equilibrium with the unsteady Laminar Flamelet model.

The basis of the non-premixed modelling approach is that under a certain set of simplifying assumptions, the instantaneous thermo-chemical state of the fluid is related to a conserved scalar quantity known as the mixture fraction,  $f$ . The mixture fraction can be written in terms of the atomic mass fraction as [Sivathanu, 1990]:

$$f = \frac{Z_i - Z_{i,OX}}{Z_{i,fuel} - Z_{i,OX}}$$

Where  $Z_i$  is the elemental mass fraction for element  $i$ . The subscript  $ox$  denotes the value at the oxidiser stream inlet and the subscript  $fuel$  denotes the value at the fuel stream inlet. If the diffusion coefficients for all species are equal, then equation is identical for all elements, and the mixture fraction definition is unique. The mixture fraction is thus the elemental mass fraction that originated from the fuel stream.

In many reacting systems, the combustion is not in chemical equilibrium and the mixture fraction concept is not a valid option to use for modelling. Other approaches can be used to model chemical non-equilibrium, including the finite-rate, the EDC, and PDF transport models, where detailed kinetic mechanisms can be incorporated.

There are three approaches in the non-premixed combustion model to simulate chemical non-equilibrium. The first is to use the rich flammability limit (RFL) option in the equilibrium model, where rich regions are modelled as a mixed but unburnt mixture of pure fuel and a leaner equilibrium burnt mixture. The second approach is the steady Laminar Flamelet model, where chemical non-equilibrium due to diffusion flame stretching by turbulence can be modelled. The third approach is the unsteady Laminar Flamelet model where slow-forming product species that are far from chemical equilibrium can be modelled.

#### ***8.3.4. Modelling premixed combustion***

In premixed combustion, fuel and oxidiser are mixed at the molecular level prior to ignition. Combustion occurs as a flame front propagating into the unburnt reactants. Examples of premixed combustion include aspirated internal-combustion engines, lean-premixed gas turbine combustors and gas-leak explosions.

Premixed combustion is much more difficult to model than non-premixed combustion. The reason for this is that premixed combustion usually occurs as a thin, propagating flame that is stretched and contorted by turbulence. For subsonic flows, the overall rate of propagation of the flame is determined by both the laminar flame speed and the turbulent eddies. The laminar flame speed is determined by the rate that species and heat diffuse upstream into the reactants and burn. To capture the laminar flame speed, the internal flame structure would need to be resolved, as well as the detailed chemical kinetics and molecular diffusion processes. Since practical laminar flame thicknesses are of the order of millimetres or smaller, resolution requirements are usually unaffordable.

The effect of turbulence is to wrinkle and stretch the propagating laminar flame sheet, increasing the sheet area and, in turn, the effective flame speed. The large turbulent eddies tend to wrinkle and corrugate the flame sheet, while the small turbulent eddies, if they are smaller than the laminar flame thickness, may penetrate the flame sheet and modify the laminar flame structure. The essence of premixed combustion modelling lies in capturing

the turbulent flame speed, which is influenced by both the laminar flame speed and the turbulence.

In premixed flames, the fuel and oxidiser are intimately mixed before they enter the combustion device. Reaction then takes place in a combustion zone, which separates unburnt reactants and burnt combustion products. Partially premixed flames exhibit the properties of both premixed and diffusion flames. They occur when an additional oxidiser or fuel stream enters a premixed system, or when a diffusion flame becomes lifted off the burner so that some premixing takes place prior to combustion.

Premixed and partially premixed flames can be modelled using finite-rate/eddy-dissipation formulation. If finite-rate chemical kinetic effects are important, the EDC model or the composition PDF transport model can be used. If the flame is perfectly premixed, so only one stream at one equivalence ratio enters the combustor, it is possible to use the premixed combustion model, as described in this chapter.

The composition PDF transport model, like the EDC model, should be used, when the interest is in simulating finite-rate chemical kinetic effects in turbulent reacting flows. With an appropriate chemical mechanism, kinetically controlled species such as CO and NO<sub>x</sub>, as well as flame extinction and ignition, can be predicted.

### 8.3.5. Discrete phase modelling

As discussed in Section 8.1.2 and 8.1.3, both smoke particulate and water spray are simulated using a discrete second phase in a Lagrangian frame of reference. These particulates and atomised water droplets are dispersed in the gaseous continuous phase. Trajectories as well as heat and mass transfer to/from these discrete phase entities are computed. A robust CFD model should provide the following discrete phase modelling options in fire analysis:

- calculation of the discrete phase trajectory using a Lagrangian formulation that includes the discrete phase inertia, hydrodynamic drag, and the force of gravity, for both steady and unsteady flows;
- prediction of the effects of turbulence on the dispersion of particles due to turbulent eddies present in the continuous phase;
- heating/cooling of the discrete phase;
- vaporisation and boiling of liquid droplets;
- combusting particles, including volatile evolution and char combustion to simulate coal combustion;
- optional coupling of the continuous phase flow field prediction to the discrete phase calculations;
- droplet breakup and coalescence.

## 8.4. Filtering turbulent scales and two-phase-phase intermittency scales

It has long been recognised within the numerical simulation community that it is not possible to capture all the relevant length scales within the fire itself with CFD models. Instead, filtered transport equations are used. [Cox, 1995 and 1998] gives details for time filtered (Reynolds-Averaged-Navier-Stokes, or RANS) equations, the most commonly used form for fire simulations. Another form is large Eddy simulation, or LES, which

employs a spatial filtering technique [Ferziger, 1996]. Implicit LES filtering, i.e. allowing the discretisation scheme to determine the lower length scales, has been used in fire driven flows [Rehm, 1997]. Once filtered, both RANS/LES equations have explicit terms representing the unresolved length and timescales that must be captured by models.

Within a fire, formal, explicit filtering of transient equations of motion should include both spatial and temporal filtering, since the transport processes involved are linked in time and space, and small length-scale processes (e.g. combustion creating density gradients creating buoyancy) are the source terms primarily responsible for driving the flow. To date this rigour has not been applied to fire problems. RANS filters the timescales explicitly but implicitly assumes that all turbulent scales are below the filter width and are therefore modelled. Transient RANS implies that transients longer than the passage of a statistically significant number of the largest turbulent structures can be resolved. LES filters the spatial scales. However, explicit temporal filters should be applied once discrete time steps are taken. In LES, explicit filtering, not tied to the grid, should permit numerical error to be separated from modelling error as it currently does in RANS by grid refinement studies.

### 8.5. Identification of local interface structure

The smoke particulates and atomised water spray are modelled using a discrete second phase in Lagrangian frame of reference. This second phase consists of spherical particles dispersed in the continuous gaseous phase. The model should compute the trajectories of these particles, as well as the heat and mass transfer to and from them. The coupling between the phases and its impact on both the discrete phase trajectories and the continuous phase should also be included.

In addition to the interface between phases, fire problems also include a flame front that propagates into the unburnt reactants. If the combustion is premixed, then the flame occurs as thin, propagates and is stretched and contorted by turbulence. The overall propagation of the flame is determined by both the laminar flame speed and the turbulent eddies. The laminar flame speed is determined by the rate that species and heat diffuse upstream into the reactant and burn. To capture the laminar flame speed, the internal flame structure need to be resolved, as well as the detailed chemical kinetics and molecular diffusion processes. Since practical laminar flame thickness are of order of millimetres or smaller, resolution requirement are usually unaffordable. Non-premixed combustion, in comparison, can be greatly simplified to a mixing problem. The essence of premixed combustion modelling lies in capturing the turbulent flame speed, which is influenced by both the laminar flame speed and the turbulence.

### 8.6. Modelling interfacial transfers

Accurate determination of droplet drag coefficients is crucial for accurate spray and smoke particulates modelling. Models should be available to provide a method that determines the droplet drag coefficient dynamically, accounting for variations in the droplet shape. Many droplet drag models assume the droplet remains spherical throughout the domain. However, as an initially spherical droplet moves through a gas, its shape is distorted significantly when the Weber number ( $We = \rho u_{rel}^2 D / \sigma$ ; where  $\rho$  is the density of the fluid,  $u$  is the fluid velocity,  $D$  is the diameter of the droplet and  $\sigma$  is the surface tension) is large. In the extreme case, the droplet shape will approach that of a disk. The drag of a disk, however, is significantly higher than that of a sphere. Since the droplet drag coefficient is highly dependent upon the droplet shape, a drag model that assumes the droplet is spherical

is unsatisfactory. The dynamic drag model should account for the effects of droplet distortion.

In addition to the simple particle injection types, fire models also require more complex injection types for sprays. For most types of injections, you will need to provide the initial diameter, position and velocity of the particles. For sprays, however, there are models available to predict the droplet size and velocity distributions. Additionally, models to predict droplet breakup and collision should be available.

### 8.7. Modelling turbulent transfers

The dispersion of particles due to turbulence in the fluid phase can be predicted using the stochastic tracking model or the particle cloud model. The stochastic tracking (random walk) model includes the effect of instantaneous turbulent velocity fluctuations on the particle trajectories using stochastic methods. The particle cloud model tracks the statistical evolution of a cloud of particles about a mean trajectory. The concentration of particles within the cloud is represented by a Gaussian PDF about the mean trajectory. In the stochastic tracking, a model should be available to account for the generation or dissipation of turbulence in the continuous phase.

The effect of turbulence is to wrinkle and stretch the propagating laminar flame sheet, increasing the sheet area, in turn, the effective flame speed. The large eddies tends to wrinkle and corrugate the flame sheet, while the small turbulent eddies, if they are smaller than the laminar flame thickness, may penetrate the flam sheet and modify the laminar flame structure.

### 8.8. Modelling wall transfer

Turbulent flows are significantly affected by the presence of walls. Obviously, the mean velocity field is affected through the no-slip condition that has to be satisfied at the wall. However, the turbulence is also changed by the presence of the wall in non-trivial ways. Very close to the wall or targets, viscous damping reduces the tangential velocity fluctuations, while kinematic blocking reduces the normal fluctuations. Toward the outer part of the near-wall region, however, the turbulence is rapidly augmented by the production of turbulence kinetic energy due to the large gradients in mean velocity.

The near-wall modelling significantly affects the fidelity of numerical solutions, inasmuch as walls are the main source of mean vorticity and turbulence. After all, it is in the near-wall region that the solution variables have large gradients, and the momentum and other scalar transports occur most vigorously. Therefore, accurate representation of the flow in the near-wall region determines successful predictions of wall-bounded turbulent flows. In fire analysis, depending on the ventilation existing in the room, the flow can be classified as either forced or buoyancy-driven. If the air is forced in the room, momentum and heat-transfer to the walls can be handled by standard wall functions since the flow there will be single-phase. In the case of buoyancy-driven flow, the standard wall function approach becomes less reliable as the flow conditions depart too much from the ideal conditions underlying the wall functions. As an alternative, a near-wall modelling method combining a two-layer model with enhanced wall functions is recommended. If the near-wall mesh is fine enough to be able to resolve the laminar sub-layer (typically  $y^+ \sim 1$ ), then the enhanced wall treatment will be identical to the traditional two-layer zonal model.

The RANS models, the RSM, and the LES model are primarily valid for turbulent core flows (i.e. the flow in the regions somewhat far from walls). Consideration therefore needs to be given as to how to make these models suitable for wall-bounded flows.

### 8.9. Validation matrix for fire analysis

In order to evaluate the capabilities of fire models for nuclear power plant applications, an international collaborative fire model project (ICFMP) was organised. The objective of the collaborative projects is to share the knowledge and resources of various organisations to evaluate and improve the state of the art of fire models for use in nuclear power plant fire safety and fire hazards analysis. The objective is divided into two-phases. The objective of the first phase is to evaluate the capabilities of current fire models for fire safety in nuclear power plants. The second phase will implement beneficial improvements to current fire models that are identified in the first phase, and extend the validation database of those models. Currently, 22 organisations from 6 countries are represented in the collaborative project.

So far, this organisation formulated five benchmark exercises. The benchmark exercise was intended to simulate a basic scenario defined in sufficient detail to allow evaluation of the physics modelled in the fire computer codes. An assessment of appropriate input parameters and assumptions, interpretation of results, and determination of the adequacy of the physical sub-models in the codes for specific scenarios will establish useful technical information regarding the capabilities and limitations of the fire computer code. Uncertainties in the predictions based on validations of each code will provide a basis for the confidence on the set of results developed in the exercise.

The USNRC has prepared a validation and verification (V&V) report of five selected fire models. These models are commonly used in support of risk-informed and performance-based fire protection at nuclear power plants. The NRC report contains six sets of fire experiments that were used in the evaluation of the selected models.

#### 8.9.1. Possible fire scenarios

The basis for the selection of these fire scenarios is as follows:

- review the range of possible configurations that contribute to fire scenarios in the commercial nuclear industry; the review focused on parameters considered important in the definition of fire scenarios;
- identify potentially risk-significant fire scenarios through review of the Individual Plant Examination for External Events (IPEEE) submittals;
- examine past industry experience with fire modelling in support of regulatory applications (other than IPEEE) to help define these fire scenarios; a questionnaire was prepared and distributed to all operating nuclear power plants in the United States concerning their experience with fire modelling; also, with support from the NRC, industry submittals were searched to identify the use of fire modelling.

Further information on nuclear power plant fire scenarios is found in [EPRI 1011989, 2005]. This reference discusses risk methods that may be used to evaluate scenarios that can be outside the applicability of the fire modelling tools evaluated in this report. Such scenarios include high-energy arcing faults, main control board fires and hydrogen fires.

### 8.9.2. Fire experiments and test selection

This section contains descriptions of the seven sets of fire experiments that can be used to validate fire models. The first six sets as shown in Table 8.1 were used in [NUREG 1824, 2007] in the evaluation of selected models. In general, the experiments established steady fires burning in simple compartment geometries. The decision to include or exclude a particular test from a particular experimental series was made for a variety of reasons and is described below. Table 8.1 summarises some of available experiments in terms of the aspects of the fire and the compartment, including the fire heat release rate ( $\dot{Q}$ ), the compartment volume (V) and compartment height (H).

**Table 8.1. Overview of the Experiments Used for Model Evaluation**

Series	$\dot{Q}$ (kW)	V (m <sup>3</sup> )	H (m)
Factory Mutual/Sandia Lab (FM/Sandia National Laboratories (SNL))	500	1400	6.1
National Bureau of Standards (NBS)	100	15	2.4
ICFMP Benchmark Exercise 2 BE #2	1800-3600	5900	19
ICFMP BE #3	400-2300	580	3.8
ICFMP BE #4	3500	74	5.7
ICFMP BE #5	400	73	5.6
IRSN (PRIZME Project)	TBD	TBD	TBD

#### FM/SNL test series

The Factory Mutual and Sandia National Laboratories (FM/SNL) test series was a series of 25 fire tests conducted in 1985 for the NRC by Factory Mutual Research Corporation (FMRC), under the direction of SNL. The primary purpose of these tests was to provide data with which to validate computer models for various types of nuclear power plant compartments. The experiments were conducted in an enclosure measuring 18 m long x 12 m wide x 6 m high (60 ft. x 40 ft. x 20 ft.), constructed at the FMRC fire test facility in Rhode Island.

All of the tests involved forced ventilation to simulate typical nuclear power plant installation practices. Four of the tests were conducted with a full-scale control room mock-up in place. Parameters varied during the experiments included fire intensity, enclosure ventilation rate and fire location.

#### NBS multi-compartment test series

The NBS, which is now called the National Institute of Standards and Technology, NIST) multi-compartment test series consisted of 45 fire tests representing nine different sets of conditions were conducted in a three-room suite. The experiments were conducted in 1985 and are described in detail in reference. The suite consisted of two relatively small rooms, connected via a relatively long corridor. The fire source, a gas burner, was located against the rear wall of one of the small compartments. Fire tests of 100 kW, 300 kW and 500 kW were conducted. [EPRI TR-108875] provides the required data for modelling

input, including information on the compartment, the fire, the ventilation and ambient conditions.

### **ICFMP benchmark exercise #2**

Benchmark exercise #2 (BE #2) consisted of eight experiments conducted in 1998 and 1999. The experiments represented three sets of conditions, and were undertaken to study the movement of smoke in a large hall with a sloped ceiling. The results of the experiments were contributed to the ICFMP for use in evaluating model predictions of fires in large volumes representative of turbine halls in nuclear power plants. The tests were conducted inside the VTT fire test hall, with dimensions of 19 m high x 27 m long x 14 m wide (62 ft. x 89 ft. x 46 ft.). [Kotsovinos, 1991] provides detailed information for model input. Each test involved a single heptane pool fire, ranging from two MW to four MW.

### **ICFMP benchmark exercise #3**

Benchmark exercise #3 (BE #3), conducted as part of the ICFMP and sponsored by the NRC, consisted of 15 large-scale experiments performed at NIST in June 2003. The experiments are documented in reference 28. The fire sizes ranged from 350 kW to 2.2 MW in a compartment with dimensions of 21.7 m x 7.1 m x 3.8 m high (71.2 ft. x 23.3 ft. x 2.5 ft.), designed to represent a compartment in a nuclear power plant containing power and control cables. A photo of the fire seen through the compartment doorway is shown in Figure 8.1. Walls and ceiling were covered with two layers of marine boards, each layer 0.0125 m (0.5 in) thick. The floor was covered with one layer of 0.0125-m (0.5-in) thick gypsum board on top of a 0.0183-m (23/32-in) layer of plywood. Thermophysical and optical properties of the marine and other materials used in the compartment are given in [Hamins, 2005]. The room had one door and a mechanical air injection and extraction system. Ventilation conditions, the fire size, and fire location were varied. Numerous measurements (approximately 350 per test) were made including gas and surface temperatures, heat fluxes and gas velocities. Detailed schematic diagrams of the experimental arrangement and data are available in [Hamins, 2005]. Figure 8.1 is a photo of a one MW heptane fire in the facility.

**Figure 8.1. Photograph of a one MW heptane fire seen through the open doorway**



### **Ventilation**

Natural Ventilation: the compartment had one door with dimensions of 2 m x 2 m (6.6 ft. x 6.6 ft.) in the middle of the west wall. Some of the tests had a closed door and no mechanical ventilation, and in those tests, the measured compartment leakage was an important consideration.

Mechanical ventilation: the mechanical ventilation and exhaust provided about five air changes per hour. The supply duct was positioned on the south wall, about two m (6.6 ft.) off the floor. An exhaust duct of equal area to the supply duct was positioned on the opposite wall at a comparable location. The flow rates through the supply and exhaust ducts were measured in detail during breaks in the testing, in the absence of a fire.

#### **ICFMP benchmark exercise #4**

Benchmark exercise (BE) #4 consisted of kerosene pool fire experiments conducted at the Institut für Baustoffe, Massivbau und Brandschutz (iBMB) of the Braunschweig University of Technology in Germany. The results of two experiments were contributed to the ICFMP and documented in [Klein, 2005]. These experiments involved relatively large fires in a relatively small [3.6 m x 3.6 m x 5.7 m (12 ft. x 12 ft. x 19 ft.)] concrete enclosure. Only a portion of test one was selected for consideration in [NUREG 1824, 2007], because a significant amount of data was lost in test one, and the measured  $\dot{Q}$  during test three exhibited significant amounts of fluctuation.

#### **ICFMP benchmark exercise #5**

Benchmark exercise (BE) #5, conducted under the ICFMP, was comprised of four large-scale tests inside a concrete enclosure with realistically routed cable trays [Riese, 2004]. This test series was conducted in the same facility as benchmark exercise #4, which was at the Institut für Baustoffe, Massivbau und Brandschutz (iBMB) of the Braunschweig University of Technology in Germany. The compartment was configured slightly differently, and the height was 5.6 m (18.4 ft.) in BE #5. Test four of the BE #5 test series was selected for the quantitative evaluation of models reported in NUREG 1824.

#### **The IRSN PRISME project**

The project will consist of a series of fire and smoke propagation tests in a dedicated facility at the French Institut de Radioprotection et de Sûreté Nucléaire (IRSN) centre at Cadarache. The facility will be used to investigate room-to-room heat and smoke propagation, the effect of network ventilation and the resulting thermal stresses to sensitive safety equipment of such room configurations. It is also planned to use data from the project to study multi-room fires and for validating fire computer codes. Several propagation modes will be studied: through a door; along a ventilation duct that crosses the room containing the fire and that ventilates an adjacent room; along a ventilation duct when flow is reversed within; and through leakages between several rooms. The project aims to provide such critical information as the time that elapses before target equipment malfunctions and to qualify computer codes modelling heat and smoke propagation phenomena. The objective is to answer questions concerning smoke and heat propagation inside an installation, by means of experiments tailored for code validation purposes.

#### **References**

- Babrauskas, V. (1986), *Fire Safety Journal*, 11:33-51.
- Cox, G. (1995), "Basic Consideration," *Combustion Fundamentals of Fire*, (G. Cox, ed.), Academic Press London, United Kingdom, pp. 1-30
- Cox, G (1998), *Phil. Trans. R. Soc. Lond. A* 356:2835-2854.
- Deliachatsios, M.A. (1987), *Combustion and Flame* 70:33-46.

- Drysdale, D. (1985), *An Introduction to Fire Dynamics*, Wiley & Sons, NY, NY.
- EPRI 1011989 and NUREG/CR-6850 (2005), “EPRI/NRC-RES Fire PRA Methodology for Nuclear Power Facilities,” U.S. Nuclear Regulatory Commission, Washington, D.C., August 2005.
- Ferziger, J.H. (1996), *New Tools in Turbulence Modelling*, (O. Metais, J. Ferziger, eds.) Springer-verlag, Berlin, Germany, pp.29-47.
- Fluent 6.3 user manual, Fluent Inc, Lebanon NH, October 2006
- Fire Modelling Code Comparison, TR-108875, Electric Power Research Institute, Palo Alto, CA.
- Klein-Heßling W. and M. Röwenkamp (2005), *Evaluation of Fire Models for Nuclear Power Plant Applications: Fuel Pool Fire Inside a Compartment*, Gesellschaft für Anlagen-und Reaktorsicherheit (GRS), Köln, Germany, May 2005.
- Kotsovinos, N.E. (1991), *Physics of Fluids A* 3(1):163-167.
- McGrattan, K.B, H.R. Baum and R.G. Rehm (1998), *Fire safety Journal* 30:161-178.
- Mell, W.E, K.B. McGrattan and H.R. Baum (1996), 26<sup>th</sup> Symposium (International) on Combustion, The Combustion Institute, Pittsburgh, PA., pp. 1523-1530.
- Mulholland, G.W., W. Liggett and H. Koseki (1996), 26<sup>th</sup> Symposium (International) on Combustion, The Combustion Institute, Pittsburgh, PA, pp. 1445-1452.
- Najm, H.N., R.W. Schefer, R.B. Milne, C.J. Mueller, K.D. Devine and S.N. Kempfka (1998), “Numerical and Experimental Investigation of Vortical Flow-Flame Interaction”, SNL, SAND98-8232.
- Nicolette, V.F. (1996), “Computational Fire Modelling for Aircraft Fire Research,” SNL, SAND96-2714, pp.22-24
- NUREG-1824 (2007), “Verification and Validation of Selected fire Models for Nuclear Power Plant Applications”, Volume 2, April 2007, Washington D.C.
- Rehm, R.G., K.B. McGrattan, H.R. Baum and K.W. Cassel (1997), *Fire Safety Science- Proceedings of the 5<sup>th</sup> International Symposium*, pp.391-402.
- Riese, O. and D. Hosser (2004), *Evaluation of Fire Models for Nuclear Power Plant Applications: Flame Spread in Cable Tray Fires*, Draft Version, Revision 1, Institut für Baustoffe, Massivbau und Brandschutz (iBMB), Braunschweig, Germany, June 2004.
- Schneider, M.E., N.R. Keltner and L.A. Kent (1989), “Thermal measurements in the Nuclear Winter Fire Test”, SNL Report, SAND88-2839.
- Sivathanu, Y.R. and G.M. Faeth (1990), “Generalised State Relationships for Scalar Properties in Non-Premixed Hydrocarbon/Air Flames”, *Combustion and Flame*, 82:211-230.
- Sung, C.J., J.B. Liu and C.K. Law (1995), *Combustion and Flame* 102:481-492.
- Tieszen, S.R. (2000), *Time and Length Scales within a Fire and Implications for Numerical Simulation*, Sandia National Lab, NM.
- Vervisch, L. and T. Pointsoot (1998), *Ann. Rev. Fluid Mech.* 30:655-691
- Vincente, W.G. and C.H. Kruger Jr. (1975), *Introduction to Physical Gas Dynamics*, Kriger Pub. Co., Huntington, NY.

Williams, F.A. (1985), *Combustion Theory*, Benjamin/Cummings Pub. Co., Menlo park, CA.

Williams, J.H. and L.A. Gritzo (1998), *27<sup>th</sup> Symposium (International) on Combustion*, The Combustion Institute, Pittsburgh, PA, pp. 2707-2714.

Zhou, X.C. and J.P. Gore (1995), *Combustion and Flame* 100:52-60.

Zhou, X.C. and J.P. Gore (1996), *27<sup>th</sup> Symposium (International) on Combustion*, The Combustion Institute, Pittsburgh, PA., pp. 2767-2773.

## 9. Verification test cases of special interest for the selected issues

The verification of a thermal-hydraulic code is necessary to evaluate the numerical scheme. The main qualities required for a numerical scheme, which have to be tested are:

- **Consistency:** ability of a system of discretised equations to tend towards the system of partial differential equations when the discretisation steps tend to zero.
- **Stability:** ability of a numerical scheme not to generate non-physical instabilities.
- **Accuracy:** ability of a system of discretised equations to approach the initial system of partial differential equations as close as possible. The accuracy generally increases when the discretisation steps tend to zero but with a given time step and space, different schemes have different accuracies.
- **Robustness:** ability of a discretisation and solving scheme to be operational and to always give the solution whatever the simulated flow configuration.
- **CPU time efficiency:** computing time required to solve a physical problem. This time depends on the time and space steps used which also influence the computing accuracy. This criterion therefore has to be examined at the same time as the accuracy criterion. To compare two schemes, the CPU time required for a given accuracy, or the accuracy obtained for a given CPU time, can for example be compared.

In system codes like TRACE, CATHARE, RELAP 5, ATHLET the main characteristics of the numerical scheme are the robustness, the efficiency in terms of CPU time and good properties of mass and energy-conservation. However, a rather high numerical diffusion is accepted due to the first order space discretisation associated with a staggered grid and to the use of rather coarse meshing. 3D modules use only structured meshing.

Looking for future CFD tools having a finer space resolution, the requirements regarding the numerical scheme have to be revisited.

### 9.1. The needs for 3D two-phase CFD codes for open medium

For 3D two-phase CFD codes, the main requirements regarding the numerical scheme are the following with decreasing priority:

- **Robustness:** capability to converge to a solution in all physical situations of the domain of simulation.
- **Adaptation to complex geometry:** for 3-D two-phase CFD codes the use of body fitted meshing with unmatched mesh capabilities or unstructured meshing is mandatory.
- **Accuracy, reducing numerical diffusion:** the modelling of fine scale processes and of turbulent diffusion is only possible when numerical diffusion is lower than the physical diffusion.

- Efficiency: 3D Two-phase CFD calculations use fine meshing and are very CPU time-consuming; any improvement of the efficiency is welcome. Parallel computing is mandatory.
- Mass and energy-conservation: good conservation properties are welcome.
- Preservation of wave propagation processes along characteristic directions: it may be important in some physical problems with pressure or void propagation phenomena.
- Well-posedness of the mathematical problem.

## 9.2. The needs for 3D codes for porous medium

In current applications of 3D codes for porous medium (component codes), the main requirements regarding the numerical scheme are the following with decreasing priority:

- Robustness: capability to converge to a solution in all physical situations of the domain of simulation.
- Accuracy, reducing numerical diffusion: in current 3D modelling rather, fine meshing may be required (up to sub-channel size) and the modelling of turbulent diffusion is only possible when numerical diffusion is lower than the physical diffusion.
- Need of unstructured meshing: in 3D modelling using fine meshing (up to the size of the sub-channel), the use of unstructured meshing may be necessary for some complex geometry.
- Efficiency: a 3D calculation using fine meshing being CPU time-consuming, any improvement of the efficiency is welcome. This may require parallel computing.
- Mass and energy-conservation: good conservation properties are required.

## 9.3. Selection of a matrix of numerical benchmarks

A benchmark matrix is to be used for each numerical method in order to measure the capabilities with respect to the requirement listed above. Criteria that are more detailed have to be defined. They can be broken down into various required potentialities. The following list was established to meet the requirements for the whole list of NRS issues identified in the previous report.

### *Operationality-robustness criteria:*

- The scheme has to be able to deal with all the two-phase flow regimes (and the whole range of void-fraction) at least with a 6-equation model + turbulence model + probably IAT equation.
- The scheme has to be able to work in a wide range of pressures and temperatures.
- The scheme has to be able to operate in an open or porous medium with complex geometries.
- The scheme has to be able to deal with flows with non-condensable (e.g. water-air, steam-H<sub>2</sub>-N<sub>2</sub> mixture).
- The scheme has to be able to deal with swollen levels and water-packing.

- The scheme has to be able to deal with incompressible and compressible flows with non-simplified equations of state.
- The scheme has to be able to deal with flows with large interfacial mass transfers (strong pressure-void-fraction coupling).
- The scheme has to be able to deal with strong hydraulic-wall conduction couplings (passing DNB, rewetting).
- The scheme has to be able to deal with flows in an extended range of velocities including at high Mach, subsonic and supersonic.

*Accuracy criteria:*

- The scheme has to be able to conserve mass and energy correctly.
- The scheme has to be able to compute the propagation of a pressure wave and of a void-fraction wave correctly.
- The scheme has to be able to compute the propagation of a temperature or concentration front correctly (Reduction of numerical diffusion).

*Numerical efficiency criterion:*

- The CPU time must remain compatible with an industrial use.

The purpose of a benchmark matrix must remain quite distinct from physical validation:

- Physical validation = quantitative computation-experiment comparison to qualify the validity of the physical models.
- Numerical benchmarks = measurement of the differences between a system of equations and its numerical solving.

In the specific two-phase situation, there are hardly any actual physical problems where an analytical solution is known apart from a few academic cases, which do not cover the physical field to be dealt with.

- A few cases exist with a known analytical solution (or approximate analytical solution) if the system of equations is simplified. They do not cover the completely physical field to be dealt with.
- Necessity to complete by test cases computed with the original physical model to complete coverage of the targeted simulation scope. Inter-comparison of numerical schemes with identical physical and/or qualitative comparison with an experiment.

Consequently, two types of tests must be selected:

- Verification tests: tests with known analytical solution:
  - a simplified system of equations and closure laws are imposed;
  - quantitative comparison between computation and analytical solution;
  - tests the accuracy of the numerical scheme;
  - tests the time step and meshing convergence;
  - CPU time measurement.

- Demonstration tests: tests with unknown analytical solution with experimental reference
  - the original system of equations is used and the adequacy of the system is checked qualitatively on the experimental result;
  - comparison between numerical schemes;
  - compares the accuracy of the numerical schemes;
  - compares the time step and meshing convergence;
  - CPU time measurement;
  - tests the operationality and robustness on an actual case;
  - tests the ability to operate with real physical laws.

A list of benchmarks was collected (See Table 9.1 below) based on information found in the fifth FP ASTAR, and ECORA actions and in the French NEPTUNE project (see Mimouni et Serre, 2001). Many of them are rather 1D tests, which were already used for 1D modules of system codes. They are defined in the Volume 6 of Multi-phase Science and Technology. They are classified with respect to the dimension of the problem (1D, 2D or 3D), the presence of phase-change or not, the relevance for open medium and/or porous medium, the type of test, either verification or demonstration. When there is an experimental basis, there can be also a validation aspect of the test.

#### **9.4. Critical analysis of the list of selected tests.**

The selected list does not pretend to be a comprehensive program of Verification for the selected NRS issues. Since the choice of the model options, for the selected issues are not fully closed it was still too early to define a frozen list of tests for each issue. Using RANS equations, or filtered equations, or even the addition of an ITM will have an impact on the verification requirements.

Many of the tests are rather 1D tests, which were already used for 1D modules of system codes. The list of really 3D tests should be extended.

The main difficulty is to find two-phase flows tests with analytical solutions. Some tests with an analytical solution exist if the system of equations is simplified but tests with the original set of equations and closure relations have only an experimental reference. In order to build new numerical benchmark tests, the method of manufactured solutions is probably the best way. It is briefly presented here below.

**Table 9.1. List of numerical benchmarks for two-phase CFD**

TITLE	1D Multi-D	Phase- Change	Open/ Porous	Verification/ Demonstration	Validation
Manometric oscillations in a U-tube	1D	No	O&P	V D	
Faucet flow	1D	No	O	V D	
Dispersed two-phase flow in a nozzle	1D	No	O/P	V	
Propagation of a passive scalar front	1D & 3D	No	O&P	V	
Laminar flow in a heated tube	2D	No	O	V	
Boiling in a channel	1D & 3D	Yes	O&P	D	
Wall heat exchange with dry-out and rewetting	1D	Yes	O&P	D	
Expulsion of steam by sub-cooled water	1D	Yes	O&P	D	
Shock tube	1D	No	O	V	
Stratified flow	2D	No	O	V D	
Static sedimentation	1D	No	O&P	V/D	
Critical flow in a nozzle (Super Moby Dick)	1D 3D	Yes	O&P	D	Val
Core uncovering (Pericles rectangular boil-up)	1D 2D	Yes	O&P	D	Val
Fast depressurisation (Super Canon)	1D	Yes	O&P	D	
Vertical air-water bubbly-slug flow (Dedale test)	1D & 3D	No	O	D	Val
Vapour explosion (OECD test case)	3D	Yes	O&P	D	
Driven cavity	3D	No	O	D	
Flooding in a vertical tube	1D & 3D	No	O&P	D	
Water-hammer	1D	Yes	O	D	Val
Condensation shock (injector condenser)	1D	Yes	O	D	
LINX: bubble plume	3D	No	O	D	Val
Boiling flow in a tube: DEBORA	2D	Yes	O&P	D	Val
Water sloshing experiment	3D	No	O	D	Val
Taylor bubble	3D	No	O	D	Val
Jet entering a free surface with bubble entrainment: Boneto-Lahey test	3D	No	O	D	Val
Water jet on inclined plate in air environment	D	No	O	D	Val
DCC on stratified flow	3D	Yes	O	D	Val

### 9.5. The method of manufactured solutions

The method of manufactured solutions (MMS) (Salari et al., 2000; Roache, 2002) is a very simple process, although some of the algebra required for implementation can become

complicated. Starting with a partial differential equation or system of PDEs for which the goal is to verify the implementation of a discretised solution procedure. Choosing a closed analytic form for the desired solution for the final test problem. Next, substituting the analytic solution into the base PDEs generates new or modified source terms in the equations. Finally, initial and boundary conditions for the test problem are obtained by evaluating the selected solution form at zero time and at whatever spatial locations constitute the boundary of the problem. For a given code, primary consideration for use of MMS is the level of difficulty involved in specifying or adding source terms to all PDEs involved in the solution.

As an example, suppose that we wish to verify a finite difference solution method for a one-dimensional transient conduction problem represented by the equation:

$$\frac{\partial T}{\partial t} - \alpha \frac{\partial^2 T}{\partial x^2} = \frac{q}{\rho c_p} \quad (1)$$

For this example, a very simple functional form is chosen for the solution.

$$T(x, t) = 300 + (0.01 - x^2)t \quad (2)$$

Evaluating the differential operators gives:

$$\frac{\partial T}{\partial t} = 0.01 - x^2, \quad \frac{\partial^2 T}{\partial x^2} = -2t, \quad \frac{\partial T}{\partial t} - \alpha \frac{\partial^2 T}{\partial x^2} = 0.01 - x^2 + 2\alpha t \quad (3)$$

As a result, the source term in the original model equation is specifically set as:

$$\frac{q}{\rho c_p} = 0.01 - x^2 + 2\alpha t \quad (4)$$

Looking at the original functional form, the initial conditions are  $T(x,0)=300$ , and boundary conditions for a 0.2 m thick metal slab would be  $T(-0.1,t)=300$  and  $T(0.1,t)=300$ .

For most general-purpose conduction solvers, the source term could be provided via tabulated input. However, complications can arise due to interpolation procedures applied to the input. For best results, the source term should be installed as a function added to the programme, or linked to the programme via an interface provided to users by the code developers.

Verification testing of the code is very similar to a Richardson extrapolation based mesh and time step sensitivity study. The error between the code and manufactured solution is followed for a sequence of mesh and a sequence of time step sizes. Any plot of error vs. mesh size (or time step) should trend clearly towards zero as the discretisation approaches zero. In addition a fit of one of these curves to the equation

$$\text{error} = ah^p \quad (5)$$

provides a check of the order of accuracy quoted for the discrete approximation to the PDE.

For best results from a manufactured solution the following rules should be followed.

- The manufactured solution should be assembled using smooth analytic functions, i.e. trigonometric, exponential or polynomial functions. This ensures that the theoretical order of accuracy can be attained and such functions are easy to differentiate.
- The solution should be general enough to exercise every term in the governing equation, including all dependent variables.
- The solution should have a sufficient number of non-trivial derivatives.
- The solution should not be a strongly varying function of space and time or have a singularity. This is accomplished by bounding a solution derivative by a relatively small constant.
- There is no requirement on physical realism or robustness. However, if the code contains assumptions, such as a positive solution or a positive equation term, make sure the manufactured solution satisfies those assumptions.

As part of a research project for the US Nuclear Regulatory Commission, use of various higher order numerical methods was studied for a two-phase, three-fluid model (vapour, continuous liquid, entrained liquid). A manufactured solution was used to check the implementation of the various difference methods (see Annex 1). Installation of the special source terms calculated by the method into the 1-D two-phase code proved to be invaluable in detecting and isolating coding errors.

## 9.6. Conclusion on verification

The initial objective of the writing group with respect to verification was to identify a matrix of numerical benchmarks of special interest for the selected NRS problems. Although the numerical capabilities to be tested were identified, and the criteria to select adequate benchmark tests were defined, the objective could not be fully reached. The difficulties of this task are now better evaluated and are related to several reasons:

- basic model options are not closed for some issues;
- 3-D two-phase problems with analytical solutions are practically limited to trivial cases;
- 3-D two-phase experiments with sufficient local measurements are also very scarce.

Therefore, it is recommended to continue the efforts made to define adequate 3D Verification tests. Two ways are recommended:

- the use of the method of manufactured solution should be promoted in two-phase CFD to produce tests with analytical solutions;
- new experiments with simple prototypic flow configurations should be produced with very well defined initial and boundary conditions and well-instrumented local measurements of possibly all principal variables; such tests could be used first as demonstration tests in the verification step and then as validation tests.

Before having a comprehensive verification matrix, it was decided to select a benchmark test (or a few) for each NRS issue to provide at least an evaluation of the present capabilities and limitations, to promote further progress. Depending on the case, the benchmark(s) can be pure validation, or a may have a “verification” aspect, or even can be a demonstration test to evaluate the capabilities of the CFD to deal with a complex industrial application. The next section presents the selected benchmarks.

### **References**

Roache, P.J. (2002), “Code Verification by the MMS,” *Trans. ASME, J. Fluids Engineering*, 124, pp. 4-10.

Salari, K. and P. Knupp (2000), *Code Verification by the MMS*, Sandia Report, SNL.

Hewitt, G., J.M. Delhaye and N. Zuber (1987), *Multi-phase Science and Technology*, Vol. 6, Eds, pp. 591-609.

Mimouni, S. and G. Serre (2001), *List of benchmarks for Simulation Tools of steam-Water two-phase flow*, ICONE 9, NICE, 8-12 April 2001.

## 10. Proposal of benchmarks relative to the selected issues

The previous sections have presented the state of the art in the use of two-phase CFD for each selected nuclear reactor safety issue. It is now more evident why the respective issues have been selected as having a good chance to be successfully treated by CFD in a reasonable period. It is also clear that further effort is necessary and that CFD tools have to be improved, validated, verified, and should better demonstrate their capabilities to reliably simulate the physical problem. In order to promote further progress of CFD tools and for a better evaluation of the present capabilities and limitations, it was decided to select a benchmark test (or a few) for each NRS issue. Each benchmark is selected taking into account what has been learnt so far and to provide the best benefit for further progress. Depending on the case, the benchmark can be pure separate-effect test validation, or a more global validation test, may have a “verification” aspect, or even can be a demonstration test to evaluate the capabilities of the CFD to deal with a complex industrial application.

The benchmarks are not proposed as ISPs (international standard problems) to avoid the heavy organisation of such exercises but rather as open exercises with a lighter procedure to be defined.

The following sections present shortly the proposed benchmarks with the objectives, the nature of the test (validation, verification, and demonstration), the expected target variable to be compared and the type of models to be evaluated with the test.

### 10.1. Proposed benchmark for dry-out

A few test cases are selected to validate the most important flow processes having an influence on the dry-out. The dry-out occurrence is governed by phenomena such as entrainment of drops from liquid film, evaporation of liquid film, deposition of drops from the gas core, presence of disturbance waves in the gas core, as well as thinning and stability of a wavy liquid film on a heated surface. Out of all these parameters, there are several that have been extensively measured and can be used as a reference for validation of computational models. The test cases that are proposed are shown in the table below, indicating the objectives and target parameters for each of the cases.

Objectives	Target parameter	Nature of test	Type of model	Reference data
To validate the mass transfer between droplets and liquid film and the resulting film thickness	Deposition rates of droplets in annular flows	Validation	a) Two-fluid b) Eulerian-Lagrangian	Jepson et al. (1989) Table 1, runs # 19, 20, 21, 22, 23; Table 2, runs # 12, 16, 19, 23, 24
To validate the mass transfer between droplets and liquid film and the resulting film thickness	Entrainment rates of droplets in annular flows	Validation	a) Two-fluid	Okawa et al. (2005) Table 4, runs # 1, 9, 13, 25
To validate the drop size prediction based on drop coalescence and breakup mechanisms	Drop size	Validation	a) Two-fluid Eulerian/Eulerian b) Eulerian-Lagrangian	Fore et al. (2002) Table 1, runs # 1, 4, 8, 9, 14, 20, 23
To validate the prediction of the dry-out occurrence based on the local liquid film thickness	Film thickness	Validation	a) Two-fluid b) Interface-tracking	Würtz (1978) Fig. 3.10.c, Fig. 3.11, Fig. 3.13.c, Fig. 3.14.c

## 10.2. Proposed benchmark for DNB

A benchmark based on both ASU data and on DEBORA data on boiling flows. Each of these experiments provides unique information:

- ASU provides velocity and turbulence measurements in boiling flow, but practically no information on bubble diameters;
- DEBORA provides information on bubble diameter profiles and on bubble diameter pdf distribution, but no information on liquid velocity and turbulence.

The objectives of the simulation of the ASU and DEBORA test are separate-effect test validation:

- forces exerted on the bubbles (drag, lift, dispersion wall force);
- coalescence, breakup and all phenomena which affect bubble interfacial area and bubble-size distribution;
- interfacial heat and mass transfer;
- wall heat transfers and associated parameters: liquid heating, wall vaporisation, quenching heat-flux, bubble departure diameter, frequency of bubble detachment, density of nucleation sites;
- wall functions for momentum equations.

Another objective is to compare several methods to take poly-dispersion of bubbles into account such as the multi-group (MUSIG) method or the method of statistical moments.

The target variables to be compared to experiment are:

- ASU test: void profile, gas and liquid velocity profile, liquid temperature profile, liquid turbulent kinetic energy;
- DEBORA test: void profile, liquid temperature profile, gas velocity profile, interfacial area profile, bubble-size distribution profile.

## 10.3. Proposed benchmark for PTS

A benchmark based on both TOPFLOW-PTS data and on a ROSA specific test on PTS is proposed.

The TOPFLOW-PTS experiment will provide data on condensation rates, volume fraction distributions (bubble entrainment below the impinging jet, wavy stratified flow in the cold leg), temperature distributions which characterise the mixing along the flow path from the ECC injection towards the down-comer as well as the thermal loads on the RPV wall and probably also some information on liquid phase velocity fields.

The objectives of the simulation of a TOPFLOW test are separate-effect test validation:

- interfacial transfers at the free surface in the cold leg;
- the effects of entrained bubbles by the plunging jet;
- the turbulence production and turbulence mixing in the cold leg;
- the phenomena at the entrance of the down-comer including heat transfers with the wall.

In addition, also the interactions of these processes can be investigated. A steady-state test should be selected as a benchmark.

The ROSA test allows a consideration of integral effects.

The objectives of simulating a ROSA specific test is to demonstrate the capability to deal with a system effects and to model the whole reactor transient by a coupling of chaining between CFD and system code calculations.

OECD-ROSA test N° 1-1 simulates natural circulation at 2% Nominal Power with stepwise decreasing mass inventory and with cold leg injection during periods of 80 seconds.

OECD-ROSA test N° 1-2 simulates a 1% Hot Leg Break with cold leg injection.

A first benchmark could consist in simulating a period of the test 1-1 with a coupling or chaining of system and CFD codes. Then the simulation of the test 1-2 would be a more complete demonstration test of the coupled (chained) calculation of the whole PTS scenario.

#### 10.4. Proposed benchmark for pool heat exchangers

The benchmark proposed here focuses on the capabilities of a CFD code to simulate the bubble plume produced by boiling on the outer surface of pool heat exchanger tubes. To minimise the number of phenomena being studied, we propose a benchmark based on air bubble plume tests in the LINX facility at the PSI in Villigen, Switzerland. The LINX vessel is 2 m in diameter and 3.4 m high with 12 glass windows for PIV, photography and visual observations. Other instrumentation includes thermo-couples, pressure transducers, electromagnetic probes, double tipped optical probes and miniature pitot tubes.

A wide range of data appropriate for CFD validation is available from the facility. PIV combined with filters on the camera permit measurement of two components of either bubble or liquid local velocities. Image processing of photographs provide probability density functions for principal axis lengths of bubbles and associated interfacial area concentration (data reduction assumes an ellipsoidal bubble shape). Double tipped optical probes provide local values for void-fraction and bubble rise velocity. An electromagnetic probe (combined with salt in the water to provide enough conductivity) is used to obtain liquid velocities in recirculation zones beyond the maximum radius of the bubble plume. Velocity measurements from the electromagnetic probe do not provide useful information on turbulence, but can be used to check CFD predictions of mean velocities.

General descriptions of the facility are available in papers by Simiano et al. (2006) and by Yadigaroglu et al. (2008). A more detailed description of instrumentation and data reduction is available in the doctoral thesis of Marco Simiano (Simiano, 2005).

A new LINX experiment would be ideal for the purposes of a blind benchmark. However, a very large amount of data has been archived from this facility. It is possible that test results could be available that have not yet been used for CFD validation.

## References

Simiano, M., R. Zboray, F. de Cachard, D. Lakehal and G. Yadigaroglu (2006), “Comprehensive experimental investigation of the hydrodynamics of large-scale, 3D, oscillating bubble plumes”, *International Journal of Multi-phase Flow*, 32, 1160-1181.

Yadigaroglu, G., M. Simiano, R. Milenkovic, J. Kubasch, M. Milelli, R. Zboray, F. de Cachard, B. Smith, D. Lakehal and B. Sigg (2008), “CFD4NRS with a focus on experimental and CMFD investigations of bubbly flows”, *Nuclear Engineering and Design*, 238, 771-785.

Simiano, M. (2005), “Experimental Investigation of Large-Scale Three-Dimensional Bubble Plume Dynamics”, Doctoral Thesis, Swiss Federal Institute of Technology Zurich, Diss. ETH No 16220, <https://www.research-collection.ethz.ch/handle/20.500.11850/148942> (accessed 28 November 2022).

## 10.5. Proposed benchmark for steam injection in a pool

One of the validation tests of potential consideration, for benchmarking the data on the steam injection in a pool, is the JICO test, which is currently ongoing at KAERI for the purpose of developing some physical models on condensing jet-induced, turbulent jet by generating a set of basic data on the local flow structures, in both the turbulent jet and global circulation in a cylinder, and of producing CFD validation data for a pool mixing analysis. The unique features of this test, when compared to previous ones, includes that the steam jet is vented to the pool upwardly or downwardly through a single nozzle inside a sub-cooled water tank. Local flow structures around the turbulent jet are measured by using special PIV techniques [Choo and Song, 2008].

This experiment provides valuable information on:

- detailed measurements of velocity characteristics around the turbulent jet-induced by a condensing steam jet discharged in a sub-cooled water pool; and
- characteristics of global circulation to determine the thermal mixing in a pool, which depends on both the steam mass flux and the pool temperature, but no detailed flow information inside the steam jet.

A high degree of turbulence generated at the interface between the steam jet and the pool water due to its large velocity difference, and the high eddy motion of small bubbles in the mixing region will be very important for understanding the thermal mixing in a pool since they can sufficiently enhance the heat and the momentum transfer in the steam jet.

The JICO testing will help us to understand the characteristics of a turbulent jet in the downstream of a condensing steam jet in detail, and to characterise the circulation flow pattern inside the pool. The JICO facility is equipped with a steam generator (Max. 10Bar; 0.023kg/s), an exchangeable sparging nozzle, and a water pool (0.8 H x 2 m D), as shown in Figure 10.1. A tentative test matrix for the validation is shown in Table 10.1.

The objectives of the simulation of the JICO test are separate-effect test for the validation:

- interfacial heat-transfer at the phasic interface around the steam jet;
- momentum exchange between steam jet and the surrounding water, which affects global picture of thermal mixing in a pool;
- thermal mixing in a pool, which is induced by the steam jet;
- wall functions for momentum equations and the free surface treatments in an analysis.

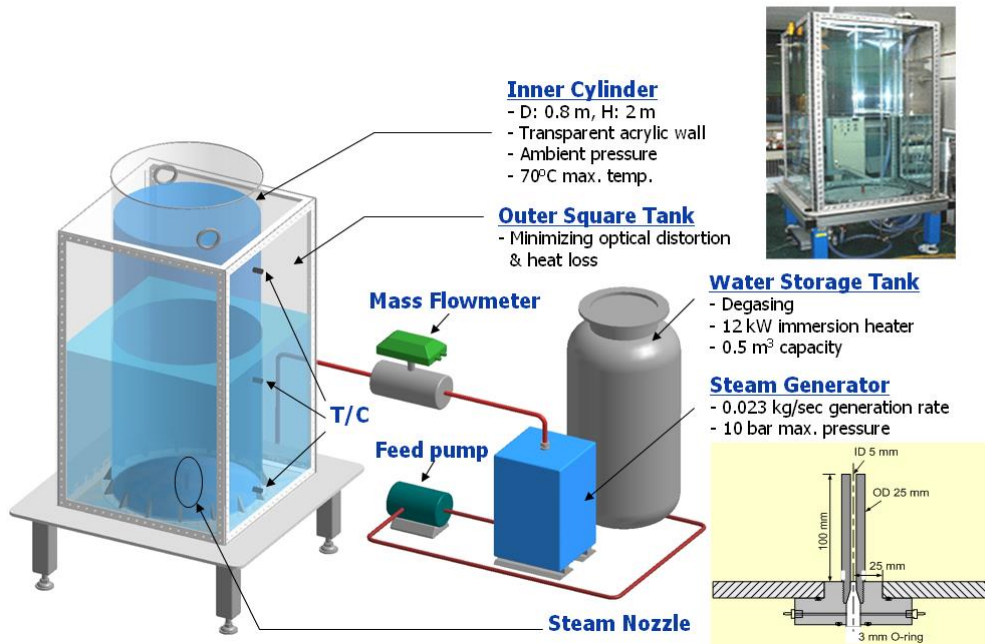
The target variables to be compared to the experiment are:

- steam jet shape;
- velocity (and temperature) distribution around the steam jet in a liquid pool; and
- global circulation pattern, which must be different from test condition.

**Table 10.1. Test conditions to be covered in the JICO test facility**

Nozzle ID (mm)	Steam mass flux (kg/m <sup>2</sup> s)	Pool temperature (°C)
5~10	300~650	20~70

**Figure 10.1. Schematic of the JICO facility**



### 10.6. Proposed benchmark for fire analysis

Benchmark exercise # 3 (BE # 3), conducted as part of the ICFMP and sponsored by the NRC is a good benchmark tests series for validation. This ICFMP exercise comprised a series of 15 large-scale fire tests, performed at NIST between five and 20 June 2003. These tests consisted of 350 kW, 1.0 MW, and 2 MW fires in a marinite room with dimensions of 21.7 m x 7.15 m x 3.7 m (71.2 ft. x 23.5 ft. x 12.1 ft.). The room had one door with dimensions of 2 m x 2 m (6.6 ft. x 6.6 ft.), and a mechanical air injection and extraction system. Ventilation conditions and fire size were varied among the 15 tests. The numerous experimental measurements included temperatures in gas layers and surfaces, heat fluxes, and gas velocities, among others. Detailed schematic diagrams of the experimental arrangement and data are available in [Hamins, 2005].

## 11. Some guidelines for two-phase CFD application to the selected NRS issues

### 11.1. Introduction

Practical guidance for the application of CFD tools to the analysis of single-phase flows in nuclear reactor safety is given by Mahaffy et al. (2007) in the report “Best Practice Guidelines for the Use of CFD in Nuclear Reactor Safety Applications”. This report covers the full range of topics for high-quality flow simulations. It comprises sections on appropriate problem definition and subsequent selection of simulation tools. Important factors in this selection are the flow processes, and the turbulence and two-phase flow scales to be resolved in the computation. The approach described by Mahaffy et al. (2007) is valid for single- and multi-phase simulations.

Since two-phase CFD application is by far less mature than single-phase CFD, a specific methodology was defined in the writing group and the application of this multi-step methodology adds some specific guidelines for two-phase applications. When this methodology will have been applied to a large number of two-phase flow situations, guidelines that are more precise could be given to CFD code users to select the right options appropriate for the specific application. At present, only limited guidelines are given as foundations of future best practice guidelines.

The report by Mahaffy et al. (2007) also describes techniques for the quantification and reduction of numerical errors. These have been developed for single-phase flows, but are equally valid for multi-phase flows: single- and multi-phase flow formulations are both based on conservation equations, and are therefore mathematically similar. There is, however, a significant additional challenge for multi-phase flows due to the presence of different phases, of sharp interfaces and of an increased tendency to instability and unsteady-state behaviour. The presence of sharp interfaces between the phases requires often a much higher grid resolution than is necessary for corresponding single-phase flows. The higher affinity to physical instabilities might be suppressed on coarse grids, but can appear under grid refinement. This characteristic and the additional model equations lead to very high computational demands for multi-phase flows.

An assessment of CFD capabilities has to ensure that different error types are properly identified and addressed. For instance, it is known from single-phase studies, that the quantification of model errors (turbulence models, etc.) can only be made if numerical and systematic errors have been reduced below an “acceptable” level. In an ideal world, this would mean that solutions are provided for grids and with time steps, which are fine enough that numerical errors become negligibly small. As this is not a trivial task, and would require very large computing resources, this ideal separation of errors cannot always be achieved. These basic difficulties are increased when multi-phase flow physics and unsteady-state effects are included in numerical simulations.

In the next sections, one will draw first some guidelines from application of the multi-step methodology and then address the control of numerical errors. The different error types that can affect a CFD simulation are listed and the most promising strategies to reduce these errors are discussed.

## 11.2. Guidelines in application of the multi-step methodology

The general methodology for two-phase CFD application to Nuclear reactor safety has been presented in Section 2. First, a checklist (Bestion, 2010) for application of the methodology is proposed. Then some information on the degree of maturity (Bestion, 2011a, 2011b) of each modelling approach is given to help in the selection of model options. Finally a series of consistency checks and a list of common errors are given.

### *11.2.1. Checklist for application of two-phase CFD to reactor thermal-hydraulic issues*

The following checklist is proposed for application of two-phase-CFD to a nuclear reactor issue. They correspond to the successive steps of the methodology presented in Section 2 and they can be grouped in the following way.

#### **A: Identification of important flow processes**

1. What is the basic process of interest in the reactor issue that I would like to predict by CFD (e.g. fluid temperature field in a component, clad temperature, a local heat-transfer, a mechanical load on some structure, a velocity field in a component, a system peak pressure...)?
2. What are all the other important basic processes, which are coupled to the process of interest?
3. What are the main non-dimensional numbers, which characterise the important flow processes?
4. What is the space and time domain of interest for the coupled processes?
5. What kind of two-phase flow regime(s) is (are) likely to be present in the domain of interest? In particular, how many separate fields are expected?
6. Is it a steady or transient situation? In case of a transient, what is the minimum time scale of interest?
7. What is the minimum space scale of interest in the process?

#### **B: Selecting basic model options**

1. Specify the time and space resolution of the simulation according to answers to questions five and six.
2. Choice of a number of fields according to answer to question four.
3. List of wall transfers (mass, momentum and energy), which may play a significant role in the whole process.
4. List of interfacial and interfiled transfers (mass, momentum and energy), which may play a significant role in the whole process.
5. List of turbulent transfers (mass, momentum and energy), which may play a significant role in the whole process.

#### **C: Review of experimental data for validation**

1. Check that the available experimental data cover all basic flow processes identified in two. If required, plan and design new experiments to cover all processes.

2. Check that the available experimental data cover all-important wall transfers, interfacial transfers and turbulent transfers identified in 9, 10 and 11. Check that they can be used to validate all-important transfer models in a separate-effect way. If required, plan and design new experimental programmes in order to be more exhaustive.
3. Check that the instrumentation and the experimental tests provide enough information to get initial conditions and boundary conditions for the simulation.
4. Check that the instrumentation and the experimental tests provide sufficient local information on flow parameters of interest to validate closure laws for wall, interfacial, and turbulent transfers identified in 9, 10 and 11.

### ***11.2.2. Applicability and degree of maturity of the various two-phase CFD approaches***

Table 11.1 below summarises the applicability and degree of maturity of the various two-phase CFD approaches to every flow regime. It may be seen that only two modelling approaches can be applied to simulate physical situations where all two-phase flow regimes may occur: the RANS (or URANS) and the LES with filtered and statistical interfaces. However, the former is more mature than the latter. The pseudo-DNS and the LES with deterministic interfaces can address all flow regimes but are practically limited by the required CPU time, which is prohibitive in the most complex flows. The LES with statistical interfaces cannot treat “large interfaces” and is intrinsically limited to dispersed flows.

The modelling needs depend a lot on the modelling approach (see Bestion, 2011b).

The pseudo-DNS and the LES with simulated interfaces have very few models to be implemented and validated

The LES with statistical interfaces has models for wall transfers, turbulent transfers and interfacial transfers for dispersed flow regime.

The RANS method has the same transfer terms as LES with statistical interfaces but for many flow regimes, which multiplies the number of models to be implemented and validated.

The LES with statistical and filtered interfaces has even more interfacial transfer models than the RANS since it considers separately large interfaces and statistical interfaces.

Attention should be paid to the availability of closure laws for all the transfers, which need to be modelled, and one must keep in mind that all current CFD codes have incomplete modelling of all transfers. Therefore, very often, for a new application, additional models have to be implemented and validated.

**Table 11.1. Applicability and degree of maturity of the various two-phase CFD approaches to every flow regime including CPU cost**

	Pseudo-DNS	LES Simulated interfaces	LES-VLES Statistical & filtered interfaces	LES-VLES Statistical interfaces	RANS-URANS Statistical & filtered interfaces
<b>Bubbly</b>	Applied	Applied	Applied	Applied	Applied
<b>Slug-Churn</b>	Possible Too expensive	Possible Too expensive	Possible	Not possible	possible
<b>Annular</b>	Possible Expensive	Possible Expensive	Possible	Not possible	Applied
<b>Annular-mist</b>	Possible Too expensive	Possible Too expensive	Possible	Not possible	possible
<b>Mist flow</b>	Applied	Applied	Applied	Applied	Applied
<b>Stratified</b>	Applied	Applied	Applied	Not possible	Applied
<b>Stratified-mist</b>	Possible Too expensive	Possible Too expensive	Possible	Not possible	Possible
<b>All flow regimes</b>	<b>Too expensive</b>	<b>Too expensive</b>	<b>Possible</b>	<b>Not possible</b>	<b>Possible</b>
<b>Degree of maturity</b>	<b>Average in some flow regimes Zero for “all flow regimes”</b>	<b>Average in some flow regimes Zero for “all flow regimes”</b>	<b>Average in some flow regimes Very low for “all flow regimes”</b>	<b>Average in dispersed flow</b>	<b>Average in some flow regimes Low for “all flow regimes”</b>

*Applied: is applicable and has been applied Not possible: cannot be applied due to intrinsic limitations*

*Possible: can be applied but not very mature Expensive: requires very high CPU time*

*Too expensive: unaffordable with current computer power*

### 11.2.3. Consistency checks

During the successive steps of the general methodology, several choices are made, which require some consistency. One can list a few required consistency checks:

- This basic choice of the number of fields must be adapted to the physical situation or to an acceptable degree of simplification of the situation. In particular, if the specific behaviour of two fields plays an important role according to the PIRT, they must be treated separately.
- The experimental SET validation matrix should be exhaustive with respect to all identified flow processes.
- The experimental SET validation matrix should be able to validate all the interfacial, interfield, turbulent and wall transfers.
- In the ideal case, the number of measured flow parameters in the validation experiments should be consistent with the complexity of the selected model to validate. A model defined by a set of  $n$  equations having a set of principal variables  $X_i$  ( $i = 1, n$ ) can be said “validable” when one can measure  $n$  parameters giving the  $n$  principal variables.
- The averaging procedure must be specified to give a clear definition of the principal variables and of the closure terms in the equations. The filtering of the turbulent scales and of two-phase intermittency must be fully consistent.

- The averaging of measured variables must be consistent with the averaging of the equations.
- A deterministic interface using an ITM requires that all phenomena having an influence on the interface are also simulated or deterministically treated.
- The choice of an adequate interfacial transfer formulation must be consistent with the interface treatment (deterministic, filtered, statistical), and with the ILIS.

#### ***11.2.4. Some frequent errors or defaults***

Due to the availability of many modelling options in commercial CFD codes such as FLUENT, STAR-CCM+, CFX, or in CFD codes specific to the nuclear community such as NEPTUNE\_CFD (Bestion and Guelfi, 2005, Guelfi and Bestion, 2007), it may happen that some non-consistent choices are made. Most errors are relative to inconsistent choices of space and/or time resolution for interfacial, wall and turbulent transfer modelling. A few examples of frequent errors are given here:

##### *1. Use of a 1D model for modelling interfacial transfer in CFD approaches*

The interfacial transfer formulation in a 3D modelling approach relates a local flux  $F_x$  of a quantity  $X$  to a difference between local phase variable  $X_k$  multiplied by a local transfer coefficient:  $C_x$

$$F_x^i = C_{x3D}^i [X_l - X_v]$$

The interfacial transfer formulation in a 1D modelling approach relates an area-averaged flux  $F_x$  of a quantity  $X$  to a difference between area-averaged phase variable  $X_k$  multiplied by a global transfer coefficient  $C_x$ :

$$\langle F_x^i \rangle = C_{x1D}^i [\langle X_l \rangle - \langle X_v \rangle]$$

Even if the flow remains unidirectional, e.g. in a pipe, there is no reason that  $C_{x3D}^i = C_{x1D}^i$  and they can differ by up to several orders of magnitude. It would be exact only in case of uniform fields of  $X_l$  and  $X_v$  which cannot be the case in a 1D model since area averaging contains boundary layers along walls in which all variables have generally strong gradients.

##### *2. Use of interfacial transfers of porous medium model in an open medium approach*

This is the same type of errors as for the previous case. In the porous medium approach, the transfer is volume-averaged in a space domain, which contains boundary layers along solid structures in which all variables have generally strong gradients.

##### *3. Use of wall transfers of porous medium model in an open medium approach*

This is a similar error to the previous one. In the porous medium approach, the wall transfer terms are homogenised due to the volume averaging in a space domain, which contains solid structures. In an open medium approach, transfers with walls generally use the wall function approach.

The wall transfer formulation in an open medium approach relates a wall flux  $F_x^w$  of a quantity  $X$  to the difference between the local value of  $X$  and the value at the wall  $X_w$  multiplied by a local transfer coefficient:  $C_x^w$

$$F_x^w = C_x^w [X - X_w]$$

The wall transfer formulation in a porous medium approach relates a volume-averaged flux  $F_x$  of a quantity  $X$  to a difference between volume-averaged phase variable  $\langle X_k \rangle$  and the value at the wall multiplied by a global transfer coefficient  $C_x$ :

$$\langle F_x^w \rangle = C_x^w [\langle X \rangle - X_w]$$

Here again the difference between the two transfer coefficients can be of several orders of magnitude for both wall friction and wall heat-transfer.

#### 4. Use a 3D two-fluid model without any turbulence modelling

The two-fluid model includes a time averaging over a long period covering all two-phase intermittency scales. Therefore all or part of the turbulence spectrum is filtered by this averaging process and this results in additional terms in momentum and energy equations for turbulent stresses (Reynolds stresses) and for turbulent diffusion which require adequate modelling.

In the case of a heated pipe with a two-phase flow, only the wall could heat the fluid meshes along the wall correctly but a turbulent transfer model in energy equations can only correctly describe the transfer to the core flow.

#### 5. Use of averaged interfacial transfer coefficients in a DNS or LES approach

This is the same inconsistency as the previous one but in a different context. The intention is here to have a fine resolution simulation with an interface-tracking technique for a deterministic treatment of interfaces.

### 11.3. Definition of errors in CFD simulations

CFD simulations have the following potential sources for errors and uncertainties:

- Numerical errors result from the difference between the exact equations and the discretised equations, which are solved, in the CFD code. For consistent discretisation schemes, these errors can be reduced by an increased spatial grid density and/or by smaller time steps.
- Model errors result from the necessity to describe flow phenomena like turbulence, combustion and multi-phase by empirical models. For turbulent flows, the necessity of using empirical models derives from the excessive computational effort to solve the exact model equations<sup>1</sup> with a DNS approach. Turbulence models are, therefore, required to bridge the gap between the real flow and the statistically averaged equations. Other examples are combustion models and models for interpenetrating continua, e.g. two-fluid models for two-phase flows.
- User errors result from inadequate use of CFD software. They are usually a result of insufficient expertise by the CFD user. They can be reduced or avoided by additional training and experience in combination with a high-quality project

---

1. I.e. THE NAVIER-STOKES equations for single-phase flows

management and by provision and use of best practice guidelines and associated checklists.

- Software errors are the result of an inconsistency between the documented equations and the actual implementation in the CFD software. They are usually a result of programming errors.
- Application uncertainties are related to insufficient information to define a CFD simulation. A typical example is insufficient information on the boundary conditions and/or the geometries.

A more detailed definition of the different errors is given by Roache (1998)] and in the ECORA best practice guidelines (2002).

#### 11.4. Strategies to reduce numerical errors

In order to reduce the numerical errors, it is necessary to have procedures for the estimation of the different errors. The main goal is to reduce solution errors to a minimum with given computer resources.

##### 11.4.1. Target variables

In order to monitor numerical errors, it is recommended to define a few characteristic target variables. The convergence of the numerical scheme can then be checked using these target variables without interpolation between different grids. Target variables should be selected using the following criteria:

1. representative of the goals of the simulation;
2. sensitive to numerical treatment and resolution;
3. available with existing post-processing tools;
4. available inside the solver and displayed during run-time (optimal).

Point 1 is self-explanatory. Point 2 should help to avoid the use of measures, which are insensitive to the resolution, like pressure-based variables in boundary layer simulations. It is best if the variable can be computed during run-time and displayed as part of the convergence history. This allows monitoring of the target variable during the iterative process.

##### 11.4.2. Iteration errors

A first indication of the convergence of an iterative solution is the reduction of residuals. Experience shows that different types of flows require different levels of residual reduction. For example, it is found regularly that swirling flows can exhibit significant changes even once more than five to six orders of magnitude have reduced the residuals. Other flows are well converged with a residual reduction of only three to four orders of magnitude.

In addition to the residual reduction, it is required to monitor the solution during convergence and to plot the predefined target variables as a function of the residual (or the iteration number). A visual observation of the solution at different levels of convergence is recommended. It is also recommended to monitor the global balances of conserved variables, like mass, momentum and energy vs. the iteration number.

Convergence is monitored and ensured by the following steps:

- reduce residuals by a pre-specified level and provide residual plots;
- plot evolution of residual with iteration number;
- report global mass balance with iteration number;
- plot target variables as function of iteration number or residual level;
- Report target variables as function of residual (table).

It is desirable to have the target variable written out at every time step or iteration in order to display it during the simulation run. Depending on the numerical scheme, the recommendations may also be relevant to the iterative convergence within the time step loop for transient simulations.

#### ***11.4.3. Spatial discretisation errors***

Spatial discretisation errors result from the numerical order of accuracy of the discretisation scheme and from the grid spacing. Second and higher order space discretisation methods are recommended to produce high-quality solutions on realistic grids. First order methods should be avoided if possible.

As the order of the scheme is given usually by the CFD software, spatial discretisation errors can mainly be influenced by the provision of adequate grids. It is important for the quality of the solution and the applicability of error estimation procedures that grids resolve the main features of the flow. This requires that grid points are concentrated in areas of large solution variation. Mahaffy et al. (2007) give guidelines for grid generation.

For grid convergence tests, simulations should be carried out for a minimum of three grids. The target quantities should be given as a function of the grid density. It is recommended that the graphical comparison between the experiments and the simulations show the grid influence for selected examples.

The following procedure should be followed:

- define target variables;
- provide three (or more) grids using the same topology (or for unstructured meshes a uniform refinement overall cells);
- compute solution on these grids:
  - ensure convergence of the target variable in the time- or iteration domain;
  - compute target variables for these solutions.
- compute and report error measure for target variables;
- plot selected variables for the different grids in a single diagram;
- check if the solution behaviour is in the asymptotic range, i.e. that error reduction is proportional to the truncation error order of the discretisation scheme.

#### ***11.4.4. Time discretisation errors***

In order to reduce time integration errors for unsteady-state simulations, it is recommended to use at least a second-order accurate time discretisation scheme. Usually, the relevant

frequencies can be estimated before the simulation. The time step should be chosen to provide at least ten to 20 steps for each period of the highest relevant frequency. In case of unsteadiness due to a moving front, the time step should be chosen as a fraction of  $\Delta t \approx \Delta x/U$ , with the grid spacing  $\Delta x$  and the front speed  $U$ .

Under strong grid and time step refinement, flow features can be resolved which are not relevant for the simulation objectives. An example is the gradual switch to a DNS for the simulation of free surface flows with a VOF method (drop formation, wave excitation for free surfaces, etc.). This is a difficult situation, as it usually means that no grid or time step converged solution exists below the DNS range, which can usually not be achieved.

In principle, the time dependence of the solution can be treated as another dimension of the problem. However, a four-dimensional grid study would be very demanding. It is therefore more practical to carry out the error estimation in the time domain separately from the space discretisation. Under the assumption that a sufficiently fine spatial discretisation is available, the error estimation in the time domain can be performed as a one-dimensional study.

Studies should be carried out with at least two and if possible three different time steps for one given spatial resolution. The following information should be provided:

- unsteady-state target variables as function of time step (graphical representation);
- error estimate based on (time-averaged) target variables;
- comparison with data for different time steps.

#### ***11.4.5. Round-off errors***

Round-off errors are usually not a significant problem. They can occur for high-Reynolds number flows where the boundary layer resolution can lead to very small cells near the wall. The number of digits of a single-precision simulation can be insufficient for such cases. The only way to avoid round-off errors with a given CFD code is the use of a double-precision version. In case of an erratic behaviour of the CFD method, the use of a double-precision version is recommended.

### **11.5. Strategies to reduce model errors**

Model errors are the most difficult errors to avoid, as they cannot be reduced systematically. The most important factor for the reduction of model errors is the quality of the models available in the CFD package and the experience of the user. There is also a strong interaction between model errors and the time and space resolution of the grid. The resolution has to be sufficient for the model selected for the application.

In principle, model errors can only be estimated in cases where the validation of the model is ‘close’ to the intended application. Model validation is essential for the level of confidence the user can have in a CFD simulation. It is therefore required that the user gathers all available information on the validation of the selected model, both from the open literature and from code developers (vendors). In case the user has personal access to a modelling expert in the required area, it is recommended to interact with the model developer or expert to ensure the optimal selection and use of the model.

In case that CFD is to be applied to a new field, it is recommended that the user carry out additional validation studies, in order to gain confidence that the physical models are adequate for the intended application. If several modelling options are available in the code

(as is usually the case for turbulence, combustion and multi-phase flows), it is recommended to carry out the simulation with different models in order to test the sensitivity of the application to the model selection.

#### ***11.5.1. Multi-phase flow models***

Multi-phase flow models are required in cases where more than one phase is involved in the simulation. There are a wide variety of multi-phase flow scenarios, with the two extremes of small-scale mixing of phases or a total separation of the phases by a sharp interface. Depending on the flow simulation, different model types are available.

The Euler-Euler formulation is most commonly used for reactor safety applications. It is based on the assumption of interpenetrating continua. A separate set of mass, momentum and energy-conservation equations is solved for each phase. Inter-phase transfer terms are modelled and included to account for the interaction of the phases. Euler-Euler methods can be applied to separated and dispersed flows by changing the interfacial transfer models.

Additional models are required for flows with mass transfer between the phases (condensation, evaporation, boiling). These models can be applied in the form of correlations for a large number of particles (bubbles) in a given control volume, or directly at the interface between the resolved phase boundaries.

#### ***11.5.2. Turbulence models***

There are different methods for the treatment of turbulent flows. The need for a model results from the inability of industrial CFD simulations to fully resolve all time and length scales of a turbulent motion. In classical CFD methods, the Navier-Stokes equations are usually time- or ensemble-averaged, reducing the resolution requirements by many orders of magnitude. The resulting equations are the RANS equations. Due to the averaging procedure, information is lost, which is then fed back into the equations by a turbulence model.

RANS methods are the most widely used approach for CFD simulations of industrial flows. Early methods, using algebraic formulations, have been largely replaced by more general transport equation models, for both implementation and accuracy considerations. The use of algebraic models is not recommended for general flow simulations, due to their limitations in generality and their geometric restrictions. The lowest level of turbulence models, which offers sufficient generality and flexibility, are two-equation models. They are based on the description of the dominant length and time scale by two independent variables. Models that are more complex have been developed and offer more general platforms for the inclusion of physical effects. The most complex RANS model used in industrial CFD applications are second moment closure (SMC) models. Instead of two equations for the two main turbulent scales, this approach requires the solution of seven transport equations for the independent Reynolds stresses and one length (or related) scale.

The amount of information, which has to be provided by the turbulence model, can be reduced if the large time and length scales of the turbulent motion are resolved. The equations for this so-called LES method are usually filtered over the grid size of the computational cells. All scales smaller than the resolution of the mesh are modelled and all scales larger than the cells are simulated. This approach is several orders of magnitude more expensive than a RANS simulation and is therefore not used routinely in industrial flow simulations. It is most appropriate free shear flows, as the length scales near solid walls are usually very small and require small cells even for the LES method.

The challenge for the user of a CFD method is to select the best model for the application from the models available in the CFD method. In most cases it cannot be specified beforehand, which model will offer the highest accuracy? However, there are indications as to the range of applicability of different model closures. This information can be obtained from validation studies carried out with the model.

In addition to the accuracy of the model, consideration has to be given to its numerical properties and the required computing power. It is often observed that more complex models are less robust and require many times more computing power than the additional number of equations would indicate. Frequently, the complex models cannot be converged at all, or, in the worst case, the code becomes unstable and the solution is lost.

It is not trivial to provide general rules and recommendations for the selection and use of turbulence and multi-phase flow models for complex applications. Different CFD groups have given preference to different models for historical reasons or personal experiences. Even experts cannot always agree as to which model offers the best cost vs. performance ratio for a new application. Mahaffy et al. (2007) give an in-depth discussion on the selection and application of turbulence and multi-phase flow models for reactor safety relevant flows.

### ***11.5.3. ERCOFTAC best practice guidelines for dispersed flow***

It is worth mentioning the existence of best practice guidelines for CFD of dispersed multi-phase flows, which were published a few years ago by the ERCOFTAC, (2008). Those guidelines are proposed both to academic and industrial users dealing with CFD simulation of disperse flows. The ERCOFTAC document lacks any reference to nuclear reactor safety problems, and does not address the verification and validation issue (although reference is made to the ERCOFTAC “Database for dispersed two-phase flow predictions”). Furthermore, this document does not address some important topics and phenomenological aspects, which are relevant in the present context, such as the poly-dispersion, the IAT, the wall heat-transfer mechanisms, the quantification of uncertainty.

On the other hand, the ERCOFTAC document provides information and discussion to a certain extent complementary to the present report and constitutes a valuable reference. For instance, it includes a checklist of best practice advice that, although meant for non-nuclear applications, has a general validity and can be referred to as long as comprehensive nuclear-oriented best practice guidelines are not available. Furthermore, the ERCOFTAC document contains an exhaustive description of the forces acting on dispersed particles (whether gaseous, liquid or solid) and of the models commonly adopted to describe them.

Although oriented towards non-nuclear industry applications, and covering a rather limited range of situations relevant to the present framework, they contain some useful advice on model selection and reduction of errors. In particular, for “bubble column” configurations (without heat-transfer) they recommend the use of a two-fluid model combined with standard  $\kappa$ - $\epsilon$  model, gravity, drag force, mean bubble diameter (4.5 mm): a set of modelling choices that is probably performing well in typical industrial situations, while it may not necessarily perform as well in bubbly flows encountered in nuclear reactors.

## **11.6. Strategies to reduce user errors**

User errors are directly related to the expertise, the thoroughness and the experience of the user. For a given user, these errors can only be minimised by good project management

and thorough interaction with others. In case of inexperienced users, day-to-day interaction with a CFD expert or project manager is required to avoid quality problems. A structured work plan with intermediate results is important for intermediate and long-term projects.

A careful study of the CFD code documentation and other literature on the numerical method as well as the physical models is highly recommended. Furthermore, benchmark studies are recommended to understand the capabilities and limitations of CFD methods. A comparison of different CFD methods is desirable, but not always possible.

### 11.7. Strategies to reduce software errors

Software errors can be detected by verification studies. They are based on a systematic comparison of CFD results with verified solutions (in the best-case analytical solutions). It is the task of the software developer to ensure the functionality of the software by systematic testing.

In most cases, existing software will be used. It is assumed that all CFD packages have been sufficiently tested to ensure that no software verification studies have to be carried out in the project (except for newly developed modules). In case that two CFD packages give different results for the same application using the same physical models, the source of these differences needs to be evaluated. In case of code errors, they should be reported to code developers and subsequently removed.

### 11.8. Strategies to reduce application uncertainties

Application uncertainties cannot always be avoided, because missing information can frequently not be recovered. The uncertainty can be minimised by interaction with the supplier of the test case. The potential uncertainties have to be documented before the start of the CFD application.

In case assumptions have to be made concerning any input to a CFD analysis, they have to be communicated to the partners in the project. Alternative assumptions should be proposed and the sensitivity of the solution to these assumptions should be evaluated by case studies (alteration of inflow profiles, different locations for arbitrary boundary conditions, etc.).

Recommendations are:

- Identify all uncertainties in the numerical set-up:
  - geometry reduction;
  - boundary condition assumptions;
  - modelling assumptions (bubble diameter, etc.).
- Perform a sensitivity analysis with at least two settings for each parameter;
- Document the sensitivity of the solution on the assumptions.

## References

Bestion, D. (2010), Applicability of two-phase CFD to nuclear reactor thermalhydraulics and elaboration of Best Practice Guidelines, presented at CFD4NRS-3, Washington, sept 2010, accepted for publication in Nuclear Engineering and Design, 2011.

Bestion, D., P. Coste, B. Niceno and S. Mimouni (2011a), Two-phase CFD: the various approaches and their applicability to each flow regime, *Multiphase Science and Technology*, Volume 23, Issue 2-4, 2011.

Bestion, D. (2011b), Status and perspective for a multiscale approach to Light Water reactor thermalhydraulic simulation, NURETH-14, Toronto, Ontario, Canada, September 25-30, 2011, to be published in a topical Issue of Nuclear Engineering and Design, 2012.

ERCOFTAC (2008), Best Practice Guidelines for Computational Fluid Dynamics of Dispersed Multiphase Flows, edited by M. Sommerfeld, B. van Wachem, R. Oliemans, Version 1, October 2008.

Mahaffy, J., B. Chung, F. Dubois, E. Graffard, F. Ducros, M. Heitsch, M. Henriksson, E. Komen, F. Moretti, T. Morii, P. Mühlbauer, U. Rohde, M. Scheuerer, B. L. Smith, C. Song, T. Watanabe and G. Zigh (2007), Best Practice guidelines for the use of CFD in NEA (2007), "Nuclear Reactor safety Applications", NEA/CSNI/R(2007)5, OECD Publishing, Paris.

Roache, P.J. (1998), *Verification and Validation in Computational Science and Engineering*, Hermosa Publishers, Albuquerque, New Mexico.

Menter, F.R. (2002), "CFD Best Practice Guidelines for CFD Code Validation for Reactor-Safety Applications," European Commission, 5<sup>th</sup> EURATOM Framework Programme, Report, EVOL-ECORA-D1.

## 12. Conclusion

The WG3 on the “extension of CFD to two-phase flow safety problems” listed and classified the NRS problems where extension of CFD to two-phase flow may bring real benefit and classified different modelling approaches. First ideas were reported about the specification and analysis of needs in terms of V&V in a first report. Then the activity was focused on a limited number of NRS issues with a high priority and a reasonable chance to be successful in a reasonable period. Six NRS problems were selected to be further analysed in more detail, the dry-out, the DNB, the two-phase PTS, the pool heat exchangers, the steam discharge in a pool, and the fire analysis. These are high priority issues from the point of view of nuclear safety with some investigations going on and CFD investigations have a reasonable chance to be successful in a reasonable period. They address both present generation of PWR and BWR and the generation three water reactors and address all flow regimes so that they may, to some extent, envelop many other issues.

A general multi-step methodology for application of two-phase CFD to nuclear safety issues was proposed. Many options are possible when using two-phase-CFD, for the basic model (one-fluid, two-fluid, multi-field,...), for the averaging or filtering of turbulent and two-phase scales (using RANS, URANS, VLES, LES,...), for the treatment of the interface either by an ITM or statistically by calculating a volume fraction, an interfacial area, .... The choices have to be justified after an in-depth analysis of the issue and an identification of all basic flow processes. Then closure relations have to be selected or developed for interfacial transfers, turbulent transfers and wall transfers and a validation test matrix has to be established to validate in a separate-effect way all the models. Many consistency checks are necessary to build the CFD application on a physically sound basis.

The method was applied to the six selected issues resulting in an updated state of the art and gaps were identified in the modelling. Available data for validation were reviewed and needs of additional data were identified. Verification tests were also identified. A few benchmarks are proposed for future activity. Although two-phase CFD is still not very mature a first approach of best practice guidelines is given which should be later complemented and updated.

The main results of this work are here summarised:

For the six selected issues, the theoretical framework was made so clear that the selection of the basic model options was possible, even if some choices remain partly open and require further benchmarking between options. The method for modelling poly-dispersion in boiling bubbly flow, the use of an ITM or a more simple large interface identification for free surfaces in PTS investigations are examples where further developments and comparisons are still necessary.

For each selected issue, an experimental test matrix already exists which provides very precious information for model validation. However, in each case, there are still some deficiencies and needs were identified for new “CFD-grade” experiments equipped with advanced local instrumentation. The present status of closure laws used for the selected issues reflects the merits and limits of the validation matrix. An updated list of available experimental data for boiling flow and DNB was implemented in 2018 in the last version of this document.

Further effort is recommended to propose a strategy of validation with a clear definition of separate-effect tests, global tests, and demonstration tests, and of their respective roles in the whole validation process.

The verification issue has to be revisited more systematically and an effort is required to define more specific 3-D benchmarks. Two ways are recommended:

- The use of the method of manufactured solution should be promoted in two-phase CFD to produce tests with analytical solutions.
- New experiments with simple prototypic flow configurations should be produced with very well defined initial and boundary conditions and well-instrumented local measurements of possibly all principal variables.

Before having a comprehensive verification matrix, it was decided to select a benchmark test (or a few) for each NRS issue to provide at least an evaluation of the present capabilities and limitations, to promote further progress.

The proposed multi-step methodology gives a first approach to best practice guidelines for two-phase CFD by inviting users to formulate and justify all their choices and by listing some necessary consistency checks. Some methods for the control of numerical errors are also given, as part of the BPG.

The work performed by the writing group confirms that two-phase CFD is becoming a complementary tool to system codes for safety investigations. It did not provide yet an estimation of safety margins for any of the selected issue, but it gives access to small-scale flow processes, and provides a better understanding of physical situations. It is already a useful tool for safety analysis and may become a tool for safety demonstration when all the steps of the methodology have been correctly addressed including uncertainty evaluation.

## 13. Glossary

### GENERAL

ADS	Automatic depressurisation system
ASME	American society of mechanical engineering
ASTAR	Advanced three-dimensional two-phase flow simulation tool for application to reactor safety (EU 5 <sup>th</sup> Framework Programme)
BC	Building condenser
BDBA	Beyond design-basis accident
BPGs	Best practice guidelines
CCFL	Counter-current flow limitation
CFD	Computational fluid dynamics
CHF	Critical heat-flux
CMT	Core make-up tank
CPU	Central processing unit
CSD	Computational structural dynamics
CSNI	Committee on the Safety of Nuclear Installations
DBA	Design-basis accident
DHR	Decay heat removal
DNB	Departure from nucleate boiling
DNS	Direct numerical simulation
DVI	Direct vessel injection
DWO	Density wave oscillations
ECC	Emergency core-cooling
ECCS	Emergency core-cooling system
ECORA	Evaluation of computational fluid-dynamic methods for reactor safety analysis (EU 5 <sup>th</sup> Framework Programme)
EOC	End of cycle
EUROFASTNET	European project for future advances in science and technology for nuclear engineering thermal-hydraulics (EU 5 <sup>th</sup> Framework Programme)
FISA-2003	The Fifth International Symposium on EU Research and Reactor Safety
GAMA	Working Group on the Analysis and Management of Accidents
HA	Hydro accumulators

HTC	Heat-transfer coefficient
HX	Heat exchange
IAC	Interfacial area concentration
IC	Isolation condenser
IRWST	In-containment refuelling water storage tank
LBLOCA	Large-break loss of coolant accident
LES	Large Eddy simulation
LIS	Large interface simulation
LOCA	Loss of coolant accident
MCPR	Minimum critical power ratio
NACUSP	Natural circulation and stability performance of BWRs (EU 5 <sup>th</sup> Framework Programme)
NEA	Nuclear Energy Agency
NRS	Nuclear reactor safety
OECD	Organisation for Economic Co-operation and Development
PBL	Pressure balance line
PCC	Passive containment cooling
PCCS	Passive containment cooling system
PRHR	Passive residual heat removal
PTS	Pressurised thermal shock
RANS	Reynolds-averaged Navier-stokes
RIA	Reactivity insertion accidents
RPT	Recirculation pump trip
RPV	Reactor pressure vessel
SARA	Severe accident re-criticality analysis
SG	Steam generator
SI	Safety injection
TH	Thermal-hydraulics
TEMPEST	Testing and enhanced modelling of passive evolutionary systems technology for containment cooling (EU 5 <sup>th</sup> Framework Programme)
UP	Upper plenum
URANS	Unsteady Reynolds-averaged Navier-stokes
VLES	Very LES
VOF	Volume of fluid
WAHALOADS	Water-hammer loads (EU 5 <sup>th</sup> Framework Programme)

**EXPERIMENTS**

CYBL	Experiment about external reactor vessel cooling
ISB	Integral test facility for VVER (Russia)
PSB	Integral test facility for VVER (Russia)
PACTEL	Integral test facility for VVER (Finland)
PANDA	Integral test facility for SBWR (Switzerland)
PMK	Integral test facility for VVER (Hungary)
SBLB	Experiment about external reactor vessel cooling
SULTAN	Experiment about external reactor vessel cooling
ULPU	Experiment about external reactor vessel cooling
UPTF	Upper plenum test facility (Germany)

**CODES**

ATHLET	System analysis code, used extensively in Germany
CATHARE	System analysis code, used extensively in France
CFX	Commercial CFD software program
FLUBOX	In-house, two-phase flow code, developed by GRS
FLUENT	Commercial CFD software program
GENFLO	In-house CFD code, developed by VTT
MELCOR	Lumped-parameter code for analysing severe accidents, developed at Sandia NL
RECRIT	Computer code for BWR re-criticality and re-flooding analyses, developed by VTT
RELAP5	System analysis code, used extensively in US and elsewhere
TRAC	Transient reactor analysis code
TRACE	TRAC/RELAP combined computational engine

**REACTORS**

ABWR	Advanced BWR
ALWR	Advanced light water reactor
BWR	Boiling water reactor
EPR	European pressurised-water reactor
SBWR	Simplified BWR
ESBWR	European simplified BWR
LWR	Light water reactor
PWR	Pressurised-water reactor
VVER (or WWER)	Russian version of the PWR

## Annex 1. Example of application of the method of manufactured solutions

As part of a research project for the US Nuclear Regulatory Commission, use of various higher order numerical methods was studied for a two-phase, three-fluid model (vapour, continuous liquid, entrained liquid). The following manufactured solution was used to check the implementation of the various difference methods.

$$\begin{aligned}
 \alpha_p &= [0.3\sin(x^2 + \omega t) + 0.5], \quad p=v,e \\
 \alpha_l &= 1 - \alpha_v - \alpha_e \\
 u_p &= u_{p0}[\sin(x^2 + \omega t) + \varepsilon], \quad p=v,l,e \\
 h_p &= h_{p0}[\sin(x^2 + \omega t) + \varepsilon], \quad p=v,l \\
 P &= P_0[\sin(x^2 + \omega t) + \varepsilon] \\
 \rho_p &= \text{const}, \quad p=v,l \\
 T &= T_0[\sin(r^2 + z^2 + \omega t) + \varepsilon]
 \end{aligned} \tag{1}$$

where  $\omega, u_{p0}, h_{p0}, P_0, T_0, \varepsilon$  are arbitrary constants,  $\varepsilon$  is small. The index  $P$  represents a corresponding field: vapour  $v$ , liquid  $l$  and entrained  $e$ . The constants are usually set to the value of one, but to avoid exceeding the thermodynamic bounds on certain variables and other code restrictions, they can be set to higher values. In this case, the amplitude of the sine function should be increased as well, to better exercise the differential operators. Note that there are many other possibilities to manufacture different solutions than the ones given by Eq. 1. A steady-state can be tested by setting  $\omega = 0$ .

In this test problem, density was set constant because the necessary verification on spatial differences was driven by the functions chosen for field volume fractions and velocities. A separate verification test was constructed to be certain that densities were properly loaded into the discrete equations.

Below, the two-phase flow equations are modified by including a new source term to balance the terms obtained by differentiation of manufactured solutions. Notation in the source terms has shifted, with subscripts included in the source name, because the results were extracted directly from MathCad

### Vapour mass conservation:

$$\frac{\partial(\alpha_v \rho_v)}{\partial t} = -\frac{\partial(\alpha_v \rho_v u_v)}{\partial x} + \Gamma''' + S'''_{vm} \tag{2}$$

$$\begin{aligned}
S_{vm} = & .3 \cdot \cos(x^2 + \omega \cdot t) \cdot \omega \cdot \rho_v \dots \\
& + .6 \cdot \cos(x^2 + \omega \cdot t) \cdot x \cdot \rho_v \cdot uv_0 \cdot (\sin(x^2 + \omega \cdot t) + \varepsilon) \dots \\
& + 2 \cdot (.3 \cdot \sin(x^2 + \omega \cdot t) + .5) \cdot \rho_v \cdot uv_0 \cdot \cos(x^2 + \omega \cdot t) \cdot x - \Gamma
\end{aligned} \quad (3)$$

**Continuous liquid mass conservation:**

$$\frac{\partial(\alpha_l \rho_l)}{\partial t} = - \frac{\partial(\alpha_l \rho_l u_l)}{\partial x} - (1 - \eta) \Gamma''' + S_D''' - S_E''' + S_{lm}''' \quad (4)$$

$$\begin{aligned}
S_{lm} = & - .6 \cdot \cos(x^2 + \omega \cdot t) \cdot \omega \cdot \rho_l - \dots \\
& + - 1.2 \cdot \cos(x^2 + \omega \cdot t) \cdot x \cdot \rho_l \cdot ul_0 \cdot (\sin(x^2 + \omega \cdot t) + \varepsilon) - \dots \\
& + - 1.2 \cdot \sin(x^2 + \omega \cdot t) \cdot \rho_l \cdot ul_0 \cdot \cos(x^2 + \omega \cdot t) \cdot x + (1 - \eta) \cdot \Gamma \dots \\
& + SE - SD
\end{aligned} \quad (5)$$

**Entrained liquid mass conservation:**

$$\frac{\partial(\alpha_e \rho_l)}{\partial t} = - \frac{\partial(\alpha_e \rho_l u_e)}{\partial x} - \eta \Gamma''' - S_D''' + S_E''' + S_{em}''' \quad (6)$$

$$\begin{aligned}
S_{em} = & .3 \cdot \cos(x^2 + \omega \cdot t) \cdot \omega \cdot \rho_l \dots \\
& + .6 \cdot \cos(x^2 + \omega \cdot t) \cdot x \cdot \rho_l \cdot ue_0 \cdot (\sin(x^2 + \omega \cdot t) + \varepsilon) \dots \\
& + 2 \cdot (.3 \cdot \sin(x^2 + \omega \cdot t) + .5) \cdot \rho_l \cdot ue_0 \cdot \cos(x^2 + \omega \cdot t) \cdot x \dots \\
& + \eta \cdot \Gamma + SD - SE
\end{aligned} \quad (7)$$

**Vapour energy-conservation:**

$$\frac{\partial(\alpha_v \rho_v h_v)}{\partial t} = - \frac{\partial(\alpha_v \rho_v h_v u_v)}{\partial x} + \Gamma''' h_e + q_{iv} + Q_{wv} + \alpha_v \frac{\partial P}{\partial x} + S_{ve}''' \quad (8)$$

$$\begin{aligned}
S_{ve} = & .3 \cdot \cos(x^2 + \omega \cdot t) \cdot \omega \cdot \rho_v \cdot hv_0 \cdot (\sin(x^2 + \omega \cdot t) + \varepsilon) \dots \\
& + (.3 \cdot \sin(x^2 + \omega \cdot t) + .5) \cdot \rho_v \cdot hv_0 \cdot \cos(x^2 + \omega \cdot t) \cdot \omega \dots \\
& + .6 \cdot \cos(x^2 + \omega \cdot t) \cdot x \cdot \rho_v \cdot uv_0 \cdot (\sin(x^2 + \omega \cdot t) + \varepsilon)^2 \cdot hv_0 \dots \\
& + 4 \cdot (.3 \cdot \sin(x^2 + \omega \cdot t) + .5) \cdot \rho_v \cdot uv_0 \cdot (\sin(x^2 + \omega \cdot t) + \varepsilon) \cdot \dots \\
& + \dots \cdot hv_0 \cdot \cos(x^2 + \omega \cdot t) \cdot x - (.3 \cdot \sin(x^2 + \omega \cdot t) + .5) \cdot P_0 \dots \\
& + \dots \cdot \cos(x^2 + \omega \cdot t) \cdot \omega - q_{iv} - \Gamma \cdot hg - Q_{wv}
\end{aligned} \quad (9)$$

**Liquid energy-conservation:**

$$\frac{\partial((1-\alpha_v)\rho_l h_l)}{\partial t} = -\frac{\partial((\alpha_l u_l + \alpha_e u_e)\rho_l h_l)}{\partial x} - \Gamma''' h_f + q_{il} + Q_{wl} + (1-\alpha_v)\frac{\partial P}{\partial t} + S'''_{le} \quad (10)$$

$$\begin{aligned} S_{le} = & .6 \cdot \cos(x^2 + \omega \cdot t) \cdot \omega \cdot \rho_l \cdot h_l \cdot (\sin(x^2 + \omega \cdot t) + \varepsilon) \dots \\ & + (1 + .6 \cdot \sin(x^2 + \omega \cdot t)) \cdot \rho_l \cdot h_l \cdot \cos(x^2 + \omega \cdot t) \cdot \omega \dots \\ & + \left[ \begin{aligned} & -1.2 \cdot \cos(x^2 + \omega \cdot t) \cdot x \cdot u_l \cdot (\sin(x^2 + \omega \cdot t) + \varepsilon) - \dots \cdot \rho_l \cdot h_l \cdot \dots \\ & + -1.2 \cdot \sin(x^2 + \omega \cdot t) \cdot u_l \cdot \cos(x^2 + \omega \cdot t) \cdot x \dots \\ & + .6 \cdot \cos(x^2 + \omega \cdot t) \cdot x \cdot u_e \cdot (\sin(x^2 + \omega \cdot t) + \varepsilon) \dots \\ & + 2 \cdot (.3 \cdot \sin(x^2 + \omega \cdot t) + .5) \cdot u_e \cdot \cos(x^2 + \omega \cdot t) \cdot x \end{aligned} \right] \cdot \rho_l \cdot h_l \cdot \dots \\ & + \left[ \begin{aligned} & \sin(x^2 + \omega \cdot t) + \varepsilon \dots \\ & + 2 \cdot \left[ \begin{aligned} & -.6 \cdot \sin(x^2 + \omega \cdot t) \cdot u_l \cdot (\sin(x^2 + \omega \cdot t) + \varepsilon) \dots \\ & + (.3 \cdot \sin(x^2 + \omega \cdot t) + .5) \cdot u_e \cdot (\sin(x^2 + \omega \cdot t) + \varepsilon) \end{aligned} \right] \cdot \rho_l \cdot h_l \cdot \dots \\ & + \cos(x^2 + \omega \cdot t) \cdot x \dots \end{aligned} \right] \cdot \rho_l \cdot h_l \cdot \dots \\ & + \left[ \begin{aligned} & -.5 \cdot .3 \cdot \sin(x^2 + \omega \cdot t) \cdot P_0 \cdot \cos(x^2 + \omega \cdot t) \cdot \omega - q_{il} + \Gamma \cdot h_f \end{aligned} \right] - Q_{wl} \end{aligned} \quad (11)$$

**Vapour momentum conservation:**

$$\alpha_v \rho_v \frac{\partial u_v}{\partial t} = -\alpha_v \rho_v u_v \frac{\partial u_v}{\partial x} - \alpha_v \rho_v g - \alpha_v \frac{\partial P}{\partial x} - \tau_{wv} - \tau_{i,vl} - \tau_{i,ve} - \Gamma_E''(u_v - (1-\eta)u_l - \eta u_e) + S'''_{vmo} \quad (12)$$

$$\begin{aligned} S_{vmo} = & (.3 \cdot \sin(x^2 + \omega \cdot t) + .5) \cdot \rho_v \cdot u_v \cdot \cos(x^2 + \omega \cdot t) \cdot \omega \dots \\ & + 2 \cdot (.3 \cdot \sin(x^2 + \omega \cdot t) + .5) \cdot \rho_v \cdot u_v \cdot (\sin(x^2 + \omega \cdot t) + \varepsilon) \cdot \dots \\ & + \cos(x^2 + \omega \cdot t) \cdot x + (.3 \cdot \sin(x^2 + \omega \cdot t) + .5) \cdot \rho_v \cdot g \dots \\ & + 2 \cdot (.3 \cdot \sin(x^2 + \omega \cdot t) + .5) \cdot P_0 \cdot \cos(x^2 + \omega \cdot t) \cdot x \dots \\ & + \tau_{wv} + \tau_{i,vl} + \tau_{i,ve} \dots \\ & + \Gamma_E \cdot \left[ \begin{aligned} & u_v \cdot (\sin(x^2 + \omega \cdot t) + \varepsilon) - \dots \\ & + -(1-\eta) \cdot u_l \cdot (\sin(x^2 + \omega \cdot t) + \varepsilon) - \dots \\ & + -\eta \cdot u_e \cdot (\sin(x^2 + \omega \cdot t) + \varepsilon) \end{aligned} \right] \end{aligned} \quad (13)$$

**Continuous liquid momentum conservation:**

$$\alpha_l \rho_l \frac{\partial u_l}{\partial t} = -\alpha_l \rho_l u_l \frac{\partial u_l}{\partial x} - \alpha_l \rho_l g - \alpha_l \frac{\partial P}{\partial x} - \tau_{wl} + \tau_{i,vl} + (1-\eta)\Gamma_C''(u_v - u_l) + S_D'''(u_e - u_l) + S_{lmo}''' \quad (14)$$

$$\begin{aligned} S_{lmo} = & - .6 \cdot \sin(x^2 + \omega \cdot t) \cdot \rho_l \cdot u_l \cos(x^2 + \omega \cdot t) \cdot \omega \dots \\ & + -1.2 \cdot \sin(x^2 + \omega \cdot t) \cdot \rho_l \cdot u_l^2 \cdot (\sin(x^2 + \omega \cdot t) + \varepsilon) \dots \\ & + \cos(x^2 + \omega \cdot t) \cdot x - .6 \cdot \sin(x^2 + \omega \cdot t) \cdot \rho_l \cdot g \dots \\ & + -1.2 \cdot \sin(x^2 + \omega \cdot t) \cdot P_0 \cos(x^2 + \omega \cdot t) \cdot x \cdot (-1 + \eta) \dots \\ & + \Gamma_C \cdot [uv_0 \cdot (\sin(x^2 + \omega \cdot t) + \varepsilon) - ul_0 \cdot (\sin(x^2 + \omega \cdot t) + \varepsilon)] \dots \\ & + -SD \cdot [ue_0 \cdot (\sin(x^2 + \omega \cdot t) + \varepsilon) - ul_0 \cdot (\sin(x^2 + \omega \cdot t) + \varepsilon)] \dots \\ & + \tau_{wl} - \tau_{vl} \end{aligned} \quad (15)$$

**Entrainment liquid momentum conservation:**

$$\alpha_e \rho_l \frac{\partial u_e}{\partial t} = -\alpha_e \rho_l u_e \frac{\partial u_e}{\partial x} - \alpha_e \rho_l g - \alpha_e \frac{\partial P}{\partial x} - \tau_{i,ve} + \eta \Gamma_C''(u_v - u_l) - S_E''(u_e - u_l) + S_{emo}''' \quad (16)$$

$$\begin{aligned} S_{emo} = & (.3 \cdot \sin(x^2 + \omega \cdot t) + .5) \cdot \rho_l \cdot u_e \cos(x^2 + \omega \cdot t) \cdot \omega \dots \\ & + 2 \cdot (.3 \cdot \sin(x^2 + \omega \cdot t) + .5) \cdot \rho_l \cdot u_e^2 \cdot (\sin(x^2 + \omega \cdot t) + \varepsilon) \dots \\ & + \cos(x^2 + \omega \cdot t) \cdot x + (.3 \cdot \sin(x^2 + \omega \cdot t) + .5) \cdot \rho_l \cdot g \dots \\ & + 2 \cdot (.3 \cdot \sin(x^2 + \omega \cdot t) + .5) \cdot P_0 \cos(x^2 + \omega \cdot t) \cdot x \dots \\ & + -\eta \cdot \Gamma_C \cdot [uv_0 \cdot (\sin(x^2 + \omega \cdot t) + \varepsilon) - ul_0 \cdot (\sin(x^2 + \omega \cdot t) + \varepsilon)] \dots \\ & + SE \cdot [ue_0 \cdot (\sin(x^2 + \omega \cdot t) + \varepsilon) - ul_0 \cdot (\sin(x^2 + \omega \cdot t) + \varepsilon)] \dots \end{aligned} \quad (17)$$

**Installation of these special source terms into the I-D two-phase code proved to be invaluable in detecting and isolating coding errors.**